INFORMATION TO USERS

This was produced from a copy of a document sent to us for microfilming. While the most advanced technological means to photograph and reproduce this document have been used, the quality is heavily dependent upon the quality of the material submitted.

The following explanation of techniques is provided to help you understand markings or notations which may appear on this reproduction.

1. The sign or "target" for pages apparently lacking from the document photographed is "Missing Page(s)". If it was possible to obtain the missing page(s) or section, they are spliced into the film along with adjacent pages. This may have necessitated cutting through an image and duplicating adjacent pages to assure you of complete continuity.

2. When an image on the film is obliterated with a round black mark it is an indication that the film inspector noticed either blurred copy because of movement during exposure, or duplicate copy. Unless we meant to delete copyrighted materials that should not have been filmed, you will find a good image of the page in the adjacent frame.

3. When a map, drawing or chart, etc., is part of the material being photographed the photographer has followed a definite method in "sectioning" the material. It is customary to begin filming at the upper left hand corner of a large sheet and to continue from left to right in equal sections with small overlaps. If necessary, sectioning is continued again–beginning below the first row and continuing on until complete.

4. For any illustrations that cannot be reproduced satisfactorily by xerography, photographic prints can be purchased at additional cost and tipped into your xerographic copy. Requests can be made to our Dissertations Customer Services Department.

5. Some pages in any document may have indistinct print. In all cases we have filmed the best available copy.

University
Microfilms
International

300 N. ZEEB ROAD, ANN ARBOR, MI 48106
18 BEDFORD ROW, LONDON WC1R 4EJ, ENGLAND

OSMAN, MOHAMMED EL-SAYED

PRESSURE ANALYSIS AND WATER FLOODING PERFORMANCE OF HETEROGENEOUS OIL RESERVOIRS

The University of Oklahoma PH.D. 1980

PLEASE NOTE:

In all cases this material has been filmed in the best possible way from the available copy. Problems encountered with this document have been identified here with a check mark ✓.

1. Glossy photographs _____
2. Colored illustrations _____
3. Photographs with dark background _____
4. Illustrations are poor copy _____
5. Print shows through as there is text on both sides of page _____
6. Indistinct, broken or small print on several pages ✓
7. Tightly bound copy with print lost in spine _____
8. Computer printout pages with indistinct print _____
9. Page(s) _____ lacking when material received, and not available from school or author
10. Page(s) _____ seem to be missing in numbering only as text follows
11. Poor carbon copy _____
12. Not original copy, several pages with blurred type _____
13. Appendix pages are poor copy _____
14. Original copy with light type _____
15. Curling and wrinkled pages _____
16. Other _____

THE UNIVERSITY OF OKLAHOMA

GRADUATE COLLEGE

PRESSURE ANALYSIS AND WATER FLOODING PERFORMANCE OF HETEROGENEOUS OIL RESERVOIRS

A DISSERTATION

SUBMITTED TO THE GRADUATE FACULTY

in partial fulfillment of the requirements for the

degree of

DOCTOR OF PHILOSOPHY

BY

MOHAMMED EL-SAYED OSMAN

Norman, Oklahoma

1980

PRESSURE ANALYSIS AND WATER FLOODING PERFORMANCE

OF HETEROGENEOUS OIL RESERVOIRS

APPROVED BY

DISSERTATION COMMITTEE

DEDICATED TO

MY

PARENTS

ACKNOWLEDGEMENTS

I wish to express my sincere gratitude to the individuals who made significant contributions to this work. Dr. D. Tiab, Assistant Professor of Petroleum and Geological Engineering and chairman of the doctoral committee, is singled out for his guidance, encouragement, and valuable suggestions. Dr. Tiab provided the computer plotting routines for this work.

Acknowledgement is extended to Dr. A. Aly, Associate Professor of Industrial Engineering, Dr. H. B. Crichlow, Associate Professor of Petroleum and Geological Engineering, Dr. D. Menzie, Professor of Petroleum and Geological Engineering, and Dr. M. Townsend, Professor of Chemical Engineering and Material Science, for being members of the dissertation committee and for their helpful comments.

The financial support for this study was furnished by the School of Petroleum and Geological Engineering of the University of Oklahoma and The National Science Foundation.

The author wishes to thank Mr. O. Abdou who assisted in drafting some of the plots, and Mrs. Wedel who typed this dissertation.

For the love and understanding I received from my wife, Wafaa, and my daughter, Hayaam, during the preparation of this manuscript, I give special thanks that cannot be expressed in words alone.

ABSTRACT

This study presents an approximate solution to the problem of unsteady state flow due to production from a single well located in the center of a multiple-layered composite reservoir. Using the technique of superposition in time, expressions for the pressure distribution anywhere in stratified composite reservoirs and the fractional flow rates from each layer of these reservoirs were developed. Both pressure drawdown and buildup behavior of the well bore were considered. Fractional flow rates and drawdown type-curve plots were generated. A type-curve matching technique to determine the reservoir characteristics and dimensions using drawdown pressure data was developed. Due to the fact that two stratified-composite reservoirs with different properties may produce similar pressure buildup curves, Horner and Miller-Dyes-Hutchinson procedures could not be used to predict the reservoir characteristics from pressure buildup.

Also, this study presents a modification to the Dykstra-Parson method to predict water flooding performance of multi-layered composite reservoirs. The modification takes into account the variations in reservoir properties and dimensions both vertically and horizontally. Two important cases, constant injection rate and constant injection pressure drop

were considered. It was found that water flooding performance in multilayered composite linear reservoirs is mainly controlled by the mobility ratio.

TABLE OF CONTENTS

LIST OF TABLES

TABLE

LIST OF FIGURES

FIGURE

FIGURE

FIGURE

FIGURE

CHAPTER 1

INTRODUCTION

The research work presented in this dissertation concentrates on fluid flow in heterogenous reservoirs. The major part deals with the bottom hole pressure behavior (drawdown and buildup) of a well located in the center of multilayered composite reservoirs. The rest of the study deals with water flooding performance of multilayered composite reservoirs.

1.1 Literature Survey

The concept of analyzing pressure-time data from a producing or shut-in oil or gas well to obtain in-situ reservoir rock properties, such as porosity, permeability, . . . etc., was first applied in 1933. A classic study by Moore, et al. (1933) presented a solution to the diffusivity equation in terms of Bessel functions for a constant rate well and a constant pressure well in an infinite reservoir. Theis (1935) presented the line source exponential integral solution to the diffusivity equation and its logarithmic approximation at large times. He also employed a semi-log graph which is commonly known as the Horner plot in the petroleum industry. Muskat (1937) developed a method to

determine the eventual static pressure of a well in a closed circular reservoir. Elkins (1946) demonstrated the use of the line source solution in interference testing between wells in an oil field to determine inter-well rock properties. Arps and Smith (1949) presented a method to determine static pressure by plotting rate of change of well shut-in pressure versus shut-in pressure.

The preceding publications laid the foundation for two important papers: by Horner (1951) and Miller, et al. (1950). Horner summarized transient pressure analysis methods for a constant rate well in an infinite reservoir and in a closed reservoir. Miller, et al. presented a behavior of a constant rate well in a circular reservoir with no-flow and constant pressure conditions at the drainage boundary of the reservoir.

Horner (1951) presented an application of the image technique proposed by Muskat (1937) to detect the presence of a sealing fault near a well from pressure data under transient flow conditions. Horner also presented a method to calculate the distance to the fault from pressure buildup data. Dolan, Einarson and Hill (1957) applied the technique to data from drill-stem tests.

Evrenos and Rejda (1965) employed superposition techniques to simulate various combinations of linear boundaries of interest in gas storage systems, and shows how a match between the actual test data with various hypothetical model

conditions can be used to arrive at a probable configuration of boundary conditions.

Witherspoon, et al. (1967) considered the effect of a linear no-flow and flow boundary and presented the dimensionless pressure behavior caused by a constant rate producing well at an observation well some distance away. They discussed techniques to analyze drawdown test data.

Matthews, Brons and Hazebroek (1954) extended Horner's determination of static pressure for bounded circular reservoir to the general case of a well in almost any position within a large variety of bounded drainage shapes. Later, Brons and Miller (1961), and Dietz (1965) developed other pressure buildup interpretive methods for these closed shapes. These studies were followed by a large number of publications on well test interpretation in bounded reservoirs of various geometrical shapes. Matthews and Russell (1967) summarized the practical aspects of the findings of these studies in a monograph.

Earlougher, et al. (1968) demonstrated that the infinite square array may be used to generate flow behavior for any rectangular shape. Earlougher and Ramey (1973) presented tables of the dimensionless pressure at the well and at several other locations within a variety of closed rectangles with a well producing at a constant rate.

Osman (1979) used superposition technique to develop MBH dimensionless pressure for a well located inside a rectangle with open or mixed boundaries. The results of his

study are presented in graphical and tabulated forms.

Russell and Prats (1962) investigated mathematically the performance of a bounded two-layer reservoir in which flow is possible from a layer of low permeability to that of higher permeability. Their studies show that except for the early time when the reservoir behaves as that of a stratified system, the performance of the reservoir is identical to that of a single layer with the same pore volume, drainage and well-bore radii. The total "Kh" and "Øh" are the sum of the individual layers. Russell and Prats conclusions have been confirmed by Katz and Tek (1962) and Pendergrass and Berry (1962) studies.

Lefkovits, et al. (1961) studied the behavior of bounded reservoirs composed of stratified layers. They found that when the shut in pressure P_{ws} is plotted versus log $(t+\Delta t)/\Delta t$, a curve with a straight-line section and subsequent leveling, rising and flattening sections is obtained. Their work showed that the time necessary to reach pseudo-steady state is much longer for two-layered reservoir than for a single layered reservoir.

Earlougher, et al. (1974) studied the behavior of pressure buildup in a closed square layered system, with variation in porosity, permeability and thickness ratios. They used the principle of superposition and the exponential integral for their calculations. The results of their study show that curves of buildup obtained for layered reservoirs vary and may

not necessarily identify layered reservoirs.

Hurst (1960) and Mortada (1960) analyzed the interference between oil fields in a common aquifer of two different permeabilities. Loucks and Guerrero (1961) presented an analysis of drawdown and buildup in radial composite systems. Carter (1968) presented an analysis of the depletion of a closed composite radial reservoir and discussed reservoir limit tests for this class of reservoirs. Ramey (1970) presented an analytical solution for unsteady state liquid flow in two-region and three-region single layer reservoirs.

Gringarten and Ramey (1973) presented the point source solution as a part of a more general theory of Green's functions. The theory is applied in combination with other techniques to yield immediate solutions to difficult flow problems. Using Green's functions, Gringarten and Ramey (1974), Gringarten, et al. (1974), Gringarten, et al. (1975), Uraiet, et al. (1977) and others presented analytical solutions for fractured reservoirs for different well and reservoir conditions.

The prediction of waterflooding performance for a stratified reservoir has been the subject of many investigations. Stiles (1949) presented a simple approach to the calculation of recovery and water cut from such stratified systems. The approach accounts for the different flood-front positions in liquid-filled, linear layers having different permeabilities

without cross flow. The Stiles method assumes that mobility ratio is unity, piston-like displacement, all beds have the same porosity and the same relative permeabilities to water behind the flood and to oil ahead of the flood.

Dykstra and Parsons (1950) introduced a semi-empirical treatment for calculating the recovery of oil by waterflooding stratified reservoirs. They developed a graphical correlation which was based on calculations applied to a layered linear model. Their correlations reflect the effect of initial fluid saturations, mobility ratio and permeability variations on the waterflooding-oil recovery. Dykstra and Parsons proposed that variations in permeability can be expressed as a log normal probability distribution.

Kufus and Lynch (1959) combined the Dykstra-Parsons technique with the Buckley-Leverett displacement theory to obtain a more nearly correct approximation of the actual conditions. Snyder and Ramey (1967) applied the Buckley-Leverett theory to stratified models.

Warren and Cosgrove (1964) developed a model approximating the effect of crossflow due to viscous forces in predicting waterflood performance from a stratified reservoir. They produced coverage charts similar to those obtained by Dykstra and Parsons. In their model, capillary and gravity forces were neglected.

Goddin, et al. (1966) and Sommers (1970) investigated the effect of crossflow due to viscous and capilary forces

for two-layered and multilayered systems, respectively, using two-phase two-dimensional models. Goddin, et al. concluded that waterflood performance with crossflow is intermediate between the performance of a uniform system and that of a reservoir with no crossflow.

Coats (1968) illustrated the effect of gravitational and capillary forces in the waterflooding of a heterogeneous linear reservoir of mixed permeability ordering. He showed that, when assuming different capillary pressure curves for each layer, the injected water may tend to finger through tighter zones due to inhibition of water from the more permeable zones.

Straight, et al. (1974) investigated the effect of rate on recovery from homogeneous and stratified reservoirs. In their work, they used three phase two-dimensional numerical models. They found that recoveries were lower at breakthrough for higher rates.

1.2 Characterization of Reservoir Heterogeneities

The presence of sediments may be said to be the one essential element of a potential petroleum provenance. Sediments provide the source of the petroleum, the reservoir rock, and the cover for the individual traps.

The reservoir rock may be divided into: fragmental (elastic), chemical and biochemical (precipitated), and miscellaneous. Fragmental reservoir rocks are aggregates of particles, fragments of minerals, or fragments of older rocks.

The constituent particles of fragmental reservoir rocks range in size from colloidal particles up to pebbles and boulders. Chemical and biochemical reservoir rocks are those that are predominantly composed of chemical or biochemical precipitates. The dominant chemical reservoir rocks are carbonate sediments, mostly limestone and dolomites. Miscellaneous reservoir rocks include the igneous and metamorphic rocks.

1.2.1 Porosity

The first essential element of a petroleum reservoir is a reservoir rock and the essential feature of a reservoir rock is porosity. Porosity, however, is not enough; the pores must be interconnected to permit the passage of oil and gas through the rock. There is a wide variation among reservoir rocks in size of the individual pores and in the arrangement of the pores with respect to one another. These variations are called primary if they are controlled by: 1. depositional environment of the rock, 2. the degree of uniformity of particle size, and 3. the nature of the material that make up the rock. The variations are called secondary if they depend on things that have happened to the rock since it was deposited; they may include: 1. fracturing and shattering, 2. solution, 3. redeposition and cementation, and 4. compaction due to increased load.

Primary porosity

The primary porosity of a rock is largely dependent upon its packing characteristics, which in turn depends largely

on the uniformity or lack of uniformity of grain size. In rock of uniform grain size, the smaller the grains are, the greater is the porosity; this effect is due to such factors as friction, adhesion, and bridging, which are greater with smaller grains because of the higher ratio of surface area to volume and mass. The shape of elastic rock particles commonly varies from round through angular to flat and mica-like, and the size from coarse to fine or even colloridal; and there are widely varying amounts of cementing material between the individual grains.

Secondary porosity

Most of the reservoir characterized by secondary porosity are in the carbonate rocks (limestones and dolomites); secondary porosity may result from and modified by: 1. solution, 2. fractures and joints, 3. recrystalization and dolomitization, and 4. cemetation and compaction.

1. Solution

Percolating surface waters containing carbonic acid and organic acids penetrate the rock along various kinds of openings, such as primary pores, fissures, fractures, joint planes, intercrystalline openings, and bedding planes. As these acid waters pass through the rock, they dissolve out the more soluable cations, including the carbonates of calcium and magnesium and salts of sodium and potasium, thereby still further opening the channels and increasing the porosity. Increased porosity develops in those parts of the rock where solution goes on more rapidly than redeposition. Some of the dissolved matter,

however, is precipitated in other parts of the rock, thus forming a cement that reduces the porosity.

2. Fractures and Joints

Fractures and joints in brittle rocks afford common and important types of secondary porosity. The brittle reservoir rocks include limestones, dolomites, cherts, shales, silicious sedimentary rocks, igneous rocks, and metamorphic rocks. Interbedded shales, sandstones, and limestones may show selective fracturing in certain beds. Since fractures afford channels for the movement of water, they are likely to be enlarged and modified by solution. They frequently combine with other types of both primary and secondary porosity to make a complex porous pattern; in fact, the presence of fractures often changes the permeability from millidarcys to darcys.

Three causes are considered to account for most fractures:

A. Diastrophism (such as folding and faulting): Some fractures may form at depth, where they accompany an increase in the volume of the rock resulting from the dilatant effect of the folding and bending of the strata.

B. Removal of the overburden by erosion in the zone of weathering: as sediments are unloaded through erosion, the upper parts expand, and incipient weaknesses in the rocks become joints, fractures and fissures.

C. Reduction in volume of shales due to loss of water: where intervening layers do not shrink, but act as dividers.

The loss of volume in the shales and siltstones is expressed in fractures, many of which have irregular forms.

3. Recrystalization

Some carbonate reservoir rocks are nearly pure limestone and some are nearly pure dolomite, but more are intimate and variable mixture of the two. The porosity of dolomite is much greater than that of limestone. This has been interpreted on molecular replacement of limestone by dolomite which would result in a volume shrinkage of 12-13 percent. Also, dolomites offer much larger intercrystaline space for the passage of dissolving solution and so present a much greater area of attack.

4. Compaction and Cementation

These two processes may occur at any time during or after deposition of the rock.

A. Cementation: Some cementation is primary; the cement may be precipitated, or it may be deposited along with the elastic material. Silica, carbonates, and other soluble materials may be precipitated contemporaneously with the deposition of detrital material. Primary cementing material is subject to recrystalization later, and it is then difficult to distinguish recrystalized cementing material from that introduced after the sediment became consolidated.

B. Compaction: Three effects of load pressure are important in the geology of petroleum: I. Compaction of the reservoir sediments, II. Compaction of the non-reservoir

sediments, especially the shales, III. Compression of the reservoir fluids.

Compaction of a reservoir rock is due chiefly to the increasing weight of the overburden. Its effect, like that of cementation, is to reduce porosity. The reduction of pore space by compaction in a sealed reservoir system causes an increase in reservoir fluid pressure. Compaction is especially significant in reservoir sediments containing shales or clays and colloidal material. Large amounts of absorbed water are squeezed out of these by an increase in load pressure, and because the clays and colloids are highly plastic, they flow between the grains to form a cementing or bonding agent and thereby reduce the porosity.

Artificial porosity

Various methods of forming, or increasing pore space and the permeability of the reservoir rocks have been devised. The fracturing of the reservoir increases the effective radius of the well bore and increases the porosity and permeability surrounding the hole and consequently permits more oil and gas to flow into the well. The response varies with different rocks depending largely on whether the explosion packs the particles tighter or fractures the rock. Forcing acids into the reservoir rock under pressure is called acidization. The acid enters the reservoir rock along connected porosity openings and dissolves the soluable materials as it penetrates the rock, thereby increasing both the permeability and the porosity.

1.2.2 Permeability

Permeability is the property that permits the passage of a fluid through the interconnected pores of a rock without damage to or displacement of the rock particles. The unit of measurement of the permeability of a rock has been named the Darcy after Henri Darcy who experimented with the passage of liquids through porous media in 1856.

Permeability is usually measured paralleled to the bedding planes of reservoir rock. Permeability across the bedding planes, or vertical permeability, is also frequently measured and is usually less than the horizontal permeability.

The reason why horizontal permeability is generally higher than vertical permeability lies largely in the arrangement and packing of the rock particles during deposition. As flat grains tend to align and overlap parallel to the depositional surface, dissolving solutions move most easily in this direction, and in so far as the solutions have a solvent action on the minerals, they increase the horizontal permeability.

High vertical permeabilities are chiefly the result of fractures and of solution along fracture and joint planes that cross the bedding. They are most commonly encountered in carbonate rocks and other brittle rocks and in elastic rocks with a high content of soluable material.

Effective and Relative Permeability

Darcy's law governing the flow of fluids through a porous material is based on the assumption that only one fluid

is present and that it completely saturates the rock. In nature, however, the reservoir pore spaces contain gas, oil, and water in varying amounts and each interferes with and impedes the flow of the others. Where a fluid does not completely saturate the rock, as is generally the case, the ability of the rock to conduct the fluid in the presence of other fluids is called its effective permeability to that fluid. It has been found that a given value of fluid saturation bears a constant relation to the effective permeability; if the one changes, the other changes proportionately. This relation, however, differs for different rocks and must be determined experimentally.

The ratio between the effective permeability to a given fluid at a partial saturation and the permeability at 100 percent saturation (the absolute permeability) is known as the relative permeability. Since the pore space of all reservoirs is full of gas, oil and/or water, in varying proportions, the relative permeability of the rock to one fluid is dependent upon the amount (saturation) and the nature of the other fluids present.

Factors Affecting Permeability

The quantitative relation between porosity and permeability is obscure and variable. Beyond the fact that permeable must also be porous, there seems to be only a general trend. As the porosity increases the permeability increases. Therefore, most of the factors affecting porosity affect the permeability as they do the porosity.

It has been found that with variable grain size, the permeability increases as the shapes of grains depart from that of true spheres. Thus the permeability of a sand composed of angular grains is greater than that of a sand composed chiefly of spherical grains of similar size, largely because the angular grains are packed more loosely and also develop bridging. Rocks composed mainly of flat, mica-shaped particles and needle-like crystals pack loosely, have a high porosity and in general have a high permeability. Decreasing grain size, on the other hand, increases porosity; but, because of the greater tortuosity and the higher capillary pressures, the relative permeability is lower.

Compaction and cementation, obviously, reduce permeability based on primary porosity, whereas solution channels increase permeability, fracturing, shattering, joint planes, and bedding planes, especially, increase permeability greatly the large cross-sectional area of the tabular openings they produce. Permeability varies inversely with the length of flow and therefore inversely with tortuosity; so whatever shortens the path increases the permeability.

1.2.3 Faults and Fractures

A fault is defined as a fracture along which there has been appreciable motion parallel to the break. There is an enormous range in the length of faults and in their displacements. Many are so small that they can be seen only under the microscope. Other faults are over one hundred miles long, and their

displacement amounts to many miles.

All faults are due to shearing and gravity plays a part in the motion of all faults, though it is not the only cause. There is a tight relation between faults and earthquakes. Many earthquakes are accompanied by visible faulting at the surface, and it is likely that in many cases there is a fault at depth.

Faults are important to the petroleum geologist not only because they make traps for oil accumulation but because the recognition of faulting where it occurs is essential to the correct interpretation of the structure. The frequency of faulting in oil-producing regions varies greatly, from practical absence of faults to an intense degree of faulting.

In general, faults are more numerous in strongly deformed than in gently dipping structures. Rigid or brittle formations like hard limestones and sandstones are more susceptible to faulting than plastic rocks like shales and clays.

The relation of faulting to oil and gas production varies greatly. Many oil and gas fields are not associated with faults and in some the faulting is incidental, while in others the fault produces the trap which causes the oil or gas accumulation. The most important structural traps associated with faults are:

Closures Against Faults

In this type of structure the fault forms the closures on one side and generally there is an anticline or nose which is

cut by the fault oil production from some structures closed against faults is fairly common in some regions. The occurrence of oil and gas in this type of structure means that the fault plane must be sealed so that oil and gas cannot migrate through it fast enough to drain the pool.

Fractures Along Fault Planes

Production from fractured rocks along fault planes does not require a typical closed structure. The production may come from any type of sedimentary rock, such as limestones, chalk, etc., which is sufficiently brittle to be extensively fractured by the faulting. Generally the reservoir becomes impervious a short distance from the fault, where it is not fractured, and this acts as a closure in all directions except along the fault. In these directions the reservoir may be sealed by the change in the direction or amount of faulting or by changes in the lithology of the rock close to the fault.

Traps Bounded by Faults

Faulting often breaks up a field into separate pools; where that happens, the fault planes may become the boundary of a pool and tightly seal it off. Water-oil contacts may be at the same or different levels in the different fault blocks, depending on whether oil can migrate across the fault planes or not.

Anticlines on Downdip Sides of Faults

In this type of trap the anticline on which the production occurs is some distance down the dip from the fault, and between

the anticlinal axis and the fault there is a reverse dip into the fault on its downthrown side. Thus a low dry belt structurally separates the oil or gas fields from the faults.

1.2.4 Hydraulic Fractures

The hydraulic fracturing technique of well stimulation is one of the recent major developments in petroleum engineering. In some areas it is the only technique which will effect commercial production; even some carbonate formations which refuse to respond to multistage acid treatment will, subsequent to hydraulic fracture treatments, yield to commercial wells. There are some cases where hydraulic fracturing is beneficial:

1. If the reservoir is composed of a low-permeability, homogeneous rock, fracturing is similar in effect to increasing the size of the hole.

2. Fracturing will eliminate formation damage due to invasion of drilling mud, deposition of mineral matter, or swelling of clays. Since there is damage only in the immediate vicinity of the well bore, only a mild fracture treatment is required.

3. Fracture radiating from the well bore acts as a gathering line connecting permeable and porous systems that are otherwise isolated from the well by impermeable barriers.

4. Aid in secondary recovery operations. In the field of secondary recovery of oil, fracturing has played two important roles: a) it has increased the capacity of the water injection well to accept fluid at a predetermined

pressure, and b) it has produced high capacity flow channels into the producing well, thus increasing efficiency of the gas or water flooding project.

5. Assist in the injection disposal of brine and industrial waste material. The large volumes of salt water produced by some oil wells threatened to limit oil production severely. However, it was found that with the aid of fracturing, a low-pressure, high-fluid-injection capacity well could be established anywhere.

1.2.5 Flow Boundaries (Fluid Contacts)

A fluid contact may be defined as the surface separating zones in a reservoir which produce different fluids. Thus, the oil-water contact separates the zones which would produce oil from the zones which would produce water. An interface is considered to be the surface separating two different fluids within an individual pore in a reservoir.

In the majority of cases the original fluid contacts in oil and gas fields are so nearly level that no tilts may be detected. The production of fluids from a reservoir produces tilts in the originally level fluid contacts in the vicinity, and in some cases tilts are produced in a field before its discovery because of production from older fields in the same reservoir. These artificially produced tilts must be carefully distinguished from the natural tilts which were present before drilling, though distinction is sometimes very difficult to make.

Causes of Tilted Fluid Contacts

During the course of geologic time all fluid contacts would become level unless there was something to prevent this. Tilted fluid contacts may therefore be classified according to the factors which keep them from becoming level. Most of these factors are reviewed below:

1. Contacts Tilted by Moving Water or Oil: Fluid contacts become tilted by the moving liquid (oil and/or water) until there is no difference in the pressures of the two liquids on opposite sides of the fluid contact. A gas-oil contact above an oil-water contact tilted by moving water would be level. A gas-oil contact above an oil-water contact tilted by moving oil would have a dip opposite to that of the oil-water contact, but at a much lower angle.

2. Tilted and Irregular Fluid Contacts Produced by Capillarity: The capillary pressures for oil saturation occurring at oil-water contacts may indicate the maximum differences in elevation of an oil-water contact which could be supported by capillarity. It would be expected that fluid contacts would be uneven, but not tilted regularly in one direction. The fluid contacts tilted or made uneven by capillarity would be expected in very fine-grained reservoir rocks of relatively low permeability, where the capillary forces are relatively large.

3. Tilted Fluid Contacts Produced Artificially: The fluid pressures in the reservoir decrease toward the older field, and the fluid contacts are tilted toward the older field

before the discovery of the newer field. Similarly, the production of fluids from a field produces tilts in the fluid contacts in the same field. It is necessary to eliminate carefully all artificial effects in order to decide which contacts are tilted by natural causes.

4. Fluid Contacts Caused by Sealing Tilting: In a number of oil fields, zones in which the pores of the reservoir rock are filled with tar or asphalt occur between the oil and water zones. If folding occurred after the development of such a tar zone, and if the tar prevents the leveling of the folded oil-water contacts, the result would be a dip of the oil-water contacts away from the crest of the anticline.

1.2.6 Mixed Boundaries

Most important combined closures (mixed boundaries) are reviewed in the section which follows:

1. Unclosed Anticlines with Reservoir Terminating Updip: These traps are closed by stratigraphic or lithologic variations in the updip direction and by dips in all other directions. In other words the oil or gas reservoir (which has such closure) would be bounded up the dip by an impervious rock and in all other directions by edge water which lies down the dip.

The termination of the reservoir up the dip may lie due to the change from one type of rock to another, or it may be due to a change in the porosity or permeability of rock of the same type as the reservoir.

2. Bald-headed Domes: The term bald-headed is applied to domes and anticlines in which truncation of the structure has removed the reservoir rock from the crestal portion. Generally this type of structure is produced by two periods of uplift separated by an interval of erosion. Subsequent to the first period of folding, the anticline is truncated by erosion and the highest permeable part of the reservoir is removed. After this the whole anticline is covered with impervious sediment, forming a seal above, and the structure is folded with approximately the same axis as before. Oil and gas pools thus formed would tend to be circular or elliptical in shape. The reservoir would be bounded up the dip by an impervious rock and down the dip by water.

3. Accumulations in Reservoirs Truncated at Unconformities: If the truncation at an angular unconformity cuts out a permeable reservoir, a trap for oil and gas accumulation is produced if the termination is up the dip and if the strata overlying the unconformity makes a good seal. The boundaries are provided up the dip by the trunction, down the dip by the regional dip and in the other two directions by anticlinal noses, stratigraphic variations, or bending in the line of truncation.

4. Traps Associated with Buried Hills and Compaction: Where sedimentary rocks of low dip overlie buried hills of considerable topographic relief, the compaction of the sediments may produce traps suitable for oil and gas accumulation. As the

sediments become compacted due to the weight of the overlying formations, a series of gentle folds is produced, with the crests of the anticlines lying over the crests of the buried hills and synclines lying over the valleys. The shrinkage of volume is especially marked in shales and is much less in limestones and other compact sedimentary rocks. As a result anticlinal folds may form over buried limestone reefs and other lenticular deposits of hard rocks.

5. Lenticular and Sheet Reservoirs on Homoclines: Many permeable rocks are deposited in broad sheets or lenses which become impervious updip. If the reservoir is partly filled with water, a trap for oil and gas accumulation is formed at the updip termination of the reservoir. If there is no anticline to determine the particular part of the updip edge most likely to form the best trap. The site of the trap will be determined entirely by the homoclinal dip and by the stratigraphic variations.

6. Traps Above Angular Unconformities: Many oil gas fields are located on traps above angular unconformities. In some cases the oil may diginate in the strator above the unconformity and rise up the dip until the reservoir rock, through which it migrates, terminates against the unconformity. This condition is likely to arise when formations containing permeable members terminate against the unconformity by overlap, provided that the termination is up the dip.

Most of the traps associated with faults have mixed boundaries. These traps are reviewed in the Section titled

"Faults and Features."

Generally, oil and gas traps may have flow boundaries (oil- or gas-water contact), no flow boundaries (faults, unconformities, lithologic variations, etc.) or mixed (flow and no flow) boundaries. Most of the oil and gas traps have mixed boundaries.

1.2.7 Multiple Layers

The most distinctive feature of sedimentary rocks is the stratification or the arrangement in layers or beds. It arises from variations in color, texture, dimensions of particles, and composition, or to temporary cessation of deposition that permit already deposited sediments to undergo some changes before renewal of deposition. Stratification has been classified as direct, or primary, and indirect or secondary. The former is that made when the sediments are first deposited. Indirect stratification develops if sediments already deposited are thrown into suspension and redeposited. Stratification varies from very regular and even to the other extreme of highly irregular. The former is likely in sediements deposited in deep or very shallow quiet water; the latter in sediments deposited in agitated waters. Many strata show no internal stratification. This may be due to continuous deposition of a single variety of sediment, but, more likely, to reworking of sediments by burrowing and scavenger organisms.

Each stratification plane tends to be parallel to the surface upon which deposition takes place, and each stratification

plane in turn becomes a surface of deposition. In a longer sequence of strata there is likely to be considerable divergence from parallelism of the stratification planes at the bottom and at the top. Initial surface of deposition are necessarily horizontal, and existing surfaces upon which deposition is taking place are undulatory and contain basins and elevation of divergent dimensions.

Dimensions of sedimentary units vary with the environments of deposition and the supply and character of composing sediments. Coarse-grained sediments, large loads, and conditions producing rapid decrease in competency for great variation in thickness and limited areal distribution. Fine-grained sediments tend to have fairly wide areal distribution and somewhat uniform thicknesses.

Deposits of alluvial fans and cones and flood plains, channels and deltas of rivers are likely to show much variation in thickness and areal extent of sedimentary units over very short distances. Sedimentary units deposited in the litteral environment and on the adjacent shallow water bottom have great dimensional variation. A unit may extend for many miles along a coast and on other parts of the same coast while another unit may extend for only a few meters.

1.2.8 Interbedding of Shale Breaks and Silt Lamination

The particles of clays and silts are commonly transported in suspension, and the particles are so small that they are effectively cushioned in both air and water against abrasion, so

that shapes are largely those of solution, decomposition, and fracture. Deposition takes place after the competences of the transporting agents have decreased to a low value. Clays and silts tend to be separated from the coarse and medium elastics with which once they may have been transported in the same currents. They may be deposited above coarse elastics of preceding currents and become overlaid by coarse elastics of succeeding currents. In many oil and gas pools, the reservoir rocks are interbedded by shale breaks and silt lamination. Knowing that shales and silts are impermeable rocks, many of the reservoir rocks, thus, consist of permeable strata separated by impermeable layers of shales of silts. In such cases, no cross-flow is dominant.

1.3. Problem Statement

Although we have been producing oil from reservoirs for over one hundred years, we still are inadequately informed about the reservoir rock itself. For a few locations in a reservoir, we know the mineral composition of the rock. Beyond this point, our real knowledge becomes sparse.

The heterogeneity of the reservoir rock, if unaccounted for, is always a detriment to any flooding process, even when the process has a favorable mobility ratio. As with any kind of fluid displacement process, large variations in the permeability of a reservoir causes poor coverage by the injected fluids. This problem can be disastrous to a miscible flood process. Where there is cross-flow between the zones of

differing permeability, transverse dispersion causes early deterioration of the slug and loss of miscibility. Where there is no cross-flow, high permeability zones tend to take a disproportionately large portion of the total slug injected. This leaves insufficient slug material to displace the oil in the less permeable zones and causes early loss of miscibility in these zones.

Linear discontinuities such as fault, sudden change in formation characteristics (including porosity, permeability, . . . etc.) and fluid contacts must be accounted for in the selection of flooding pattern.

Thus, the development of improved methods for predicting fluid flow in heterogeneous reservoirs is of vital interest in oil reservoir engineering and ground-water hydrology.

1.4 Objectives of Study

The purpose of this study is to obtain a set of expressions and procedures that can be used to determine the reservoir characteristics from both pressure drawdown and buildup data for a well located in the center of composite layered reservoir. Equations were derived to express dimensionless pressure and time terms for both drawdown and buildup cases. Those equations were used to generate type curve plots for two-layered composite reservoir for pressure drawdown and buildup analysis. A proposed type curve matching technique was discussed.

Also, a mathematical approach to predict water flooding

performance for linear composite layered reservoirs was presented. Two important cases, constant injection pressure and constant injection rate, were considered.

1.5 Organization of Study

Chapter Two presents an approximate solution to the problem of single phase flow through multilayered composite reservoir. Both dimensionless time and dimensionless pressure behavior for a single well located in the center of the reservoir were presented. Details of the mathematical treatment are presented in Appendices A and B. Chapter Three deals in details with the case of two-layer composite reservoirs. Type curves are generated and discussed in that chapter. Chapter Four discusses pressure buildup analysis for the model considered in Chapter Two.

Chapter Five discusses a technique to predict water flooding performance for multilayered composite systems. The general conclusions reached by this study are presented in Chapter Six.

CHAPTER 2

AN APPROXIMATE SOLUTION FOR UNSTEADY STATE SINGLE PHASE FLOW IN LAYERED COMPOSITE RESERVOIRS

2.1 Basic Flow Equation

The pressure transient analysis techniques presented in this study are based on the diffusivity equation describing the fluid flow through porous media. The diffusivity equation is generally written in cylindrical coordinates as:

$$\frac{1}{r}\frac{\partial}{r}\left(r\frac{\partial P}{\partial r}\right) = \frac{1}{\eta}\frac{\partial P}{\partial t} \qquad 2.1\ *$$

This equation is obtained by the combination of the material balance equation and Darcy's flow equation. The assumptions implicit in the use of the diffusivity equation are as follows:

1. The porous medium is isotropic, horizontal, incompressible, homogeneous, uniform in thickness, and has constant permeability and porosity.

2. A single-phase fluid is present and occupies the entire volume.

---

*See Nomenclature.

3. Viscosity and compressibility of the fluid remain constant at all pressures.

4. The well completely penetrates the formation, and gravity forces are negligible.

5. Isothermal conditions prevail.

6. The fluid flow in the porous media is laminar.

7. The pressure gradient is small.

8. Fluid density is governed by the equation:

$$\rho = \rho_0 \quad e^{c(P-P_0)} \qquad 2.2$$

where ρ_0: fluid density at some reference pressure P_0.

c : fluid compressibility.

2.2 Reservoir Model

The reservoir model used in this study is a composite-layered infinite system, as shown in Figure 2.1. The reservoir is divided vertically into n layers, and there is no communication between them except at the well bore. The reservoir is overlaid and underlaid by impermeable layers. Each layer of the reservoir consists of two regions. Region 1 has radius a_j which varies from layer to layer and region 2 extends from a_j to infinity. The rock and fluid properties vary from layer to layer and from region to region. The reservoir is initially at a uniform pressure P_i. All the layers are penetrated at the center of region 1 by a single well producing at a constant flow rate. The pressures in all

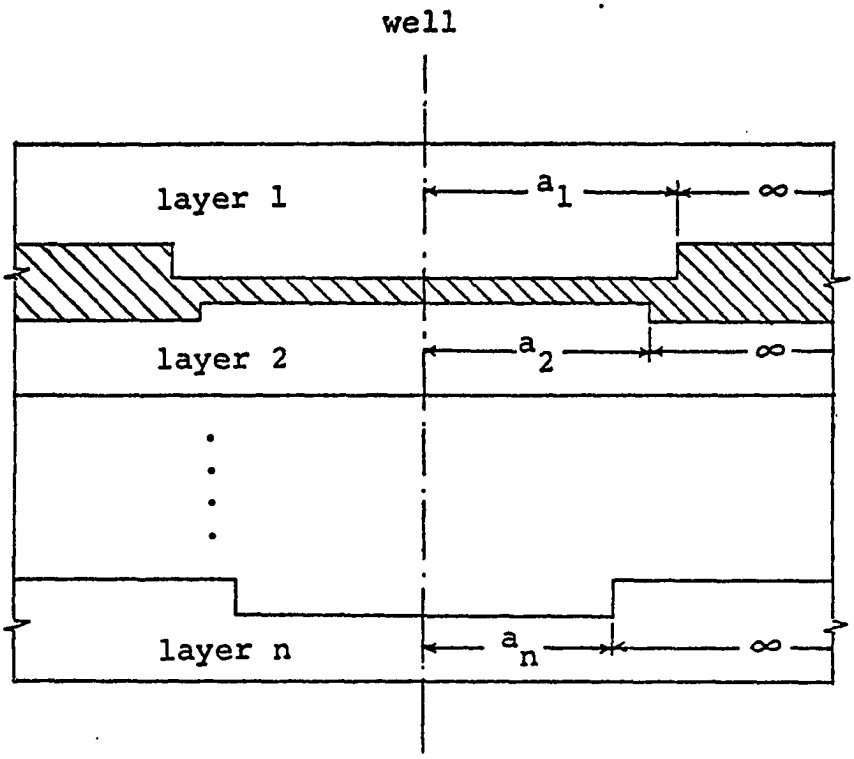

(a)

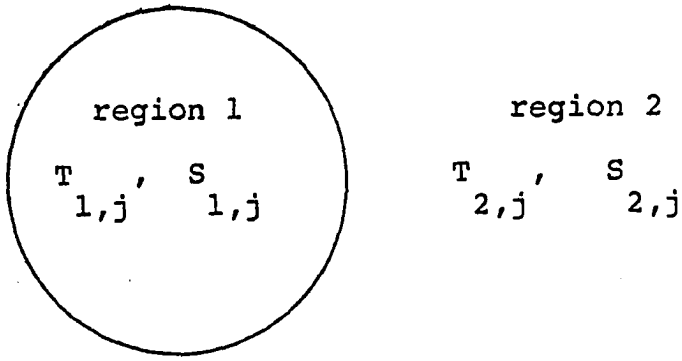

(b)

Figure 2.1 : (a) Layered composite reservoir
(b) Radial changes of reservoir characteristics of jth layer

layers at the well bore are equal. All the assumptions followed in Equation 2.1 hold for any particular region in a particular layer.

The diffusivity equations for the above-mentioned system is given as:

$$\frac{1}{r}\frac{\partial}{\partial r}\left(r\frac{\partial P_{1,j}}{\partial r}\right)=\frac{1}{\eta_{1,j}}\frac{\partial P_{1,j}}{\partial t}\ ,$$

$$0 \leq r \leq a_j\ ,\quad j = 1, 2, \ldots n \qquad 2.3$$

$$\frac{1}{r}\frac{\partial}{\partial r}\left(r\frac{\partial P_{2,j}}{\partial r}\right)=\frac{1}{\eta_{2,j}}\frac{\partial P_{2,j}}{\partial t}\ ,$$

$$a_j \leq r \leq \infty\ ,\quad j = 1, 2, \ldots n \qquad 2.4$$

The initial and boundary conditions for the system understudy are:

a. Inner boundary conditions:

$$\lim_{r \to 0} r\frac{\partial P_{1,j}}{\partial r}=\frac{q_j}{2\pi T_{1,j}}\ ,$$

$$t > 0,\ j = 1, 2, \ldots n \qquad 2.5$$

b. Interface conditions:

$$P_{i,j} = P_{2,j}\ ,\ r = a_j\ ,\ t > 0,\ j = 1,2, \ldots n \qquad 2.6$$

Since there is no accumulation at the interface;

$$q_j = r\, T_{1,j} \frac{\partial P_{1,j}}{\partial r} = r\, T_{2,j} \frac{\partial P_{2,j}}{\partial r} ,$$

$$r = a_j,\ t \geq 0,\ j = 1,2,\ldots n \qquad 2.7$$

c. Outer boundary conditions:

$$\lim_{r \to \infty} P_{2,j} = P_i ,$$

$$t \geq 0,\quad j = 1,2,\ldots n \qquad 2.8$$

d. Initial conditions:

$$P_{1,j} = P_{2,j} = P_i,\ t = 0,\ j = 1,2,\ldots n \qquad 2.9$$

2.3 Drawdown Dimensionless Pressure Term

Using Boltzman transform in the form:

$$Z = \frac{r^2}{4\, \eta_{1,1} t} \qquad 2.10$$

Equations 2.3 and 2.4 can be transformed into:

$$Z\frac{d^2 P_{1,j}}{d^2 Z} + \left(1 + Z\frac{\eta_{1,1}}{\eta_{1,j}}\right) \frac{dP_{1,j}}{dZ} = 0,$$

$$0 \leq r \leq a_j,\ j = 1,2,\ldots n \qquad 2.11$$

and

$$Z\frac{d^2 P_{2,j}}{d^2 Z} + \left(1 + Z\frac{\eta_{1,1}}{\eta_{2,1}}\right) \frac{dP_{2,j}}{dZ} = 0,$$

$$a_j \leq r \leq \infty,\ j = 1,2,\ldots n \qquad 2.12$$

Equations 2.11 and 2.12 are linear ordinary differential equations. Their solutions are readily given by Ramey (1970) as:

$$P_{1,j} = C_j Ei(-Z\frac{\eta_{1,1}}{\eta_{1,j}}) + D_j,$$

$$j = 1,2,. \; . \; . \; n \qquad 2.13$$

$$P_{2,j} = F_j Ei(-Z\frac{\eta_{1,1}}{\eta_{2,1}}) + G_j,$$

$$j = 1,2,. \; . \; . \; n \qquad 2.14$$

Using initial and boundary conditions defined by Equations 2.5 through 2.9, C_j, D_j, F_j and G_j are obtained.

The following transforms are used:

$$\eta = \frac{T}{S}$$

$$r = r_D r_W$$

$$f_j = \frac{q_j}{Q}$$

$$a_j = r_{D\,aj} \cdot r_W$$

$$Z = \frac{r^2}{4t}\frac{S}{T}$$

Applying the superposition technique in time to take into account flow rate* variations in layer j, the pressure

*The oil production rate "at the well."

distribution in region one of layer j is given as:

$$P_{1,j}(r,t) = P_i + \frac{Q}{4\pi}\left[\sum_{i=1}^{N} (f_{j,i}-f_{j,i-1})R_j(t_N-t_{i-1})\right],$$

$$0 < r \leq a_j,\ j = 1,2,\ldots n \qquad 2.15$$

where

$$R_j(t-t_{i-1}) = \frac{1}{T_{1,j}}\left[Ei\left(\frac{-r_D^2 r_W^2}{4(t-t_{i-1})}\frac{S_{1,j}}{T_{1,j}}\right) - Ei\left(\frac{-r_{D\,aj}^2 r_W^2}{4(t-t_{i-1})}\frac{S_{1,j}}{T_{1,j}}\right)\right]$$

$$+ \frac{1}{T_{2,j}} e^{\frac{-r_{D\,aj}^2 r_W^2}{4(t-t_{i-1})}\left(\frac{S_{1,j}}{T_{1,j}} - \frac{S_{2,j}}{T_{2,j}}\right)} Ei\left(\frac{-r_{D\,aj}^2 r_W^2}{4(t-t_{i-1})}\frac{S_{2,j}}{T_{2,j}}\right) \qquad 2.16$$

$f_{j,i}$ & $f_{j,i-1}$ are fractional flow rates from layer j at time levels i & i-1 respectively.

Similarly, the pressure distribution in region two of layer j is given as:

$$P_{2,j}(r,t) = P_i + \frac{Q}{4\pi}\left[\sum_{i=1}^{N} (f_{j,i}-f_{j,i-1})\ V_j(t-t_{i-1}),\right.$$

$$a_j \leq r_j \leq \infty\ ,\ j = 1,2,\ldots\ n \qquad 2.17$$

where

$$V_j(t-t_{i-1}) = \frac{1}{T_{2,j}} \; e^{\frac{-r_{D\,aj}^2 r_W^2}{4(t-t_{i-1})} \left(\frac{S_{1,j}}{T_{2,j}}\right)} \; Ei\left(\frac{-r_D^2 r_W^2}{4(t-t_{i-1})} \frac{S_{2,j}}{T_{2,j}}\right) \quad 2.18$$

Neglecting gravity effects, the pressure at the well bore is the same for all layers and equals to P_W. Thus Equation 2.15 can be written as:

$$\frac{4\pi\,(P_i - P_W)}{Q} = -\sum_{i-1}^{N} (f_{j,i} - f_{j,i-1})\; R_j(t-t_{i-1}),$$

$$j = 1,2,\ldots \text{or } n \qquad 2.19$$

where R_j is expressed by Equation 2.16 with $R_D = 1$.

Multiplying both sides of Equation 2.19 by the system transmissibility (T_S) yields an expression for P_{Dw} term as:

$$P_{Dw} = -\sum_{i=1}^{N} (f_{j,i} - f_{j,i-1})\; T_S(t-t_{i-1})\; R_j(t-t_{i-1}) \quad 2.20$$

where T_S: system transmissibility to be expressed in next section.

Detailed derivation of Equation 2.20 starting with Equation 2.3 is presented in Appendix A.

A material balance about the well bore gives

$$f_{1,i} + f_{2,i} + \ldots + f_{n,i} = 1 \qquad 2.21$$

Keeping in mind that at any point of time the left hand side of Equation 2.19 is the same for all layers, Equations 2.19 and 2.21 represent n equations in n unknowns. These equations can be solved for fractional flow rates from different layers. The reader is referred, for more details, to Appendix A. Knowing the fractional flow rates, Equations 2.15, 2.16 and 2.20 can be used to describe pressure behavior in the system.

2.4 Drawdown Dimensionless Time Term

For a well located in the center of composite-layered reservoir, t_D term can be expressed by:

$$t_{Dw} = \frac{t}{r_w^2} \cdot \frac{T_s}{S_s} \qquad 2.22$$

Where T_s and S_s are the transmissibility and the storage of the system under study respectively. They are expressed as:

$$T_s = \frac{\sum_{j=1}^{n} T_j \, r_{D\,invj}^2}{\sum_{j=1}^{n} r_{D\,invj}^2} \qquad 2.23$$

$$S_s = \frac{\sum_{j=1}^{n} S_j \, r^2_{D\,invj}}{\sum_{j=1}^{n} r^2_{D\,invj}} \qquad 2.24$$

where: a. $t \leq t_{aj}$

$$T_j = T_{1,j} \qquad 2.25$$

$$S_j = S_{1,j} \qquad 2.26$$

$$r^2_{D\,invj} = \frac{4}{r_w^2} \frac{T_{1,j}}{S_{1,j}} t \qquad 2.27$$

b. $t \geq t_{aj}$

$$T_j = \frac{T_{i,j} \, r^2_{D\,aj} + T_{2,j}(r^2_{D\,invj} - r^2_{D\,aj})}{r^2_{D\,invj}} \qquad 2.28$$

$$S_j = \frac{S_{1,j} \, r^2_{D\,aj} + S_{2,j}(r^2_{D\,invj} - r^2_{D\,aj})}{r^2_{D\,invj}} \qquad 2.29$$

$$r_{D\,invj} = r_{D\,aj} + \frac{2}{r_w} \left(\frac{T_{2,j}}{S_{2,j}}\right)^{0.5} (t-t_{aj})^{0.5} \qquad 2.30$$

$$t_{aj} = \frac{r_{D\,aj}^2 \cdot r_w^2}{4} \frac{S_{1,j}}{T_{1,j}} \quad , \; j = 1,2,\ldots n \qquad 2.31$$

Substituting Equations 2.24 and 2.25 into Equation 2.23 yields:

$$t_{Dw} = \frac{t}{r_w^2} \cdot \frac{\sum_{j=1}^{n} T_j \, r_{D\,inv\,j}^2}{\sum_{j=1}^{n} S_j \, r_{D\,inv\,j}^2} \qquad 2.32$$

Theoretical background and detailed derivation of Equations 2.23, 2.24 and 2.32 are presented in Appendix B of this dissertation.

Thus this chapter presents an approximate solution, using line source solution, for the problem of slightly compressible fluid flow in layered composite reservoirs. The solution can be used to predict pressure at any point of reservoir. Equation 2.20 is used to generate type curves, for two-layer two-region system, which can be used to predict reservoir characteristics and dimensions. The theoretical treatment presented in this chapter can be easily extended to multilayer multiregion systems.

CHAPTER 3

DRAWDOWN DIMENSIONLESS PRESSURE BEHAVIOR IN TWO-LAYER COMPOSITE RESERVOIRS

3.1 Introduction

Chapter Two and Appendices A and B of this study present a theoretical analysis of a multi-layered composite reservoir. Mathematical expressions for drawdown dimensionless pressure and time terms were derived. A proposed technique to calculate fractional flow rates from each layer was briefly discussed.

In this chapter, the unsteady state solution presented in the previous chapter is applied for two-layer composite reservoir to obtain expressions for drawdown dimensionless pressure and time terms. These expressions are used to develop type curves that are necessary to analyze both drawdown and buildup data.

In the present study, the properties (transmissibility, storage and width) of all layers and regions are related (by correlating factors) to the properties of the first region of the top layer. The following transforms are introduced:

$$T_{1,1} = T$$

$$S_{1,1} = S$$

$$T_{2,1} = x_1 T$$

$$T_{1,2} = x_2 T$$

$$T_{2,2} = x_3 T$$

$$S_{2,1} = y_1 S$$

$$S_{1,2} = y_2 S$$

$$S_{2,2} = y_3 S$$

$$a_2 = z\, a_1$$

$$r_{Da2}^2 = z^2\, r_{Da1}^2$$

where x_1 to x_3, y_1 to y_3 and z are correlating factors that correlate the properties and dimension of each homogeneous block of the system to those of the reference block (first region of the top layer).

3.2 Transmissibility and Storage of Two-Layer Two-Region System

Dimensionless pressure and time terms are presented in this section as follows:

Equation 2.24 can be written for two-layer system as:

$$T_s = \frac{T_1\, r_{D\,inv1}^2 + T_2\, r_{D\,inv2}^2}{r_{D\,inv1}^2 + r_{D\,inv2}^2} \qquad 3.1$$

Also S_s term can be expressed using Equation 2.25 as:

$$S_s = \frac{S_1\, r_{D\,inv1}^2 + S_2\, r_{D\,inv2}^2}{r_{D\,inv1}^2 + r_{D\,inv2}^2} \qquad 3.2$$

where Equations 2.26 and 2.27 or Equations 2.29 and 2.30, depending on time, are used to express transmissibility and storage for each layer. In this situation, four possibilities arise. They are considered below.

3.2.1 $t \leq t_{a1}$ and $t \leq t_{a2}$

Where the time is less than both times of radii of investigation arrivals to the end of region one in both layers, transmissibilities and storages are given as:

$$T_1 = T \quad , \quad T_2 = x_2 T$$
$$S_1 = S \quad , \quad S_2 = y_2 S \qquad 3.3$$

Substituting Equation 3.3 into Equations 3.1 and 3.2 yields:

$$T_s = \frac{r_{D\,inv1}^2 + x_2\, r_{D\,inv2}^2}{r_{D\,inv1}^2 + r_{D\,inv2}^2}\, T \qquad 3.4$$

$$S_s = \frac{r_{D\,inv1}^2 + y_2\, r_{D\,inv2}^2}{r_{D\,inv1}^2 + r_{D\,inv2}^2}\, S \qquad 3.5$$

Where $r_{D\,inv1}$ and $r_{D\,inv2}$ are expressed by Equation 2.28.

3.2.2 $t \leq t_{a1}$ and $t \geq t_{a2}$

This represents the case where the time less than the time at which $r_{inv1} = a_1$ and greater than that at which $r_{inv2} = a_2$. In this case, storages and transmissibilities are given as:

$$T_1 = T \qquad 3.6$$

$$T_2 = \frac{x_2 z^2\, r_{Da1}^2 + x_3 (r_{D\,inv2}^2 - z^2 r_{Da1}^2)}{r_{D\,inv2}^2} \qquad 3.7$$

$$S_1 = S \tag{3.8}$$

$$S_2 = \frac{y_2 z^2 r_{Da1}^2 + y_3 (r_{D\,inv2}^2 - z^2 r_{Da1}^2)}{r_{D\,inv2}^2} S \tag{3.9}$$

Substituting Equations 3.6 and 3.7 into Equation 3.1 gives:

$$T_s = \frac{r_{D\,inv1}^2 + x_2 z^2 r_{Da1}^2 + x_3 (r_{D\,inv2}^2 - z^2 r_{Da1}^2)}{r_{D\,inv1}^2 + r_{D\,inv2}^2} T \tag{3.10}$$

From Equations 3.2, 3.8 and 3.9, S_s is expressed as:

$$S_s = \frac{r_{D\,inv1}^2 + y_2 z^2 r_{Da1}^2 + y_3 (r_{D\,inv2}^2 - z^2 r_{Da1}^2)}{r_{D\,inv1}^2 + r_{D\,inv2}^2} S \tag{3.11}$$

Where $r_{D\,inv1}$ is expressed by Equation 2.28 and

$r_{D\,inv2}$ is expressed by Equation 2.31.

3.2.3 $t \geq t_{a1}$ and $t \leq t_{a2}$:

In this case, transmissibilities and storages for both layers are epxressed as:

$$T_1 = \frac{r_{Da1}^2 + x_1 (r_{D\,inv1}^2 - r_{Da1}^2)}{r_{D\,inv1}^2} T \tag{3.12}$$

$$T_2 = x_2 T \tag{3.13}$$

$$S_1 = \frac{r_{Da1}^2 + y_1 (r_{D\,inv1}^2 - r_{Da1}^2)}{r_{D\,inv1}^2} S \tag{3.14}$$

$$S_2 = y_2 S \tag{3.15}$$

Substituting Equations 3.12 and 3.13 into Equation 3.1 gives:

$$T_s = \frac{r_{Da1}^2 + x_1(r_{D\,inv1}^2 - r_{Da1}^2) + x_2\, r_{D\,inv2}^2}{r_{D\,inv1}^2 + r_{D\,inv2}^2}\, T \tag{3.16}$$

Substituting Equations 3.14 and 3.15 into Equation 3.2 yields:

$$S_s = \frac{r_{Da1}^2 + y_1(r_{D\,inv1}^2 - r_{Da1}^2) + y_2\, r_{D\,inv2}^2}{r_{D\,inv1}^2 + r_{D\,inv2}^2}\, S \tag{3.17}$$

Where $r_{D\,inv1}$ and $r_{D\,inv2}$ are given by Equations 2.31 and 2.28 respectively.

3.2.4 $t \geq t_{a1}$ and $t \geq t_{a2}$

Transmissibilities and storages for both layers are given as:

$$T_1 = \frac{r_{Da1}^2 + x_1(r_{D\,inv1}^2 - r_{Da1}^2)}{r_{D\,inv1}^2}\, T \tag{3.18}$$

$$T_2 = \frac{x_2 z^2 r_{Da1}^2 + x_3(r_{D\,inv2}^2 - z^2 r_{Da1}^2)}{r_{D\,inv2}^2}\, T \tag{3.19}$$

$$S_1 = \frac{r_{Da1}^2 + y_1(r_{D\,inv1}^2 - r_{Da1}^2)}{r_{D\,inv1}^2}\, S \tag{3.20}$$

$$S_2 = \frac{y_2 z^2 r_{Dal}^2 + y_3 (r_{D\,inv2}^2 - z^2 r_{Dal}^2)}{r_{D\,inv2}^2} S \qquad 3.21$$

Substituting Equations 3.18 and 3.19 into Equation 3.1 yields:

$$T_s = \frac{r_{Dal}^2 (1+x_2 z^2) + x_1 (r_{D\,inv1}^2 - r_{Dal}^2) + x_3 (r_{D\,inv2}^2 - z^2 r_{Dal}^2)}{r_{D\,inv1}^2 + r_{D\,inv2}^2} T \qquad 3.22$$

Similarly, substituting Equations 3.20 and 3.21 in Equation 3.2 results in an expression for S_s as:

$$S_s = \frac{r_{Dal}^2 (1+y_2 z^2) + y_1 (r_{D\,inv1}^2 - r_{Dal}^2) + y_3 (r_{D\,inv2}^2 - z^2 r_{Dal}^2)}{r_{D\,inv1}^2 + r_{D\,inv2}^2} S \qquad 3.23$$

Where $r_{D\,inv1}$ and $r_{D\,inv2}$ are radii of investigations in layers one and two respectively.

3.3 Fractional Flow Rates

The flow rate from a particular layer of the two-layer two-region system varies with time. The line source solution used in this study is based on the assumption that the flow rate is constant. Thus superposition in time should be used to account for the variations in the flow rates.

As mentioned in Chapter Two, Equations 2.19 and 2.21 can be solved to determine the fractional flow rate from each layer of the system. This is applied for two-layer composite systems as follows:

Equation 2.19 can be written for the two-layer system as:

$$\frac{4\pi(P_i-P_w)}{Q} = -\sum_{i=1}^{N}\left[(f_{1,i}-f_{1,i-1})\ R_1(t-t_{i-1})\right]$$

$$= -\sum_{i=1}^{N}\left[(f_{2,i}-f_{2,i-1})\ R_2(t-t_{i-1})\right]$$

Then

$$\sum_{i=1}^{N}\left[(f_{1,i}-f_{1,i-1})\ R_1(t-t_{i-1})\right] = \sum_{i=1}^{N}\left[(f_{2,i}-f_{2,i-1})R_2(t-t_{i-1})\right] \qquad 3.24$$

Also, at any particular time level i;

$$f_{1,i} + f_{2,i} = 1. \qquad 3.25$$

In this work, the calculations were made at progressive time steps. The time at $i^{\underline{th}}$ level is calculated as:

$$t_i = \sum_{j=1}^{i} \Delta t_j \qquad 3.26$$

Where Δt_j is time interval at $j^{\underline{th}}$ level.

At N = 1, Equation 3.24 can be written as

$$(f_{1,1}-f_{1,0})\ R_1(t_1-t_0) = (f_{2,1}-f_{2,0})\ R_2(t-t_0)$$

but $t_0 = f_{1,0} = f_{2,0} = 0$

Then;

$$f_{1,1}\, R_1(t_1) = f_{2,1}\, R_2(t_1) \qquad 3.27$$

Where t_1 is the time at first time level (N = 1). Solving Equations 3.25 and 3.27 for $f_{1,1}$ and $f_{2,1}$ yields:

$$f_{1,1} = \frac{R_2(t_1)}{R_1(t_1) + R_2(t_1)} \qquad 3.28$$

$$\text{and } f_{2,1} = 1 - f_{1,1} = \frac{R_1(t_1)}{R_1(t_1) + R_2(t_2)} \qquad 3.29$$

At N = 2, Equation 3.24 can be written as:

$$f_{1,1}R_1(t_2) + (f_{1,2}-f_{1,1})R_1(t_2-t_1)$$

$$= f_{2,1}R_2(t_2) + (f_{2,2}-f_{2,1})\, R_2(t_2-t_1)$$

Substituting, $f_{2,2} = 1 - f_{1,2}$, in the above equation and solving for $f_{1,2}$ yields:

$$f_{1,2} = \frac{R_2(t_2-t_1)+f_{2,1}[R_2(t_2)-R_2(t_2-t_1)]-f_{1,1}[R_1(t_2)-R_1(t_2-t_1)]}{R_1(t_2-t_1) + R_2(t_2-t_1)} \qquad 3.30$$

Thus $f_{2,2}$ is given as:

$$f_{2,2} = \frac{R_1(t_2-t_1)-[f_{2,1}\, R_2(t_2)-R_2(t_2-t_1) -f_1\, R_1(t_2)-R_1(t_2-t_1)\ ]}{R_1(t_2-t_1) + R_2(t_2-t_1)} \qquad 3.31$$

Similarly, at N = 3, $f_{1,3}$ and $f_{2,3}$ can be expressed as:

$$f_{1,3}=\{f_{2,1}[R_2(t_3)-R_2(t_3-t_1)]+f_{2,2}[R_2(t_3-t_1)-R_2(t_3-t_2)] + R_2(t_3-t_2)-f_{1,1}[R_1(t_3)-R_1(t_3-t_1)]-f_{1,2}[R_1(t_3-t_1)-R_1(t_3-t_2)]\} \div [R_1(t_3-t_2)+R_2(t_3-t_2)] \quad 3.32$$

$$f_{2,3} = 1 - f_{1,3} = \{-f_{2,1}[R_2(t_3)-R_2(t_3-t_1)]-f_{2,2}[R_2(t_3-t_1)-R_2(t_3-t_2)] + R_1(t_3-t_2)+f_{1,1}[R_1(t_3)-R_1(t_3-t_1)]+f_{1,2}[R_1(t_3-t_1)-R_1(t_3-t_2)]\} \div [R_1(t_3-t_2)+R_2(t_3-t_2)] \quad 3.33$$

Generally, at any time t which corresponds to time level N, the fractional flow rates from layer one and layer two are expressed as:

$$f_{1,N} = \frac{R_2(t-t_{N-1}) + \sum_{k=0}^{N-1} \sum_{\ell=1}^{2} \{(-1)^{\ell} f_{\ell,k}[R_\ell(t-t_{k-1})-R_\ell(t-t_k)]\}}{R_1(t-t_{N-1}) + R_2(t-t_{N-1})} \quad 3.34$$

$$f_{2,N} = \frac{R_1(t-t_{N-1}) - \sum_{k=0}^{N-1} \sum_{\ell=1}^{2} (-1)^{\ell} f_{\ell,k}[R_\ell(t-t_{k-1})-R_\ell(t-t_k)]}{R_1(t-t_{N-1}) + R_2(t-t_{N-1})} \quad 3.35$$

In Equations 3.24 through 3.35, R terms are evaluated using Equation 2.20.

Using the transforms listed in Section 3.1, Equation 2.16 is written for layer one and layer two as:

$$R_1(t-t_{i-1})=\frac{1}{T}\left\{Ei\left(\frac{-r_w^2}{4(t-t_{i-1})}\frac{S}{T}\right) - Ei\left(\frac{-r_{Dal}^2 r_w^2}{4(t-t_{i-1})}\cdot\frac{S}{T}\right)\right.$$

$$\left. + \frac{1}{x_1}\, e^{\frac{-r_{Dal}^2 r_w^2}{4(t-t_{i-1})}\frac{S}{T}\left(\frac{x_1-y_1}{x_1}\right)}\, Ei\left(\frac{-r_{Dal}^2 r_w^2}{4(t-t_{i-1})}\frac{S}{T}\cdot\frac{y_1}{x_1}\right)\right\} \qquad 3.36$$

$$R_2(t-t_{i-1})=\frac{1}{T}\left\{\frac{1}{x_2}\left[Ei\left(\frac{-r_w^2}{4(t-t_{i-1})}\frac{S}{T}\frac{y_2}{x_2}\right) - Ei\left(\frac{-z^2 r_{Dal}^2 r_w^2}{4(t-t_{i-1})}\frac{S}{T}\cdot\frac{y_2}{x_2}\right)\right]\right.$$

$$\left. + \frac{1}{x_3}\, e^{\frac{-z^2 r_{Dal}^2 r_w^2}{4(t-t_{i-1})}\frac{S}{T}\left(\frac{y_2}{x_2}-\frac{y_3}{x_3}\right)}\, Ei\left(\frac{-z^2 r_{Dal}^2 r_w^2}{4(t-t_{i-1})}\frac{S}{T}\frac{y_3}{x_3}\right)\right\} \qquad 3.37$$

Equations 3.34 and 3.35 are explicit expressions to calculate the fractional flow rates from each layer at any time level N. At N = 1, the summation term is canceled and Equations 3.28 and 3.29 are obtained.

Equation 3.34 is used to calculate the fractional flow rates from layer 1 of several different systems. The results are presented in semilog plots (f_1 versus t_{Dw}). These results are discussed in Section 3.6.

3.4 Dimensionless Drawdown Pressure and Time Terms

The pressure distribution in two-layered composite reservoir is obtained from Equations 2.15 through 2.18 and from the transforms listed in Section 3.1. The pressure distribution in the reference block is given as:

$$P_{1,1}(r,t) = P_i + \frac{Q}{4\pi T} \sum_{i=1}^{N} [(f_{1,i}-f_{1,i-1}) \cdot$$

$$\{Ei(\frac{r^2}{4(t-t_{i-1})} \frac{S}{T}) - Ei(\frac{-r_{Da1}^2 r_w^2}{4(t-t_{i-1})} \frac{S}{T}) +$$

$$\frac{1}{x_1} e^{\frac{-r_{Da1}^2 r_w^2}{4(t-t_{i-1})} \frac{S}{T} (\frac{x_1-y_1}{x_1})} Ei(\frac{-r_{Da1}^2 r_w^2}{4(t-t_{i-1})} \frac{S}{T} \frac{y_1}{x_1}) \}],$$

$$r \leq a_1 \qquad 3.38$$

The pressure distribution in the second region of layer 1 is given as:

$$P_{2,1}(r,t) = P_i + \frac{Q}{4\pi T x_1} \sum_{i=1}^{N} [(f_{1,i} - f_{1,i-1}) \cdot$$

$$e^{\frac{-r_{Da1}^2 r_w^2}{4(t-t_i)} \frac{S}{T} (\frac{x_1-y_1}{x_1})} \cdot Ei(\frac{-r^2}{4(t-t_{i-1})} \frac{S}{T} \frac{y_1}{x_1})],$$

$$r \geq a_1 \qquad 3.39$$

The pressure distribution in region 1 of layer 2 is given as:

$$P_{1,2}(r,t) = P_i + \frac{Q}{4\pi T} \sum_{i=1}^{N} [(f_{2,i} - f_{2,i-1}) \cdot$$

$$\{ \frac{1}{x_2}[Ei(\frac{-r^2}{4(t-t_{i-1})} \frac{S}{T} \frac{y_2}{x_2}) - Ei(\frac{-z^2 r_{Da1}^2 r_w^2}{4(t-t_{i-1})} \frac{S}{T} \cdot \frac{y_2}{x_2})]$$

$$+ \frac{1}{x_3} e^{\frac{-z^2 r_{Da1}^2 r_w^2}{4(t-t_{i-1})} \frac{S}{T}(\frac{y_2}{x_2} - \frac{y_3}{x_3})} Ei(\frac{-z^2 r_{Da1}^2 r_w^2}{4(t-t_{i-1})} \frac{S}{T} \frac{y_3}{x_3}) \}],$$

$$r \leq z\ a_1 \qquad 3.40$$

and the pressure distribution in region 2 of layer 2 is given as:

$$P_{2,2}(r,t) = P_i + \frac{Q}{4\pi T x_3} \sum_{i=1}^{N} [(f_{1,i} - f_{1,i-1}) \cdot$$

$$e^{\frac{-z^2 r_{Da1}^2 r_w^2}{4(t-t_{i-1})} \frac{S}{T}(\frac{y_2}{x_2} - \frac{y_3}{x_3})} Ei(\frac{r^2}{4(t-t_{1-i})} \frac{S}{T} \frac{y_3}{x_3})] ,$$

$$r \geq z\ a_1 \qquad 3.41$$

Thus the pressure any where in a two-layer composite reservoir can be evaluated using Equations 3.38 through 3.41. It is

well known that the pressure distribution is very important for solving many reservoir engineering problems especially the uses of material balance equations (MBE).

Equations 2.21 and 2.23 express respectively the dimensionless pressure drawdown and time terms for multi-layered composite systems. The well bore dimensionless pressure term, P_{Dw}, for two-layer composite system is obtained by using Equation 2.21 in terms of layer 1 characteristics as:

$$P_{Dw} = - \sum_{i=1}^{N} (f_{1,i}-f_{1,i-1}).T_s(t-t_{i-1}).R_1(t-t_{i-1}) \qquad 3.42$$

Substituting Equation 3.36 into Equation 3.42 yields:

$$P_{Dw} = \frac{-1}{T} \sum_{i=1}^{N} \{(f_{1,i}-f_{1,i-1}).T_s(t-t_{i-1}).[Ei(\frac{-r_w^2}{4(t-t_{i-1})} \frac{S}{T}) - Ei(\frac{-r_{Da1}^2 r_w^2}{4(t-t_{i-1})} \frac{S}{T}) + \frac{1}{x_1} e^{\frac{-r_{Da1}^2 r_w^2}{4(t-t_{i-1})} \frac{S}{T}(\frac{x_1-y_1}{x_1})} Ei(\frac{-r_{Da1}^2 r_w^2}{4(t-t_{i-1})} \frac{S}{T} \frac{y_1}{x_1})]\} \qquad 3.43$$

The dimensionless time term for two layer composite system at time t is expressed by Equation 2.23 in the form:

$$t_{Dw} = \frac{t}{r_w^2} \cdot \frac{T_s(t)}{S_s(t)} \qquad 3.44$$

Where T_s and S_s are respectively the system transmissibility and storage evaluated at time t as outlined in Section 3.2.

Equations 3.43 and 3.44 are used to generate type curves for several different systems where the reservoir properties change from layer to layer and from region to region. In computations, the typical parameters were:

$T = 1000.$ md.ft/cp

$S = 0.00002$ ft/psi

$r_w = 0.5$ ft

$a_1 = 500.$ ft

The independent parameter was time (t) and not the dimensionless time (t_{Dw}). The first time interval (Δt) = 2×10^{-3} hours and it was doubled every 10 steps afterward. The computations covered the time from 2×10^{-3} to 2×10^{3} hours with 166 time steps for each system.

The results are presented in semi-log and log-log plots. The following sections discuss these results.

3.5 Behavior of Dimensionless Well Pressure

Properties and dimensions of the two-layer two-region system under study are related by fractional factors to the properties of the first region (from the well) of the top layer. These relations are listed in Section 3.1. The effects of transmissibilities, storages and dimensions of the reservoir are respectively presented in Sections 3.5.1, 3.5.2 and 3.5.3.

3.5.1 Effect of Transmissibility

Figure 3.1 shows a family of curves for seven different systems. The storages of all blocks in a particular system are the same and equal to that of the reference block in that particular system. Also, the radii of region one in both layers are the same.

The system represented by Curve seven of Figure 3.1 consists of four blocks which have exactly the same properties and dimensions. As expected, this system behaves exactly as a single layer homogeneous reservoir of infinite dimension. Plotting P_{Dw} vs log t_{Dw} for this system (Curve 7 of Plot 3.1) yields an exact straight line of slope 1.151. This curve (Curve 7) has been included in P_{Dw} vs t_{Dw} plots to detect the anomalies in reservoir pressure behavior due to changes in it's properties vertically and horizontally.

The first region of the two layers have the same transmissibility in all seven systems. Thus, as expected, all of them follow the same behavior, in early time (Period AB), of infinite acting reservoir. Then the drawdown curves bend upward. Curve 1 represents a system of four homogeneous blocks where $T_{2,1} = 5T_{1,1}$, $T_{1,2} = T_{1,1}$ and $T_{2,2} = 10T_{1,1}$. For this system, P_D increases (Portions BCD of the curve) due to increased depletion of more permeable regions ($T_{2,1}$ and $T_{2,2}$). However, the region of $T_{2,2}$ is depleted faster ($T_{2,2} = 10T_{1,1}$) and results in higher pressure drop (Portion BC). Then P_{Dw} goes through transition period (Portion CD) after which the curve levels off and

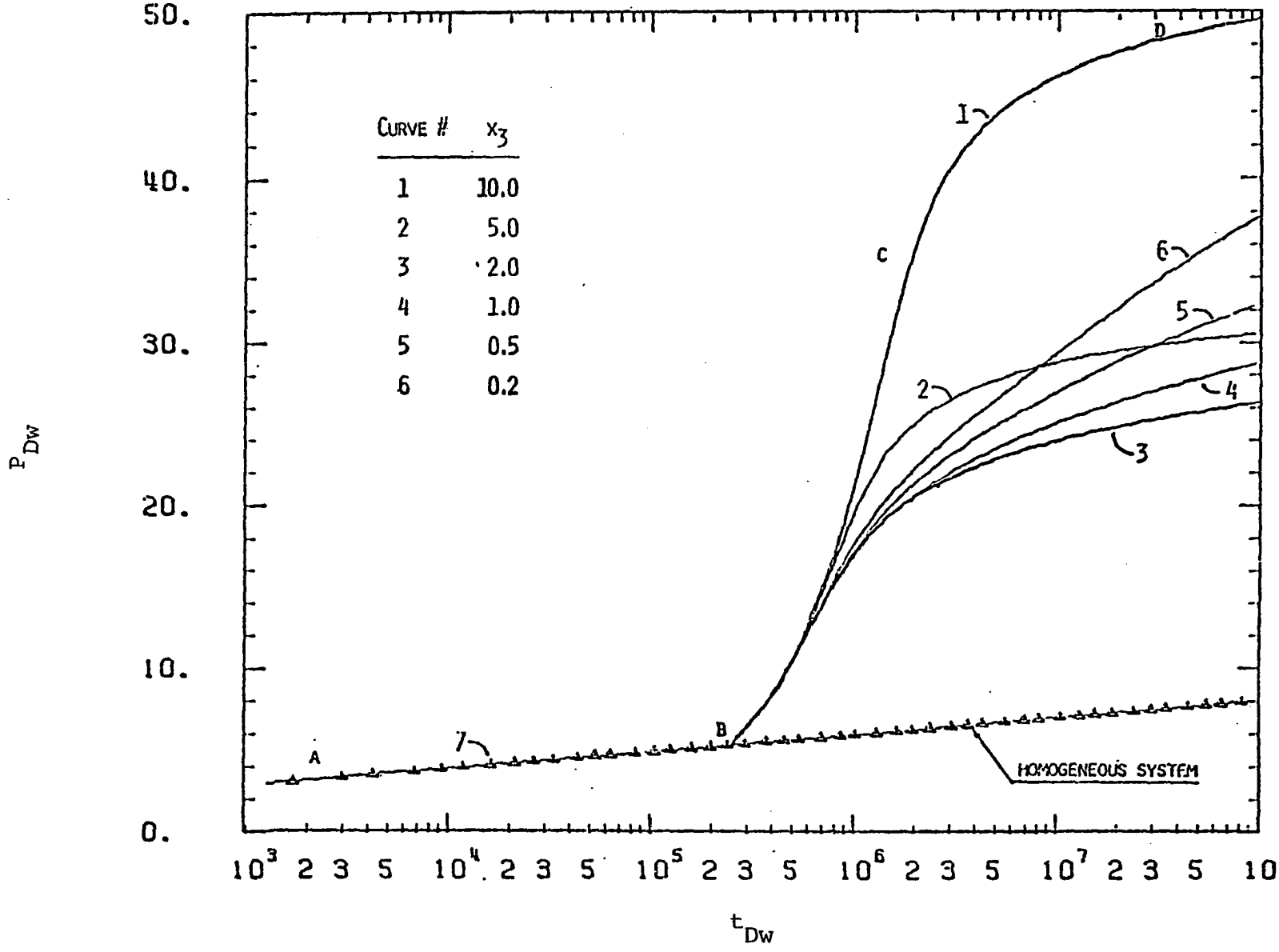

Figure 3.1: Semilog plot of P_{Dw} versus t_{Dw} for a two-layer two-region system with $x_2=y_1=y_2=y_3=z=1.$ and $x_1=5.$.

reaches stabilized conditions (Segment DE).

The second regions of the two layers presented by Curve 2 have the same transmissibilities ($T_{1,2} = T_{2,2} = 5T_{1,1}$). Thus the system behaves as a single layer two-region reservoir. The two layers of the second region are depleted at the same rate and thus the system stabilizes at the pseudosteady state conditions faster than the other systems (excluding System 7).

The rest of the seven systems behave in a fashion similar to that of System 1. However, the second region of the second layer of each of these systems has lower transmissibility and thus less depletion and lower P_{Dw} values.

Type curve plots of P_{Dw} versus t_{Dw} for the seven systems presented in Figure 3.1 are presented in Figure 3.2. Figure 3.2 shows the same features of P_{Dw} function as Figure 3.1 does.

Figure 3.3 shows a family of curves for six different systems in addition to the straight line that represents the homogeneous system. The first region of each of these six systems consists of two blocks of the same dimensions and transmissibilities $T_{1,1}$ and$_{1,2} = 5T_{1,1}$. As expected, the behavior of the six systems in early production time are similar (Segment AB). However, the initial Segment AB has a slope different from that of an infinite-acting reservoir (1.151). This is an indication that in the case of composite layered reservoirs where transmissibility varies considerably from layer to layer in region one, the early portion of

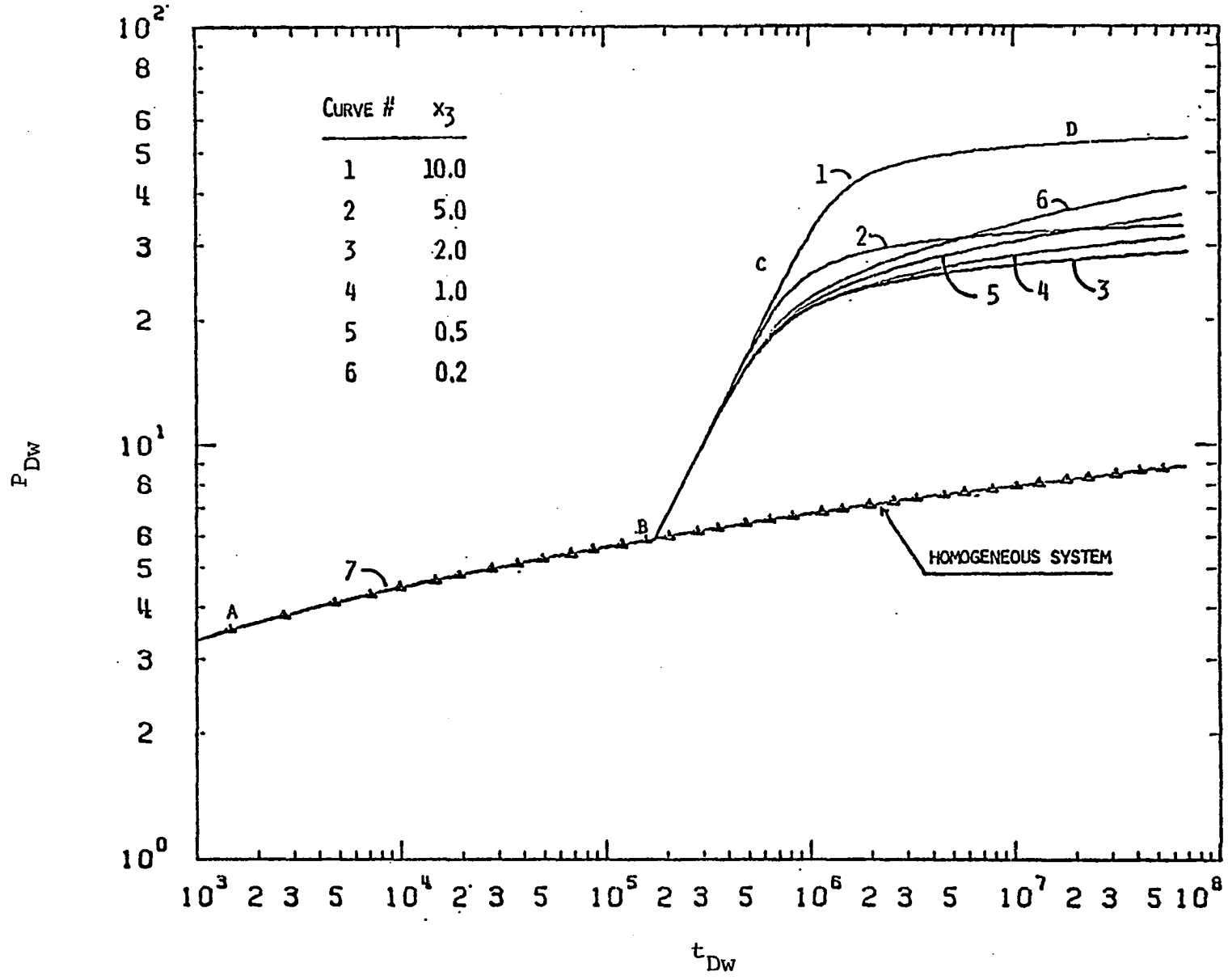

Figure 3.2: Type-curve plot of P_{Dw} versus t_{Dw} for a two-layer two-region system with $x_2=y_1=y_2=y_3=z=1.$ and $x_1=5.$.

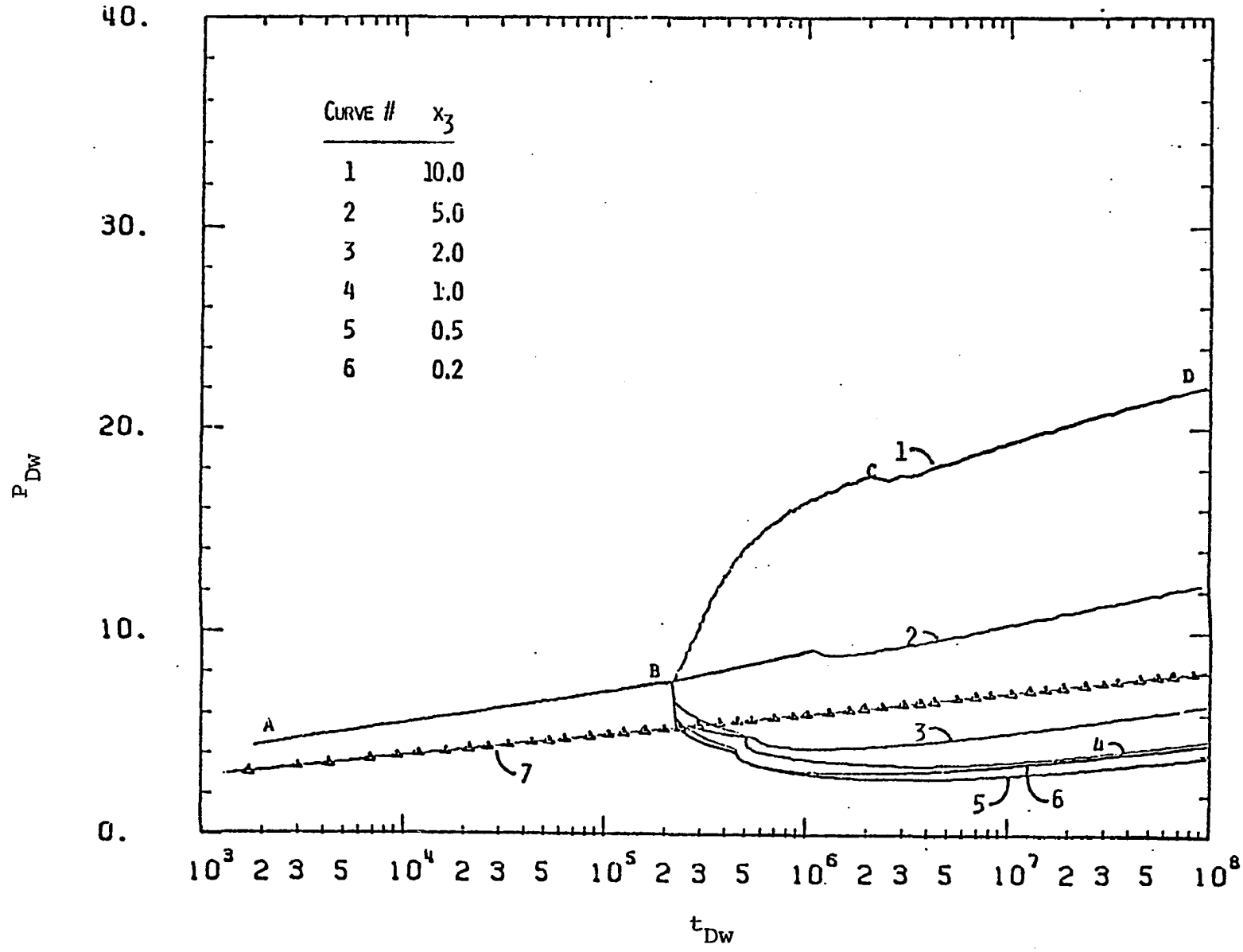

Figure 3.3: Semilog plot of P_{Dw} versus t_{Dw} for a two-layer two-region system with $y_1=y_2=y_3=z=1.$, $x_1=0.5$ and $x_2=5.$.

the pressure drop should not be expected to have the same slope as that of infinite-acting reservoir.

As the well starts producing, pressure disturbances occur due to fluid flow and travel through the porous media. These pressure disturbances travel faster through zones of higher permeabilities than through those of lower permeabilities. Thus, for any particular system represented in Figure 3.3, Portion BC of that system's curve reflects the effect of the second region of the second layer of that particular system. For example, $T_{1,2}$ of system 1 (represented by Curve #1 of Figure 3.3) = $5T_{1,1}$ and thus the pressure disturbance arrives to region (2,2) before it arrives to region (1,2). Then section BC corresponds to the region of high transmissibility $T_{2,2}$ = $10T_{1,1}$. The rise in BC portion of Curve 1 is due to the increased depletion of the more permeable region.

Point C represents the arrival time of the pressure disturbance to region (2,1) of $T_{2,1} = 0.5T_{1,1}$. Since this region has low transmissibility, its effect (shown by Segment CD) is small compared to that caused by the more permeable regions.

Figure 3.4 is a log-log plot of P_{Dw} versus t_{Dw} using the same data as in Figure 3.3.

Figures 3.1 through 3.4 show that, for two-layered two-region reservoir, the dimensionless time needed to reach pseudo-steady state conditions varies with the transmissibilities of

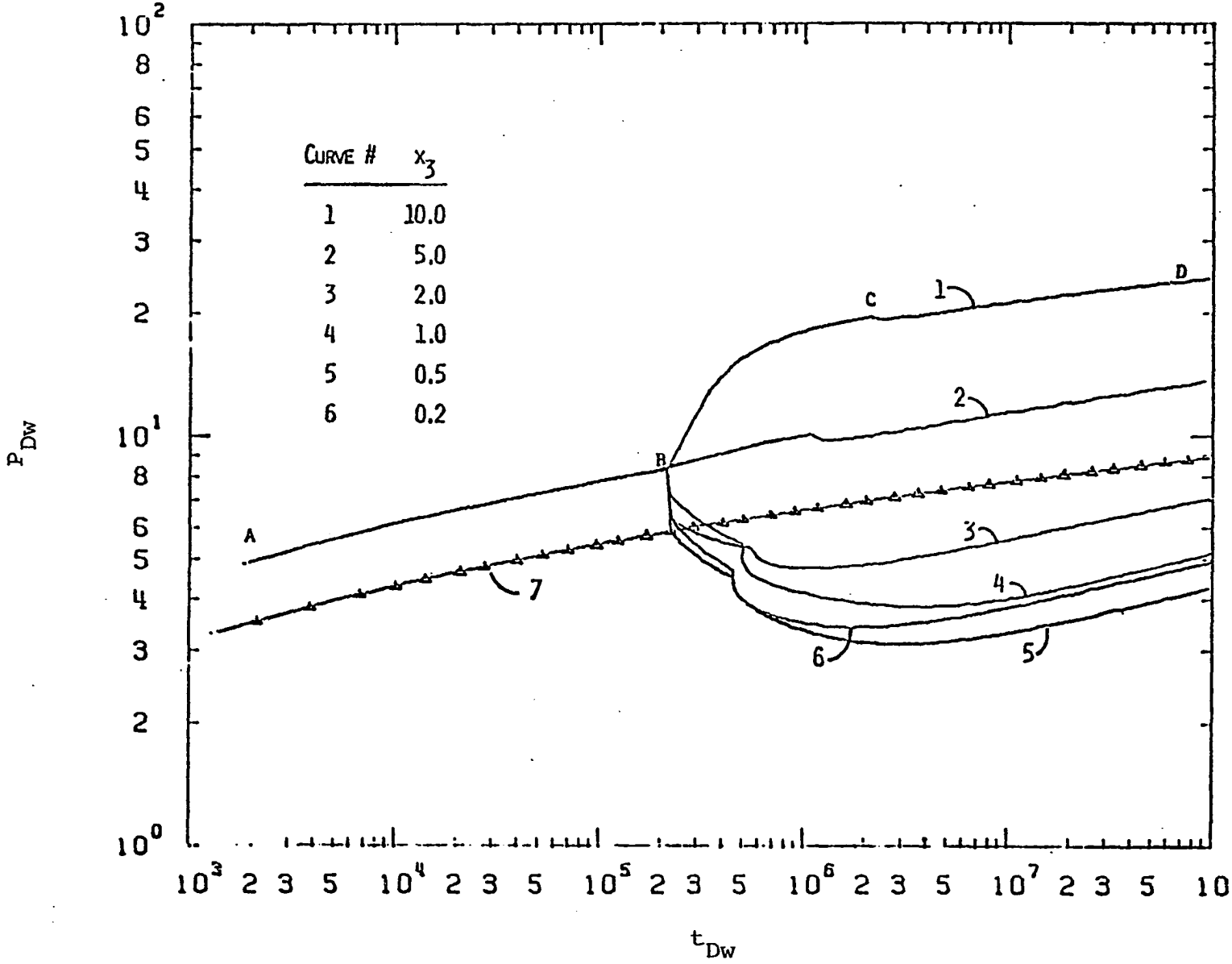

Figure 3.4: Type-curve plot of P_{Dw} versus t_{Dw} for a two-layer two-region system with $y_1=y_2=y_3=z=1.$, $x_1=0.5$ and $x_2=5.$.

different homogeneous blocks of the reservoir. The reason for this lies mainly in the changing rates of production from the layers of the reservoir.

3.5.2 Effect of Storage

Figure 3.5 shows a family of curves for seven different systems. The transmissibility anywhere in a particular system is the same. Also, the dimensions of layer one are identical to those of layer two. However, the storage varies from block to block within the system and each system is different from the others. Figure 3.5 shows that the effect of storage on pressure behavior is negligible. Curves 1 and 6 of Figure 3.5 present two extremes. Curve 1 presents one extreme where the storage of layer 2 decreases from 1. $S_{1,1}$ in region 1 to 0.2 $S_{1,1}$ in region 2 of that layer. The other extreme is presented by Curve 6 where the storage of layer 2 increases from 1. $S_{1,1}$ to 10 $S_{1,1}$. However, the behavior of the dimensionless pressure drop of the two systems are very similar to that of single layer homogeneous systems except for the appearance of a discontinuity on Curve 1. Comparing the two systems presented by Curves 1 and 6, it is noted that the storage of region (2,2) of the system presented by Curve 6 is 50 times that of the same region of the other system (Curve 1). However, the dimensionless pressure behavior of the two systems are very much similar.

Figure 3.6 shows the dimensionless pressure behavior for other six different systems. For each system, storage of block (2,1) is twice that of block (1,1). Thus during early

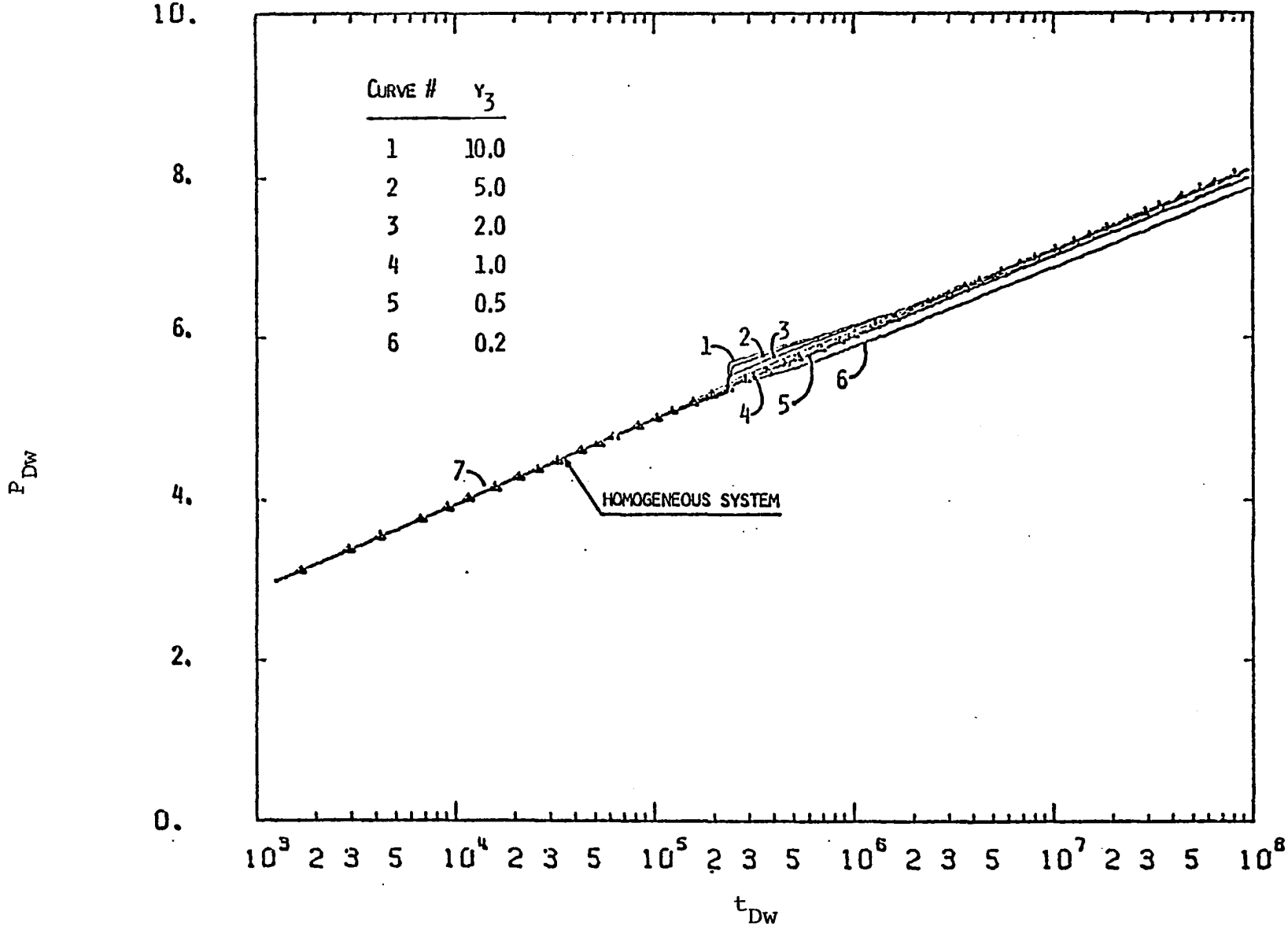

Figure 3.5: Semilog plot of P_{Dw} versus t_{Dw} for a two-layer two-region system with $x_1=x_2=x_3=y_2=z=1.$ and $y_1=2.$.

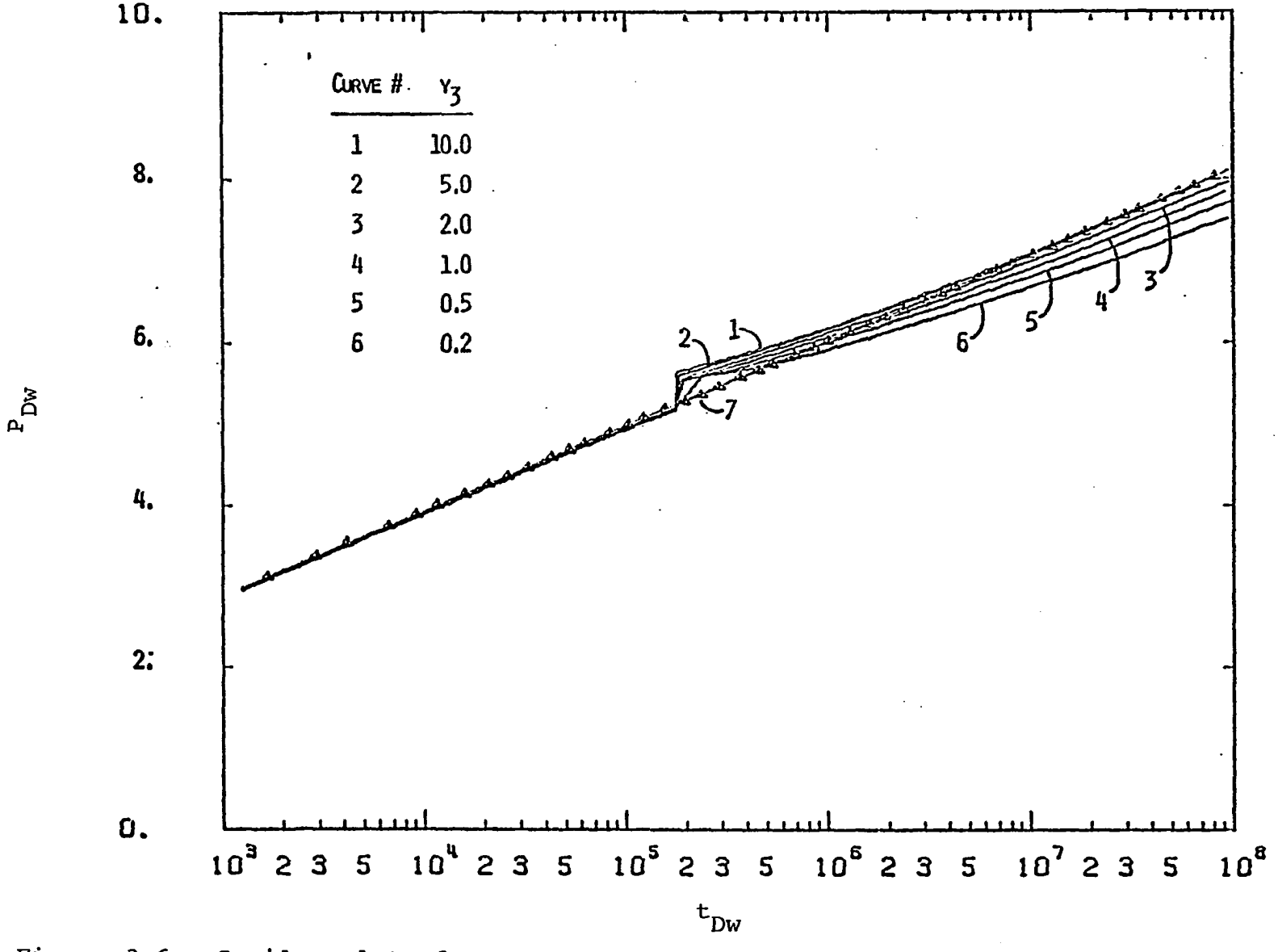

Figure 3.6: Semilog plot of P_{Dw} versus t_{Dw} for a two-layer two-region system with $x_1=x_2=x_3=z-1.$, $y_1=10.$ and $y_2=2.$.

time of production (Segment AB) the six systems behave in a typical manner. However, their behavior is very much similar to that of single layer homogeneous reservoir. Also, for each system, the storage of layer 1 increases from $S_{1,1}$ in block (1,1) to 10 $S_{1,1}$ in block (2,1). As the case of Figure 3.5, Curves 1 and 6 present two extremes. While Curve 1 presents the behavior of dimensionless pressure drop of the system where storage of layer 2 decreases from 2 $S_{1,1}$ in block (1,2) to 0.2 $S_{1,1}$ in block (2,2), Curve 6 presents the case where storage of layer 2 increases from 2. $S_{1,1}$ in block (1,2) to 10 $S_{1,1}$ in block (2,2). However, the behavior of the two systems are similar except for the appearance of a discontinuity on Curve 1.

Figures 3.5 and 3.6 indicate that the storage, whether it changes horizontally or vertically, has very little effect on the behavior of the well bore dimensionless pressure. This is not unexpected either from physical or from mathematical point of views. From the physical point of view, the fluid flow through porous media is mainly controlled by the system transmissibility and not by its storage. From the mathematical point of view, P_{Dw} is a direct function of system transmissibility (T_s) and not the system storage (S_s) as can be seen from Equation 3.38. However, storage terms are very important in estimating the reserve of any reservoir. The type curve matching technique presented in Section 3.7 of this dissertation can be used to estimate the average storage of the

system under study.

Based on the conclusion reached from the above discussion of Figures 3.5 and 3.6 and other figures not included here, the system storages will not be further studied in the rest of the dissertation.

3.5.3 Effect of Region 1 Dimensions

Figure 3.7 shows the same six systems presented in Figure 3.3 with the exception that the radius of region 1 of layer 2 is 1.5 times that of the reference block (z = 1.5). It can be noted from Figure 3.7 that the discontinuity points B are closer to the discontinuity points C than the cases presented by Figure 3.3. With z = 2., the same systems are presented in Figure 3.8. The figure (Figure 3.8) shows that the discontinuity points B are very close to the point C such that the discontinuity points C are very difficult to identify. With a higher value for z, say z = 2.2 or so, points B and C for each system may coincide and pressure behavior curve may look like one of those presented in Figure 3.1. That is to say that, depending on region 1 dimensions, the characteristics of the pressure behavior for systems like those presented in Figure 3.7 may be very much similar to the behavior of those presented in Figure 3.1. In the case of systems presented in Figure 3.1, the transmissibility of region 1 does not vary from layer to layer which is not the case of the systems presented in Figure 3.7.

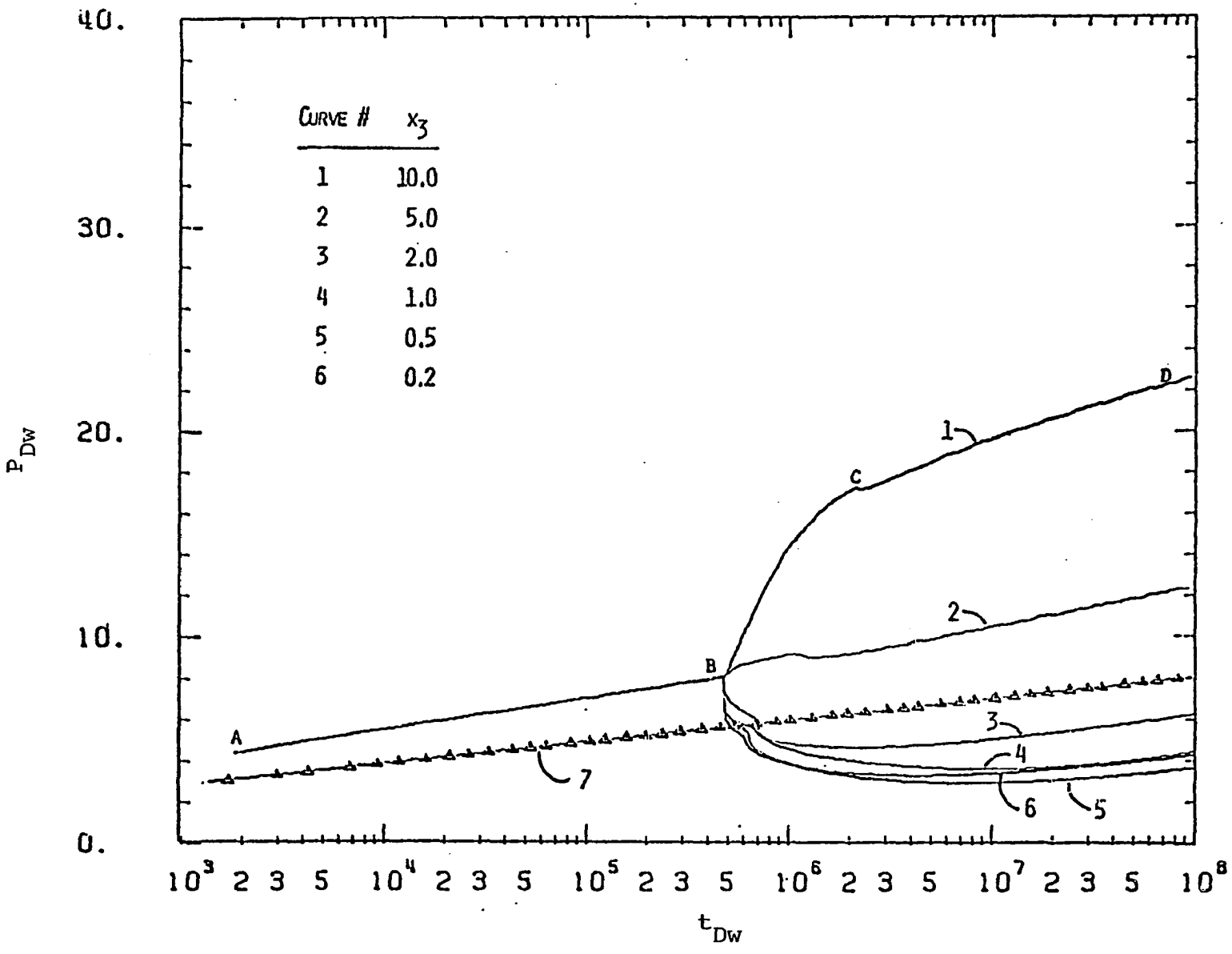

Figure 3.7: Semilog plot of P_{Dw} versus t_{Dw} for a two-layer two-region system with $y_1=y_2=y_3=1.$, $z=1.5$, $x_1=0.5$ and $x_2=5.$.

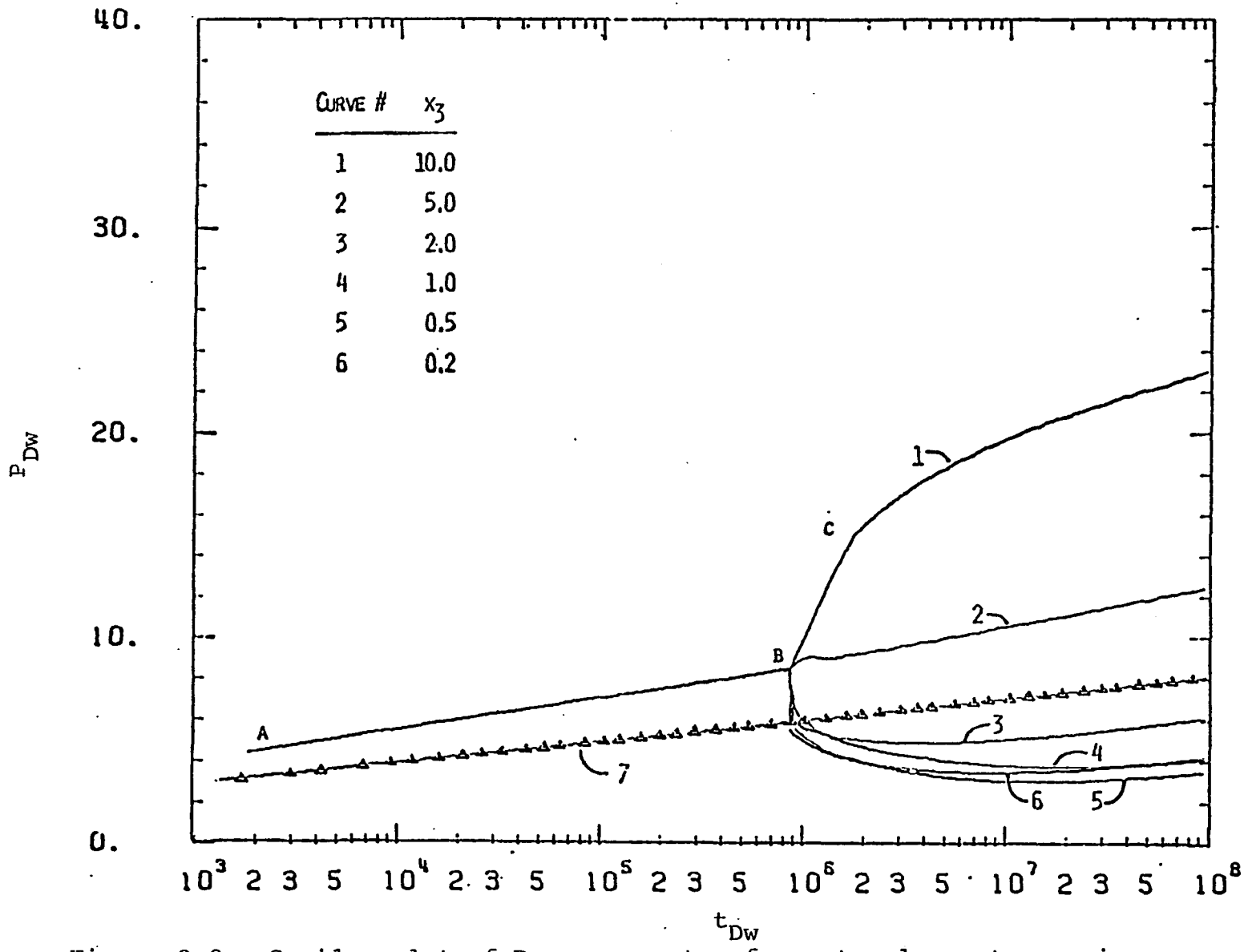

Figure 3.8: Semilog plot of P_{Dw} versus t_{Dw} for a two-layer two-region system with $y_1=y_2=y_3=1.$, $z=2.$, $x_1=0.5$ and $x_2=5.$.

As explained before, points B and C (for different curves of Figures 3.3, 3.4, 3.7 and 3.8) present the arrival time of the pressure disturbance in layers 2 and 1 respectively. In other words, interval BC represents the time lag between pressure disturbance arrivals to region 2 in both layers. As the dimension of region 1 of layer 2 increases ($z = 1.5$, Figure 3.7 and $z = 2.$, Figure 3.8) this time lag decreases till it becomes zero and points B and C coincide. For larger values of z, the lag in time develops again and points B and C become far from each other. However, points B and C would represent the arrival time of pressure disturbance to region 2 in layers 1 and 2 respectively. For $z < 1.$, discontinuity points B would be encountered at earlier time than that in Figure 3.3.

Perhaps the best thing that enables the engineer to differentiate between the different types of the reservoirs is the slope of early time data (portion AB). If the slope of the segment AB of P_w versus log (t) plot is 1.151, the transmissibility of region one does not vary from layer 1 to layer 2 even if two discontinuity points appear. Otherwise, the transmissibility varies from layer to layer in region one even if only one discontinuity point appears on the P_w versus log (t) curve.

Figures 3.9 and 3.10 are the log-log of P_{Dw} versus T_{Dw} of Figures 3.7 and 3.8 respectively.

In addition to the plots presented in Section 3.5, other log-log plots for other different systems are presented

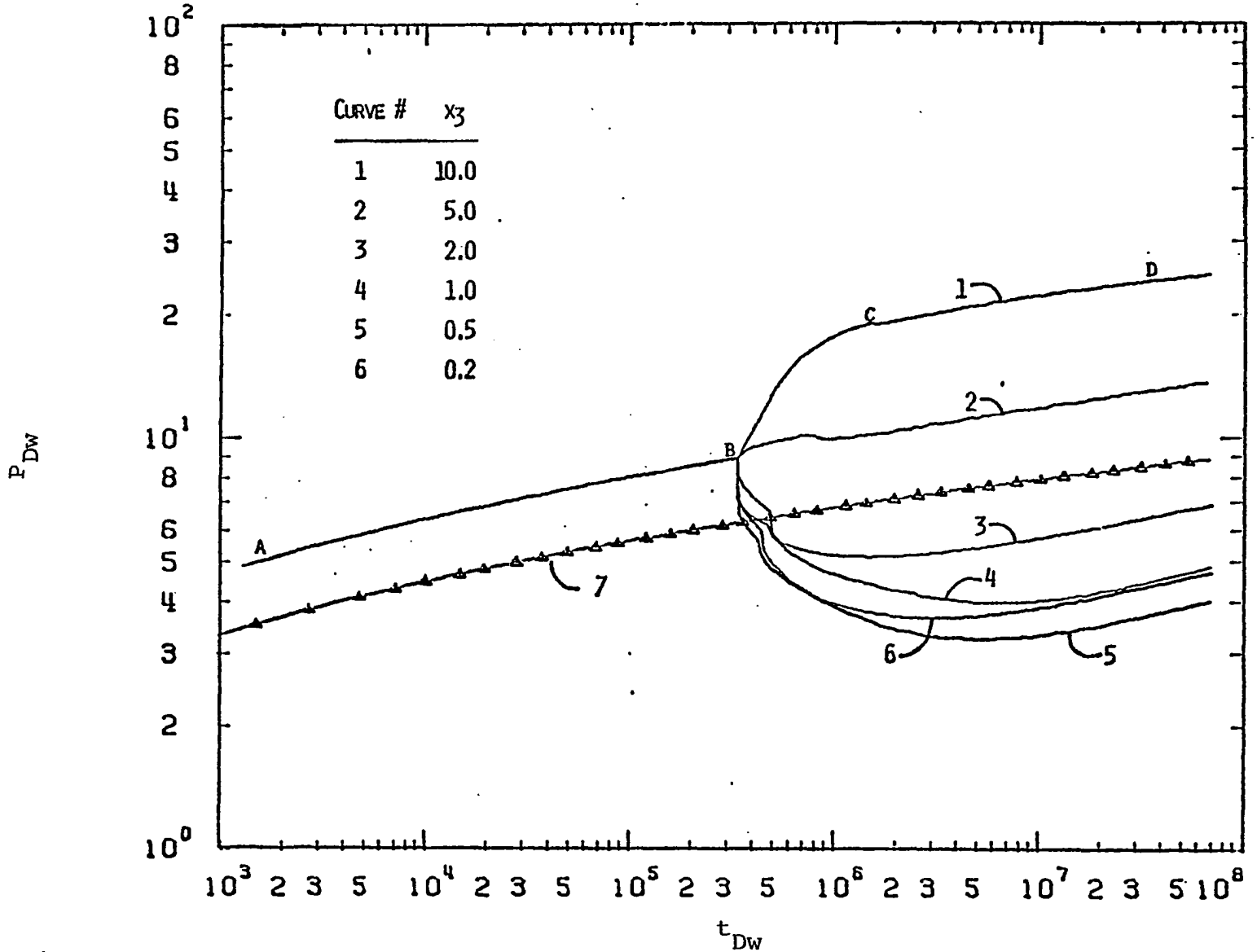

Figure 3.9: Type-curve plot of P_{Dw} versus t_{Dw} for a two-layer two-region system with $y_1=y_2=y_3=1.$, $z=1.5$, $x_1=0.5$ and $x_2=5.$.

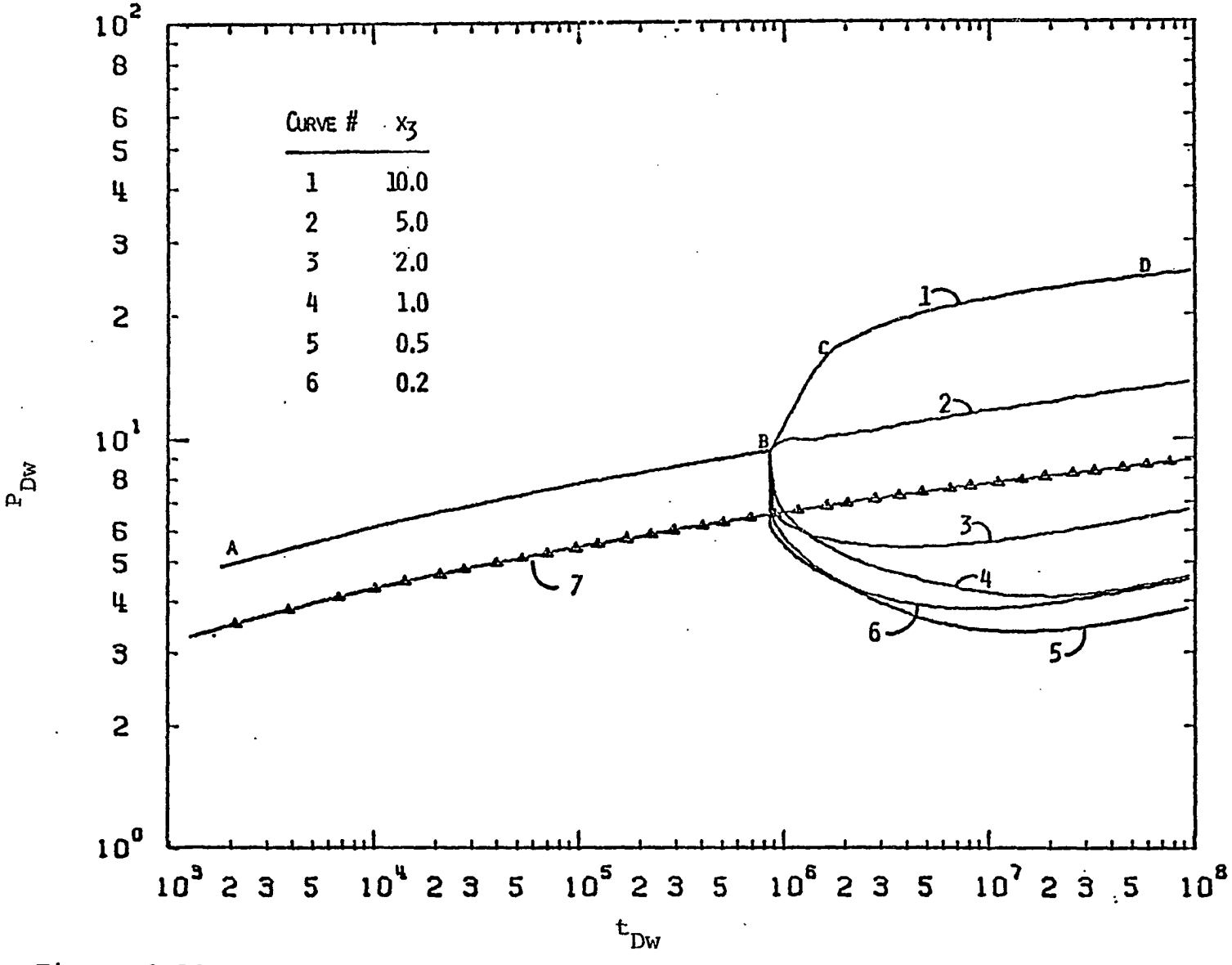

Figure 3.10: Type-curve plot of P_{Dw} versus t_{Dw} for a two-layer two-region system with $y_1=y_2=y_3=1.$, $z=2.$, $x_1=0.5$ and $x_2=5.$.

in Appendix D. The log-log plots presented in this chapter and those presented in Appendix D of this dissertation can be used to determine different reservoir parameters using the proposed type curve matching technique presented in Section 3.7.

3.6 Behavior of Fractional Flow Rates

Figure 3.11 shows a family of curves for six different systems. They are the same six systems presented in Figure 3.1. The properties and dimensions of Blocks (1,1) and (1,2) are identical. During the first period, where the pressure disturbance has not been felt yet by the second region, the fractional flow rate from layer one is exactly half of that from the system (segment AB). For the system presented by curve 2, the transmissibilities of the second region of the two layers are equal. Thus the fractional flow rate from layer 1 is equal to that from the other layer ($f_1 = 0.5$).

For the system presented by curve 6 of Figure 3.11, the fractional flow rate from layer one of this system increases with time (segment BC). This is due to the fact that the transmissibility of the second region of layer one is higher than that of the second region of the other layer. After a long time of production, the fractional flow rate curve will stabilize later (not shown in the figure) at a constant value.

The fractional flow rates from layer one of the other systems presented by curves 3, 4 and 5 follow the same trend as the one presented by curve 1. However, curve 3 tends to stabilize faster than curve 4 which tends to stabilize faster

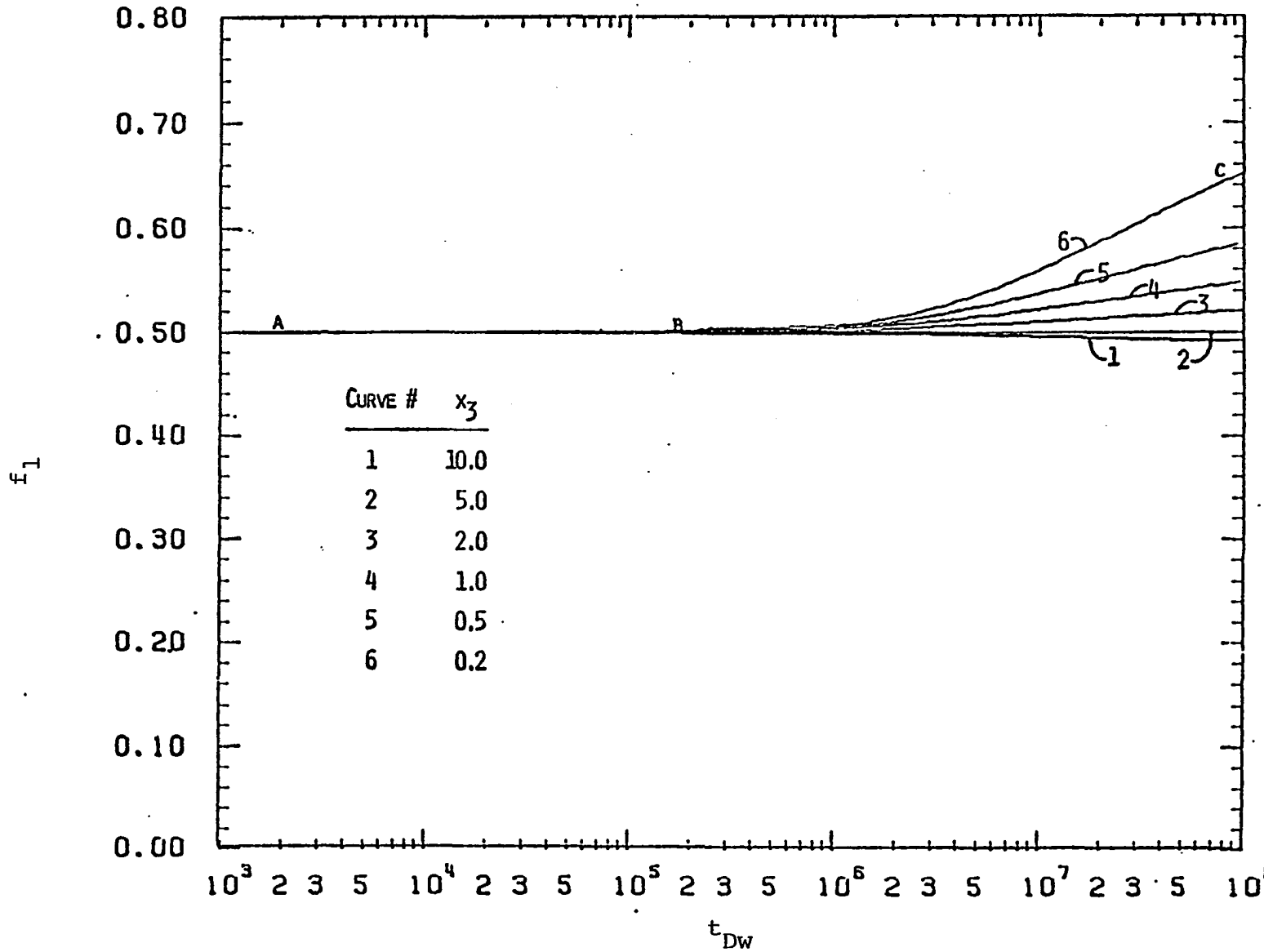

Figure 3.11: Fractional flow rate from layer 1 of a two-layer region system with x_1=0.5 and x_2=y_1=y_2=y_3=z=1..

than Curve 5 and so on. This is due to the fact that the transmissibility ratio of region two ($T_{1,2}/T_{2,2}$) for the system presented by Curve 3 is lower than that of Curve 4 which is lower than that of Curve 5, and so on. This leads us to the conclusion that a reservoir with drastic changes in its transmissibilities may reach steady state after a long production time compared to that required for a reservoir with slight changes.

Segment BC of curve 1 of Figure 3.11 shows a decrease in the fractional flow rate from layer 1 of the system presented by this curve. This is due to the fact that transmissibility of region two of layer 1 is lower than that of region two of the other layer.

Figure 3.12 shows the fractional flow behavior of six additional systems. They are the same six systems presented in Figure 3.2. Although the properties and dimensions of the first region are identical for the six systems, the transmissibility varies from layer to layer of that region.

As expected, the fractional flow behavior of the six systems are identical during the early time of production (segment AB) where the influence of the second region properties has not been reflected yet on the behavior of each system. The fractional flow rates from layer one decreases with time till it experiences pseudosteady state conditions or the influence of the second region properties.

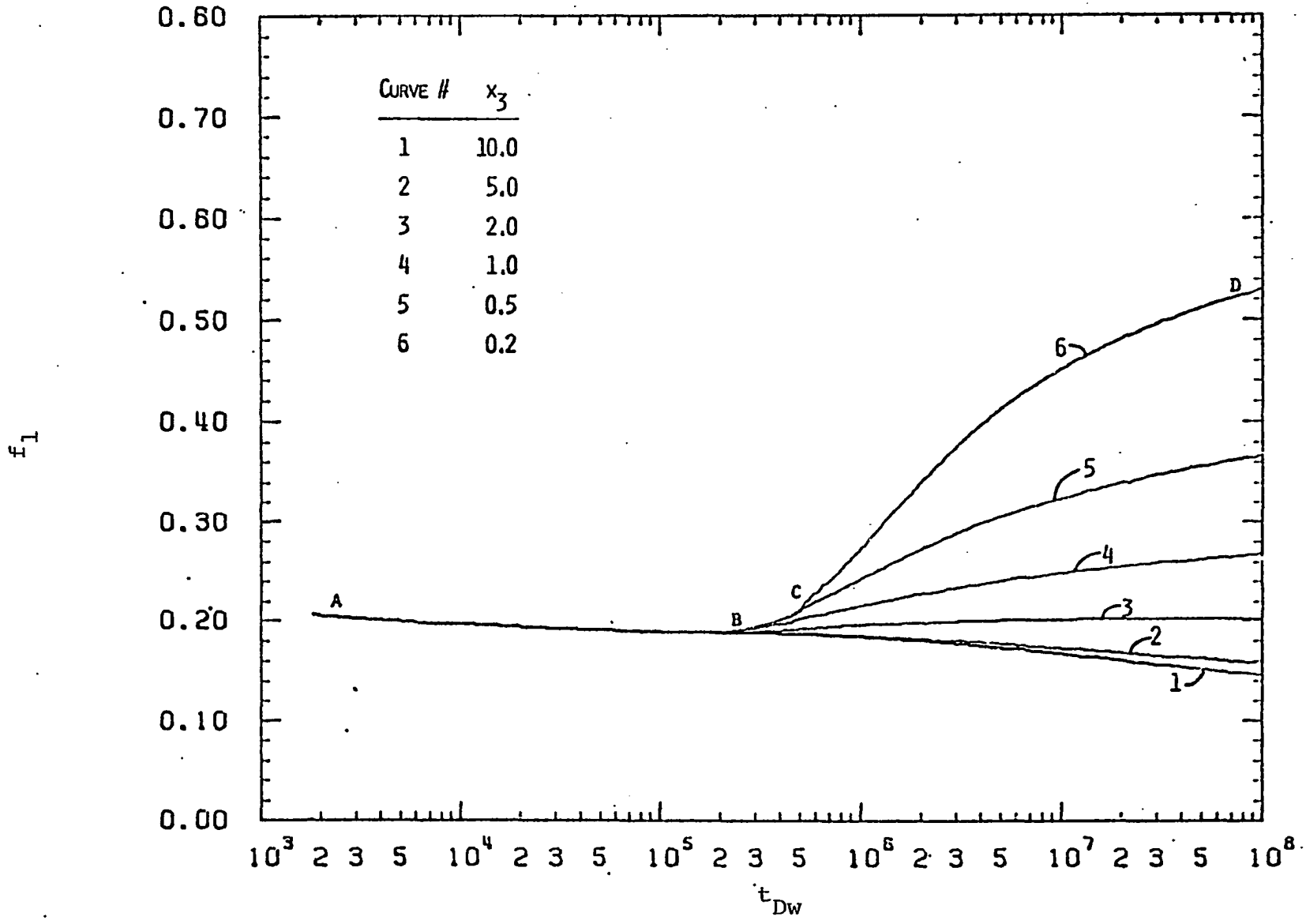

Figure 3.12: Fractional flow rate from layer 1 of a two-layer two-region system with x_1=.5, x_2=5. and y_1=y_2=y_3=z=1..

Since $T_{1,2} = 5T_{1,1}$, the pressure disturbance occurred due to early time production travels in layer two faster than in layer one. Thus the fractional flow rates experience the effect of block (2,2) properties (segment BC of each curve) earlier than that of block (1,2) properties which is reflected later as shown by segment CD of all the curves. For the systems presented by curves 1, 2, 3, and 4, the transmissibility of layer two decreases from region one to region two. This explains why the fractional flow rates from layer 1 increases during the periods presented by segments BC and CD. The reverse is true for the system presented by Curve 6 of the figure. Figure 3.12 shows that the reservoirs with slight changes in their transmissibilities reach pseudosteady state conditions faster than those with drastic changes. Figures 3.11 and 3.12 show that, depending on the contrast of different blocks properties, there is always differential depletion between the two layers even during pseudosteady state periods. Additional plots of f_1 versus t_{Dw} for other different cases are presented in Appendix E of this dissertation.

3.7 Drawdown Type-Curve Match Technique

Section 3.5 and Appendix D present type-curve plots for different two-layer two-region systems. To make use of these plots, a type curve matching technique is presented in this section.

3.7.1 Basic Equations

The dimensionless pressure term P_{Dw} is defined in oil field units as:

$$P_{Dw} = \frac{T_s}{141.2\ Q\ B_0}\ \Delta\ P_w \qquad 3.45$$

where $\Delta P_w = P_i - P_w$

Thus the transmissibility of the system is given as;

$$T_s = 141.2\ Q\ B_0\ \frac{P_{DwM}}{\Delta P_{wM}} \qquad 3.46$$

where P_{DwM} and P_{wM} are respectively P_{Dw} and ΔP_w at a convenient match point.

Combining Equations 3.4 and 3.46 yields an expression for the reference block transmissibility as:

$$T = 141.2\ Q\ B_0\ \frac{r_{D\,inv1}^2 + r_{D\,inv2}^2}{r_{D\,inv1}^2 + x_2\ r_{D\,inv2}^2} \cdot \frac{P_{DwM}}{\Delta P_{wM}} \qquad 3.47$$

Substituting Equation 2.27 into the above Equation and using the transforms listed in Section 3.1 yields:

$$T = 141.2\ Q\ B_0\ \frac{(1 + x_2/y_2)}{(1 + x_2^2/y_2)} \cdot \frac{P_{DwM}}{\Delta P_{wM}} \qquad 3.48$$

Then:

$$T_{2,1} = x_1 \, T \tag{3.49}$$

$$T_{1,2} = x_2 \, T \tag{3.50}$$

$$T_{2,2} = x_3 \, T \tag{3.51}$$

Equations 3.48 through 3.51 express the transmissibility of the four blocks of two-layer two-region reservoir.

Similarly, dividing Equation 3.5 by Equation 3.4 gives:

$$\frac{S_s}{T_s} = \frac{1 + x_2}{1 + \frac{x_2^2}{y_2}} \cdot \frac{S}{T} \tag{3.52}$$

Equation 2.22 is written in field units as:

$$\frac{S_s}{T_s} = \frac{0.0002637}{r_w^2} \cdot \frac{t_M}{t_{DwM}} \tag{3.53}$$

From Equations 3.52 and 3.53, the storage of the reference block is given as:

$$S = \frac{0.0002637}{r_w^2} \cdot \frac{1 + x_2^2/y_2}{1 + x_2} \cdot T \cdot \frac{t_M}{t_{DwM}} \tag{3.54}$$

Where T is given by Equation 3.48 and t_M and t_{DwM} are t and t_{Dw} at a convenient match point.

As can be noted from Figures 3.11, 3.12 and E.1 through E.23, the fractional flow rates from each layer can be assumed constant during early production time without introducing significant error. This explains why Equations 3.4 and 3.5 were used to obtain Equations 3.48 and 3.54. Equations (3.10 and 3.11), (3.16 and 3.17) or (3.22 and 3.23) can also be used. However, the variations in flow rates may have to be considered and the simplicity of type-curve technique may be obscured.

Using Equation 2.31 and the transforms listed in Section 3.1, (t_{a1}/t_{a2}) ratio can be written as:

$$\frac{t_{a1}}{t_{a2}} = \frac{x_2}{y_2\, z^2} \qquad 3.55$$

Using Equation 2.31, the reservoir dimensions are calculated as follows:

$$a_1 = 2\,(0.0002637\, t_{d1}\, \frac{T}{S})^{0.5} \qquad \frac{t_{a1}}{t_{a2}} \leq 1. \qquad 3.56$$

$$a_2 = z\, a_1$$

$$a_2 = 2\,(0.0002637\, t_{d1}\, \frac{x_2^2 T}{y_2 S})^{0.5}$$

$$\frac{t_{a1}}{t_{a2}} > 1 \qquad 3.57$$

$$a_1 = a_2/z$$

3.7.2 Stepwise Type-Curve Match Procedure

1. Plot well testing data, draw down pressure versus time, on log-log paper using the same scale as that of the master curve.
2. Select the proper master curve which has the same trend as that of field data obtained in step 1.
3. The type curve data is placed on the chosen master curve. The coordinate axes of the two curves are kept parallel and shifted to a position which represents the best fit of the data to the master curve.
4. Pick any convenient match point and read the corresponding values of P_{DwM} and t_{DwM} from the master type-curve, and P_{wM}, t_M and t_{dl} (time of first discontinuity point) from the type curve data plot. Read the correlating factors x_1 to x_3, y_1 to y_3 and Z from the master curve.
5. Use the data obtained in step 4 to calculate transmissibilities, storages and dimensions of the reservoir using the basic equations listed in Section 3.7.1.

3.7.3 Drawdown Type-Curve Example

A. Reservoir Data

$Q = 300$ bbl/D

$\mu = 0.8$ cp

$c_t = 1.05 \times 10^{-5}$ psi^{-1}

$B_0 = 1.1$

$r_w = 0.25$ ft

B. Pressure Drawdown Simulated Data

(shown by Figure 3.13)

Solution:

From the master curve read

$y_1 = y_2 = y_3 = z = 1.$

$x_1 = 0.5$

$x_2 = 5$

$x_3 = 10$

At the match point read

$P_{DM} = 6.15$

$\Delta P_{wM} = 130.$ psi

$t_{DwM} = 10^5$

$t_m = 2.2$ hrs

At the first discontinuity points read

$t_{dl} = 5.8$ hr

1. Transmissibility terms

Using Equation 3.48:

$$T = 141.2 \quad QB_0 \left(\frac{1 + \frac{x_2}{y_2}}{1 + \frac{x_2^2}{y_2}}\right) \frac{P_{DwM}}{\Delta P_{wM}}$$

$$= 141.2 \times 300 \times 1.1 \left(\frac{1 + \frac{5}{1}}{1 + \frac{5^2}{1}}\right) \frac{18.}{130.}$$

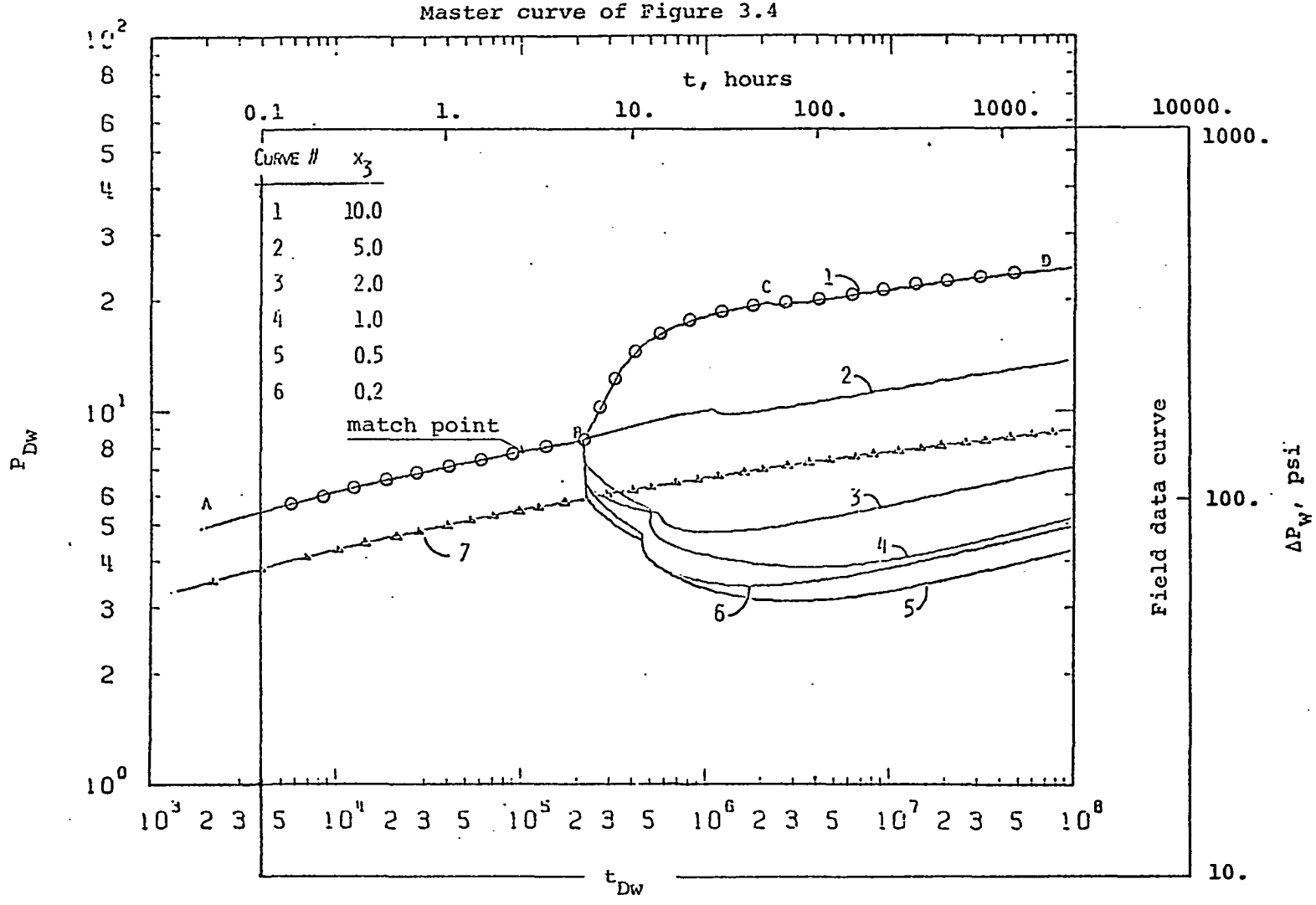

Figure 3.13: Drawdown type-curve match example.

$$T_{1,1} = 508.7 \text{ md} \cdot \text{ft/cp}$$

$$(kh)_{1,1} = T \cdot \mu$$

$$= 508.7 \times 0.8 = 407.0 \text{ md} \cdot \text{ft}$$

$$T_{2,1} = x_1 T \cdot = 0.5 \times 508.7$$

$$= 254.4 \text{ md} \cdot \text{ft/sec}$$

$$(kh)_{2,1} = T_{2,1} \cdot \mu$$

$$= 254.4 \times 0.8 = 203$$

Similarly

$$T_{1,2} = 2543.5 \text{ md} \cdot \text{ft/cp}$$

$$(kh)_{1,2} = 2034.8 \text{ md} \cdot \text{ft}$$

$$T_{2,2} = 5087. \text{ md} \cdot \text{ft/cp}$$

$$(kh)_{2,2} = 4069.6 \text{ md} \cdot \text{ft}$$

2. Storage terms

Using Equation 3.53

$$S = \frac{0.0002637}{r_w^2} \cdot \left(\frac{1 + x_2^2/y_2}{1 + x_2}\right) T \cdot \frac{t_M}{t_{DwM}}$$

$$= 5.12 \times 10^{-5} \text{ ft} \cdot \text{psi}^{-1}$$

$$\phi h = \frac{S}{c_t} = \frac{5.12 \times 10^{-5}}{1.7 \times 10^{-5}} = 4.88 \text{ ft}$$

Since $y_1 = y_2 = y_3$

$$(\phi h)_{1,1} = (\phi h)_{2,1} = (\phi h)_{1,2} = (\phi h)_{2,2} = 4.88 \text{ ft}$$

3. Reservoir dimensions

$$\frac{t_{al}}{t_{a2}} = \frac{x_2}{y_2 z^2} = 5. > 1.$$

Using Equation 3.57:

$$a_2 = 2(0.0002637 \cdot t_{dl} \cdot \frac{x_2 T}{y_2 S})^{0.5}$$

$$= 2(0.0002637 \times 5.8 \times \frac{5 \times 508.7}{1 \times 5.12 \times 10^{-5}})^{0.5}$$

$$= 551.3 \text{ ft}$$

$$a_1 = \frac{a_2}{z} = \frac{551.3}{1} = 551.3 \text{ ft}$$

CHAPTER 4

PRESSURE BUILDUP BEHAVIOR IN MULTILAYER COMPOSITE RESERVOIR

4.1 Introduction

The most popular transient well testing technique, pressure buildup testing, has been treated widely in the literature. Pressure buildup testing requires shutting in a producing well after the well has been producing at constant rate. Because of the absence of the operational problems which are frequently associated with drawdown tests, a buildup test will usually give the most dependable results. The main problem that may be encountered is that prohibited long shut-in times may be required before stabilization is attained specially in tight formations. However, long shut-in periods may be avoided when a proper analysis of the transient pressure-time data is possible.

In this chapter; pressure buildup behavior for single well located in the center of layered composite system is treated. The system considered here and the assumptions associated with it are the same as those described and listed in Sections 2.1 and 2.2. Two conventional methods of analyzing pressure buildup data are considered. The two methods are Horner plot and Miller-Dyes-Hutchinson (Abreviated MDH) plot.

4.2 Multilayer Composite System

The powerful principle of superposition, which was used in Chapters 2 and 3 to develop expressions for drawdown dimensionless pressure, can also be used to develop interperative methods for analyzing the behavior of shut-in well pressure, P_{Ws}, during buildup well testing. For multi-layered composite reservoirs, the fractional flow rates from each layer vary with time during production period. Therefore, the superposition technique was used to develop P_{Dw} term. During shut-in period, the flow rate from the well and consequently from each layer is zero.

Suppose that the well, which is in the center of multi-layered composite reservoir, produced oil at constant rate Q for time t_p and then shut-in for period Δt_s. Let us assume that the production time, t_p, corresponds to time level κ and the time $t = t_p + \Delta t_s$ Corresponds to time level N. So, the difference in $N^{\underline{th}}$ and $\kappa^{\underline{th}}$ time levels represents the shut-in time interval, Δt_s. While the fractional flow rate from each layer of the system varies with time during production period t_p, it is constant and equals to zero during shut-in period Δt_s. Thus the change in the fractional flow rate from layer j just after shutting-in the well is $-f_{j,\kappa}$, where $f_{j,\kappa}$ is the fractional flow rate from layer j just before shutting-in the well.

Applying the superposition technique in time, Equation 2.15 is modified to express pressure distribution in region one of layer

j of the layered composite reservoir during shut-in time as:

$$P_{1,j}(r,t) = P_i + \frac{Q}{4\pi} \left[\left\{ \sum_{i=1}^{\kappa} (f_{j,i} - f_{j,i-1})\, R_j(t-t_{i-1}) \right\} \right.$$

$$\left. - f_{j,\kappa}\, R_j(\Delta t_s) \right],$$

$$0 \leq r \leq a_j, \quad j = 1,2, \ldots n \qquad 4.1$$

Similarly, the pressure distribution in region two of layer j is obtained from Equation 2.17 as:

$$P_{2,j} = P_i + \frac{Q}{4\pi} \left[\left\{ \sum_{i=1}^{\kappa} (f_{j,i} - f_{j,i-1})\, V_j(t-t_{i-1}) \right\} \right.$$

$$\left. - f_{j,\kappa}\, V_j(\Delta t_s) \right],$$

$$a_j \leq r \leq \infty, \quad j = 1,2, \ldots n \qquad 4.2$$

In Equations 4.1 and 4.2, R_j and V_j are respectively defined by Equations 2.16 and 2.18. The fractional flow rates, $f_{j,i}$, are calculated by using Equations 2.19 and 2.21.

Replacing $P_{1,j}(r,t)$ by P_{ws} in Equation 4.1 yields an

expression for the well bore shut-in pressure as:

$$\frac{4\pi(P_i-P_{ws})}{Q} = f_{j,\kappa}\, R_j(\Delta t_s) - \sum_{i=1}^{\kappa} [(f_{j,i}-f_{j,i-1})\cdot$$

$$R_j(t-t_{i-1})], j = 1,2,\ldots n \qquad 4.3$$

where R_j is obtained by substituting $r_D = 1$ into Equation 2.16.

Multiplying both sides of Equation 4.3 by the system transmissibility ($T_s = \frac{\bar{K}\bar{h}}{\bar{\mu}}$) yields:

$$\frac{4\pi\bar{K}\bar{h}(P_i-P_{ws})}{Q} = f_{j,\kappa}\cdot T_s(\Delta t_s)\, R_j(\Delta t_s)$$

$$- \sum_{i=1}^{\kappa} (f_{j,i}-f_{j,i-1})\cdot T_s(t-t_{i-1})\cdot R_j(t-t_{i-1})],$$

$$j = 1,2,\ldots n \qquad 4.4$$

The left hand side of Equation 4.4 is the definition of the dimensionless pressure buildup of a well located in the center of multilayered composite reservoir, P_{Ds}. Thus:

$$P_{Ds} = f_{j,\kappa} \cdot T_s(\Delta t_s)\, R_j(\Delta t_s) - \sum_{i=1}^{\kappa} (t_{j,i} - f_{j,i-1}) \cdot T_s(t-t_{i-1}) \cdot R_j(t-t_{i-1})], \quad j = 1,2, \ldots n \qquad 4.5$$

The system transmissibility term, T_s, is evaluated using Equation 2.23.

Horner's graph for multi-layered composite system is obtained by plotting P_{Ds}, expressed by Equation 4.5, versus log $[(t_p + \Delta t_s)_D / (\Delta t_s)_D]$. The two terms, $(t_p + \Delta t_s)_D$ and Δt_{Ds}, are expressed by Equation 2.23 as:

$$(t_p + \Delta t_s)_D = \frac{(t_p + \Delta t_s)}{r_w^2} \cdot \frac{T_s(t_p + \Delta t_s)}{S_s(t_p + \Delta t_s)} \qquad 4.6$$

where T_s and S_s are system transmissibility and storage evaluated at time $(t_p + \Delta t_s)$.

$$\Delta t_{Ds} = \frac{\Delta t_s}{r_w^2} \cdot \frac{T_s(\Delta t_s)}{S_s(\Delta t_s)} \qquad 4.7$$

where T_s and S_s are evaluated at time (Δt_s).

Miller-Dyes-Hutchinson plot can be obtained by plotting P_{Ds} given by Equation 4.5 versus log Δt_{Ds} expressed by Equation 4.7.

4.3 Two-layer Composite Reservoir

The previous section of this chapter treated the case of multi-layer composite systems. This section concentrates on the case of two-layered composite system. A mathematical expression for dimensionless pressure buildup behavior is presented. The dimensionless time terms required to develop Horner and MDH plots are also presented. The results are discussed in Section 4.4.

4.3.1 Dimensionless Pressure Buildup Term (P_{Ds})

The dimensionless pressure buildup behavior for a well located in the center of two-layer two-region reservoir and shut-in for time Δt_s after producing at a constant flow rate Q for time t_p is obtained from Equation 4.5 in terms of layer one characteristics as:

$$P_{Ds} = f_{1,\kappa} \cdot T_s(\Delta t_s) \cdot R_1(\Delta t_s) - \sum_{i=1}^{\kappa} [(f_{1,i}-f_{1,i-1}) \cdot T_s(t-t_{i-1}) \cdot R_1(t-t_{i-1})], \; j = 1,2, \ldots . n \qquad 4.8$$

Substituting Equation 3.36 into Equation 4.8 yeilds:

$$P_{Ds} = f_{1,\kappa} \cdot \frac{T_s(\Delta t_s)}{T} \{ Ei \left(\frac{-r_w^2}{4\,\Delta t_s} \frac{S}{T}\right) - Ei \left(\frac{-r_{Dal}^2\, r_w^2}{4\,\Delta t_s} \frac{S}{T}\right)$$

$$+\frac{1}{x_1}\, e^{\frac{-r_{Da1}^2\, r_w^2}{4\, t_s}\frac{S}{T}\left(\frac{x_1-y_1}{x_1}\right)}\; Ei\left(\frac{-r_{Da1}^2\, r_w^2}{4\, t_s}\frac{S}{T}\frac{y_1}{x_1}\right)\}$$

$$-\frac{1}{T}\sum_{i=1}^{\kappa}\{(f_{1,i}-f_{1,i-1})\cdot T_s(t-t_{i-1})\cdot[Ei\left(\frac{-r_w^2}{4(t-t_{i-1})}\frac{S}{T}\right)$$

$$-Ei\left(\frac{-r_{Da1}^2}{4(t-t_{i-1})}\frac{S}{T}\right)+\frac{1}{x_1}\, e^{\frac{-r_{Da1}^2\, r_w^2}{4(t-t_{i-1})}\frac{S}{T}\left(\frac{x_1-y_1}{x_1}\right)}\cdot$$

$$Ei\left(\frac{-r_{Da1}^2\, r_w^2}{4(t-t_{i-1})}\frac{S}{T}\frac{y_1}{x_1}\right)]\} \qquad 4.9$$

where κ is the time level of shutting-in the well. The fractional flow rate from layer one during production (up to time level κ) is calculated by Equation 3.34.

Horner's graph for a two-layer composite system is obtained by plotting P_{Ds}, expressed by Equation 4.9, versus $\log[(t_p+\Delta t_s)_D/\ \Delta t_{Ds}\ ]$. MDH plot is obtained by plotting P_{Ds} term versus $\log \Delta t_{Ds}$. The two terms $(t_p+\Delta t_s)_D$ and Δt_{Ds} are expressed by Equations 4.6 and 4.7 respectively. The transmissibility and storage terms (T_s and S_s) are evaluated as outlined in Section 3.2.

Equations 4.6, 4.7 and 4.9 are used to generate type curves (Horner and MDH plots) for several different systems where the reservoir properties vary from layer to layer and

from region to region. The parameters used in drawdown calculations were used in buildup computations. Thus the fractional flow rates calculated in drawdown calculations were used to evaluate P_{Ds} term. The production time t_p was taken 2×10^3 hrs. The buildup calculations were run at time intervals. The first time interval was 5×10^{-4} hrs. and was doubled every 10 steps afterward with the restriction that the time interval $\leq$ 10 hrs. The computations covered the time from 5×10^{-4} to 6×10^2 hours with 194 time steps. The results are presented in semilog and of both Horner and MDH plots. These results are discussed in the following section.

4.4 Behavior of Buildup Dimensionless Well Pressure:

The behavior of buildup dimensionless well pressure has been studied for several different reservoirs. As it has been mentioned earlier in Section 3.5.2 the effect of storage terms on pressure drawdown behavior is negligible. Thus, storage effects on pressure buildup behavior are not considered. The effects of transmissibility and reservoir dimensions are discussed in Sections 4.4.1 and 4.4.2 respectively.

4.4.1 Effect of Transmissibility

Figure 4.1 shows a family of curves for seven different systems. These seven systems are the same as those presented by Figure 3.1. The storage anywhere in a particular system is the same. The dimensions of the two layers in a particular system are the same.

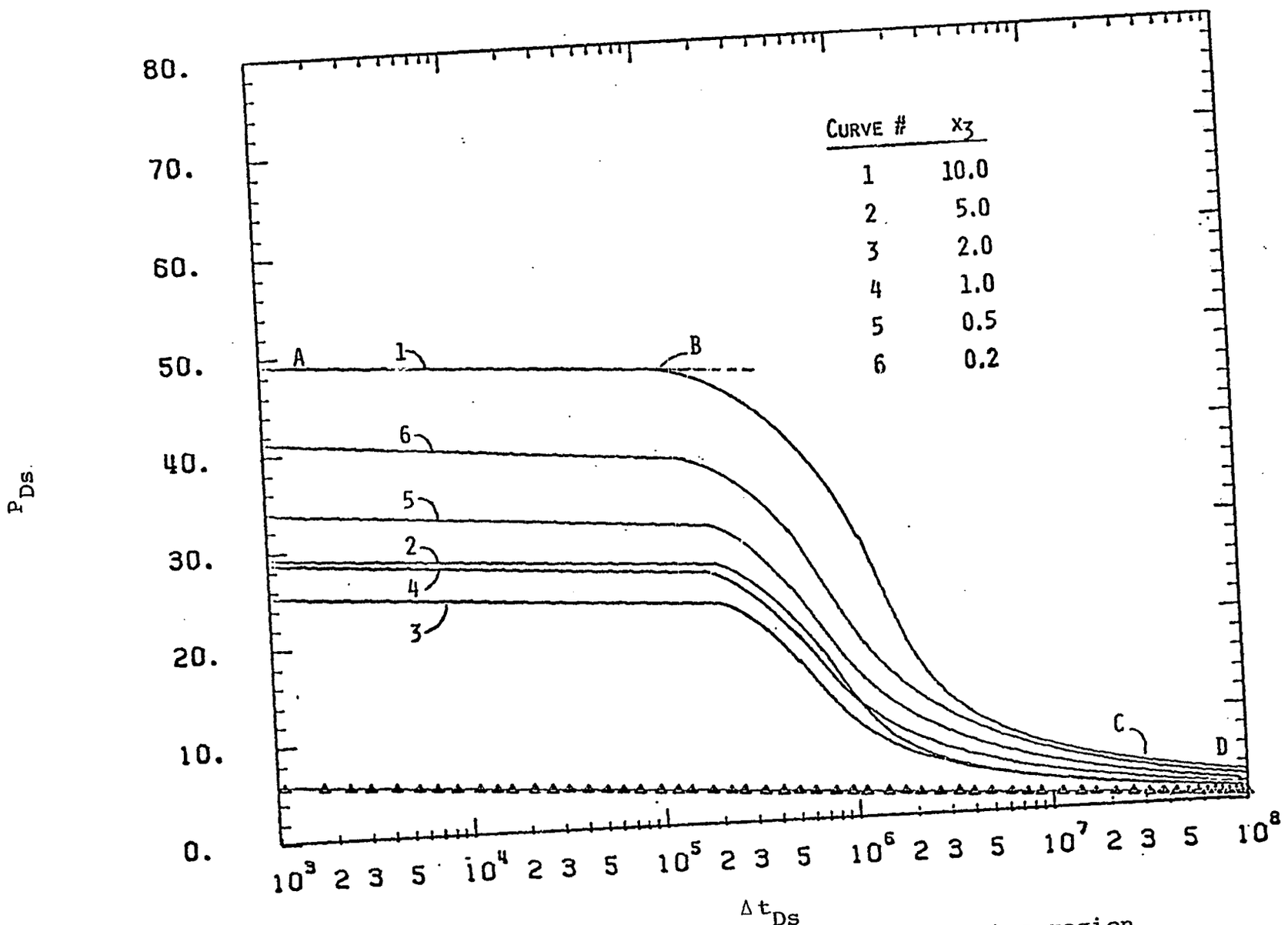

Figure 4.1: Miller-Dyes-Hutchinson buildup graph for a two-layer two-region system with $x_2=y_1=y_2=y_3=z=1.$ and $x_1=5.$.

The properties are the same anywhere in the system presented by curve 7 of Figure 4.1. Thus, as expected, this system behaves exactly as a single layer homogeneous infinite reservoir and P_{Ds} versus Δt_{Ds} is a straight line of slope 1.151. Curve 7 is included in buildup plots (P_{Ds} versus Δt_{Ds}) to compare the behavior of homogeneous system and that of multi-layered composite systems. Segments AB of curves 1 through 6 are straight lines and represent the early time behavior of pressure buildup for the six different systems (excluding the homogeneous system). Although the properties of the first region of the six systems are identical, the slopes of segment AB vary from system to system. This is unlike the case of drawdown where the early time behavior of the six systems are identical (Segment AB of Figure 3.1). Furthermore, in the case of drawdown behavior, each system is assumed to have initial and uniform pressure P_i. This is not the case for buildup.

As explained in Section 3.6, during drawdown period there is always differential depletion between the two layers of two-layered composite system and that differential depletion stabilizes at a constant value after a specific time of production which depends on the contrast in reservoir properties. At that time the reservoir reaches pseudosteady state conditions. If the well is shut-in during the pseudosteady state conditions, the early time pressure buildup behavior follows a straight line which does not reflect only the properties of

region one of a particular system but reflects also the properties of region two of that system. This explains why the slope of segments AB varies from system to system. However, the properties of region one are the dominant factors that control pressure buildup behavior during early shut-in time.

At point B, P_{Ds} function deviates from the straight line AB as Δt_{Ds} increases. The P_{Ds} function goes through a transition period BC and then follows another straight line CD where $P_{Ds} \rightarrow 0$ as $\Delta t_{Ds} \rightarrow \infty$. Point B represents the time at which the influence of the second region properties are felt at the well.

Curve 1 represents a system where $T_{2,1}$ and $T_{2,2}$ are respectively 5 and 10 times that of the reference block. These blocks of higher transmissibility are "recharged" with pressure as are depleted during drawdown, faster than the other blocks of lower transmissibilities. This explains why the well bore pressure builds up, and P_{Ds} decreases, faster as shown by segment BC of curve 1.

The second region of the system presented by curve 2 has the same transmissibilities ($T_{1,2} = T_{2,2} = 5\ T_{1,1}$) and thus it behaves as a single layer two-region reservoir. The two blocks of the second region are recharged with fluid at the same rate and thus the system stabilizes at the pseudosteady state conditions faster than the other systems (excluding system 7).

The rest of the seven systems behave in a fashion similar to that of system 1. However, the second region of the

second layer of each of these systems has lower transmissibility, thus slower "recharging," and slower drop in P_{Ds} values. Horner's semilog plot of P_{Ds} versus $(t_p + \Delta t_s)_D/\Delta t_{Ds}$ for the same systems are presented by Figure 4.2. Figure 4.2 shows the same features of P_{Ds} function as Figure 4.1 does.

Figure 4.3 shows a family of curves (P_{Ds} versus Δt_{Ds}) for another set of six different systems in addition to the straight line which represents the homogeneous system. Segment AB of each curve shows the early shutting-in time behavior of the corresponding system. The first region of each of these six systems consists of two blocks of the same dimensions and transmissibilities $T_{1,1}$ and $T_{1,2} = 10\ T_{1,1}$. However, the slope of segment AB varies from system to system. As explained earlier, segment AB of each curve reflects the effects of all reservoir properties.

Shutting-in the well after producing at a constant flow rate Q for time t_p creates a pressure disturbance at the well which travels through the porous media with a speed that depends on the fluid and porous media properties. For all the systems presented by Figure 4.3 (excluding the homogeneous system), $T_{1,2} = 10\ T_{1,1}$. Thus the pressure disturbance during early shut-in time (segment AB) travels faster through layer 2 than through layer 1. Thus point B represents the arrival time of the pressure disturbance to the end of region 1 of layer 2. Segment BC of each curve reflects the effect of block (2,2)

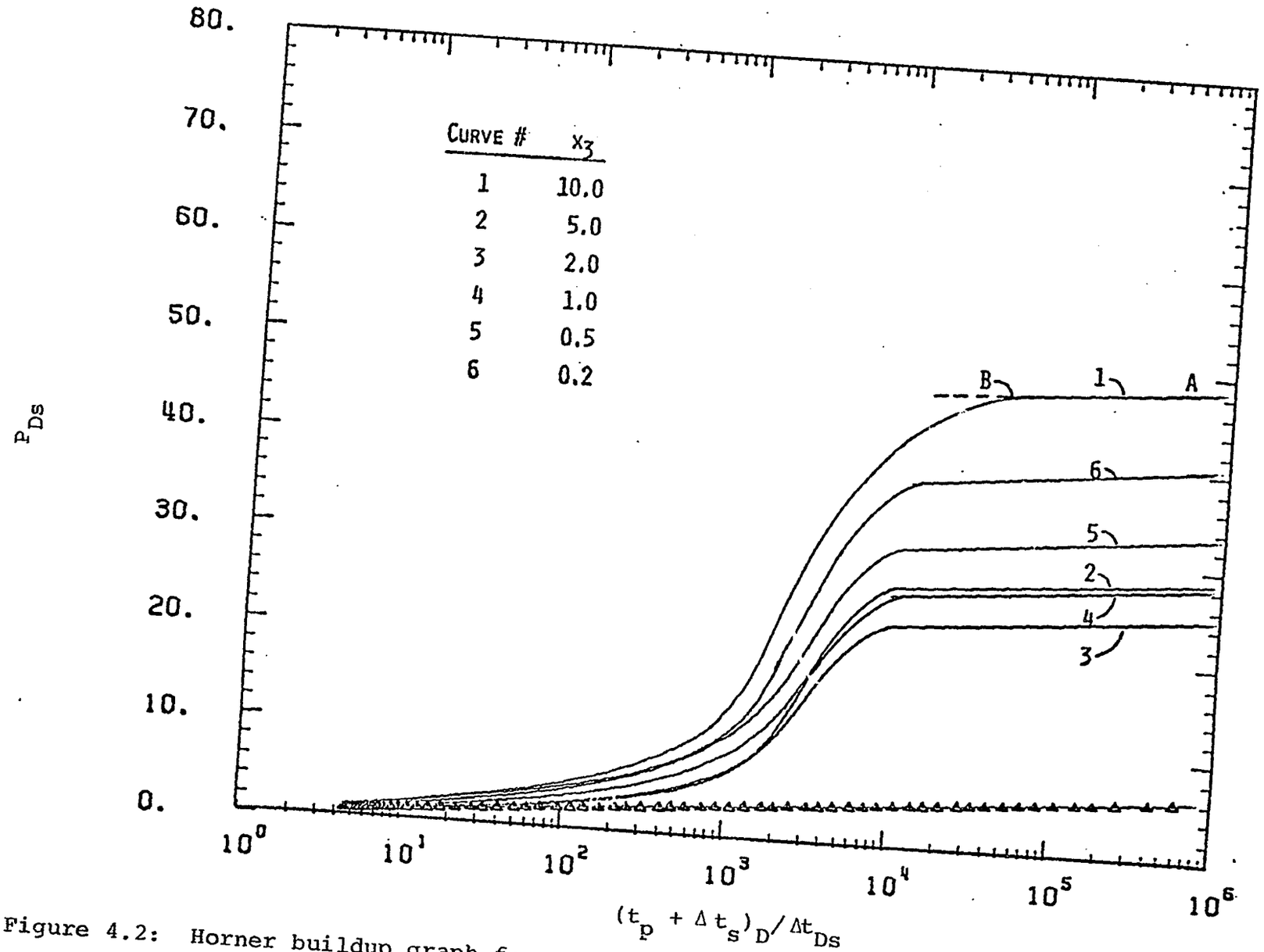

Figure 4.2: Horner buildup graph for a two-layer two-region system with $x_2=y_1=y_2=y_3=z=1.$ and $x_1=5.$.

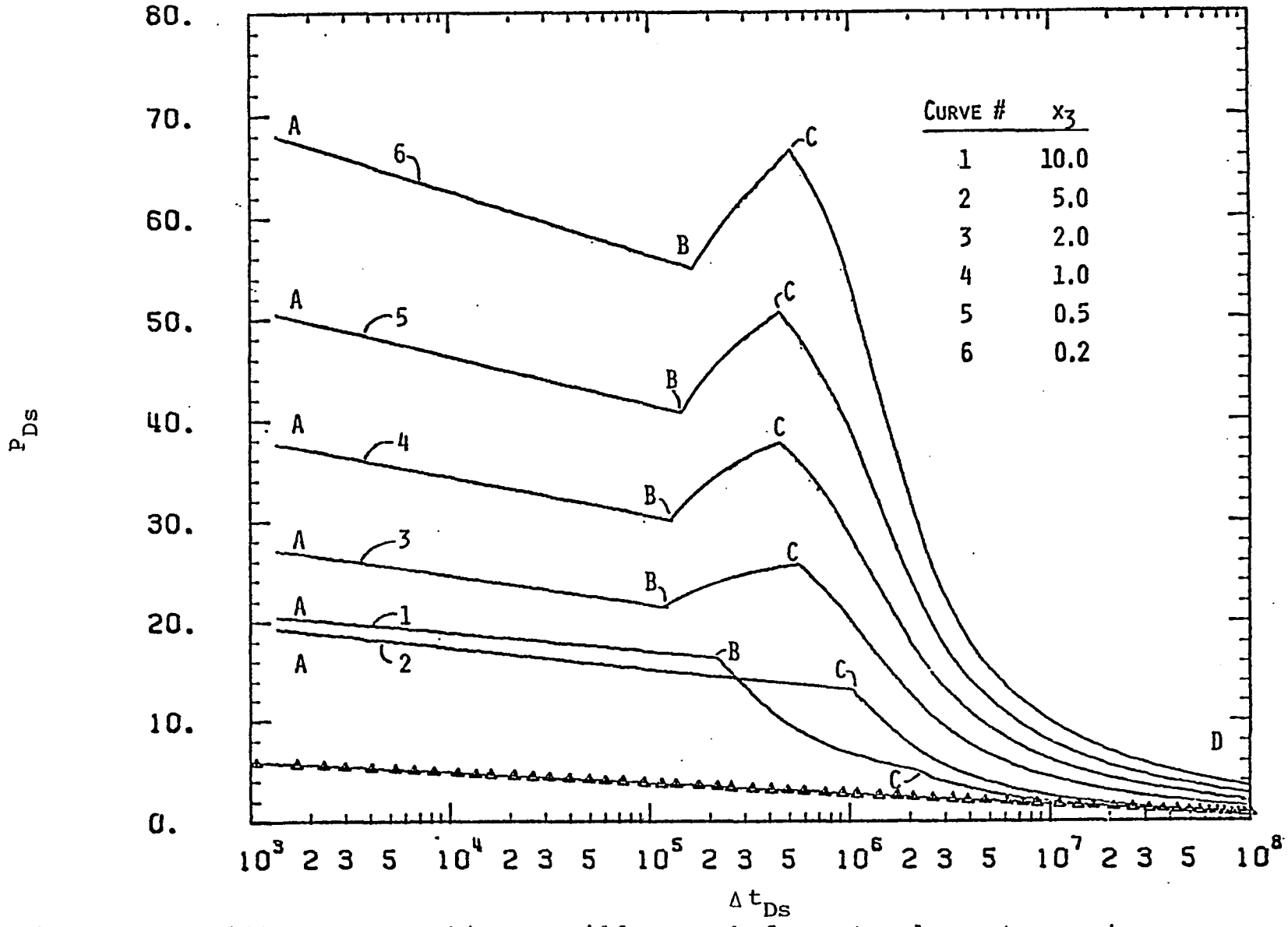

Figure 4.3: Miller-Dyes-Hutchinson Buildup graph for a two-layer two-region system with $y_1=y_2=y_3=z=1.$, $x_1=10.$ and $x_2=5.$.

properties on the pressure buildup behavior.

Segment BC of each curve reflects the effects of block (2,2) properties on the pressure buildup behavior. Curve 6 presents the case where $T_{2,2} = 0.2\ T_{1,1}$. In that case, the pressure disturbance in layer 2 travels from block (1,2) (where $T_{1,2} = 5\ T_{1,1}$) into less permeable block (2,2) (where $T_{2,2} = 0.2\ T_{1,1}$). The block (2,2) is recharged with pressure much slower than the block (1,2). This results in less pressure buildup and consequently higher P_{Ds} as Δt_{Ds} increases (segment BC). For the case presented by curve 2, there is no change in the transmissibility from block (1,2) to block (2,2), $T_{1,2} = T_{2,2} = 5\ T_{1,1}$. For this case, the discontinuity point B disappears. For the case presented by curve 1, the transmissibility of layer 2 changes from $5\ T_{1,1}$ in block (1,2) to $10\ T_{1,1}$ in block (2,2). Block (2,2) is recharged with pressure faster than block (1,2). This explains why portion BC of curve 1 shows that P_{Ds} decreases as Δt_{Ds} increases.

Segment CD of each curve shows the effect of block (2,1) transmissibility on P_{Ds} behavior. The transmissibility of block (2,1) of each of the six systems is ten times that of the reference block. Point C on each curve marks the arrival time of the pressure disturbance in layer 1 to block (2,1). For all the systems presented in Figure 4.3, excluding the homogeneous system, the transmissibility of layer 1 increases from $T_{1,1}$ in the reference block to $T_{2,1} = 10\ T_{1,1}$. Thus P_{Ds} decreases as Δt_{Ds} increases.

Finally, curves 6 and 1 show, respectively, drastic and slight changes in P_{Ds} function. This is due to the fact that the corresponding systems are respectively characterized by drastic and slight changes in the transmissibility. For all the systems (including the homogeneous system), as $\Delta t_{Ds} \rightarrow \infty$, $P_{Ds} \rightarrow 0$.

Horner's semilog plot of P_{Ds} versus $(tp + \Delta t_s)_D/\Delta t_{Ds}$ for the same systems presented by Figure 4.3 is presented by Figure 4.4. Both Miller-Dyes-Hutchinson (MDH) and Horner plots (Figures 4.3 and 4.4 respectively) show the same characteristics for these six systems.

4.4.2 Effect of Region 1 Dimensions

Figure 4.5 presents the same six systems presented by Figure 4.1 with the exception that the radius of region 1 of layer 2 for each system is double that of the reference block ($z = 2.$). Figure 4.5 shows that the discontinuity point B of a particular system is very close to the discontinuity point C of that system. For a higher value of z, say $z = 2.2$ or so, points B and C for each system may coincide and pressure behavior curve may look like one of those presented in Figure 4.1. That is to say that, depending on dimensions of region 1, the characteristics of the pressure behavior for systems as those presented by Figure 4.5 may be very much similar to the behavior of those presented by Figure 4.1. In the case of the systems presented by Figure 4.1, the transmissibility of region 1 does not vary from layer to layer which is not the case for

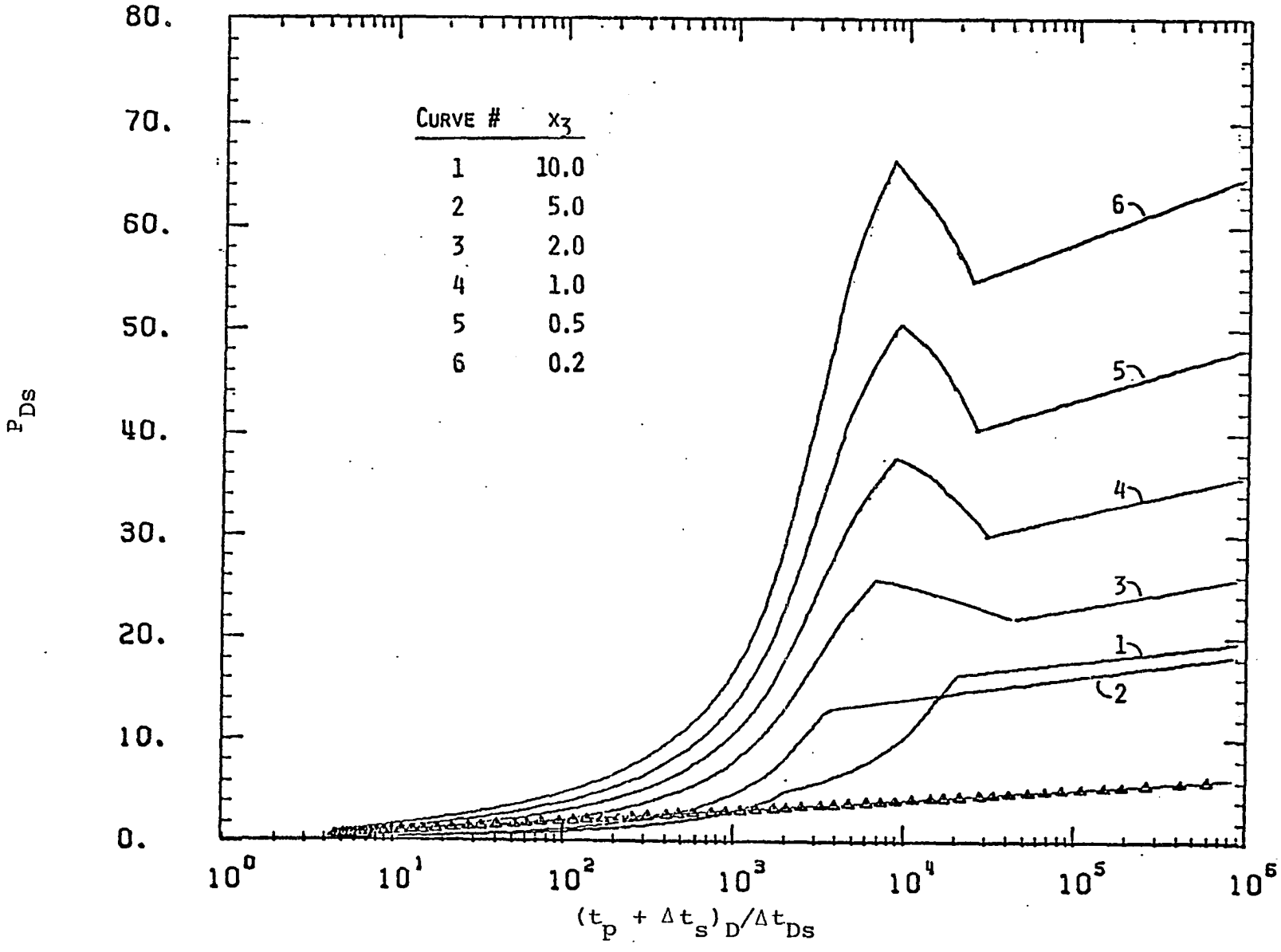

Figure 4.4: Horner buildup graph for a two-layer two-region system with $y_1=y_2=y_3=z=1.$, $x_1=10.$ and $x_2=5.$.

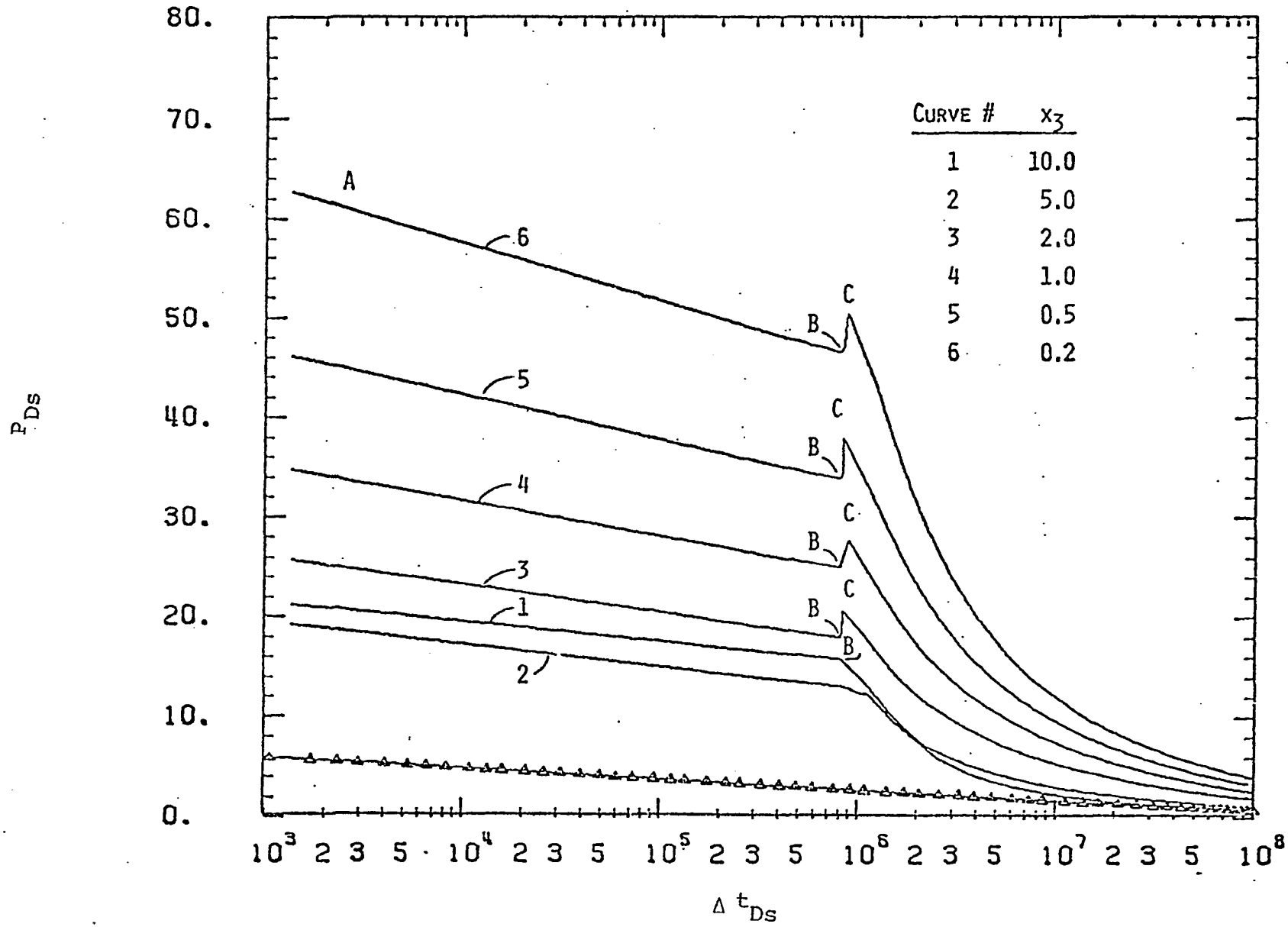

Figure 4.5: Miller-Dyes-Hutchinson buildup graph for a two-layer two-region system with $y_1=y_2=y_3=1.$, $z=2.$, $x_1=10.$ and $x_2=5.$.

the systems presented by Figure 4.5.

As mentioned earlier, points B and C for a particular system represent the arrival time of shutting-in well pressure disturbance to the second region in layer 2 and layer 1 of that system respectively. In other words, interval BC represents the time lag between pressure disturbance arrivals to region 2 in both layers. As the dimension of region 1 of layer 2 increases (z = 2, Figure 4.5) this time lag decreases until it becomes zero and points B and C coincide. For larger values of z, the lag in time would develop again and points B and C becomes far from each other. However, points B and C would represent the arrival time of the pressure disturbance to region 2 in layers 1 and 2 respectively. For z less than 1., the discontinuity points B would be encountered at earlier time than that shown by Figure 4.1.

This leads us to the conclusion that the well bore pressure buildup behavior of a particular multilayered composite reservoir may be very much similar to that of another different reservoir. Unlike the case of drawdown behavior, the slope of early time data (segment AB of buildup curves) does not help to differentiate between the different types of the reservoirs. This is due to the fact that segment AB of buildup curves does not only reflect the effects of region one properties but also reflect those of region 2.

Unless the dimensions of the reservoir blocks are known, Miller-Dyes-Hutchinson (MDH) and Horner's loglog plots cannot

be used to predict the reservoir properties and dimensions using a type curve matching technique similar to that presented in Chapter 3 of this dissertation.

Surprisingly, the most famous procedures (MDH and Horner) used for many years in the oil industry to predict homogeneous reservoir properties from pressure buildup data cannot be used to predict properties and dimensions of multi-layered composite systems.

Horner's semilog plot is presented by Figure 4.6.

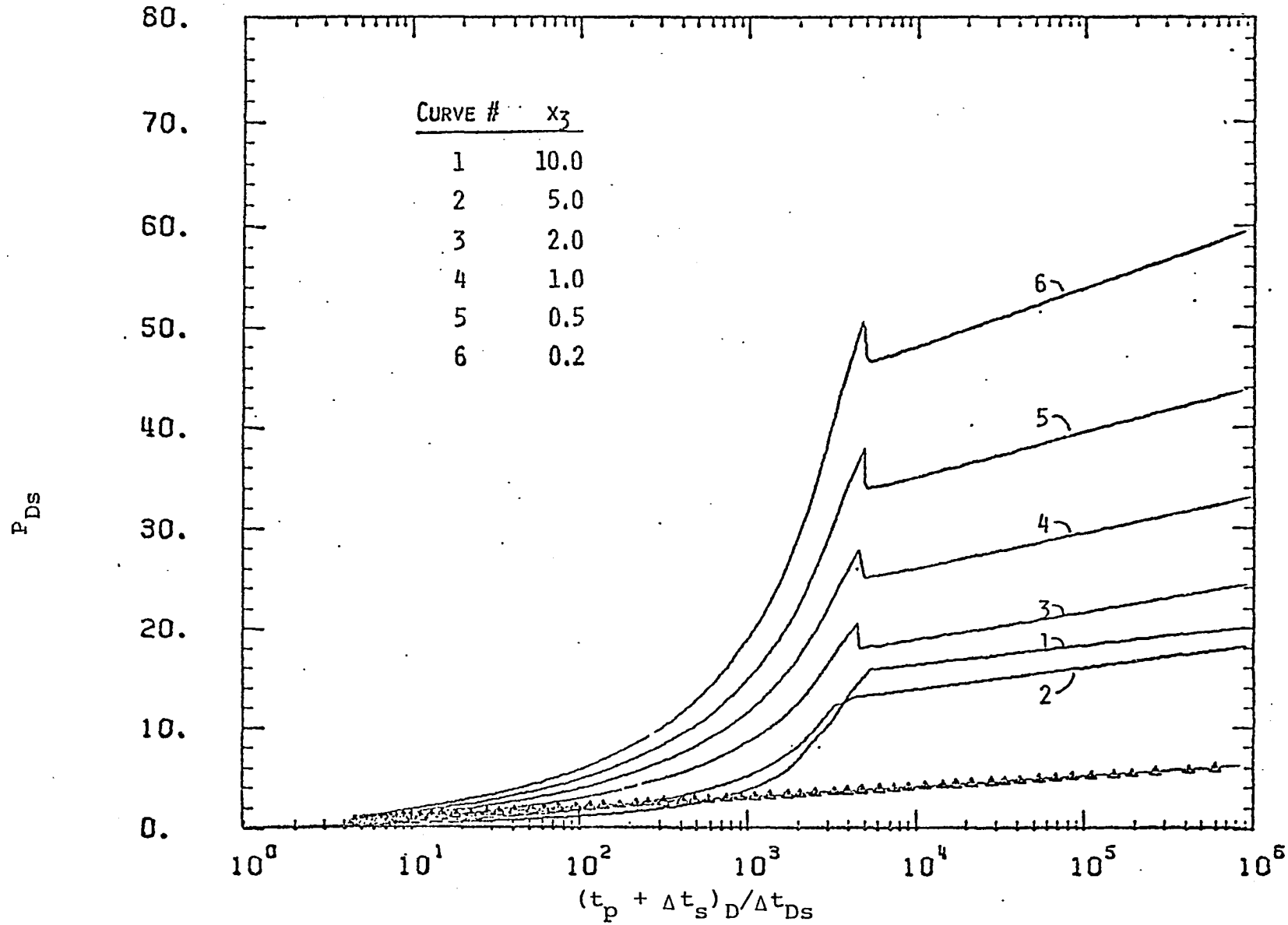

Figure 4.6: Horner buildup graph for a two-layer two-region system with $y_1=y_2=y_3=1.$, $z=2.$, $x_1=10.$ and $x_2=5.$.

CHAPTER 5

PREDICTING WATER FLOODING PERFORMANCE IN MULTILAYERED COMPOSITE RESERVOIRS

5.1 Introduction

Water flooding is dominant among fluid injection methods and is responsible for the current high level of producing rate and reserves within the United States of America and Canada. Its popularity is accounted for by the general availability of water, water's efficiency in displacing oil, the ability with which water spreads through an oil-bearing formation and the water hydraulic head that eases the injection process.

One of the most popular and recommended methods of predicting water flood performance of stratified reservoirs is Dykstra-Parsons method. However, their method is not applicable to composite layered reservoirs where rock properties vary vertically from layer to layer and horizontally from region to region. In this chapter, an approach, which is in fact a modification to Dykstra-Parsons method, to predict water flooding performance in composite layered reservoir is presented. The details of the mathematical treatment presented here are available in Appendix C.

5.2 Reservoir Model

Let us consider the case of a reservoir (shown by Figure 5.1) that consists of n-layers and each layer consists of two regions. Figure 5.1.b shows schematically the details of j^{th} layer of that reservoir. The properties of that layer are ϕ_j, K_j, ℓ_j and h_j for the region that is close to the injector and ϕ'_j, K'_j, $(L - \ell_j)$ and h'_j for the second region that is close to the producer. The width (W) is the same for both regions in all layers. Since the distance between the injector and producer is the same for all layers, the lengths of all layers are the same and equal to L. When the injection into-production from the above described system is under way, the water advances in the system at a speed which varies from layer to layer and from time to time. Also, the proportion of flowing water in each layer varies from layer to layer and from time to time.

The procedure (modification of the Dykstra-Parson method) outlined in this chapter assumes that:

1. Although the dimensions and properties vary from layer to layer and from region to region, a specific region in a particular layer is assumed to be homogeneous and isotropic and filled with incompressible fluids.

2. The reservoir has horizontal and linear geometry and thus the flow in the system is linear and horizontal.

3. All the layers are separated by impermeable zones and consequently vertical or cross-flow is not allowed between

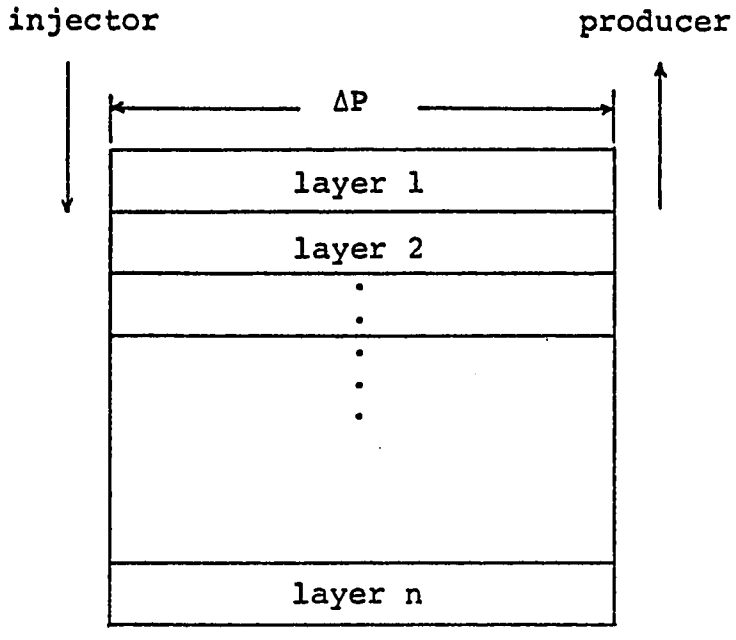

(a)

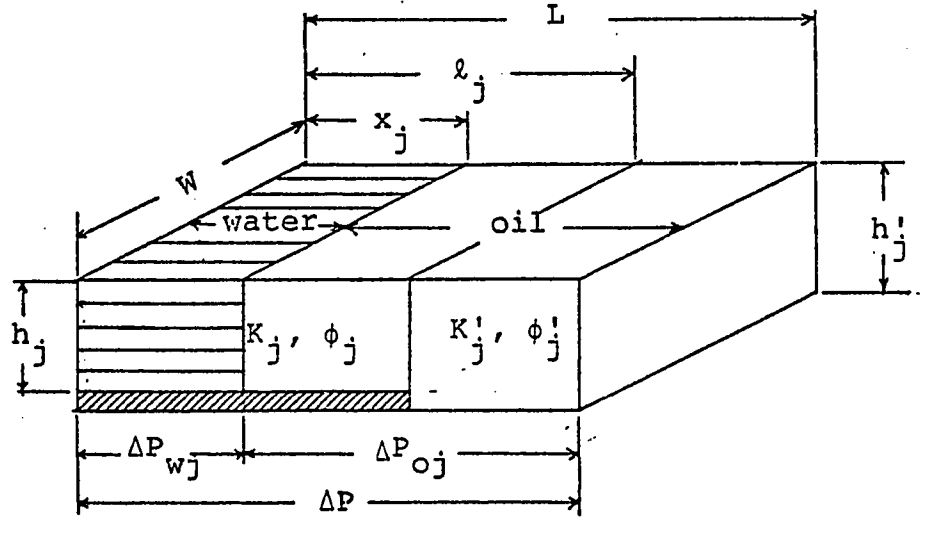

(b)

Figure 5.1 : Schematic diagram showing water flooding in a multilayer composite system

the permeable layers.

4. Since the fluids (oil and water) are assumed to be incompressible, any volume of water injected into the system before break through results in producing the same volume of oil.

5. The oil is produced by a piston-like displacement and consequently the production from any layer, at break through of that layer, changes abruptly from oil to water.

6. At any time of water injection, the pressure drop in a particular layer is equal to those in the other layers.

7. The capilary and gravity forces are negligible.

8. The position of the layers are in an ascending order with respect to their times of break through. In other words, layer one breaks through the first and layer n breaks through the last.

9. Applicability of Darcy's law.

10. Initial water saturation equals to its irreducable saturation.

11. The water front leaves behind it oil at its irreducable saturation.

12. Relative permeability to water behind its front is the same for all swept portions of the reservoir. Also, relative permeability to oil is the same for all unswept portions of the system.

5.3 Pressure Drop

At any point of injection time, pressure drop in a particular layer (j) is equal to that in any of the other layers. The pressure drop in a specific layer j(ΔP) is given as:

$$\Delta P = \Delta P_{0j} + \Delta P_{wj} \quad , j = 1,2,\ldots n \qquad 5.1$$

where ΔP_{0j} and ΔP_{wj} are pressure drops due to the flow of oil and water respectively.

Before break through of a certain layer j, the water front in that layer is at a distance x_j from the injector. The distance x_j increases from zero, at the start of water injection, to ℓ_j when the water front crosses the interface of the two regions in that particular layer j. Then, x_j increases from ℓ_j to L at break through time of that layer j. The pressure drop (ΔP) in layer j is obtained, using Darcy's law for three beds in series, as

$$\Delta P = \frac{q_j \mu_w L}{W K_{rw} K_j h_j} \left[(1-M) \frac{x_j}{L} + M \left(1 - \frac{1}{M'_j}\right) \frac{\ell_j}{L} + \frac{M}{M'_j}\right],$$

$$0 \leq x_j \leq \ell_j, \; j = 1, 2, \ldots n \qquad 5.2$$

The effective velocity in region 1 of layer j is defined as:

$$\frac{dx_j}{dt} = \frac{q_j}{wh_j\phi_j} \tag{5.3}$$

or

$$\frac{q_j}{w} = h_j\phi_j \frac{dx_j}{dt} \tag{5.4}$$

From Equations 5.2 through 5.4, the pressure drop in layer j is given as:

$$\Delta P = M''_{1,j}\left[(1-M)\frac{x_j}{L} + \frac{M}{M'_j}\left\{(M'_j - 1)\frac{\ell_j}{L} + 1\right\}\right]\frac{dx_j}{dt},$$

$$x_j \leq \ell_j,\ j = 1, 2, \ldots n \tag{5.5}$$

Similarly,

$$\Delta P = \frac{M''_{2,j}}{M'_j}\left[(1-M)\frac{x_j}{L} + (M'_j - 1)\frac{\ell_j}{L} + M\right]\frac{dx_j}{dt},$$

$$\ell_j \leq x_j \leq L,\ j = 1, 2, \ldots n \tag{5.6}$$

where:

M = mobility ratio

$$= \frac{K_{rw}}{K_{ro}} \cdot \frac{\mu_o}{\mu_w}$$

$$M'_j = K'_j h'_j / K_j h_j \qquad 5.7$$

$$M''_{1,j} = \frac{\mu_w}{K_{rw}} \cdot \frac{\phi_j}{K_j} \qquad 5.8$$

$$M''_{2,j} = \frac{\mu_w}{K_{rw}} \cdot \frac{\phi'_j \, h'_j}{K_j \, h_j} \qquad 5.9$$

5.4 Water Front Locations

It is a common practice to follow one of two techniques of water flooding: either inject the water at a constant rate and consequently the pressure drop (ΔP) varies with time or keep pressure drop constant and let injection rate varies with time. The two techniques are considered in the following sections.

5.4.1 Constant Injection Rate

Although the pressure drop varies with time, the pressure drops on layers 1 to n, at a certain point of time, are the same and equal to ΔP.

When the i^{th} layer has just broken through, the water front location in the j^{th} layer ($j > i$) is given as

$$\frac{x_j}{L} = \frac{-b_j + \sqrt{b_j^2 - 4\, a'_j \, (c_i/E_j + c_j)}}{2\, a'_j} \qquad 5.10$$

where:

$$\left.\begin{aligned} a'_j &= 1 - M \\ b_j &= 2\,\frac{M}{M'_j}\left[(M'_j - 1)\,\frac{\ell_j}{L} + 1\right] \\ c_j &= 0 \\ E_j &= M''_{1,j} \end{aligned}\right\}, \quad 0 \le x_j \le \ell_j \qquad 5.11$$

$$\left.\begin{aligned} a'_j &= (1-M)/M'_j \\ b_j &= \frac{2}{M'_j}\left[(M'_j - 1)\,\frac{\ell_j}{L} + M\right] \\ c_j &= \frac{M''_{1,j}}{M''_{2,j}}\left(\frac{\ell_j}{L}\right)\left[\left\{1-M+\frac{2M}{M'_j}(M'_j-1)\right\}\frac{\ell_j}{L} + \frac{2M}{M'_j}\right] \\ &\quad + \frac{1}{M'_j}\,\frac{\ell_j}{L}\left[(1+M-2M'_j)\frac{\ell_j}{L} - 2M\right] \\ E_j &= M''_{2,j} \end{aligned}\right\}, \quad \ell_j \le x_j \le L \qquad 5.12$$

$$c_i = -M''_{1,j}\,\frac{\ell_i}{L}\left[\left\{1-M+2\frac{M}{M'_i}\,(M'_i-1)\right\}\frac{\ell_i}{L} + 2\,\frac{M}{M'_i}\right]$$

$$- \frac{M''_{2,j}}{M'_i}\,\left(1-\frac{\ell_i}{L}\right)\left[(1-M)\left(1+\frac{\ell_i}{L}\right)+2(M'_i-1)\frac{\ell_i}{L}+2M\right] \qquad 5.13$$

5.4.2 Constant Injection Pressure

In this case, both injector and producer bottom hole pressures are kept constant during water injection process. The water injection rate varies with time. The time of water front arrival to the interface of the two regions of layer j ($t_{\ell j}$) is obtained by integrating Equation 5.5 as:

$$t_{\ell j} = \frac{1}{2}\frac{L}{\Delta P} M''_{1,j} \left(\frac{\ell_j}{L}\right)\left[\left\{1-M+2\frac{M}{M'_j}(M'_j-1)\right\}\frac{\ell_j}{L} + 2\frac{M}{M'_j}\right] ,$$

$$j = 1, 2, \ldots n \qquad 5.14$$

Similarly, break through time of layer j (t_{Lj}) is given as:

$$t_{Lj} = \frac{1}{2}\frac{L}{\Delta P}\left\{M''_{1,j}\frac{\ell_j}{L}\left[\left\{1-M+2\frac{M}{M'_j}(M'_j-1)\right\}\frac{\ell_j}{L} + 2\frac{M}{M'_j}\right]\right.$$

$$\left. + \frac{M''_{2,j}}{M'_j}\left(1-\frac{\ell_j}{L}\right)\left[(1-M)\left(1+\frac{\ell_j}{L}\right)+2(M'_j-1)\frac{\ell_j}{L} + 2M\right]\right\} ,$$

$$j = 1, 2, \ldots n \qquad 5.15$$

The water front location is given as:

$$\frac{x_j}{L} = \frac{-b_j + \sqrt{b_j^2 + 4\,a'_j\left[2\frac{\Delta P}{L}\frac{1}{E_j}(t - v_j) + d_j\right]}}{2\,a_j} ,$$

$$j = 1, 2, \ldots n \qquad 5.16$$

where

$$\begin{aligned} d_j &= 0 \\ E_j &= M''_{1,j} \qquad , 0 \leq x_j \leq \ell_j \\ v_j &= 0 \end{aligned} \tag{5.17}$$

$$\begin{aligned} d_j &= \frac{\ell_j}{L}\left[(2M'_j - M - 1)\,\frac{\ell_j}{L} + 2M\right] \\ E_j &= M''_{2,j} \qquad , \ell_j \leq x_j \leq L \\ v_j &= t\,\ell_j \end{aligned} \tag{5.18}$$

5.5 Break Through Order

In deriving Equations 5.10 through 5.13, it was assumed that the positions of the layers are in ascending order with respect to their times of break through. In other words, layer one breaks through first and layer n breaks through last.

Unlike Dykstra-Parson method, the properties and dimensions are not enough evidence to detect the order of break through of different layers. For the case of constant injection pressure, Equation 5.15 can be used to determine break through time of any layer j. So the order of layers with respect to their break through time can be determined. Also, Equation 5.14 can be used to determine whether the water front in a specific layer j lies in the first or in the second region of that particular layer.

For the case of constant injection rate, a trial and error procedure should be used to predict the order with which

the layers break through. For two-layer composite system, the order of break through can be obtained as follows:

a - assume that layer one breaks through before layer two and layer one has just broken through,

b - predict water front location ($\frac{x_2}{L}$) in layer two using Equation 5.10, 5.12 and 5.13, and

c - if x_2 predicted in step b is less than L, the assumption made in step a is correct. Otherwise, layer two breaks through before layer one.

The above trial and error technique can be used to predict the order of break through of n layers. Also, trial and error procedure should be used to predict the region, of layer j, in which the water front lies. This is as follows:

a - predict $\frac{x_j}{L}$ using Equations 5.10, 5.11 and 5.13, and

b - if predicted x_j satisfies the condition that $0 \leq x_j \leq \ell_j$, the water front lies in the first region. Otherwise, the water front lies in the second region if the layer has not broken through yet.

5.6 Water Oil Ratio

Before break through, water production is zero and consequently water-oil ratio is zero. After break through the water production and consequently the water-oil ratio increases with time. Perhaps the water-oil ratio is the main factor that determines when the water injection process should be stopped.

For the system under study, when the j^{th} layer has broken through, the water-oil ratio is given as:

$$WOR = \frac{\sum_{i=1}^{j} \frac{K_i h_i}{\ell_i/L + 1/M_i'(1 - \ell_i/L)}}{\sum_{i=j+1}^{n} K_i h_i/Y_i} \qquad 5.21$$

where:

$$Y_i = \frac{x_i}{L} + M[(\frac{\ell_i}{L} - \frac{x_i}{L}) + \frac{1}{M_i'}(1 - \frac{\ell_i}{L})],$$

$$0 \leq x_i \leq \ell_i \qquad 5.20$$

$$Y_i = \frac{\ell_i}{L} + \frac{1}{M_i'}[(\frac{x_i}{L} - \frac{\ell_i}{L}) + M(1 - \frac{x_i}{L})],$$

$$\ell_i \leq x_i \leq L \qquad 5.21$$

5.7 Special Case (M = 1)

For the mobility ratio equals unity, the water front locations are given as follows:

a - constant injection rate

$$\frac{x_j}{L} = \frac{A_i}{E_j A_j}[M''_{1,i}\frac{\ell_i}{L} + M''_{2,i}(1 - \frac{\ell_i}{L})] + H_j ,$$

$$j = 1, 2, \ldots n \qquad 5.22$$

where

$$A_r = \frac{1}{M'_r}\left[(M'_r - 1)\frac{\ell_r}{L} + 1\right], \quad r = i \text{ or } j$$

$$H_j = 0, \quad x_j \leq \ell_i$$

$$H_j = (1 - M''_{1,j}/M''_{2,j})\,\ell_j/L, \quad x_j \geq \ell_j \qquad 5.23$$

b - constant injection pressure

$$\frac{x_j}{L} = \frac{M'_j}{E_j}\,\frac{\Delta p}{L}\,\frac{t}{[(M'_j-1)\frac{\ell_j}{L} + 1.]} + H_j,$$

$$j = 1, 2, \ldots n \qquad 5.24$$

Water-oil ratio is given as:

$$WOR = \frac{\sum_{i=1}^{j}\left[\frac{K_i\,h_i}{\ell_i/L+1/M'_i(1-\ell_i/L)}\right]}{\sum_{i=j+1}^{n}\left[\frac{K_i\,h_i}{\ell_i/L+1/M'_i(1-\ell_i/L)}\right]} \qquad 5.25$$

5.8 Coverage

Coverage is defined as the cross-sectional area contacted by the injected fluid divided by the cross-sectional area enclosed in all layers behind the injected water front. For n-layer composite system with j^{th} layer broken through, coverage (Cov_j) as defined above is given as:

$$Cov_j = \frac{\sum_{i=1}^{j} \left[\frac{\ell_i}{L} h_i + \left(1 - \frac{\ell_i}{L}\right) h_i'\right] + \sum_{i=j+1}^{n} F_i'}{\sum_{i=1}^{n} \left[\frac{\ell_i}{L} h_i + \left(1 - \frac{\ell_i}{L}\right) h_i'\right]} \qquad 5.26$$

where:

$$F_i' = \frac{x_i}{L} h_i, \quad 0 < x_i < \ell_i \qquad 5.27$$

$$F_i' = \frac{\ell_i}{L} h_i + \left(\frac{x_i}{L} - \frac{\ell_i}{L}\right) h_i', \quad \ell_i \leq x_i \leq L \qquad 5.28$$

5.9 Cumulative Oil Recovery

Assuming that the water front in any layer leaves oil at the residual oil saturation, which is assumed to be the same for all layers, the recovery when the j^{th} layer has broken through is given as:

$$N_{pj} = \frac{(S_{oi}-S_{or})W\,L \sum_{i=1}^{n} [\frac{\ell_i}{L}h_i\phi_i+(1-\frac{\ell_i}{L})\,h_i'\phi_i'] \; Cov_j E_s}{B_0},$$

$$j = 1, 2, \ldots n \qquad 5.29$$

where E_s: sweep efficiency which is mainly a function of water flooding pattern, mobility ratio and reservoir heterogeneities

Some investigators proposed prediction methods to account specifically for areal sweep and recovery at break through and their increase after break through. Some of those methods are experimental and others are numerical. The graphical correlations proposed by Dyes, et al. (1954) and Kimbler, et al. (1964), which are widely used, are suggested to be used in this study. The use of their correlations in conjunction with the present approach is illustrated in sample calculations presented later in the next section.

5.10 Water Flooding Performance Example

The previous section of this chapter presented an approach to predict water flooding performance of multilayered composite reservoir. Two important cases (constant injection pressure and constant injection rate) were considered. This section presents the application of this approach.

5.10.1 Description of the Reservoir

Let us consider the case of 20-layered 2-regions reservoir to be water flooded in a five-spot pattern. The graphical correlations proposed by Dyes, et al. (1954), were used to predict the areal sweep efficiency of the system under study. The reservoir rock and fluid properties are:

L (length)	= 1000. ft
W (width)	= 1. ft
S_W (initial water saturation)	= 0.2
S_{or} (residual oil saturation)	= 0.15
B_0	= 1. res. bbl/STB
B_w	= 1. res. bbl/STB
K_{ro} (relative permeability to oil)	= 0.75
K_{rw} (relative permeability to water)	= 0.1244
μ_w (water viscosity)	= 1. cp

oil viscosity

(M = 0.1)	= 0.6029 cp
(M = 0.5)	= 3.0145 cp
(M = 1.)	= 6.029 cp
(M - 2.)	= 12.058 cp
(M = 10.)	= 60.29 cp

The properties of each layer are presented in Table 5.1. The layers are arranged in an ascending order with respect to the permeabilities of the first region from the injector. The calculations were made for different values of

TABLE 5.1:VARIABLE LAYER PROPERTIES OF TWENTY LAYERED COMPOSITE MODEL

LAYER NUMBER	REGION ONE FRACTIONAL LENGTH	REGION ONE PROPERTIES			REGION TWO PROPERTIES		
		POROSITY	PERMEABILITY	THICKNESS	POROSITY	PERMEABILITY	THICKNESS
1	0.500	0.230	185.0	5.00	0.245	125.0	6.00
2	0.420	0.220	157.0	6.00	0.225	600.0	4.50
3	0.580	0.217	134.0	5.50	0.205	200.0	5.00
4	0.600	0.207	120.0	6.20	0.185	78.0	6.00
5	0.330	0.205	109.0	6.80	0.165	26.0	7.30
6	0.700	0.195	100.0	4.50	0.235	120.0	6.00
7	0.280	0.192	91.0	4.20	0.215	330.0	5.00
8	0.800	0.183	82.5	7.30	0.195	125.0	5.80
9	0.750	0.180	74.0	7.50	0.175	47.0	8.00
10	0.450	0.170	63.0	7.00	0.155	11.6	8.20
11	0.600	0.150	61.0	7.10	0.150	10.6	5.00
12	0.550	0.180	58.0	7.30	0.145	30.0	6.00
13	0.390	0.170	53.0	7.50	0.140	40.0	5.50
14	0.450	0.175	49.0	6.00	0.130	50.0	7.00
15	0.900	0.200	42.0	7.20	0.125	60.0	7.50
16	0.870	0.120	41.0	6.80	0.140	55.0	4.20
17	0.820	0.150	38.0	5.40	0.142	45.0	6.20
18	0.760	0.160	35.0	6.00	0.190	65.0	5.40
19	0.670	0.130	34.0	4.50	0.185	70.0	6.10
20	0.850	0.190	15.0	6.80	0.172	15.0	6.90

injection rate, pressure drop and mobility ratios. The results are included in tables 5.2 through 5.10.

5.10.2 Results and Discussions

Tables 5.2 and 5.3 show the water flooding performance for constant flow rates, 80 and 100 BPD respectively. Tables 5.4 and 5.5 show the results for constant injection pressure drop 200 and 250 psi respectively. In all cases, the mobility ratio is the same and equals 0.1. The first column of these tables shows that the breakthrough order of the layers is exactly the same for the different four cases. Also, the last four columns of these tables show that the water-oil ratio, coverage, cumulative water injection and cumulative oil production are not functions of injection flow rate or pressure drop. Tables 5.2 through 5.5 show that oil production rate increases as the injection rate and/or pressure drop increases. From a practical point of view, there are two limitations: the injection rate should not exceed the available pumping capacity and the injection pressure should not exceed the formation fracturing pressure.

Tables 5.3 and 5.6 through 5.9 show the results of water flooding performance for mobility ratios 0.1, 0.5, 1., 2. and 10. respectively. In these cases, the injection rate is constant and equal to 100 BPD. The first column of these tables shows that the breakthrough order of the layers is not the same. For example, at M = 0.5, layer 8 breaks through just before layer 6; but at M = 1., layer 6 breaks through

TABLE 5.2: WATER FLOODING PERFORMANECE FOR TWENTY LAYERED COMPOSITE MODEL WITH VARIABLE PRESSURE DROP, CONSTANT INJECTION RATE (Q= 80.0) AND MOBILITY RATIO = 0.10.

B. T. LAYER	PRESSURE DROP, PSI	OIL PROD. RATE, BPD	WATER PROD. RATE, BPD	WATER OIL RATIO	COVERAGE, FRACTION	CUMULATIVE WATER INJECTION, BBL	CUMULATIVE OIL PRODUCTION, BBL
2	114.58	71.89	8.11	0.11	0.513	3920.29	3918.73
3	142.74	64.38	15.62	0.24	0.670	5289.93	5117.39
7	149.67	57.63	22.37	0.39	0.708	5653.71	5406.11
1	151.27	51.54	28.46	0.55	0.716	5756.30	5472.20
4	157.46	45.94	34.05	0.74	0.751	6175.16	5735.80
8	167.41	38.92	41.08	1.06	0.799	6853.57	6105.77
6	173.88	33.21	46.79	1.41	0.838	7487.52	6401.22
9	177.57	28.10	51.90	1.85	0.861	7993.39	6578.89
16	180.03	25.10	54.90	2.19	0.878	8408.35	6709.06
13	181.24	22.47	57.53	2.56	0.887	8662.71	6780.51
14	182.64	19.28	60.72	3.15	0.899	9023.18	6867.37
12	183.60	16.70	63.30	3.79	0.907	9310.30	6927.30
17	187.60	13.43	66.57	4.96	0.946	10863.68	7225.25
5	187.66	11.20	68.80	6.14	0.946	10901.74	7230.58
15	188.90	7.99	72.01	9.01	0.962	11800.88	7346.73
18	189.05	5.88	74.12	12.61	0.963	11996.35	7361.09
11	189.42	4.74	75.26	15.87	0.968	12574.18	7395.34
19	189.65	2.93	77.07	26.29	0.971	13252.49	7420.19
10	190.52	1.27	78.73	62.15	0.983	16668.61	7507.67

TABLE 5.3: WATER FLOODING PERFORMANECE FOR TWENTY LAYERED COMPOSITE MODEL WITH VARIABLE PRESSURE DROP, CONSTANT INJECTION RATE (Q= 100.0) AND MOBILITY RATIO = 0.10.

B. T. LAYER	PRESSURE DROP, PSI	OIL PROD. RATE, BPD	WATER PROD. RATE, BPD	WATER OIL RATIO	COVERAGE, FRACTION	CUMULATIVE WATER INJECTION, BBL	CUMULATIVE OIL PRODUCTION, BBL
2	143.23	89.87	10.13	0.11	0.513	3920.28	3918.73
3	178.42	80.47	19.53	0.24	0.670	5289.93	5117.39
7	187.09	72.04	27.96	0.39	0.708	5653.72	5406.11
1	189.09	64.42	35.58	0.55	0.716	5756.31	5472.20
4	196.83	57.43	42.57	0.74	0.751	6175.16	5735.80
8	209.26	48.65	51.35	1.06	0.799	6853.57	6105.77
6	217.36	41.51	58.49	1.41	0.838	7487.52	6401.22
9	221.97	35.12	64.88	1.85	0.861	7993.39	6578.89
16	225.04	31.37	68.63	2.19	0.878	8408.33	6709.06
13	226.55	28.09	71.91	2.56	0.887	8662.70	6780.51
14	228.30	24.10	75.90	3.15	0.899	9023.16	6867.37
12	229.49	20.87	79.13	3.79	0.907	9310.29	6927.30
17	234.50	16.79	83.21	4.96	0.946	10863.66	7225.25
5	234.58	14.00	86.00	6.14	0.946	10901.72	7230.58
15	236.12	9.99	90.01	9.01	0.962	11800.86	7346.73
18	236.31	7.35	92.65	12.61	0.963	11996.33	7361.09
11	236.77	5.93	94.07	15.87	0.968	12574.16	7395.34
19	237.06	3.66	96.34	26.29	0.971	13252.47	7420.19
10	238.15	1.58	98.42	62.15	0.983	16668.59	7507.67

TABLE 5.4: WATER FLOODING PERFORMANECE FOR TWENTY LAYERED COMPOSITE MODEL
WITH VARIABLE INJECTION RATE, CONSTANT PRESSURE DROP (DP= 200.0)
AND MOBILITY RATIO = 0.10.

B. T. LAYER	INJECTION RATE, BPD	OIL PROD. RATE, BPD	WATER PROD. RATE, BPD	WATER OIL RATIO	COVERAGE, FRACTION	CUMULATIVE WATER INJECTION, BBL	CUMULATIVE OIL PRODUCTION, BBL
2	139.63	125.49	14.15	0.11	0.513	3920.28	3918.73
3	112.09	90.20	21.89	0.24	0.670	5289.93	5117.39
7	106.90	77.01	29.89	0.39	0.708	5653.72	5406.10
1	105.77	68.14	37.63	0.55	0.716	5756.31	5472.19
4	101.61	58.36	43.26	0.74	0.751	6175.16	5735.80
8	95.57	46.49	49.08	1.06	0.799	6853.56	6105.77
6	92.01	38.19	53.82	1.41	0.838	7487.52	6401.22
9	90.10	31.65	58.46	1.85	0.861	7993.38	6578.89
16	88.87	27.88	60.99	2.19	0.878	8408.33	6709.07
13	88.28	24.80	63.48	2.56	0.887	8662.69	6780.51
14	87.61	21.11	66.50	3.15	0.899	9023.15	6867.37
12	87.15	18.19	68.96	3.79	0.907	9310.28	6927.30
17	85.29	14.32	70.97	4.96	0.946	10863.65	7225.25
5	85.26	11.94	73.32	6.14	0.946	10901.72	7230.58
15	84.70	8.46	76.24	9.01	0.962	11800.85	7346.73
18	84.63	6.22	78.42	12.61	0.963	11996.33	7361.09
11	84.47	5.01	79.46	15.87	0.968	12574.15	7395.34
19	84.37	3.09	81.28	26.29	0.971	13252.46	7420.20
10	83.98	1.33	82.65	62.15	0.983	14668.58	7507.68

TABLE 5,5: WATER FLOODING PERFORMANECE FOR TWENTY LAYERED COMPOSITE MODEL
WITH VARIABLE INJECTION RATE, CONSTANT PRESSURE DROP (DP= 250.0)
AND MOBILITY RATIO = 0.10.

B. T. LAYER	INJECTION RATE, BPD	OIL PROD. RATE, BPD	WATER PROD. RATE, BPD	WATER OIL RATIO	COVERAGE, FRACTION	CUMULATIVE WATER INJECTION, BBL	CUMULATIVE OIL PRODUCTION, BBL
2	174.54	156.86	17.68	0.11	0.513	3920.28	3918.73
3	140.12	112.75	27.36	0.24	0.670	5289.93	5117.39
7	133.63	96.27	37.36	0.39	0.708	5653.72	5406.10
1	132.21	85.18	47.04	0.55	0.716	5756.31	5472.20
4	127.02	72.95	54.07	0.74	0.751	6175.16	5735.80
8	119.47	58.12	61.35	1.06	0.799	6853.56	6105.77
6	115.02	47.74	67.28	1.41	0.838	7487.52	6401.22
9	112.63	39.56	73.07	1.85	0.861	7993.38	6578.89
16	111.09	34.85	76.24	2.19	0.878	8408.33	6709.07
13	110.35	31.00	79.35	2.56	0.887	8662.69	6780.51
14	109.51	26.39	83.12	3.15	0.899	9023.15	6867.37
12	108.94	22.74	86.20	3.79	0.907	9310.28	6927.30
17	106.61	17.90	88.71	4.96	0.946	10863.65	7225.25
5	106.57	14.92	91.65	6.14	0.946	10901.72	7230.58
15	105.88	10.57	95.31	9.01	0.962	11800.85	7346.73
18	105.79	7.77	98.02	12.61	0.963	11996.33	7361.09
11	105.59	6.26	99.33	15.87	0.968	12574.15	7395.34
19	105.46	3.86	101.60	26.29	0.971	13252.46	7420.20
10	104.98	1.66	103.31	62.15	0.993	16668.58	7507.68

TABLE 5.6:WATER FLOODING PERFORMANECE FOR TWENTY LAYERED COMPOSITE MODEL
WITH VARIABLE PRESSURE DROP. CONSTANT INJECTION RATE (Q= 100.0)
AND MOBILITY RATIO = 0.50.

B. T. LAYER	PRESSURE DROP, PSI	OIL PROD. RATE, BPD	WATER PROD. RATE, BPD	WATER OIL RATIO	COVERAGE, FRACTION	CUMULATIVE WATER INJECTION, BBL	CUMULATIVE OIL PRODUCTION, BBL
2	178.33	87.39	12.61	0.14	0.357	2197.09	2186.85
7	197.89	78.09	21.91	0.28	0.526	3485.52	3289.58
3	199.46	70.19	29.81	0.42	0.540	3689.62	3422.84
1	205.71	61.30	38.70	0.63	0.594	4338.11	3870.16
4	213.40	53.85	46.15	0.86	0.669	5434.38	4510.43
8	216.15	46.96	53.04	1.13	0.699	6058.65	4828.50
6	217.74	41.41	58.59	1.42	0.717	6466.42	4997.34
9	224.74	34.31	65.69	1.91	0.792	8079.02	5022.33
16	226.57	30.90	69.10	2.24	0.812	8676.85	5819.98
14	228.22	26.96	73.04	2.71	0.833	9542.65	6053.41
13	230.30	23.43	76.57	3.27	0.860	10672.75	6340.83
12	232.77	19.74	80.26	4.06	0.897	12324.98	6704.50
17	233.08	17.29	82.71	4.78	0.902	12779.68	6783.11
18	234.77	14.14	85.86	6.07	0.928	14267.93	7022.96
19	234.96	11.94	88.06	7.38	0.930	14719.26	7076.86
15	235.18	8.42	91.58	10.87	0.933	15323.87	7127.78
5	235.64	5.47	94.53	17.27	0.938	16005.26	7165.06
11	238.40	3.12	96.88	31.07	0.975	22087.80	7451.48
10	238.69	1.36	98.64	72.50	0.982	24015.14	7502.89

TABLE 5.7: WATER FLOODING PERFORMANECE FOR TWENTY LAYERED COMPOSITE MODEL WITH VARIABLE PRESSURE DROP, CONSTANT INJECTION RATE (Q= 100.0) AND MOBILITY RATIO = 1.00.

B. T. LAYER	PRESSURE DROP, PSI	OIL PROD. RATE, BPD	WATER PROD. RATE, BPD	WATER OIL RATIO	COVERAGE, FRACTION	CUMULATIVE WATER INJECTION, BBL	CUMULATIVE OIL PRODUCTION, BBL
2	239.22	83.08	16.92	0.20	0.217	1232.23	1207.47
7	239.22	73.52	26.48	0.36	0.363	2321.18	2093.40
3	239.22	64.25	35.75	0.56	0.423	2944.17	2536.58
1	239.22	54.99	45.01	0.82	0.487	3766.30	3032.47
4	239.22	48.26	51.74	1.07	0.598	5243.14	3816.75
6	239.22	42.59	57.41	1.35	0.604	5514.48	3932.33
8	239.22	35.63	64.37	1.81	0.610	5936.19	4082.57
9	239.22	30.08	69.92	2.32	0.731	8684.64	5016.56
16	239.22	27.05	72.95	2.70	0.753	9501.87	5248.59
14	239.22	23.44	76.56	3.27	0.769	10401.94	5459.59
13	239.22	20.46	79.54	3.89	0.838	12924.59	6034.06
17	239.22	18.06	81.94	4.54	0.856	14038.57	6235.19
19	239.22	15.89	84.11	5.30	0.866	14894.83	6371.21
18	239.22	13.29	86.71	6.53	0.886	16421.67	6594.48
12	239.22	10.34	89.66	8.67	0.889	17417.66	6697.51
15	239.22	6.85	93.15	13.60	0.900	19267.74	6844.47
5	239.22	4.04	95.96	23.77	0.919	22485.67	7023.50
11	239.22	2.79	97.21	34.90	0.981	34441.75	7497.67
10	239.22	1.14	98.86	86.56	0.981	34525.88	7498.63

TABLE 5.8 WATER FLOODING PERFORMANECE FOR TWENTY LAYERED COMPOSITE MODEL WITH VARIABLE PRESSURE DROP, CONSTANT INJECTION RATE (Q= 100.0) AND MOBILITY RATIO = 2.00.

B. T. LAYER	PRESSURE DROP, PSI	OIL PROD. RATE, BPD	WATER PROD. RATE, BPD	WATER OIL RATIO	COVERAGE, FRACTION	CUMULATIVE WATER INJECTION, BBL	CUMULATIVE OIL PRODUCTION, BBL
2	356.13	74.81	25.19	0.34	0.228	1182.44	1145.65
7	331.32	63.32	36.68	0.58	0.319	1887.50	1666.56
3	307.29	54.08	45.92	0.85	0.410	2767.41	2219.27
1	284.69	44.56	55.44	1.24	0.469	3629.91	2660.65
6	281.83	40.30	59.70	1.48	0.548	4772.49	3175.78
8	275.06	33.72	66.28	1.97	0.584	5681.62	3515.55
4	273.37	26.44	73.56	2.78	0.594	6619.37	3763.45
9	261.23	23.65	76.35	3.23	0.711	9753.71	4612.75
16	258.88	21.05	78.95	3.75	0.732	10813.17	4849.34
14	258.15	17.38	82.62	4.75	0.740	11869.23	5032.91
19	254.09	16.38	83.62	5.11	0.793	14069.54	5430.31
17	251.58	14.67	85.33	5.82	0.820	15625.24	5679.00
13	249.72	12.19	87.81	7.20	0.837	17245.70	5893.84
18	248.85	9.79	90.21	9.21	0.847	18897.04	6055.57
15	246.41	7.08	92.92	13.13	0.873	22373.57	6350.96
12	245.22	4.51	95.49	21.16	0.883	25515.17	6512.34
5	243.43	2.35	97.65	41.60	0.908	29608.47	6694.66
10	240.58	1.84	98.16	53.38	0.976	46663.01	7192.19
11	239.83	0.89	99.11	111.46	0.984	50395.87	7255.25

TABLE 5.9: WATER FLOODING PERFORMANECE FOR TWENTY LAYERED COMPOSITE MODEL WITH VARIABLE PRESSURE DROP, CONSTANT INJECTION RATE (Q= 100.0) AND MOBILITY RATIO = 10.00.

B. T. LAYER	PRESSURE DROP, PSI	OIL PROD. RATE, BPD	WATER PROD. RATE, BPD	WATER OIL RATIO	COVERAGE, FRACTION	CUMULATIVE WATER INJECTION, BBL	CUMULATIVE OIL PRODUCTION, BBL
2	818.44	42.11	57.89	1.37	0.174	1214.17	913.23
7	669.78	25.85	74.15	2.87	0.217	2291.32	1258.96
3	520.93	22.16	77.84	3.51	0.342	5120.63	2037.68
1	437.60	17.67	82.33	4.66	0.405	7413.43	2496.02
6	410.86	12.96	87.04	6.71	0.439	9564.11	2812.12
8	369.36	11.00	89.00	8.09	0.511	13728.36	3332.10
4	339.69	8.59	91.41	10.64	0.552	17407.71	3680.46
19	318.68	11.35	88.65	7.81	0.659	22191.14	4281.39
9	305.58	7.91	92.09	11.64	0.673	25184.24	4521.51
14	295.84	6.39	93.61	14.65	0.690	28134.98	4706.59
16	291.60	4.03	95.97	23.80	0.694	30787.74	4801.48
17	281.76	4.43	95.57	21.55	0.757	39314.89	5233.21
18	276.46	3.23	96.77	29.98	0.779	42950.29	5384.96
13	265.25	3.85	96.15	24.96	0.822	49692.99	5682.81
15	261.27	1.48	98.52	66.72	0.830	51956.27	5741.21
12	253.90	1.13	98.87	87.39	0.868	66246.87	6004.60
5	248.03	0.50	99.50	198.25	0.895	79277.44	6191.66
10	243.99	0.44	99.56	223.91	0.966	144827.87	6680.87
11	240.84	0.47	99.53	211.35	0.991	168252.81	6852.43

just before layer 8.

Figure 5.2 shows cumulative water injection versus cumulative oil production for mobility ratios 0.1, 0.5, 1.0, 2. and 10. During early injection time (before breakthrough), cumulative oil production is equal to cumulative water injection. It can be concluded that as the mobility ratio increases, the reservoir breaks through earlier. After breakthrough, the cumulative water injection increases asymptotically as cumulative oil production increases. For a particular value of cumulative water injection, the cumulative oil production increases as the mobility ratio decreases. This explains why the mobility ratio is called favorable if it is less or equal to unity and unfavorable if it is greater than unity.

Figure 5.3 shows pressure drop versus cumulative oil production for different mobility ratios. For mobility ratio (M) = 1., the pressure drop during the water flood life is constant. This is due to the fact that for a certain flow rate, the necessary pressure gradient is the same in the swept and the unswept portions of the reservoir. For mobility ratio greater (less) than 1., this pressure gradient in the swept portions is less (greater) than that in the unswept portions of the reservoir. This explains why the pressure drop decreases (increases) as cumulative oil production increases.

Figure 5.4 shows oil production rate versus cumulative oil production for different values of mobility ratios. Figure 5.4 shows that after breakthrough, except for the case of M =

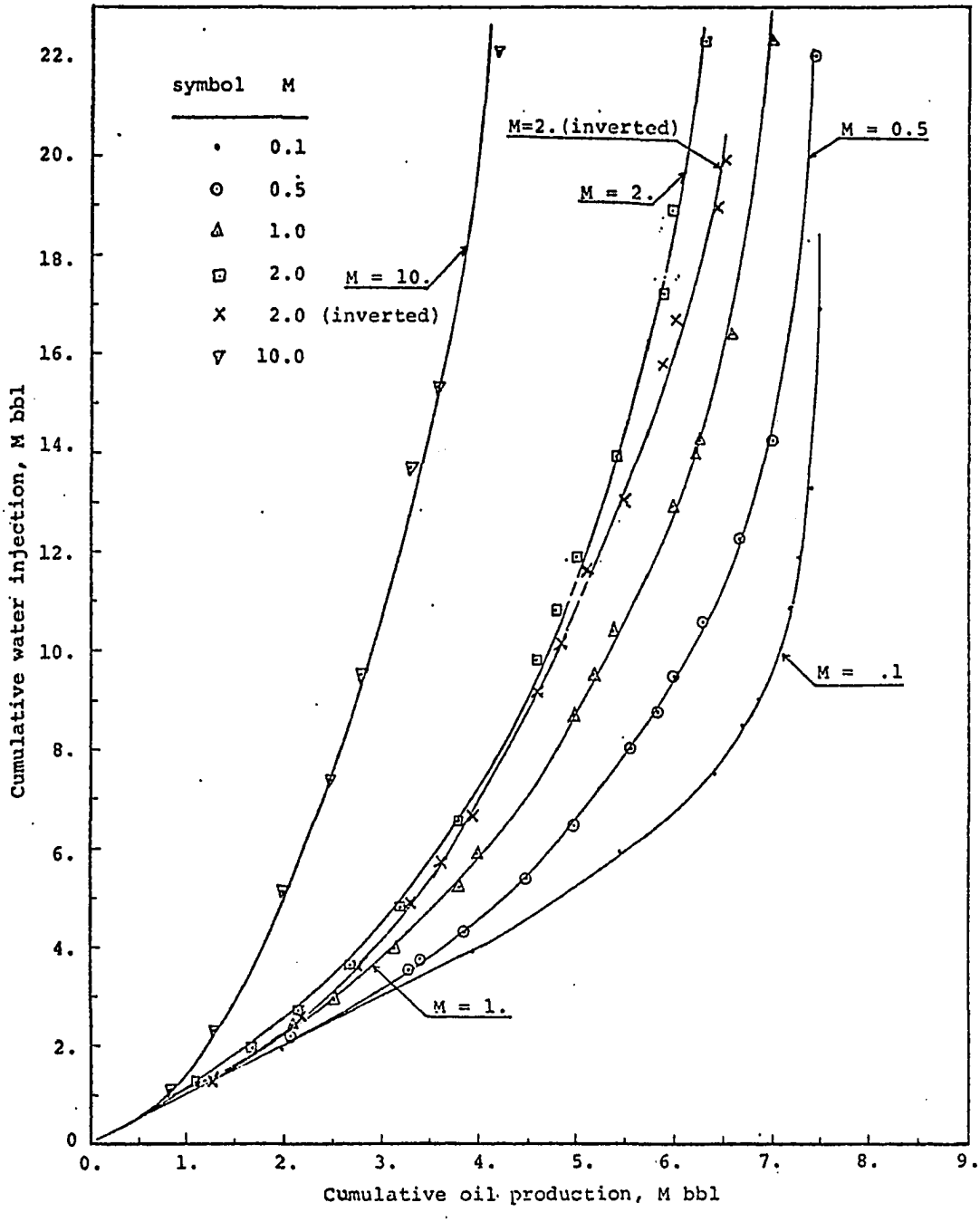

Figure 5.2: Cumulative water injection versus cumulative oil production with Q = 100. BPD

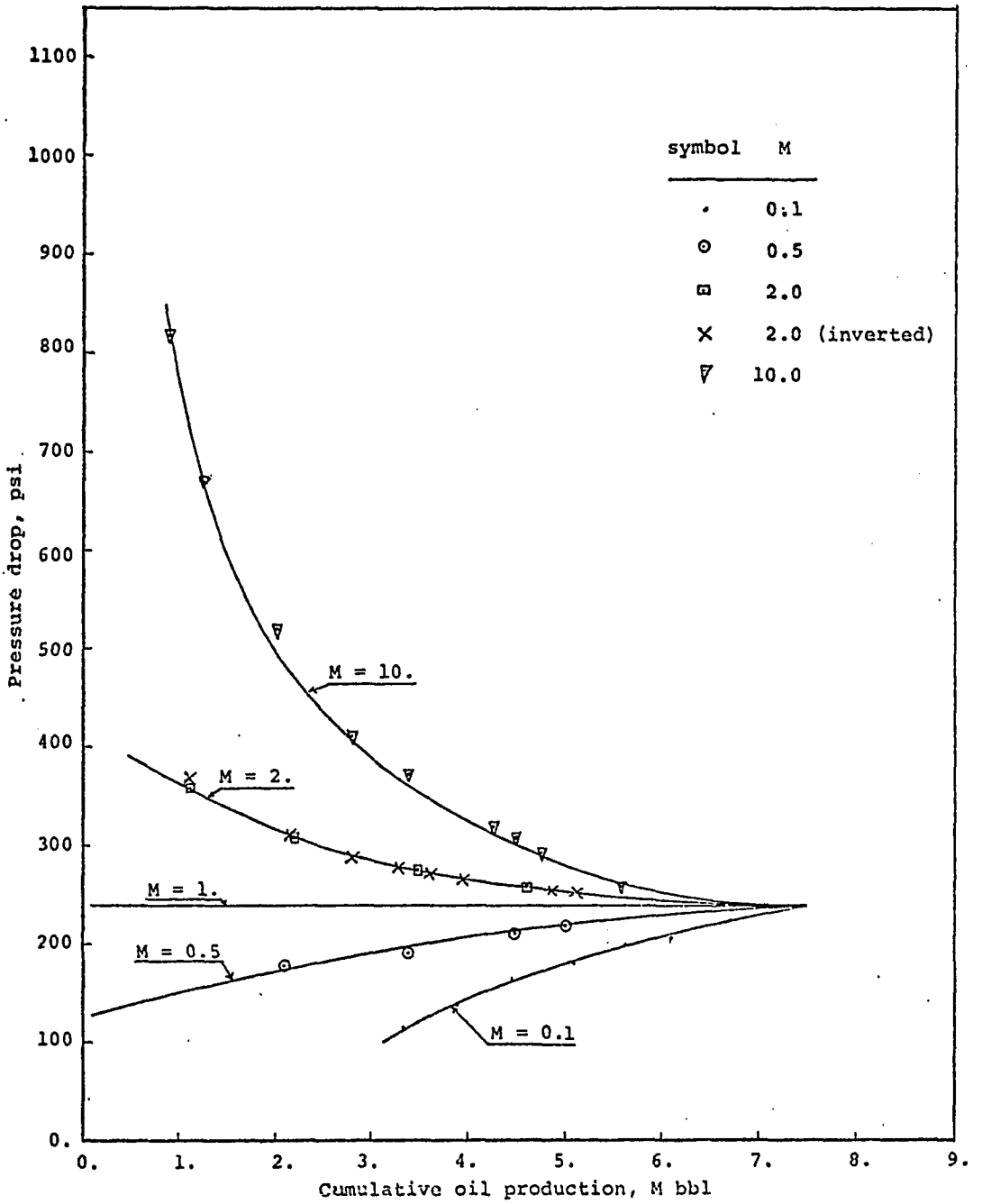

Figure 5.3: Pressure drop versus cumulative oil production with Q = 100. BPD

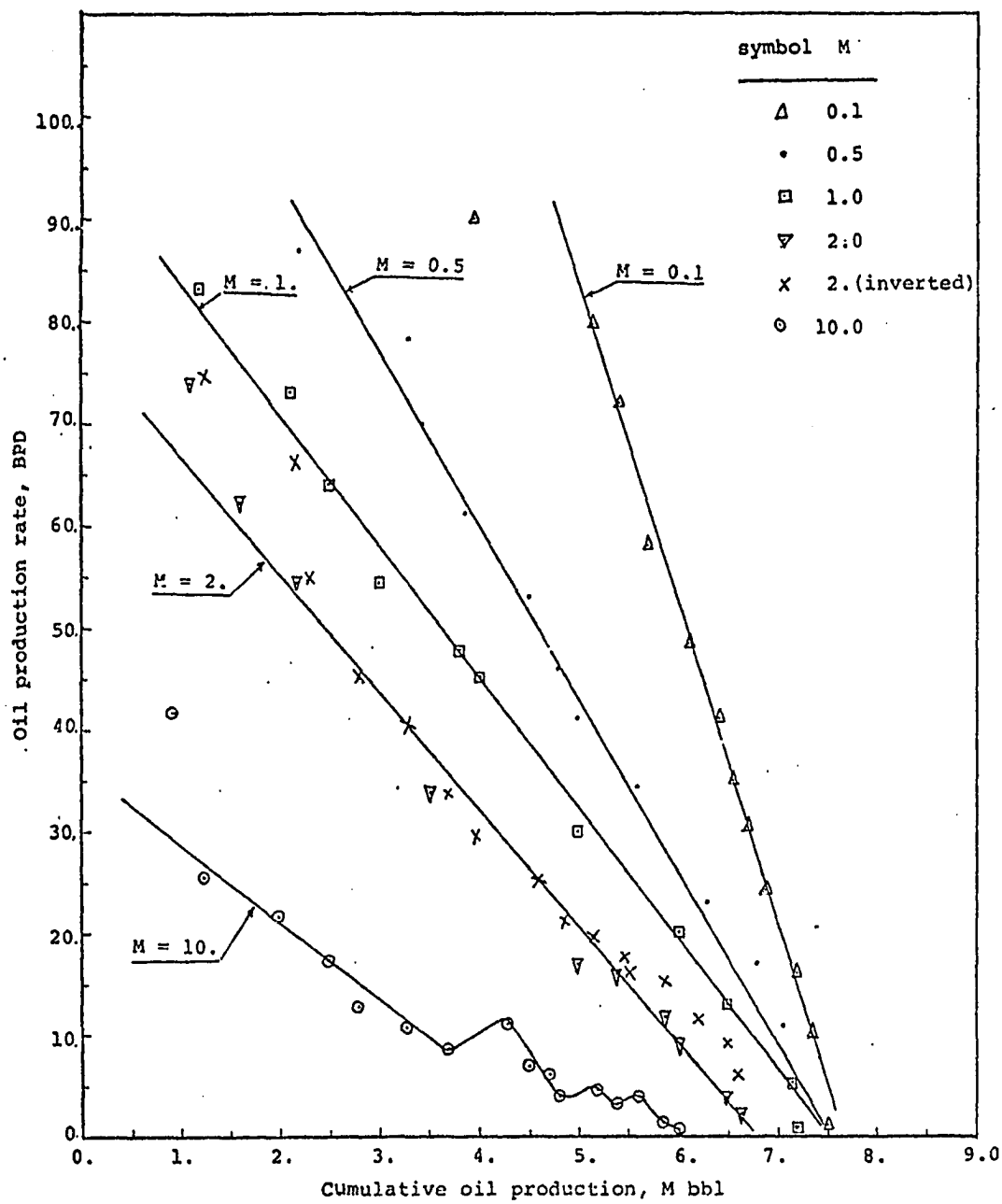

Figure 5.4: Oil production rate versus cumulative oil production with Q = 100. BPD

10, oil production rate is linearly related to the cumulative oil production; as the cumulative oil production increases the oil production rate decreases. For the case of M = 10, the pressure gradient in the swept portions is lower than that in the unswept portions. That is to say as the swept portions increase, the system pressure drop decreases and consequently the flow rate through the broken through layers decrease. Since the injection rate is constant, flow rates through the unbroken through layers increase which results in a higher oil production rate. On the other hand, as the number of broken through layers increases, oil production rate decreases. This explains why the oil production rate fluctuates during the water flooding life. This also explains why the WOR for M = 10 fluctuates as shown by Figure 5.5. This phenomena does not exist for the case of M = 2. because the decrease in oil production due to the increase of broken through layers is higher than the increase due to the decrease in pressure drop. For mobility ratio less than unity, the two factors act in the direction of decreasing the oil production rate. Thus the oil production rate decreases and WOR increases as the cumulative oil production increases as shown by Figures 5.4 and 5.5 respectively.

This leads us to the conclusion that at very high mobility ratios, both oil production rate and WOR are fluctuating during the water flooding life.

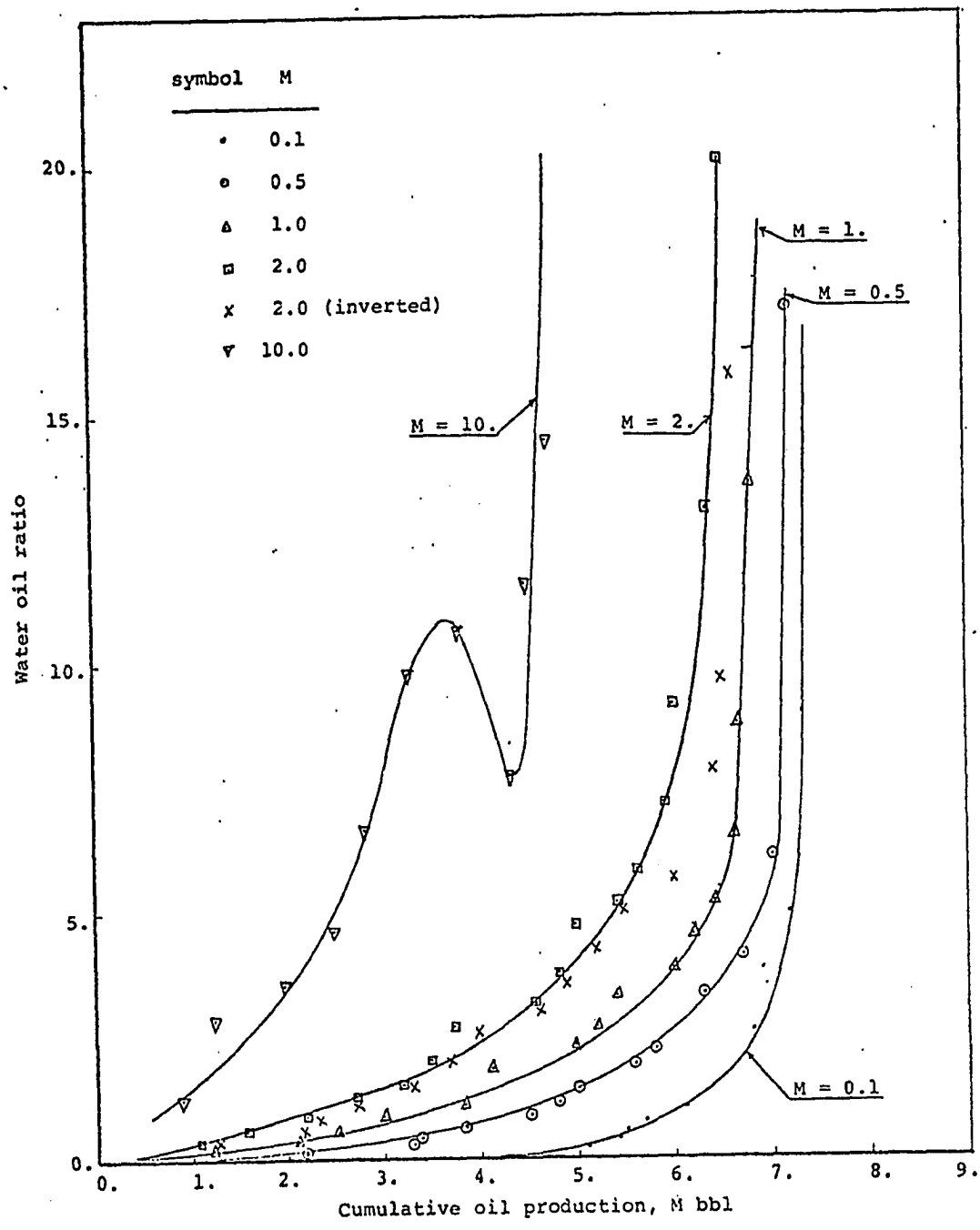

Figure 5.5: Water oil ratio versus cumulative oil production with Q = 100. BPD

Table 5.10 shows the results of water flooding performance for the same system presented in Section 5.10.1 with the exception that the injector (producer) is inverted to the producer (injector) before starting water flooding. These results are for a mobility ratio equal to 2. The first column of tables 5.8 and 5.10 show that the breakthrough orders of the reservoir layers for both cases (normal and inverted) are different. The cumulative water injection, the pressure drop, oil production rate and water oil ratio results are presented (by symbol "x") in figures 5.2 through 5.5 respectively. By comparing the two curves of M = 2 (normal and inverted) of Figure 5.2, it can be noticed that for a certain cumulative water injection, the cumulative oil production is higher for the inverted case. This can be related to WOR behavior presented in Figure 5.5 which shows that for a particular WOR, the cumulative oil production is higher for the inverted case. Figure 5.3 shows that the injection pressure drop is the same for the two cases. However, Figure 5.4 shows that oil production rate is slightly higher for the inverted case than for the normal case.

This shows the importance of selecting the locations of the injectors and the producers in a water flooding project.

TABLE 5.10:WATER FLOODING PERFORMANECE FOR TWENTY LAYERED COMPOSITE MODEL
WITH VARIABLE PRESSURE DROP, CONSTANT INJECTION RATE (Q= 100.0)
AND MOBILITY RATIO = 2.00, "INVERTED CASE".

B. T. LAYER	PRESSURE DROP, PSI	OIL PROD. RATE, BPD	WATER PROD. RATE, BPD	WATER OIL RATIO	COVERAGE, FRACTION	CUMULATIVE WATER INJECTION, BBL	CUMULATIVE OIL PRODUCTION, BBL
2	363.68	74.27	25.73	0.35	0.265	1326.80	1282.98
7	307.58	65.95	34.05	0.52	0.418	2490.25	2163.74
3	303.22	54.69	45.31	0.83	0.432	2795.73	2330.80
1	290.20	45.40	54.60	1.20	0.491	3635.92	2767.62
4	276.13	40.28	59.72	1.48	0.573	4858.65	3324.21
8	270.15	33.70	66.30	1.97	0.608	5769.19	3663.98
6	267.09	28.13	71.87	2.56	0.629	6645.91	3929.73
9	257.94	24.61	75.39	3.06	0.716	9096.65	4612.34
16	255.40	22.11	77.89	3.52	0.742	10220.75	4877.07
14	253.08	19.01	80.99	4.26	0.767	11617.16	5163.79
13	250.24	16.80	83.20	4.95	0.803	13365.96	5487.54
12	246.32	15.07	84.93	5.64	0.854	15824.91	5904.27
17	245.59	12.85	87.15	6.78	0.863	16952.86	6049.23
18	242.19	11.43	88.57	7.75	0.900	19441.06	6368.24
19	241.83	9.37	90.63	9.68	0.903	20628.10	6479.41
15	241.58	5.93	94.07	15.87	0.907	23441.18	6646.19
5	241.35	3.18	96.82	30.44	0.913	26100.05	6730.77
11	240.32	2.34	97.66	41.78	0.964	37122.85	7108.64
10	240.10	0.78	99.22	127.35	0.974	41077.44	7182.38

CHAPTER 6

CONCLUSIONS

An approximate solution for unsteady state single phase flow for a single well located in the center of a multi-layered composite reservoir was obtained. The powerful superposition technique in time was used to take into account the variations in flow rates from each layer. Also, the same technique was used to calculate the fractional flow rates from each layer. A thorough analysis of a single well located in the center of a two-layer two-region reservoir was conducted. For this case, drawdown and buildup analysis were considered.

It was found that the drawdown type-curve matching technique is a powerful tool to determine the transmissibility of different homogeneous blocks of the reservoir. The same technique was found useful in estimating the dimensions and the average storage of the system. For the pressure buildup case, it was found that different reservoirs with different dimensions may behave in a very similar fashion. Thus the famous procedures (Horner and MDH) that have been used for a long time in the oil industry to predict the reservoir properties are not recommended to be used to predict the characteristics of multilayered composite systems.

Also, a modification to the Dykstra-Parson method to predict water flooding performance of multilayered composite reservoirs was presented. The modification takes into account the variations in reservoir properties and dimensions vertically and horizontally. Although the Dykstra-Parson method is limited to the case of constant injection rate, the modifications presented in this study treated the two cases of constant injection rate and constant injection pressure.

The following specific conclusions are reached from this study:

I. Pressure Analysis of Heterogeneous Reservoirs

1. The transmissibilities and dimensions of multilayered composite reservoirs are the main factors that affect the pressure and fractional flow rate behavior of these systems. However, the storage variation from layer to layer and from region to region has little effect. This is due to the fact that fluid flow in porous media is mainly controlled by the system transmissibility and not by its storage.

2. In multilayered composite reservoirs, the dimensionless time needed to reach stability varies with the properties and dimensions of different homogeneous blocks of these reservoirs. Reservoirs with significant changes in their properties stabilize at longer times than those required for the reservoirs with minor changes to reach stability. The reason for this lies mainly in the changing rates of production from each layer which depends on the reservoir characteristics.

3. A plot of flowing well pressure versus time on a semilog graph yields a straight line for the early production data. The slope of this straight line depends on region 1 characteristics. For the case that region 1 is homogeneous, the slope of this straight line is 1.151., otherwise the slope is different from 1.151. This finding can be used to select the proper master-curve for applying the type-curve matching technique as outlined in Section 3.7.

4. The drawdown type-curve plots presented in Chapter 3 and Appendix D can be used to determine the dimensions and transmissibilities of each homogeneous block of two-layer composite reservoirs. Although the variation in storage from layer to layer and from region to region cannot be determined by using these type-curve plots, an average value can be obtained in absence of other better means.

5. The fractional flow rate from each layer of multi-layered composite reservoirs depends on the reservoir properties and dimensions. During the early production time, the fractional flow rates experience minor changes. As the production time increases, the fractional flow rate changes significantly, for the cases where the reservoir properties vary drastically from region to region, and then stabilizes at a constant value.

6. The approximate solution presented in Chapter 2 can be used to calculate the fractional flow rates from, and the pressure distribution in, each layer of the multilayered

composite system. Thus the MBE can be applied on each layer separately and better results may be obtained.

7. Like the case of drawdown, the main factors that control the pressure buildup behavior are the reservoir transmissibilities and dimensions.

8. A plot of shut-in pressure versus shut-in time on a semilog graph for two-layer two-region system yields a straight line for the early shut-in time. Unlike the case of drawdown, the slope of this straight line (which varies from system to system) does not only reflect the effect of properties of region 1 but also reflects the effect of region 2 properites.

9. Two stratified composite reservoirs with different characteristics may produce similar pressure buildup curves. Unlike the case of drawdown behavior, the slope of early time data does not help to differentiate between the different types of reservoirs. Surprisingly, the most famous procedures (MDH and Horner) used for many years in the oil industry to predict homogeneous reservoir properties from pressure buildup data cannot be used to predict properties and dimensions of multi-layered composite systems.

II. Water Flooding Performance

10. For a particular mobility ratio; water oil ratio, coverage, cumulative water injection and cumulative oil production are not functions of injection flow rate or pressure drop. This is due to the assumption that the oil is displaced by a piston-like displacement. However, oil production rate increases

as the injection rate and/or pressure drop increases.

11. For a particular stratified composite reservoir, the breakthrough order of its layer depends on the mobility ratio. Also, as the mobility ratio increases the reservoir breaks through earlier.

12. For mobility ratio equal to 1. and constant injection rate, the pressure drop (injector bottom hole pressure minus producer bottom hole pressure) is constant during water flooding life. However, for mobility ratio greater (less) than 1 the pressure drop and consequently the injection pressure decreases (increases) during the water flooding life.

13. Except for a very high mobility ratio, oil production rate is linearly related to the cumulative oil production; as the cumulative oil production increases the oil production rate decreases. At high mobility ratios, oil production rate fluctuates during the water flooding life.

14. Before breakthrough, no water is produced and consequently WOR is zero. After breakthrough, except for very high mobility ratio, the WOR increases asymptotically as cumulative oil production increases. However, at high mobility ratios, WOR may fluctuate during water flooding life.

15. For the same flow rate and mobility ratio, proper selection of the injector and the producer locations may result in higher oil recovery and production rate and lower WOR and cumulative water injection.

NOMENCLATURE

a_j radius of region 1 in layer j

a'_j layer j constant defined by Equations 5.11 and 5.12

A_r parameter is obtained by substituting M = 1 into Equations C.13 or C.14

b_j layer j constant defined by Equations 5.11 and 5.12

B_0 oil formation volume factor, res vol/std vol

B_w water formation volume factor, res vol/std vol

c compressibility

c_i layer i (that has just broken through) constant defined by Equation 5.13

c_j layer j constant defined by Equations 5.11 and 5.12

c_t effective total compressibility

C_j a constant of integration defined by Equation A.7

Cov_j coverage (vertical sweep efficiency) when layer j has broken through

d_j layer j constant defined by Equation C.20

D_j a constant of integration defined by Equation A.13

e = 2.71828·· (Napierian base)

$Ei(-x)$ exponential integral = $-\int_x^\infty \frac{e^{-u}}{u}\,du$

E_j layer j constant defined by Equations 5.11 and 5.12

E_s areal sweep efficiency

f_j fractional flow rate from layer j of cylindrical system

$f_{j,i}$ fractional flow rate from layer j of cylindrical system at time level i

F_j a constant of integration defined by Equation A.12

F_i' parameter of layer i defined by Equations 5.27 and 5.28

G_j a constant of integration defined by Equation A.8

h thickness

$\bar{h}_j$ average thickness of layer j of cylindrical system

$h_{1,j}$ thickness of region 1 of layer j of cylindrical system

$h_{2,j}$ thickness of region 2 of layer j of cylindrical system

h_j thickness of region 1 of layer j from the injector of linear system

h_j' thickness of region 2 of layer j from the injector of linear system

h_s average thickness of multilayered composite cylindrical system

H_j parameter defined by Equation 5.23

K permeability

K_j permeability of region 1 of layer j of the linear system

K_j' permeability of region 2 of layer j of the linear system

K_{ro} relative permeability to oil

K_{rw} relative permeability to water

L distance between the injector and the producer of the linear system

M mobility ratio defined by Equation C.5

M'_j	layer j constant defined by Equation C.7
$M''_{1,j}$	a constant for region 1 of layer j defined by Equation 5.8
$M''_{2,j}$	a constant for region 2 of layer j defined by Equation 5.9
n	number of layers
N	time level corresponding to time t
N_{pj}	cumulative oil recovery when layer j has broken through
P	pressure
P_0	reference pressure
P_{Dw}	dimensionless drawdown pressure
P_{Ds}	dimensionless shut-in pressure
P_i	initial pressure
$P_{1,j}$	pressure distribution of region 1 of layer j of the cylindrical system
$P_{2,j}$	pressure distribution of region 2 of layer j of the cylindrical system
P_w	drawdown bottom hole pressure
ΔP	pressure drop in the linear system
ΔP_{0j}	pressure drop in the unswept portion of layer j
ΔP_{wj}	pressure drop in the swept portion of layer j
q_j	flow rate through layer j
q_{0j}	oil flow rate through layer j of the linear system
q_{wj}	water flow rate through layer j of the linear system
Q	total injected or produced flow rate
r	radius

r_D dimensionless radius

r_{Daj} dimensionless radius of region 1 of layer j of the cylindrical system

$r_{D\,invj}$ dimensionless radius of investigation of layer j

r_w well bore radius

R_j layer j parameter defined by Equation 2.16

S storage

S_j storage of layer j

$S_{1,j}$ storage of region 1 of layer j of the cylindrical system

$S_{2,j}$ storage of region 2 of layer j of the cylindrical system

S_{0i} initial oil saturation

S_{0r} residual oil saturation

S_w initial water saturation

t time

t_{aj} time of pressure-disturbance arrival to layer j interface

t_D dimensionless time

t_{Dw} drawdown dimensionless time

$t_{\ell j}$ time of water-front arrival to layer j interface

t_{Lj} break through time of layer j

t_p time of shutting-in the well

Δt_i time interval at time level i

Δt_s shut-in time

T transmissibility

T_j transmissibility of layer j

$T_{1,j}$ transmissibility of region 1 layer j

$T_{2,j}$ transmissibility of region 2 layer j

T_s system transmissibility

v_j layer j parameter defined by Equations 5.17 and 5.18

V_j layer j parameter defined by Equation 2.18 (cylindrical system)

W width of the linear system

WOR water oil ratio

x_1, x_2, x_3 factors that correlate different blocks transmissibilities to that of the reference block (region 1 of the top layer) of the cylindrical system

x_j water-front location (from the injector) in layer j (linear system)

y_1, y_2, y_3 factors that correlate different blocks storages to that of the reference block (region 1 of the top layer) of the cylindrical system

Y_i parameter defined by Equations 5.20 and 5.21

z a factor that correlates radius of region 1 of layer 2 to that of the reference block (two-layer two-region cylindrical system)

Z Bolizman transform defined by Equation 2.10

Δ difference operator

η diffusivity constant

$\eta_{1,j}$ diffusivity constant of region 1 of layer j

$\eta_{2,j}$ diffusivity constant of region 2 of layer j

λ	mobility
λ_j	mobility of oil in layer j
$\lambda_{1,j}$	mobility of oil in region 1 of layer j
$\lambda_{2,j}$	mobility of oil in region 2 of layer j
μ	viscosity, cp
μ_0	oil viscosity, cp
μ_w	water viscosity, cp
ρ	density
ρ_0	density at reference pressure P_0
ϕ	porosity
ϕ_j	porosity of region 1 of layer j of the linear system
ϕ'_j	porosity of region 2 of layer j of the linear system
ℓ_j	length of region 1 of layer j of the linear system
π	3.1459
κ	shutting-in time level

REFERENCES

Arps, J. J. and A. E. Smith. "Practical Use of Bottom-Hole Pressure Buildup Curves," Drill and Prod. Prac., API (1949): 155.

Brons, F. and W. C. Miller. "A Simple Method for Correcting Spot Pressure Readings," JPT (Aug. 1961): 803-805.

Carter, R. D. "Pressure Behavior of a Limited Circular Composite Reservoir," SPEJ (Dec. 1966): 328.

Coats, K. H. "An Analysis for Simulating Reservoir Performance Under Pressure Maintenance by Gas and/or Water Injection," SPEJ (Dec. 1968): 331-340.

Dietz, D. N. "Determination of Average Pressure from Build-up Surveys," JPT (Aug. 1965): 955.

Dolan, J. R., C. A. Einarsen and G. A. Hill. "Special Applications of Drill Stem Test Pressure Data," Trans., AIME (1957): 210, 318 - 324.

Dyes, A. B., B. H. Caudle and R. A. Erickson. "Oil Production After Breakthrough - As Influenced by Mobility Ratio," Trans., AIME (1954): 201, 81-86.

Dykstra, H. and R. L. Parsons. "The Prediction of Oil Recovery by Waterflooding," Secondary Recovery of Oil in the United States, 2nd Ed., API, New York (1950): 160-174.

Earlougher, R. C., Jr., H. J. Ramey, Jr., F. G. Miller and T. D. Mueller. "Pressure Distribution in Rectangular Reservoirs," JPT (Feb. 1968): 199.

Earlougher, R. C., Jr. and H. J. Ramey, Jr. "Interference Analysis in Bounded Systems," J. Canad. Pet. Tech., (Oct.-Dec. 1973): 33.

Earlougher, R. C., Jr., K. M. Kersh and W. J. Kunzman. "Some Characteristics of Pressure Buildup Behavior in Bounded Multiple-Layered Reservoirs without Crossflow," JPT, (Oct. 1974): 1178.

Elkins, L. F. "Reservoir Performance and Well Spacing, Silica Arhuckle Pool, Kansas," Drill. and Prod. Prac., API (1946): 109.

Evrenos, A. I. and E. A. Rejda. "A Digital Computer Application to the Investigation of Aquifer Properties," JPT (July 1965): 827-838.

Goddin, C. S., Jr., F. F. Craig, Jr., J. O. Wilkes and M. R. Tek. "A Numerical Study of Waterflood Performance in a Stratified System with Crossflow," Trans. AIME (1966) Vol. 237, pp. 765-771.

Gringarten, A. C. and H. J. Ramey, Jr. "The Use of Source and Green's Functions in Solving Unsteady-Flow Problems in Reservoirs," SPEJ (Oct. 1973): 285.

Gringarten, A. C. and H. J. Ramey, Jr. "Unsteady-State Pressure Distributions Created by a Well with a Single Horizontal Fracture, Partial Penetration, or Restricted Entry," SPEJ (Aug. 1974): 413.

Gringarten, A. C., H. J. Ramey, Jr. and R. Raghavan. "Unsteady-State Pressure Distributions Created by a Well with a Single Infinite-Conductivity Vertical Fracture," SPEJ (Aug. 1974): 347.

Gringarten, A. C., H. J. Ramey, Jr. and R. Raghaven. "Applied Pressure Analysis for Fractured Wells," JPT (July 1975): 887.

Horner, D. R. "Pressure Buildup in Wells," Proc., Third World Pet. Cong., E. J. Brill, Leiden (1951): II, 503.

Hurst, W. "Interference Between Oil Fields," Trans. AIME, Vol. 219 (1960): 175.

Katz, M. L. and M. L. Tek. "A Theoretical Study of Pressure Distribution and Fluid Flux in Bounded Stratified Porous Systems with Crossflow," SPEJ (March 1962): 68.

Kimbler, O. K., B. H. Candle and H. E. Cooper, Jr. "Areal Sweepout Behavior in a Nine-Spot Injection Pattern," Trans., AIME (1964): 231, 199-202.

Kufus, H. B. and E. J. Lynch. "Linear Frontal Displacement in Multilayer Sands," Prod. Monthly (Dec. 1959): Vol. 24, No. 12, 32-35.

Lefkovits, M. C., P. Hazekbrock, E. E. Allen and C. S. Matthews. "A Study of the Behavior of Bounded Reservoirs Composed of Stratified Layers," Trans., AIME, Vol. 222, (1961): 43.

Loucks, T. L. and E. T. Guerrero. "Pressure Drop in a Composite Reservoir," SPEJ (Sept. 1961): 170.

Matthews, C. S., F. Brons and P. Hazebrock. "A Method for Determination of Average Pressure in a Bounded Reservoir," Trans., AIME (1954): 201, 182-191.

Matthews, C. S. and D. G. Russell. "Pressure Buildup and Flow Tests in Wells," SPE Monograph, Vol. 1, Society of Pet. Eng. of AIME, Dallas Texas (1967).

Miller, C. C., A. B. Dyes and C. A. Hutchinson, Jr. "The Estimation of Permeability and Reservoir Pressure from Bottom-Hole Pressure Buildup Characteristics," Trans., AIME (1950): 189, 91-106.

Moore, T. V., R. J. Schilthuis and W. Hurst. "The Determination of Permeability from Field Data," Proc., API Bull. 211 (1933): 4.

Mortada, M. "Oilfield Interference of Aquifers of Non-Uniform Properties," Trans. AIME, Vol. 219 (1960): 412.

Muskat, M. The Flow of Homogeneous Fluids Through Porous Media. McGraw-Hill Book Co., Inc., New York (1937).

Osman, M. "Matthews, Brons and Hazebrock Dimensionless Pressures for a Well Located Anywhere Inside a Rectangle with Closed, Open and Mixed Boundaries," General Exam. Report, Univ. of Oklahoma, Norman, Oklahoma, Nov. 1979.

Pendergrass, J. D. and V. J. Berry, Jr. "Pressure Transient Performance of a Multilayered Reservoir with Cross-Flow," SPE of AIME, Production Research Symposium, Tulsa, Oklahoma, April, 1962, 92.

Ramey, H. J., Jr. "Approximate Solutions for Unsteady Liquid Flow in Composite Reservoirs," J. of Canad. Pet. Tech. (Jan.-March 1970).

Russell, D. G. and M. Prats. "Performance of Layered Reservoirs with Cross Flow-Single-Compressible-Fluid Case," SPEJ, (March 1962): 53.

Snyder, R. W. and H. J. Ramey, Jr. "Application of Buckley-Leverett Displacement Theory to Noncommunicating Layered Systems," JPT (Nov. 1967): 1500-1506.

Sommers, G. E. "The Effect of Cross Flow in a Stratified Reservoir During a Waterflood," M.S. Thesis, Texas A&M University, Texas (Aug. 1970).

Stiles, W. E. "Use of Permeability Distribution in Water Flood Calculations," Trans. AIME, Vol. 186 (1949): 9.

Stright, D. H., D. W. Bennion and K. Aziz. "Influence of Production Rate on the Recovery of Oil from Horizontal Waterfloods," paper SPE 5127 presented at the SPE-AIME 49th Annual Fall Meeting, Houston, Oct. 1974, 6-9.

Theis, C. V. "The Relationship Between the Lowering of Piezometric Surface and Rate and Duration of Discharge of Wells Using Ground-Water Storage," Trans, AGU (1935): II, 519.

Uraiet, A., R. Raghavan and G. W. Thomas. "Determination of the Orientation of Vertical Fracture by Interference Tests," JPT (January 1977): 73.

Warren, J. E. and J. J. Cosgrove. "Prediction of Waterflood Behavior in a Stratified System," SPEJ (June 1964): 194-157.

Witherspoon, P. A., I. Javandel, S. P. Neuman and R. A. Freeze. "Interpretation of Aquifer Gas Storage Conditions from Water Pumping Tests," Monograph on Project NS-38, American Gas Association, Inc., New York, 1967.

APPENDIX A

DIMENSIONLESS DRAWDOWN TERM FOR A WELL LOCATED IN THE CENTER OF COMPOSITE-LAYERED RESERVOIR

In this appendix, a mathematical treatment of dimensionless well bore pressure behavior of a single well located in the center of a composite layered reservoir is presented. The basic assumptions and description of the reservoir model are listed in the first two sections of Chapter 2 of this study.

The diffusivity equations are:

$$\frac{1}{r}\frac{\partial}{\partial r}\left(r\frac{\partial P_{1,j}}{\partial r}\right) = \frac{1}{\eta_{1,j}}\frac{\partial P_{1,j}}{\partial t},$$

$$0 \leq r \leq a_j, \quad j = 1,2,\ldots n \qquad 2.3$$

$$\frac{1}{r}\frac{\partial}{\partial r}\left(r\frac{\partial P_{2,j}}{\partial r}\right) = \frac{1}{\eta_{2,j}}\frac{\partial P_{2,j}}{\partial t},$$

$$a_j \leq r \leq \infty \text{ and } j = 1,2,\ldots n \qquad 2.4$$

The initial and boundary conditions for this system are:

a. Inner Boundary Conditions

$$\lim_{r \to 0} r\frac{\partial P_{1,j}}{\partial r} = \frac{q_j}{2\pi T_{1,j}}$$

$$t > 0, \quad j = 1,2,\ldots n \qquad 2.5$$

b. Interface Conditions

$$P_{i,j} = P_{2,j} \qquad r = a_j,\ t \geq 0,\ j = 1,2,\ldots n \qquad 2.6$$

Since there is no accumulation at the interface;

$$q_j = r\, T_{1,j} \frac{\partial P_{1,j}}{\partial r} = r\, T_{2,j} \frac{\partial P_{2,j}}{\partial r}$$

$$r = a_j,\ t \geq 0,\ j = 1,2,\ldots n \qquad 2.7$$

c. Outer Boundary Conditions

$$\lim_{r \to \infty} P_{2,j} = P_i,$$

$$t \geq 0\ , \quad j = 1,2,\ldots n \qquad 2.8$$

d. Initial Conditions

$$P_{1,j} = P_{2,j} = P_i,\ t = 0,\ j = 1,2,\ldots n \qquad 2.9$$

Boltzman transform can be written as:

$$Z = \frac{r^2}{4\eta_{1,1}t} \qquad 2.10$$

where: $\eta_{1,1}$ = hydraulic diffusifity of region 1 of the top layer (reference block).

from chain rule: $\frac{\partial P}{\partial r} = \frac{dP}{dz} \cdot \frac{Z}{r}$

from Equation 2.10: $\frac{\partial z}{\partial r} = \frac{2r}{4\eta_{1,1}t}$

$$r \frac{\partial P}{\partial r} = r \cdot \frac{2r}{4\eta_{1,1} t} \cdot \frac{dP}{dZ}$$

$$= 2Z \frac{dP}{dZ} \qquad \text{A.1}$$

$$\frac{r \frac{\partial P_{1,j}}{\partial r}}{\partial r} = \frac{\partial (2Z \frac{dP}{dZ})}{\partial r}$$

$$= \frac{d(2Z \frac{dP}{dZ})}{dZ} \cdot \frac{\partial Z}{\partial r}$$

$$= \frac{2r}{4\eta_{1,1} t} \cdot \frac{d(2Z \frac{dP}{dZ})}{dZ}$$

Then: $\frac{1}{r} \frac{\partial}{\partial r} (r \frac{\partial P_{1,j}}{\partial r}) = \frac{2Z}{r^2} \frac{d}{dZ} (2Z \frac{dP}{dZ})$ A.2

Similarly: $\frac{\partial P}{\partial t} = \frac{dP}{dZ} \cdot \frac{\partial z}{\partial t}$

From equation 2.10: $\frac{\partial Z}{\partial t} = \frac{-r^2}{4\eta_{1,1} t^2} = \frac{-Z}{t}$

Then $\frac{\partial P}{\partial t} = \frac{-Z}{t} \frac{dP}{dZ}$

$$= \frac{4\eta_{1,1} Z^2}{r^2} \frac{dP}{dZ} \qquad \text{A.3}$$

Substituting Equations A.2 and A.3 into Equation 2.3, yields:

$$\frac{2Z}{r^2} \frac{d}{dZ} (2Z \frac{dP_{1,j}}{dZ}) = \frac{1}{\eta_{1,j}} (\frac{-4\eta_{1,1} Z^2}{r^2}) \frac{dP_{1,j}}{dZ}$$

$$Z \frac{d^2P_{1,j}}{dZ^2} + (1 + Z \frac{\eta_{1,1}}{\eta_{1,j}}) \frac{dP_{1,j}}{dZ} = 0$$

$$0 \leq r \leq a_j, \; j = 1, 2, \ldots n \qquad 2.11$$

Similarly, Equation 2.4 is written as:

$$Z \frac{d^2P_{2,j}}{dZ^2} + (1 + Z \frac{\eta_{1,1}}{\eta_{2,j}}) \frac{dP_{2,j}}{dZ} = 0$$

$$\text{and } a_j \leq r \leq \infty, \; j = 1, 2, \ldots n \qquad 2.12$$

Equations 2.11 and 2.12 are linear ordinary differential equations. Their solutions are readily given by Ramey [1970] as:

$$P_{i,j} = C_j Ei[-Z \frac{\eta_{1,1}}{\eta_{1,j}}] + D_j \qquad 2.13$$

$$P_{2,j} = F_j Ei[-Z \frac{\eta_{1,1}}{\eta_{2,j}}] + G_j \qquad 2.14$$

where C_j, D_j, F_j are parameters to be determined from initial and boundary conditions as follows:

From Equations 2.5 and A.1:

$$\lim_{r \to 0} r \frac{\partial P_{1,j}}{\partial r} = \lim_{Z \to 0} 2Z \frac{dP_{1,j}}{dZ}$$

$$= \frac{q_j}{2 \pi T_{1,j}} \qquad j = 1,2,\ldots n \quad A.4$$

differentiate equation 2.13 with respect to Z as:

$$\frac{dP_{1,j}}{dZ} = C_j \frac{d}{dZ} \left[E_i \left(-Z \frac{\eta_{1,1}}{\eta_{1,j}}\right)\right]$$

$$= C_j \frac{d}{dZ} \int_{Z\frac{\eta_{1,1}}{\eta_{1,j}}}^{\infty} \frac{e^{-Z\frac{\eta_{1,1}}{\eta_{1,j}}}}{Z\left(\frac{\eta_{1,1}}{\eta_{1,j}}\right)} d\left(Z \frac{\eta_{1,1}}{\eta_{1,j}}\right)$$

$$= C_j \frac{d}{dZ} \int_{Z\frac{\eta_{1,1}}{\eta_{1,j}}}^{\infty} \frac{e^{-Z\frac{\eta_{1,1}}{\eta_{1,j}}}}{Z} dZ$$

Then: $$\frac{dP_{1,j}}{dZ} = \frac{C_j}{Z} e^{-Z\frac{\eta_{1,1}}{\eta_{1,j}}} \qquad \text{A.5}$$

Similarly

$$\frac{dP_{2,j}}{dZ} = \frac{F_j}{Z} e^{-Z\frac{\eta_{1,1}}{\eta_{2,j}}} \qquad \text{A.6}$$

Substituting Equation A.5 into Equation A.4,

$$\lim_{Z \to 0} 2Z\frac{dP_{i,j}}{dZ} = \lim_{Z \to 0} 2Z \cdot \frac{C_j}{Z} e^{-Z\frac{\eta_{1,1}}{\eta_{1,j}}}$$

$$= 2C_j \lim_{Z \to 0} e^{-Z\frac{\eta_{1,1}}{\eta_{1,j}}}$$

$$= 2C_j$$

$$= \frac{q_j}{2\pi T_{1,j}}$$

Then $C_j = \frac{q_i}{4\pi T_{1,j}}$, $j = 1,2,\ldots n$ A.7

From Equations 2.8 and 2.14

$$\lim_{r \to \infty} P_{2,j} = \lim_{Z \to \infty} P_{2,j}$$

$$= \lim_{Z \to \infty} [F_j Ei(-Z\frac{\eta_{1,1}}{\eta_{2,j}})] + G_j] = G_j$$

Then: $G_j = P_i$

$j = 1,2,\ldots n$ A.8

Combining Equations 2.7, A.1 and A.5 yields:

$$T_{1,j}\,(r\frac{\partial P_{1,j}}{\partial r}) = 2C_j\, T_{1,j}\; e^{(-Z\frac{\eta_{1,1}}{\eta_{1,j}})},$$

$r = a_j$, $j = 1,2,\ldots .n$ A.9

Similarly, from equations 2.7, A.1 and A.6,

$$T_{2,j}(r\frac{\partial P_{2,j}}{\partial r}) = 2F_j\, T_{2,j} \cdot e^{(-Z\frac{\eta_{1,1}}{\eta_{2,j}})},$$

$r = a_j$, $j = 1,2,\ldots n$ A.10

from Equations 2.7, A.9 and A.10,

$$F_j = \frac{T_{1,j}}{T_{2,j}} \; C_j \; e^{-Z\eta_{1,1}\left(\frac{1}{\eta_{1,j}} - \frac{1}{\eta_{2,j}}\right)}$$

Substituting Equation A.7 into the above equation yields:

$$F_j = \frac{T_{1,j}}{T_{2,j}} \cdot \frac{q_j}{4\,T_{1,j}} \; e^{-Z\eta_{1,1}\left(\frac{1}{\eta_{1,i}} - \frac{1}{\eta_{2,j}}\right)}$$

$$j = 1,2,\ldots n \qquad \text{A.11}$$

$$\text{at } r = a_j, \quad Z\Big|_{a_j} = \frac{r^2}{4\eta_{1,1}t}\Big|_{r=a_j} = \frac{a_j^2}{4\eta_{1,1}t} \cdot \frac{r^2}{r^2}$$

$$= Z\,\frac{a_j^2}{r^2}$$

Thus Equation A.11 is written as:

$$F_j = \frac{q_i}{4\pi T_{2,j}} \; e^{-Z\frac{a_j^2}{r^2}\eta_{1,1}\left(\frac{1}{\eta_{1,j}} - \frac{1}{\eta_{2,j}}\right)} \qquad \text{A.12}$$

At the interface of layer $j(r=a_j)$ $P_{1,j} = P_{2,j}$. Thus from Equations 2.13 and 2.14,

$$C_j Ei\left(-Z\frac{a_j^2}{r^2}\;\frac{\eta_{1,1}}{\eta_{1,j}}\right) + D_j = F_j\, Ei\left(-Z\frac{a_j^2}{r^2}\;\frac{\eta_{1,1}}{\eta_{2,j}}\right) + G_j$$

$$D_j = F_j\, Ei\left(-Z\frac{a_j^2}{r^2}\;\frac{\eta_{1,1}}{\eta_{2,j}}\right) + G_j - C_j\, Ei\left(-Z\frac{a_j^2}{r^2}\,\frac{\eta_{1,1}}{\eta_{1,j}}\right)$$

Substituting Equations A.7, A.8 and A.12 into the above equation yields:

$$D_j = P_i + \frac{q_i}{4\pi}\left[\frac{1}{T_{2,j}}\, e^{-Z\frac{a_j^2}{r^2}\eta_{1,1}}\left(\frac{1}{\eta_{1,j}} - \frac{1}{\eta_{2,j}}\right) Ei\left(-Z\frac{a_j^2}{r^2}\frac{\eta_{1,1}}{\eta_{2,1}}\right)\right.$$

$$\left. - \frac{1}{T_{1,j}}\, Ei\left(-Z\,\frac{a_j^2}{r^2}\,\frac{\eta_{1,1}}{\eta_{2,j}}\right)\right]$$

$$j = 1,2,\ldots n \qquad \text{A.13}$$

Parameters C_j, G_j, F_j and D_j are expressed by Equations A.7, A.8, A.11 and A.13 respectively.

Thus the pressure distribution in region one of layer j is obtained by substituting Equations A.7 and A.13 into Equation 2.13 as:

$$P_{1,j}(r,t) = P_i + \frac{q_j}{4\pi}\left[\frac{1}{T_{1,j}}\left(Ei\left[-Z\frac{\eta_{1,1}}{\eta_{1,j}}\right] - Ei\left[-Z\frac{a_j^2}{r^2}\,\frac{\eta_{1,1}}{\eta_{2,j}}\right]\right)\right.$$

$$\left. + \frac{1}{T_{2,j}}\, e^{-Z\frac{a_j^2}{r^2}\eta_{1,1}}\left(\frac{1}{\eta_{1,j}} - \frac{1}{\eta_{2,j}}\right)\, Ei\left(-Z\frac{a_j^2}{r^2}\,\frac{\eta_{1,1}}{\eta_{2,j}}\right)\right]$$

$$r \leq a_j,\ j = 1,2,\ldots n \qquad \text{A.14}$$

Similarly, the pressure distribution in region two of layer j is obtained by substituting Equations A.8 and A.12

into Equation 2.14 as:

$$P_{2,j} = P_i + \frac{q_j}{4\pi T_{2,j}} e^{-z\frac{a_j^2}{r^2}\eta_{1,1}\left(\frac{1}{\eta_{1,j}} - \frac{1}{\eta_{2,j}}\right)} Ei\left(-z\frac{\eta_{1,1}}{\eta_{2,j}}\right),$$

$$j = 1,2,\ldots n \qquad A.15$$

It should be noted that Equations A.14 and A.15 are applicable only if q_j is constant which is not the case. Thus, superposition in time should be applied to take into account the flow rate variations. Applying superposition technique in time and using Equation 2.10, Equations A.14 and A.15 are rewritten as:

$$P_{1,j}(r,t) = P_i + \frac{Q}{4\pi}\left[\sum_{i=1}^{N} (f_{j,i} - f_{j,i-1}) \cdot R_j(t - t_{i-1})\right],$$

$$r \geq a_j,\ j = 1,2,\ldots n \qquad 2.15$$

where:

$$R_j(t-t_{i-1}) = \frac{1}{T_{1,j}}\left[Ei\left(\frac{-r_D^2 r_W^2}{4(t-t_{i-1})}\frac{S_{1,j}}{T_{1,j}}\right) - Ei\left(\frac{-r_{D\,aj}^2 r_W^2}{4(t-t_{i-1})}\frac{S_{1,j}}{T_{1,j}}\right)\right]$$

$$+ \frac{1}{T_{2,j}} e^{-\frac{r_{Daj}^2 r_W^2}{4(t-t_{i-1})}\left(\frac{S_{1,j}}{T_{1,j}} - \frac{S_{2,j}}{T_{2,j}}\right)} Ei\left(\frac{-r_{Daj}^2 r_W^2}{4(t-t_{i-1})}\frac{S_{2,j}}{T_{2,j}}\right) \qquad 2.16$$

$f_{j,i}$ and $f_{j,i-1}$ are fractional flow rates from layer j at time levels i and i-1 respectively.

Similarly, the pressure distribution in region two of layer j is given as:

$$P_{2,j} = P_i + \frac{Q}{4\pi}\left[\sum_{i=1}^{N}(f_{j,i} - f_{j,i-1}) - V_j(t - t_{i-1})\right],$$

$$a_j \leq r_j \quad , j = 1,2,\ldots n \qquad 2.17$$

where:

$$V_j(t - t_{i-1}) = \frac{1}{T_{2,j}} e^{-\frac{r_D^2 a_j r_W^2}{4(t-t_{i-1})}\left(\frac{S_{1,j}}{T_{1,i}} - \frac{S_{2,j}}{T_{2,j}}\right)} \cdot Ei\left(-\frac{r_D^2 r_W^2}{4(t-t_{i-1})}\frac{S_{2,j}}{T_{2,j}}\right)$$

2.18

To obtain an expression for the term P_D for the system under study, Equation 2.15 is further munipulated as follows:

$$\eta = \frac{K}{\phi c} = \frac{Kh}{\mu} \cdot \frac{1}{\phi ch} = \frac{T}{S} \qquad A.16$$

Then, $$Z \left.\frac{\eta_{1,1}}{\eta_{1,j}}\right|_{r=r_w} = \frac{r_w^2}{4\eta_{1,1}t} \cdot \frac{\eta_{1,1}}{\eta_{1,j}}$$

$$= \frac{r_w^2}{4t} \cdot \frac{S_{1,j}}{T_{1,j}} \qquad A.17$$

$$Z \left.\frac{a_j^2}{r^2} \frac{\eta_{1,1}}{\eta_{1,j}}\right|_{r=r_w} = \frac{r_w^2}{4\eta_{1,1}t} \cdot \frac{a_j^2}{r_w^2} \cdot \frac{\eta_{1,1}}{\eta_{1,j}}$$

$$= \frac{a_j^2}{4t} \cdot \frac{\eta_{1,j}}{T_{1,j}} \qquad A.18$$

Similarly

$$Z \frac{a_j^2}{r^2} \left. \frac{\eta_{1,1}}{\eta_{2,j}} \right|_{r=r_w} = \frac{a_j^2}{4t} \cdot \frac{S_{2,j}}{T_{2,j}} \qquad \text{A.19}$$

$$Z \frac{a_i^2}{r^2 \eta_{1,1}} \left(\frac{1}{\eta_{1,j}} - \frac{1}{\eta_{2,j}}\right) = \frac{a_j^2}{4t} \left(\frac{S_{1,j}}{T_{1,j}} - \frac{S_{2,j}}{T_{2,j}}\right) \qquad \text{A.20}$$

$$P_{i,j}(r,t) \Big|_{r=r_w} = P_w \qquad \text{A.21}$$

Substituting Equations A.16 through A.21 into Equation A.14 yields:

$$P_w = P_i + \frac{q_i}{4\pi} \left[\frac{1}{T_{1,j}} \; Ei\left(\frac{-r_w^2}{4t} \frac{S_{1,j}}{T_{1,j}}\right) - Ei\left(\frac{-a_j^2}{4t} \frac{S_{1,j}}{T_{1,j}}\right)\right.$$

$$\left. + \frac{1}{T_{2,j}} e^{\frac{-a_j^2}{4t}\left(\frac{S_{1,j}}{T_{1,j}} - \frac{S_{2,j}}{T_{2,j}}\right)} Ei\left(-\frac{a_j^2}{4t} \frac{S_{2,j}}{T_{2,j}}\right)\right],$$

$$j = 1,2,\ldots n \qquad \text{A.22}$$

let Q = total flow rate,

f_j = fractional flow rate from layer j,

$q_j = Q\, f_i$, and

$a_j = r_{D\,aj} \cdot r_w$

Thus Equation A.22 is rewritten as:

$$\frac{4\pi(P_i - P_w)}{Q} = -f_j \left[\frac{1}{T_{1,j}} \left\{Ei\left(\frac{-r_w^2}{4t} \cdot \frac{S_{1,j}}{T_{1,j}}\right) - Ei\left(\frac{-r_{aj}^2 \cdot r_w^2}{4t} \cdot \frac{S_{1,j}}{T_{1,j}}\right)\right\}\right.$$

$$+\frac{1}{T_{2,j}}\, e^{\frac{-r_{aj}^2\, r_w^2}{4t}\left(\frac{S_{1,j}}{T_{1,j}}-\frac{S_{2,j}}{T_{2,j}}\right)}\, Ei\left(\frac{-r_{aj}^2 . r_w^2}{4t}\cdot\frac{S_{2,j}}{T_{2,j}}\right)],$$

$$j = 1,2,\ldots n \qquad \text{A.23}$$

let $\quad \frac{\bar{K}\bar{h}}{\bar{\mu}} = T_s$

Multiply both sides of Equation A.23 by the above equation to get:

$$\frac{4\pi\ (P_i-P_w)\ \bar{K}\bar{h}}{Q\ \bar{\mu}} = -T_s f_j\ [\ \frac{1}{T_{1,j}}\ \{Ei(\frac{-\ r_w^2}{4t}\ .\ \frac{S_{1,j}}{T_{1,j}}) - Ei(\frac{-r_{aj}^2 r_w^2}{4t}\cdot\frac{S_{1,j}}{T_{1,j}})\}$$

$$+\frac{1}{T_{2,j}}\, e^{\frac{-r_{aj}^2 . r_w^2}{4t}\left(\frac{S_{1,j}}{T_{1,j}}-\frac{S_{2,j}}{T_{2,j}}\right)}\, Ei\left(\frac{-r_{aj}^2\, r_w^2}{4t}\,\frac{S_{2,1}}{T_{2,j}}\right)]$$

The L.H.S. of the above equation is the definition of P_{Dw} term for the system under study. Substitution $a_j = r_{Daj}.r_w$ in the R.H.S., one can get:

$$P_{Dw} = -T_s f_j\ \ [\frac{1}{T_{1,j}}\{Ei(\frac{-r_w^2}{4t}\cdot\frac{S_{1,j}}{T_{1,j}}) - Ei(\frac{-r_{Daj}^2\, r_w^2}{4t}\,\frac{S_{1,j}}{T_{1,j}})\}$$

$$+ \frac{1}{T_{2,j}} e^{\frac{-r_{Daj}^2 r_w^2}{4t}\left(\frac{S_{i,j}}{T_{1,j}} - \frac{S_{2,j}}{T_{2,j}}\right)} Ei\left(-\frac{r_{Daj}^2 r_w^2}{4t} \frac{S_{2,j}}{T_{2,j}}\right)]$$

$$j = 1,2,3,\ldots n \qquad A.24$$

Equation A.24 expresses the dimensionless draw down pressure term of a system of n layers and two-regions. Again, superposition in time should be applied with this equation to take into account the variation in the fractional flow rates from each layer.

Thus P_{Dw} term for the system is gives as:

$$P_{Dw} = -\sum_{i=1}^{N} (f_{j,i} - f_{j,i-1}) \cdot T_s(t - t_{i-1}) \cdot R_j(t - t_{i-1}),$$

$$j = 1,2,3,\ldots n \qquad 2.20$$

where:

$T_s(t - t_{i-1})$ = System transmissibility evaluated at time $(t - t_{i-1})$.

The fractional flow rates from each layer, that must be known to make use of the presented solution, are evaluated by applying superposition technique in time on Equation A.14, for $r = r_w$ and $P_{i,j} = P_w$, to yield:

$$\frac{4\pi(P_i - P_w)}{Q} = -\sum_{i=1}^{N} [(f_{j,i} - f_{j,i-1}) \cdot R_j(t - t_{i-1})],$$

$$j = 1,2,\ldots n \qquad 2.19$$

Since L.H.S. of Equation 2.19 is the same for all layers at a certain point of time, then:

$$\sum_{i=1}^{N} (f_{1,i}-f_{1,i-1})\, R_1(t-t_{i-1}) = \sum_{i=1}^{N} (f_{2,i}-f_{2,i-1})\, R_2(t-t_{i-1}) \quad \text{A.25.1}$$

$$= \sum_{i=1}^{N} (f_{3,i}-f_{2,i-1})\, R_3(t-t_{i-1}) \quad \text{A.25.2}$$

$$\vdots$$

$$= \sum_{i=1}^{N} (f_{n,i}-f_{n,i-1})\, R_n(t-t_{i-1}) \quad \text{A.25.n-1}$$

Also,

$$(f_{1,i}-f_{1,i-1}) + (f_{2,1}-f_{2,i-1}) + \ldots + (f_{n,i}-f_{n,i-1})$$

$$= 1 \text{ for } i = 1$$

$$= 0 \text{ for } i \geq 2 \quad \text{A.25.n}$$

At the first time step where N = 1 and consequently i = 1, Equation A.25 can be solved to obtain the values of fractional flow rates. As the time progresses, the same equation can be used to calculate the variation in fractional flow rates $(f_{j,i}-f_{j,i-1})$ and consequently the fractional flow rates.

APPENDIX B

DIMENSIONLESS DRAWDOWN TIME TERM FOR A WELL LOCATED IN THE CENTER OF COMPOSITE-LAYERED RESERVOIRS

The dimensionless time term for a well located in a homogeneous reservoir is given as:

$$t_D = \frac{K\ t}{\phi\ \mu c_t\ r_w^2}$$

$$= \frac{Kh}{\mu} \cdot \frac{1}{\phi c_t h} \cdot \frac{t}{r_w^2}$$

or $$t_D = \frac{t}{r_w^2} \cdot \frac{T}{S} \qquad \text{B.1}$$

where T = transmissibility of the reservoir

S = storage of the reservoir

For multi-layered composite reservoir, t_D is expressed as:

$$t_{Dw} = \frac{t}{r_w^2} \cdot \frac{T_s}{S_s} \qquad 2.22$$

where T_s = transmissibility of multilayered composite system

S_s = storage of multilayered composite system

It is common in literature that $\bar{K}\,\bar{h}$ and $\bar{\phi}\,\bar{h}$ products and consequently T_s and S_s are approximated by summing up their products for each homogeneous layer of the multilayered reservoir. This would be true representation for heterogeneous reservoirs under steady state conditions. In the present study, volumetric averages—based on the radius of investigation in each layer—of the system properties are used to express T_s and S_s. The radii of investigations are a function of time and so are T_s and S_s.

Whenever the radius of investigation in a particular layer is less than or equal to the radius of the first region of that particular layer, the fluid flow is completely controlled by the properties of the first region of that layer and so are the average transmissibility and storage of that layer. Otherwise, volumetric average based on the radius of investigation of both regions charactertistics are used to express the transmissibility and storage of a certain layer. Then, based on the radii of investigations of all layers, volumetric average properties are used to express T_s and S_s.

The radius of investigation in layer j, $r_{inv\,j}$, is given as:

$$r^2_{inv\,j} = 4\,t\,\frac{T_j}{S_j}\,,\quad j = 1,2,\ldots n \qquad \text{B.2}$$

or

$$t = \frac{r^2_{inv\,j}}{4}\cdot\frac{S_j}{T_j}\,,\quad j = 1,2,\ldots n \qquad \text{B.3}$$

where:

T_j = transmissibility of layer j

S_j = storage of layer j

Define t_{aj} as the time at which the radius of investigation equal to the radius of the first region of layer j and $r_{Daj} = \frac{a_j}{r_w}$. The transmissibility and storage of each layer can be expressed as follows:

a. at $t \leq t_{aj}$

$$T_j = T_{1,j}, \quad j = 1,2,. \; . \; .n \qquad 2.25$$

$$S_j = S_{1,j}, \quad j = 1,2,. \; . \; .n \qquad 2.26$$

Substituting Equations 2.25 and 2.26 into Equation B.3 yeilds,

$$t_{aj} = \frac{r_{Daj}^2 . r_w^2}{4} \cdot \frac{S_{1,j}}{T_{1,j}}, \quad j = 1,2,. \; . \; .n \qquad 2.31$$

b. at $t \geq t_{aj}$

$$r_{inv\,j} = a_j + \Delta r$$

$$r_{D\,inv\,j} = r_{Daj} + \frac{\Delta r}{r_w}$$

$$= r_{Daj} + \frac{2}{r_w} \left(\frac{T_{2,j}}{S_{2,j}}\right)^{0.5} (t-t_{aj})^{0.5},$$

$$j = 1,2,. \; . \; .n \qquad 2.30$$

where t_{aj} is defined by Equation 2.31.

The volumetric average of fluid mobility ($\lambda = \frac{T}{h}$) is given as:

$$\lambda_j = \frac{\lambda_{1,j}\,\pi a_j^2\, h_{1,j} + \lambda_{2,j}\,[\pi(r_{invj}^2 - a_j^2)\, h_{2,j}]}{\pi\, r_{invj}^2\, h_j}$$

but $\lambda h = T$,

$r_{invj} = r_w \cdot r_{Dinvj}$, and

$a_j = r_w \cdot r_{Daj}$

Then,

$$T_j = \frac{T_{1,j}\, r_{Daj}^2 + T_{2,j}\,(r_{Dinvj}^2 - r_{Daj}^2)}{r_{Dinvj}^2}\ ,\ j=1,2,\ldots n \qquad 2.28$$

Similarly, volumetric average value of ϕc_t for layer j is expressed by:

$$(c_t\phi)_j = \frac{(c_t\phi)_{1,j}\ a_j^2\, h_{1,j} + (c_t\phi)_{2,j}[r_{invj}^2 - a_j^2]\, h_{2,j}}{\pi\, r_{invj}^2\, h_j}$$

but

$$c_t \phi h = S$$

Then,

$$S_j = \frac{S_{1,j}\, r_{Daj}^2 + S_{2,j}\,(r_{Dinvj}^2 - r_{Daj}^2)}{r_{Dinvj}^2},\ j = 1,\ 2,\ \ldots\ n \qquad 2.29$$

Then the transmissibility and storage of the system under study are obtained as follows:

The volumetric average of the system mobility is given by:

$$\lambda_s = \frac{\sum_{j=1}^{n} \lambda_j \; r_{inv\,j}^2 \; h_j}{h_s \sum_{j=1}^{n} \pi r_{inv\,j}^2}$$

Then,

$$T_s = \frac{\sum_{j=1}^{n} T_j \; r_{Dinv\,j}^2}{\sum_{j=1}^{n} r_{Dinv\,j}^2} \qquad 2.23$$

Similarly, the storage term for the system is expressed by:

$$(c_t\phi)_s = \frac{\sum_{j=1}^{n} (c_t\phi)_j \; \pi \; r_{inv\,j}^2 \; h_j}{h_s \sum_{j=1}^{n} \pi \; r_{inv\,j}^2}$$

Then,

$$S_s = \frac{\sum_{j=1}^{n} S_j \; r_{Dinv\,j}^2}{\sum_{j=1}^{n} r_{Dinv\,j}^2} \qquad 2.24$$

Depending on the time, T_j and S_j are expressed by Equations (2.25 or 2.28) and (2.26 or 2.29) respectively.

Equations 2.23 and 2.24 are used to express the transmissibility and storage of multilayer composite systems. Both terms, T_s and S_s, are functions of $r_{D\,inv\,j}$ which is a function of time. It should be noted that h_s is not an exact dimension of the system under study. Rather, it expresses average thickness. Since T_s and S_s terms appear as a ratio in Equation 2.22, h_s is canceled and has no effect on t_{Dw} calculations.

Substituting Equations 2.23 and 2.24 into Equation 2.22 yields:

$$t_{Dw} = \frac{t}{r_w^2} \cdot \frac{\sum_{j=1}^{n} T_j \, r_{Dinv\,j}^2}{\sum_{j=1}^{n} S_j \, r_{Dinv\,j}^2} \qquad 2.32$$

APPENDIX C

MATHEMATICAL TREATMENT OF WATER FLOODING PERFORMANCE IN LAYERED COMPOSITE RESERVOIRS

A mathematical treatment of a proposed approach to predict water flooding performance is presented in this appendix. The approach is a modification of Dykstra-Parson method to take into account the changes in rock properties laterally. The basic assumptions and description of the reservoir model considered in this study are listed in Chapter 5.

C.1 Pressure Drop

The pressure drop in any layer j before breakthrough of that layer is given as:

$$\Delta P = \Delta P_{0j} + \Delta P_{wj},\ j = 1, 2, \ldots n \qquad 5.1$$

Each layer of the reservoir under study consists of two regions of different characteristics. After a certain period of water injection, the water front location in layer j lies either in the first region or in the second region of that layer.

For the first case, where the water front in layer j lies in region one of that layer, the pressure drop in the unswept portion of that layer (ΔP_{0j}) is given as:

$$\Delta P_{0j} = \frac{q_{0j}\,\mu_0}{W\,K_{r0}}\left[\frac{\ell_j - x_j}{K_j\,h_j} + \frac{L-\ell_j}{K_j'\,h_j'}\right],$$

$$x_j \leq \ell_j,\ j = 1,2,\ldots n \qquad C.1$$

and the pressure drop in the swept portion is given as:

$$\Delta P_{wj} = \frac{q_{wj}\,\mu_w}{W\,K_{rw}} \cdot \frac{x_j}{K_j\,h_j},\ x_j \leq \ell_j,\ j = 1,2,\ldots n \qquad C.2$$

It is assumed that both oil and water are incompressible fluids and the displacement is piston-like. Thus,

$$q_{0j} = q_{wj} = q_j,\ j = 1,2,\ldots n \qquad C.3$$

From Equations 5.1 and C.1 through C.3, the pressure drop in layer j is given as:

$$\Delta P = \frac{q_j\,\mu_w}{W\,K_{rw}}\left[\frac{x_j}{K_j\,h_j} + \frac{K_{rw}\,\mu_0}{K_{r0}\,\mu_w}\left(\frac{\ell_j - x_j}{K_j\,h_j} + \frac{L-\ell_j}{K_j'\,h_j'}\right)\right],$$

$$x_j \leq \ell_j,\ j = 1,2,\ldots n \qquad C.4$$

The mobility ratio M is

$$M = \frac{K_{rw}\ \mu_0}{K_{r0}\ \mu_w} \qquad C.5$$

Substituting Equation C.5 into Equation C.4 yields:

$$\Delta P = \frac{q_j\ \mu_w}{W\ K_{rw}\ K_j\ h_j}\left[x_j + M\left\{(\ell_j - x_j) + \frac{K_j\ h_j}{K_j'\ h_j'}(L - \ell_j)\right\}\right],$$

$$x_j \leq \ell_j\ ,\ j = 1,2,\ldots n \qquad C.6$$

$$\text{let } M_j' = \frac{K_j'\ h_j'}{K_j\ h_j}\ ,\ j = 1,2,\ldots n \qquad C.7$$

Thus Equation C.6 can be written as:

$$\Delta P = \frac{q_j\ \mu_w}{W\ K_{rw}\ K_j\ h_j}\left[\frac{x_j}{L} + M\frac{\ell_j}{L} - M\frac{x_j}{L} + \frac{M}{M_j'} - \frac{M}{M_j'}\ \frac{\ell_j}{L}\right]$$

$$= \frac{q_j\ \mu_w\ L}{W\ K_{rw}\ K_j\ h_j}\left[(1-M)\frac{x_j}{L} + M\left(1-\frac{1}{M_j'}\right)\frac{\ell_j}{L} + \frac{M}{M_j'}\right],$$

$$x_j \leq \ell_j\ ,\ j = 1,2,\ldots n \qquad 5.2$$

The effective velocity in region 1 of layer j is given as:

$$\frac{dx_j}{dt} = \frac{q_j}{W\ h_j\ \phi_j} \qquad 5.3$$

Then $\frac{q_j}{W} = h_j \, \phi_j \, \frac{dx_j}{dt}$, $j = 1,2,\ldots n$ 5.4

let $M''_{1,j} = \frac{\mu_w}{K_{rw}} \cdot \frac{\phi_j}{K_j}$, $j = 1,2, \ldots n$ 5.8

From Equations 5.2, 5.4 and 5.8

$$\Delta P = M''_{1,j}\left[(1-M)\frac{x_j}{L} + \frac{M}{M'_j}\left\{(M'_j - 1)\frac{\ell_j}{L} + 1\right\}\right] \frac{dx_j}{dt},$$

$$x_j \leq \ell_j \ , \quad j = 1,2,\ldots n \qquad 5.5$$

Similarly, for the second case where the water front lies in region two of layer j, an expression for the pressure drop (ΔP) is given as:

$$\Delta P = \left(\frac{M''_{2,j}}{M'_j}\right)\left[(1-M)\frac{x_j}{L} + (M'_j - 1)\frac{\ell_j}{L} + M\right]\frac{dx_j}{dt} \ ,$$

$$x_j \geq \ell_j \ , \ j = 1,2,\ldots n \qquad 5.6$$

where: $M''_{2,j} = \frac{\mu_w}{K_{rw}} \cdot \frac{\phi'_j \, h'_j}{K_j \, h_j}$ 5.9

C.2 Water Front Locations

Some water flooding operators inject the water at a constant rate and consequently the pressure drop (ΔP) varies with time and some others follow the reverse. The

two situations are treated in the following sections.

C.2.1 Constant Injection Rate

In this case the water injection rate is kept constant and the pressure drop (ΔP) varies with time. However, at any time the pressure drops on layers 1 to n are the same and equal to ΔP.

Let us consider a system of n layers and assume that the i^{th} layer breaks through before $(i + 1)^{th}$ one. The pressure drop on particular layer is expressed either by Equation 5.5 or Equation 5.6 depending on water front location (x_j) in that particular layer. When the i^{th} layer has just broken through, the water front location in j^{th} layer, $(j > i)$, is determined as follows:

At any time of water injection, pressure drop on all layers are equal. Thus:

$$\Delta P_{\text{layer } i} = \Delta P_{\text{layer } j}$$

Substituting Equations 5.5 and/or 5.6 in the above equation and integrating as:

$$M''_{1,i}\int_0^{\ell_i}\left[(1-M)\frac{x_i}{L}+\frac{M}{M'_i}\left(M'_i-1\right)\frac{\ell_i}{L}+1\right]dx_i$$

$$+\frac{M''_{2,i}}{M'_i}\int_{\ell_i}^{L}\left[(1-M)\frac{x_i}{L}+\left(M'_i-1\right)\frac{\ell_i}{L}+M\right]dx_i$$

$$=M''_{1,j}\int_0^{\alpha}\left[(1-M)\frac{x_j}{L}+\frac{M}{M'_j}\left(M'_j-1\right)\frac{\ell_j}{L}+1\right]dx_j$$

$$\frac{M''_{2,j}}{M'_j}\int_{\ell_j}^{x_j}\left[(1-M)\frac{x_j}{L}+\left(M'_j-1\right)\frac{\ell_j}{L}+M\right]dx_j\ ,$$

$$i=1,2,\ldots n-1,\ j=i+1,\ldots n \qquad \text{C.8}$$

where: $\alpha = x_j$ and $\beta = 0$ for $0 \le x_j \le \ell_j$

$\alpha = \ell_j$ and $\beta = 1$ for $\ell_j \le x_j \le L$

Integrals on the left side of Equation C.8 are evaluated as follows:

$$\int_0^{\ell_i}\left[(1-M)\frac{x_i}{L}+\frac{M}{M'_i}\left\{\left(M'_i-1\right)\frac{\ell_i}{L}+1\right\}\right]dx_i$$

$$= \frac{L}{2} \left[(1-M) \left(\frac{\ell_i}{L}\right)^2 + 2\frac{M}{M_i'} (M_i' - 1) \left(\frac{\ell_i}{L}\right)^2 + \frac{\ell_i}{L} \right.$$

$$= \frac{L}{2} \left(\frac{\ell_i}{L}\right) \left[\left\{1-M + 2 \frac{M}{M_i'} (M_i' - 1)\right\} \frac{\ell_i}{L} + 2 \frac{M}{M_i'} \right. \qquad \text{C.9}$$

$$\int_{\ell_i}^{L} \left[(1-M)\frac{x_i}{L} + (M_i' - 1) \frac{\ell_i}{L} + M \right] dx_i$$

$$= \frac{L}{2} \left[(1-M) \left(1 - \left(\frac{\ell_i}{L}\right)^2\right) + 2(M_i' - 1) \frac{\ell_i}{L} \left(1 - \frac{\ell_i}{L}\right) + 2M\left(1 - \frac{\ell_i}{L}\right) \right]$$

$$= \frac{L}{2}\left(1 - \frac{\ell_i}{L}\right) \left[(1-M) \left(1 + \frac{\ell_i}{L}\right) + 2(M_i' - 1) \frac{\ell_i}{L} + 2M \right] \qquad \text{C.10}$$

The integral terms on the right side of Equation C.8 are evaluated as follows:

For the case of $0 \leq x_j \leq \ell_j$, the second integral is canceled and the upper limit of first integration is x_j. Then:

$$\int_0^{x_j} \left[(1-M) \frac{x_j}{L} + \frac{M}{M_j'} \left\{ (M_j' - 1) \frac{\ell_j}{L} + 1 \right\} \right] dx_j$$

$$= \frac{L}{2} \left[(1-M) \left(\frac{x_j}{L}\right)^2 + 2\frac{M}{M_j'} \left\{ (M_j' - 1) \frac{\ell_j}{L} + 1 \right\} \frac{x_j}{L} \right.$$

$$0 \leq x_j \leq \ell_j \qquad \text{C.11}$$

For the case of $\ell_j \leq x_j \leq L$, the upper limit of the first integral equals to ℓ_j and $\beta = 1$. Then:

$$\int_0^{\ell_j} \left[(1-M)\frac{x_j}{L} + \frac{M}{M_j'}\left\{(M_j' - 1)\frac{\ell_j}{L} + 1\right\}\right] dx_j$$

$$= \frac{L}{2}\left(\frac{\ell_j}{L}\right)\left[(1-M)\frac{\ell_j}{L} + 2\frac{M}{M_j'}\left\{(M_j' - 1)\frac{\ell_j}{L} + 1\right\}\right]$$

$$= \frac{L}{2}\left(\frac{\ell_j}{L}\right)\left[1-M + 2\frac{M}{M_j'}(M_j' - 1)\frac{\ell_i}{L} + 2\frac{M}{M_j'}\right]$$

$$0 \leq x_j \leq \ell_j \qquad \text{C.12.a}$$

$$\int_{\ell_j}^{x_j} \left[(1-M)\frac{x_j}{L} + (M_j' - 1)\frac{\ell_j}{L} + M\right] dx_j$$

$$= \frac{L}{2}\left\{(1-M)\left(\frac{x_j}{L}\right)^2 - (1-M)\left(\frac{\ell_j}{L}\right)^2 + 2\left[(M_j' - 1)\frac{\ell_j}{L}\frac{x_j}{L}\right.\right.$$

$$\left.\left. -(M_j'-1)\left(\frac{\ell_j}{L}\right)^2 + M\frac{x_j}{L} - M\frac{\ell_j}{L}\right]\right\}$$

$$= \frac{L}{2}\left\{(1-M)\left(\frac{x_j}{L}\right)^2 + 2\left[(M_j'-1)\frac{\ell_j}{L} + M\right]\frac{x_j}{L}\right.$$

$$\left. + \frac{\ell_j}{L}\left[(1+M-2M_j')\frac{\ell_j}{L} - 2M\right]\right\},$$

$$\ell_j \leq x_j \leq L \qquad \text{C.12.b}$$

Substituting Equations C.9 through C.11 into Equation C.8 yields:

$$\frac{M''_{1,i}}{M''_{1,j}} \frac{\ell_i}{L} \left[\left\{ (1 - M + 2\frac{M}{M'_i} (M'_i - 1) \right\} \frac{\ell_i}{L} + 2 \frac{M}{M'_i} \right] +$$

$$\frac{M''_{2,i}}{M''_{1,j}} \frac{}{M'_i} (1 - \frac{\ell_i}{L}) \left[(1 - M)(1 + \frac{\ell_i}{L}) + 2 (M'_i - 1) \frac{\ell_i}{L} + 2M \right]$$

$$= (1 - M) (\frac{x_j}{L})^2 + 2 \frac{M}{M'_j} \left\{ (M'_j - 1) \frac{\ell_j}{L} + 1 \right\} \frac{x_j}{L} ,$$

$$0 \leq x_j \leq \ell_j, \quad i = 1,2,\ldots n-1, \quad j = i + 1, \ldots n \qquad C.13$$

Substituting Equation C.9, C.10 and C.12 into Equation C.8 yields:

$$\frac{M''_{1,i}}{M''_{2,j}} \frac{\ell_i}{L} \left[\left\{ (1 - M + 2 \frac{M}{M'_i}(M'_i - 1) \right\} \frac{\ell_i}{L} + 2 \frac{M}{M'_i} \right] +$$

$$\frac{M''_{2,i}}{M''_{2,j}} \frac{}{M'_i} (1 - \frac{\ell_i}{L}) \left[(1 - M)(1 + \frac{\ell_i}{L}) + 2 (M'_i - 1) \frac{\ell_i}{L} + 2M \right]$$

$$= \frac{M''_{1,j}}{M''_{2,j}} \frac{\ell_j}{L} \left[\left\{ 1 - M + \frac{2M}{M'_j}(M'_j - 1) \right\} \frac{\ell_j}{L} + \frac{2M}{M'_j} \right] + \frac{1}{M'_j} \frac{\ell_j}{L} \left[(1 + M - 2M'_j) \frac{\ell_j}{L} - 2M \right]$$

$$+ \frac{1}{M'_j} \left[(1 - M) (\frac{x_j}{L})^2 + 2 (M'_j - 1) \frac{\ell_j}{L} + M \frac{x_j}{L} \right] ,$$

$$\ell_j \leq x_j \leq L, \quad i = 1,2,\ldots n-1, \quad j = i + 1,\ldots n \qquad C.14$$

Solving Equations C.13 and C.14 for $\frac{x_j}{L}$ yields:

$$\frac{x_j}{L} = \frac{- b_j \pm \sqrt{b_j^2 - 4a'_j(c_i/E_j + c_j)}}{2a_j}$$

For the case where i^{th} and j^{th} layers have same dimensions and properties, $x_j/L = 1$. Thus the sign before the radical must be positive. Then:

$$\frac{x_j}{L} = \frac{- b_j + \sqrt{b_j^2 - 4a'_j(c_i/E_j + c_j)}}{2a_j} ,$$

$$M \neq 1, \text{ and } j = 1,2,\ldots n \qquad 5.10$$

where:

$$\left.\begin{aligned} a'_j &= (1 - M) \\ b_j &= 2\frac{M}{M'_j}\left[(M'_j - 1)\frac{\ell_j}{L} + 1\right] \\ c_j &= 0 \\ E_j &= M''_{1,j} \end{aligned}\right\} , \; 0 \leq x_j \leq \ell_j \qquad 5.11$$

$$\left.\begin{aligned} a'_j &= (1 = M)/M'_j \\ b_j &= \frac{2}{M'_j}\left[(M'_j - 1)\frac{\ell_i}{L} + M\right] \\ c_j &= \frac{M''_{1,j}}{M''_{2,j}}\left(\frac{\ell_j}{L}\right)\left[1-M+\frac{2M}{M'_j}(M'_j-1)\frac{\ell_j}{L} + \frac{2M_j}{M'_j}\right] \\ &\quad + \frac{1}{M'_j}\frac{\ell_i}{L}\left[(1+M-2M'_j)\frac{\ell_j}{L} - 2M\right] \\ E_j &= M''_{2,j} \end{aligned}\right\} , \ell_i \leq x_i \leq L, \qquad 5.12$$

$$c_i = M''_{1,i}\frac{\ell_i}{L}\left[\left\{1-M+2\frac{M}{M'_i}(M'_i-1)\right\}\frac{\ell_i}{L} + 2\frac{M}{M'_i}\right]$$

$$+ \frac{M''_{1,i}}{M'_i}\left(1-\frac{\ell_i}{L}\right)\left[(1-M)\left(1+\frac{\ell_j}{L}\right)+2(M'_i-1)\frac{\ell_i}{L} + 2M\right] \quad 5.13$$

C.2.2 Constant Injection Pressure:

In this case, both injector and producer bottom hole pressures are kept constant during water injection process. The water injection rate varies with time. The time of water-front arrival to the interface between the two regions of layer j ($t_{\ell j}$) is obtained by integrating Equation 5.5 as follows:

$$\int_0^{t_{Lj}} dt = \frac{M''_{1,j}}{\Delta P}\int_0^{\ell_j}\left[(1-M)\frac{x_j}{L} + \frac{M}{M'_j}\left\{(M'_j-1)\frac{\ell_j}{L} + 1\right\}\right] dx_j$$

$$t_{\ell j} = \frac{1}{2}\left(\frac{L}{\Delta P}\right)M''_{1,j}\left(\frac{\ell_j}{L}\right)\left[\left\{1-M+2\frac{M}{M'_j}(M'_j-1)\right\}\left(\frac{\ell_j}{L}\right) + 2\frac{M}{M'_j}\right],$$

$$j = 1,2,\ldots n \quad 5.14$$

The time of j^{th} layer breakthrough (t_{Lj}) is obtained by integrating Equation 5.6 as follows:

$$\int_{t_{\ell j}}^{t_{Lj}} dt = \frac{M''_{2,j}}{\Delta P\, M'_j}\int_{\ell_j}^{L}\left[(1-M)\frac{x_j}{L} + (M'_j-1)\frac{\ell_j}{L} + M\right] dx_j$$

$$t_{Lj} = t_{1j} + \frac{1}{2}\left(\frac{L}{\Delta P}\right)\frac{M''_{2,j}}{M'_j}\left(1 - \frac{\ell_j}{L}\right)\left[(1 - M)\left(1+\frac{\ell_j}{L}\right)\right.$$

$$\left. + 2(M'_j - 1)\frac{\ell_j}{L} + 2M\right], \quad j = 1,2,\ldots n \qquad \text{C.15}$$

Substituting Equation 5.14 into Equation C.15 yields:

$$t_{Lj} = \frac{1}{2}\left(\frac{L}{\Delta P}\right)\left\{M''_{1,j}\frac{\ell_j}{L}\left[\left\{1-M-2\frac{M}{M'_j}(M'_j - 1)\right\}\frac{\ell_j}{L} + 2\frac{M}{M'_j}\right]\right.$$

$$\left. + \frac{M''_{2,j}}{M'_j}\left(1 - \frac{\ell_j}{L}\right)\left[(1-M)\left(1+\frac{\ell_j}{L}\right) + 2(M'_j-1)\frac{\ell_j}{L} + 2M\right]\right\},$$

$$j = 1,2,\ldots n \qquad 5.15$$

The water front location in layer j, for the case of $x_j \leq \ell_j$, at time t is obtained by integrating Equation 5.5 as follows:

$$\int_0^t dt = \frac{M''_{1,j}}{\Delta P}\int_0^{x_j}\left[(1-M)\frac{x_j}{L} + \frac{M}{M'_j}\left\{(M'_j-1)\frac{\ell_j}{L} + 1\right\}\right] dx_j$$

$$t = \frac{1}{2}\left(\frac{L}{\Delta P}\right) M''_{1,j}\left[(1-M)\left(\frac{x_j}{L}\right)^2 + 2\frac{M}{M'_j}\left\{(M'_j-1)\frac{\ell_j}{L} + 1\right\}\frac{x_j}{L}\right],$$

$$j = 1,2,\ldots n \qquad \text{C.16}$$

Solving Equation C.16 for $\frac{x_j}{L}$ yields:

$$\frac{x_j}{L} = \frac{-b_j + \sqrt{b_j^2 + 8(\Delta P/L)(a_j'/M''_{1,j})t}}{2a_j'} ,$$

$$M \neq 1,\ x_j \leq \ell_j ,\ j = 1,2,\ldots n \qquad C.17$$

For the other case where $x_j \geq \ell_j$, the water front location at time t is obtained by integrating Equation 5.6 as follows:

$$\int_{t_{\ell j}}^{t} dt = \frac{M''_{2,j}}{P\ M'_j} \int_{\ell_j}^{x_j} \left[(1-M)\frac{x_j}{L} + (M'_j - 1)\frac{\ell_j}{L} + M\right] dx_j$$

$$t - t_{\ell j} = \frac{1}{2}\left(\frac{L}{P}\right)\frac{M''_{2,j}}{M'_j}\left[(1-M)\left(\frac{x_j}{L}\right)^2 + 2\left\{(M'_j-1)\frac{\ell_j}{L} + M\right\}\frac{x_j}{L}\right.$$

$$\left. - \frac{\ell_j}{L}\left\{(2M'_j - M - 1)\frac{\ell_j}{L} + 2M\right\}\right] ,$$

$$\ell_j \leq x_j \leq L,\ j = 1,2,\ldots n \qquad C.18$$

Solving Equation C.18 for $\frac{x_j}{L}$ yields:

$$\frac{x_j}{L} = \frac{-b_j + \sqrt{b_j^2 + 4a_j'\left\{2\frac{\Delta P}{L}\frac{1}{M''_{2,j}}(t-t_{\ell j}) + d_j\right\}}}{2a_j} ,$$

$$M \neq 1,\ \ell_j \leq x_j \leq L,\ j = 1,2,\ldots n \qquad C.19$$

where:

$$d_j = \frac{\ell_j}{L}\left[(2M'_j - M - 1)\frac{\ell_j}{L} + 2M\right] / M'_j \qquad C.20$$

a'_j and b_j are determined using Equation 5.11 or Equation 5.12 depending on whether $x_j \leq \ell_j$ or $x_j \geq \ell_j$ respectively.

Equation C.17 and C.19 give the water front location at any time (t). Thus the flow rate in each layer can be calculated using Darcy's law for three beds in a series.

C.3 Water Oil Ratio

For the system under study, when the j^{th} layer has broken through, water oil ratio is defined as:

$$WOR = \sum_{i=1}^{j} q_{wi} / \sum_{i=j+1}^{n} q_{0i} \qquad C.21$$

Before break through, the water production is zero and thus water oil ratio is zero. After break through the water oil ratio increases with time. After break through of a certain layer j, the water production from that layer is given as:

$$q_{wj} = \frac{\Delta P}{\frac{\mu_w L}{K_j h_j K_{rw} W}\left[\frac{\ell_j}{L} + \frac{1-(\ell_j/L)}{M'_j}\right]} \quad , j=1,2,\ldots n \qquad C.22$$

For layer j that has not broken through yet, the oil production from that layer is given as:

$$q_{oj} = \frac{\Delta P}{\frac{\mu_w L}{W K_{rw} K_j h_j} \{(\frac{x_j}{L}) + M[(\frac{\ell_j}{L} - \frac{x_j}{L}) + (1 - \frac{\ell_i}{L})/M'_j]\}},$$

$$x_j \leq \ell_j, \quad j = 1,2,\ldots n \qquad C.23$$

$$= \frac{\Delta P}{\frac{\mu_w L}{W K_{rw} K_j h_j} [\frac{\ell_j}{L} + \frac{1}{M'_j} (\frac{x_j}{L} - \frac{\ell_j}{L}) + \frac{M}{M'_j}(1 - \frac{x_j}{L})]},$$

$$x_j \geq \ell_j, \quad j = 1,2,\ldots n \qquad C.24$$

Substituting Equations C.22 and C.23 or C.24 into Equation C.21 yields an expression for WOR as:

$$WOR = \frac{\sum_{i=1}^{j} \frac{K_i h_i}{\frac{\ell_i}{L} + \frac{1}{M'_i}(1 - \frac{\ell_i}{L})}}{\sum_{i=j+1}^{n} \frac{K_i h_i}{Y_i}} \qquad 5.19$$

where

$$Y_i = \frac{x_i}{L} + M[(\frac{\ell_i}{L} - \frac{x_i}{L}) + \frac{1}{M'_i}(1 - \frac{\ell_i}{L}),$$

$$x_i \leq \ell_i \qquad 5.20$$

$$= \frac{\ell_i}{L} + \frac{1}{M'_i}\left[\left(\frac{x_i}{L} - \frac{\ell_i}{L}\right) + M\left(1 - \frac{x_i}{L}\right)\right],$$

$$x_i \geq \ell_i \qquad 5.21$$

C.4 Special Case (M = 1)

For the mobility ratio equals unity, Equations C.10, C.17 and C.19 fail to predict the water front location during water front process. Such case is treated in this section.

C.4.1 Water Front Location (Constant Injection Rate)

Substituting M = 1 into Equations C.13 and C.14 yeilds an expression for the water front as:

$$\frac{x_j}{L} = \frac{A_i}{E_j A_j}\left[M''_{1,i}\frac{\ell_i}{L} + M''_{2,i}\left(1 - \frac{\ell_i}{L}\right)\right] + H_j \qquad 5.22$$

where $A_r = \frac{1}{M'_r}\left[(M'_r - 1)\frac{\ell_r}{L} + 1\right]$, r = i or j

$$E_j = M''_{1,j}, \quad x_j \leq \ell_j$$

$$= M''_{2,j}, \quad x_j \geq \ell_j$$

$$H_j = 0, \quad x_j \leq \ell_j$$

$$= \left(1 - \frac{M''_{1,j}}{M''_{2,j}}\right)\frac{\ell_j}{L}, \quad x_j \geq j$$

C.4.2 Water Front Location (Constant Injection Pressure)

Substituting M = 1 into Equation 5.15 gives an expression for break through time of layer j as:

$$t_{Lj} = \frac{L}{\Delta P\ M'_j}\left[(M'_j-1)\frac{\ell_j}{L} + 1\right]\left[M''_{1,j}\frac{\ell_j}{L} + M''_{2,j}\left(1 - \frac{\ell_j}{L}\right)\right] ,$$

$$j = 1,2,\ldots n \qquad \text{C.25}$$

Substituting M = 1 into Equation C.16 gives:

$$\frac{x_j}{L} = \frac{M'_j}{M''_{1,j}}\frac{\Delta P}{L}\frac{t}{\left[(M'_j-1)\frac{\ell_i}{L}+1\right]} \quad , x_j \leq \ell_j \qquad \text{C.26.a}$$

Substituting M = 1 into Equation C.18 gives:

$$\frac{x_j}{L} = \frac{\frac{M'_j}{M''_{2,j}}\cdot\frac{\Delta P}{L}(t-t_{1j}) + \frac{\ell_j}{L}\left[(M'_j-1)\frac{\ell_j}{L}+1\right]}{(M'_j-1)\frac{\ell_j}{L}+1} \qquad \text{C.26.b}$$

where $t_{\ell j}$ is obtained by substituting M = 1 into Equation 6.14 as:

$$t_{\ell j} = \frac{L}{\Delta P}\frac{M''_{1,j}}{M'_j}\left(\frac{\ell_j}{L}\right)\left[(M'_j - 1)\frac{\ell_j}{L} + 1\right] \qquad \text{C.27}$$

From Equations C.26 and C.27, $\frac{x_j}{L}$ is written as:

$$\frac{x_j}{L} = (1-\frac{M''_{1,j}}{M''_{2,j}})\frac{\ell_j}{L} + \frac{M'_j}{M''_{2,j}} \frac{\Delta P}{L} \frac{t}{[(M'_j-1)\frac{\ell_j}{L} + 1]}, \quad x_j \geq \ell_j \qquad 5.24$$

C.4.3 Water Oil Ratio

Substituting M = 1 into Equations C.23 and C.24 yields an expression for oil flow from layer j as:

$$q_{oj} = \frac{\Delta P}{\frac{\mu_w L}{W K_{rw} K_j h_j} [\frac{\ell_j}{L} + \frac{1-\frac{\ell_j}{L}}{M'_j}]} \qquad C.28$$

Substituting M = 1 into Equation 5.20 and 5.21 gives:

$$Y_i = \frac{\ell_j}{L} + \frac{(1-\frac{\ell_j}{L})}{M'_j}$$

Thus water oil ratio, when the j^{th} layer has broken through, is given as:

$$WOR = \sum_{i=1}^{j} [\frac{K_i h_i}{\frac{\ell_i}{L} + \frac{1}{M'_i}(1 - \frac{\ell_i}{L})}] \Big/ \sum_{i=j+1}^{n} [\frac{K_i h_i}{\frac{\ell_i}{L} + \frac{1}{M'_i}(1 - \frac{\ell_i}{L})}] \qquad 5.25$$

APPENDIX D

DRAWDOWN TYPE-CURVE PLOTS FOR DIFFERENT SYSTEMS WITH CONSTANT STORAGE ($y_1=y_2=y_3=1.$)

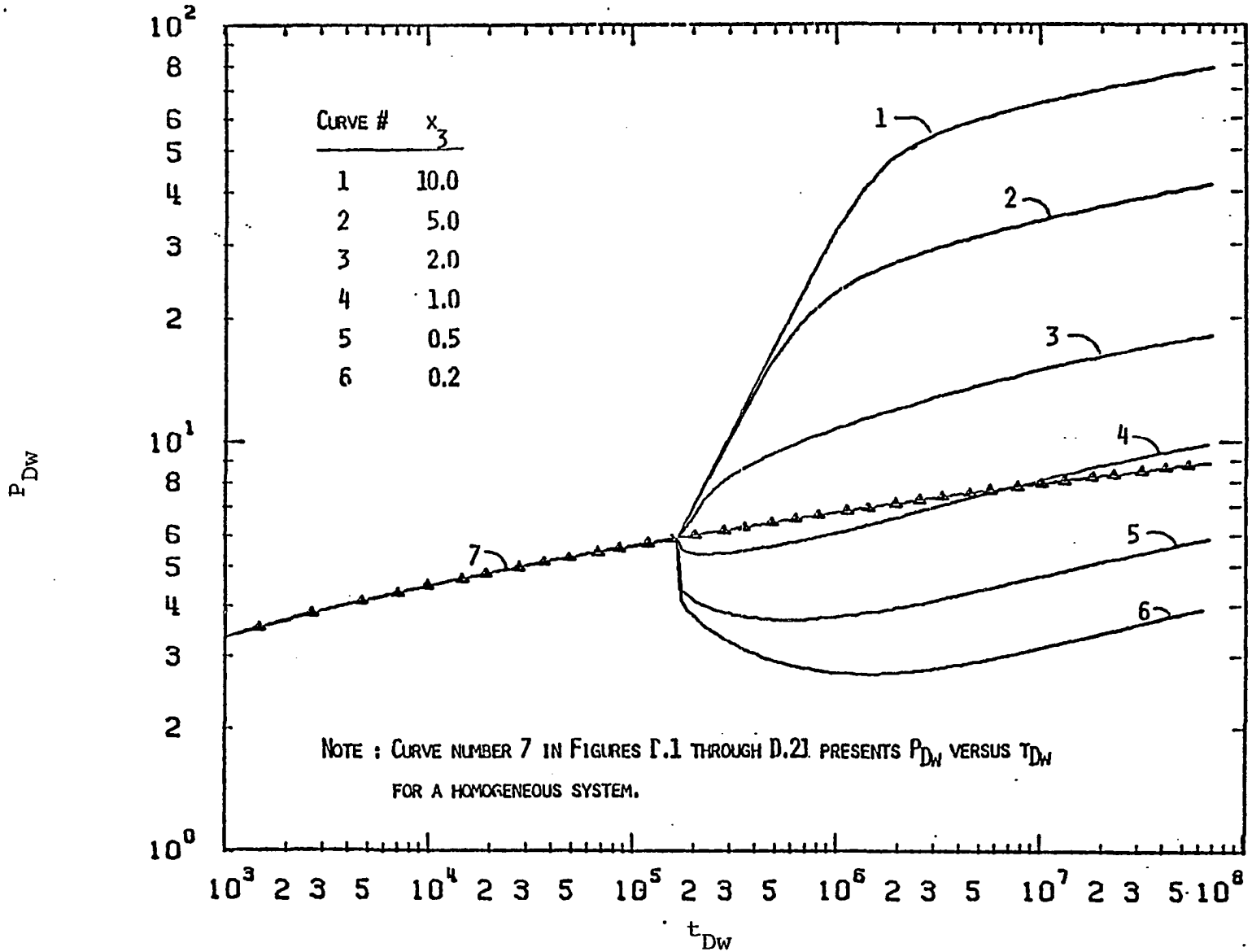

Figure D.1: Type-curve plot of P_{Dw} versus t_{Dw} for a two-layer two region system with z=1., x_1=0.2 and x_2=1..

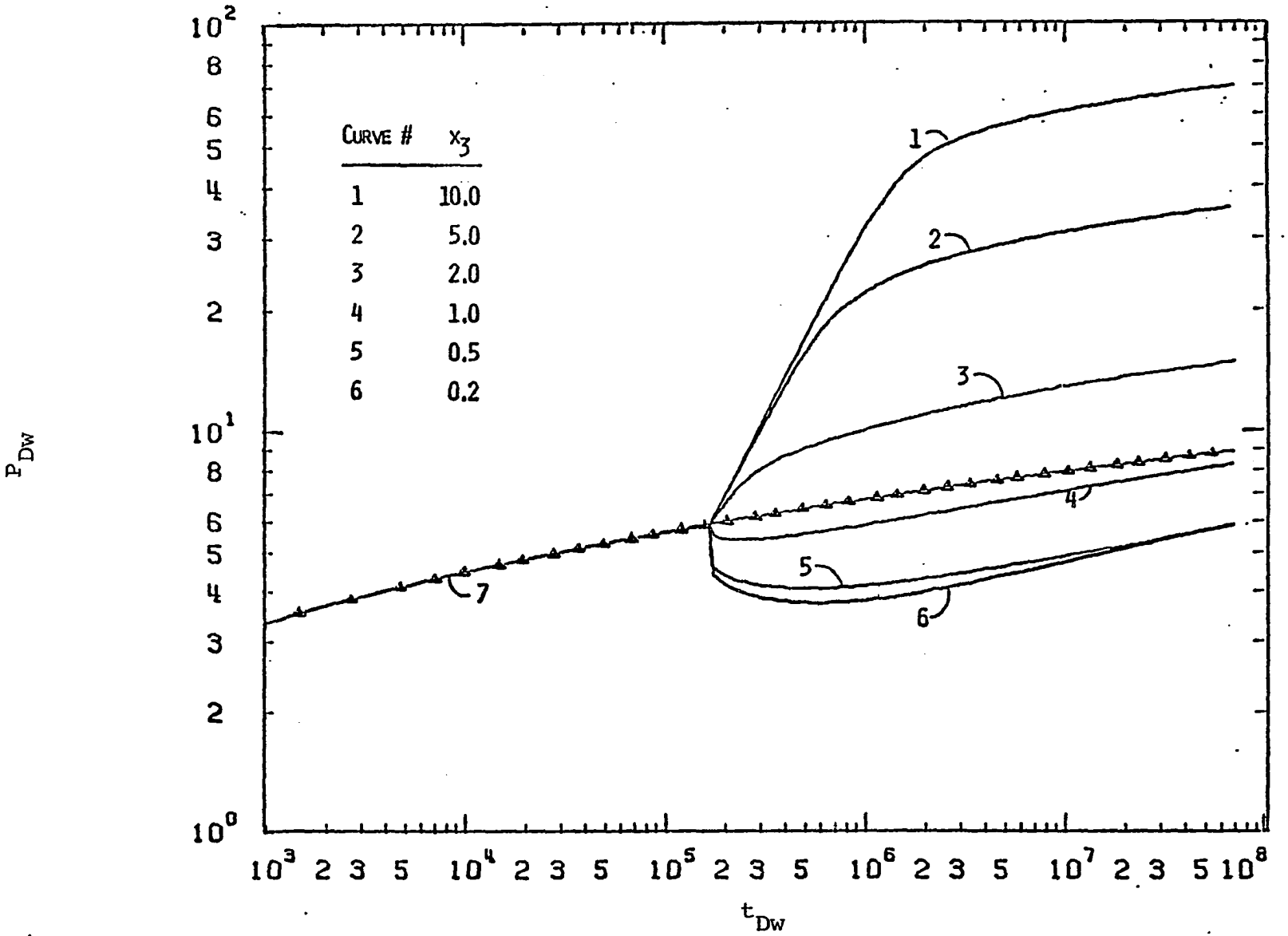

Figure D.2: Type-curve plot of P_{Dw} versus t_{Dw} for a two-layer two-region system with z=1., x_1=0.5 and x_2=1..

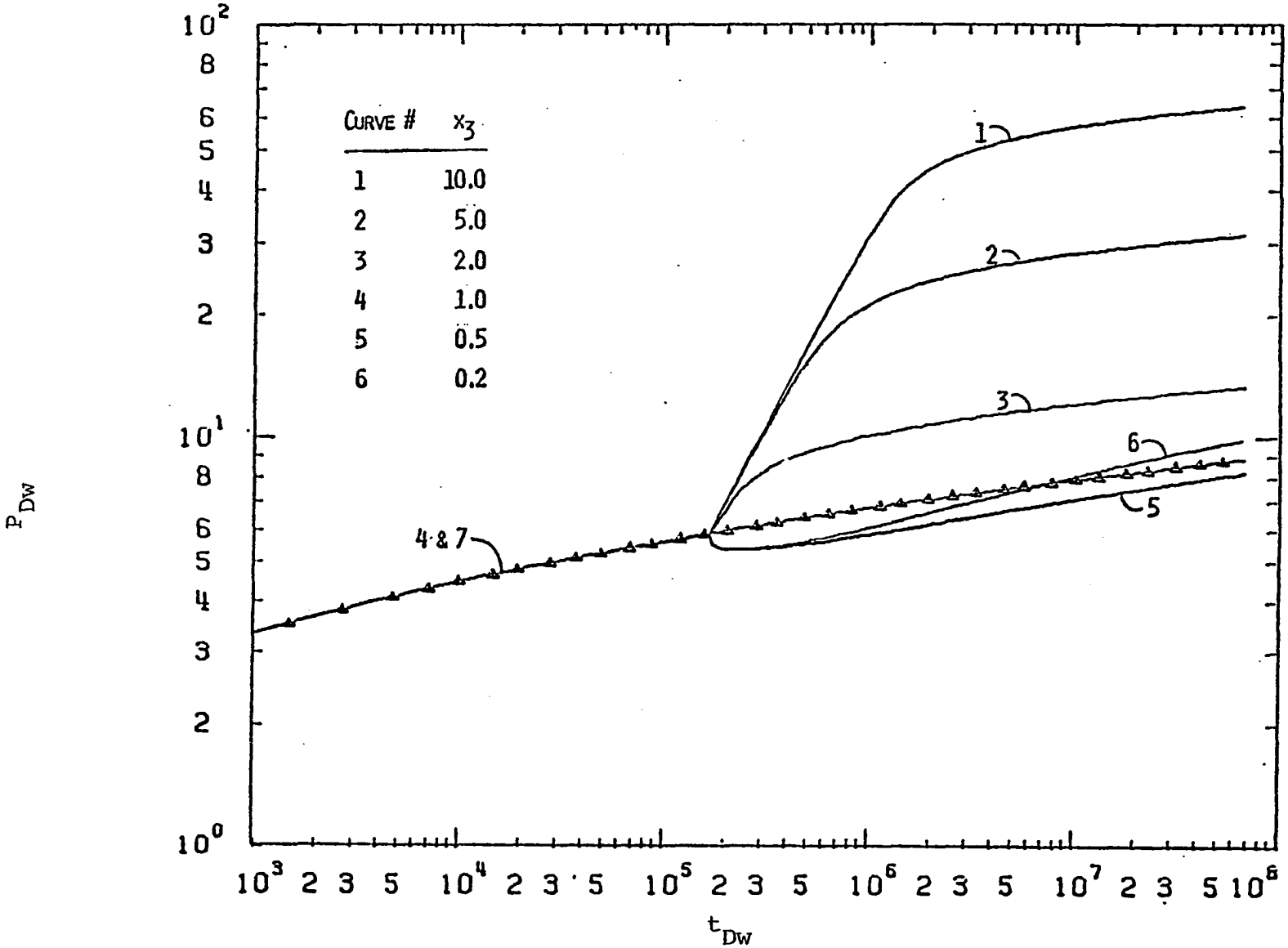

Figure D.3: Type-curve plot of P_{Dw} versus t_{Dw} for a two-layer two-region system with z=1., x_1=1. and x_2=1..

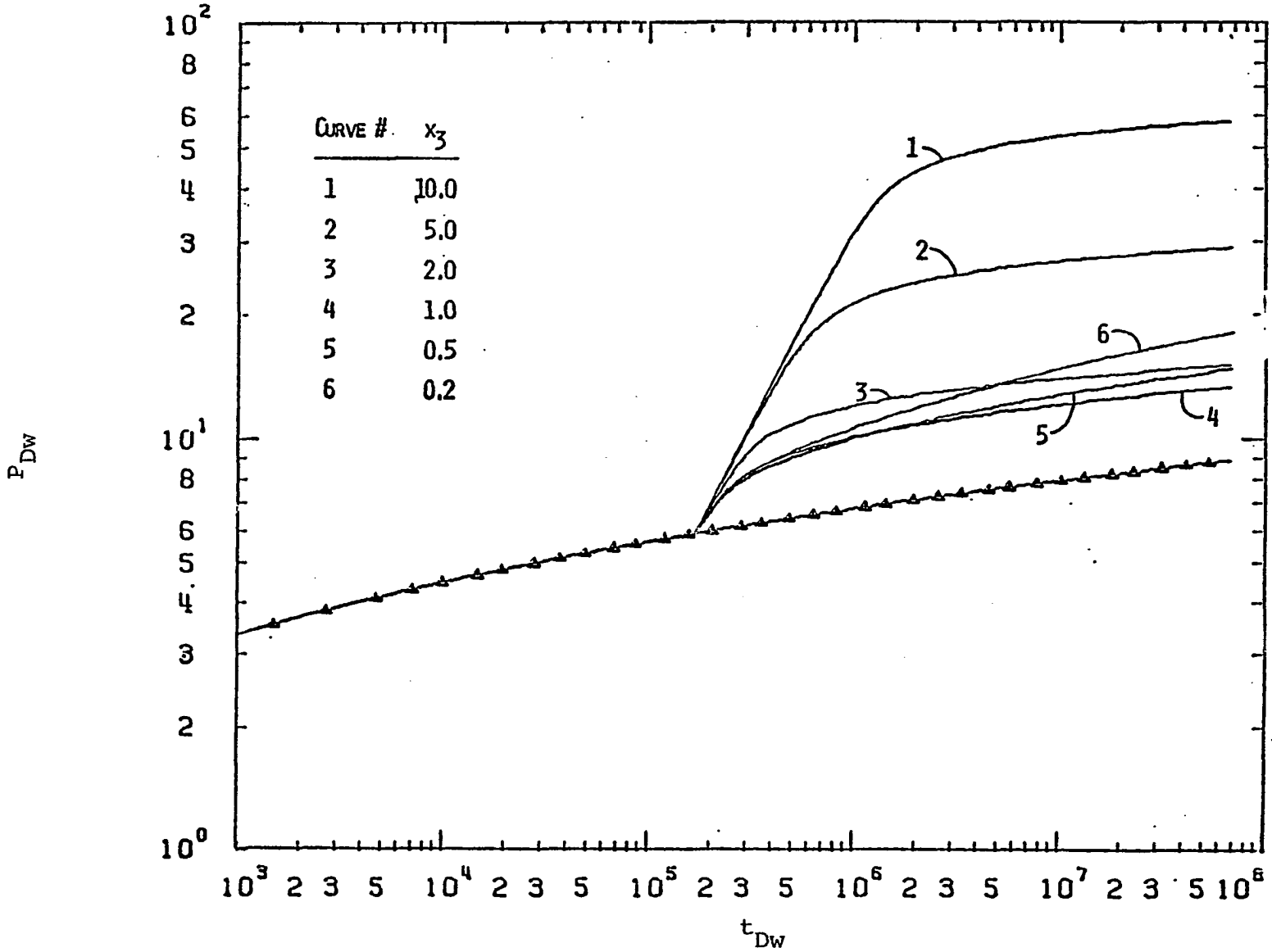

Figure D.4: Type-curve plot of P_{Dw} versus t_{Dw} for a two-layer two-region system with z=1., x_2=2. and x_2=1..

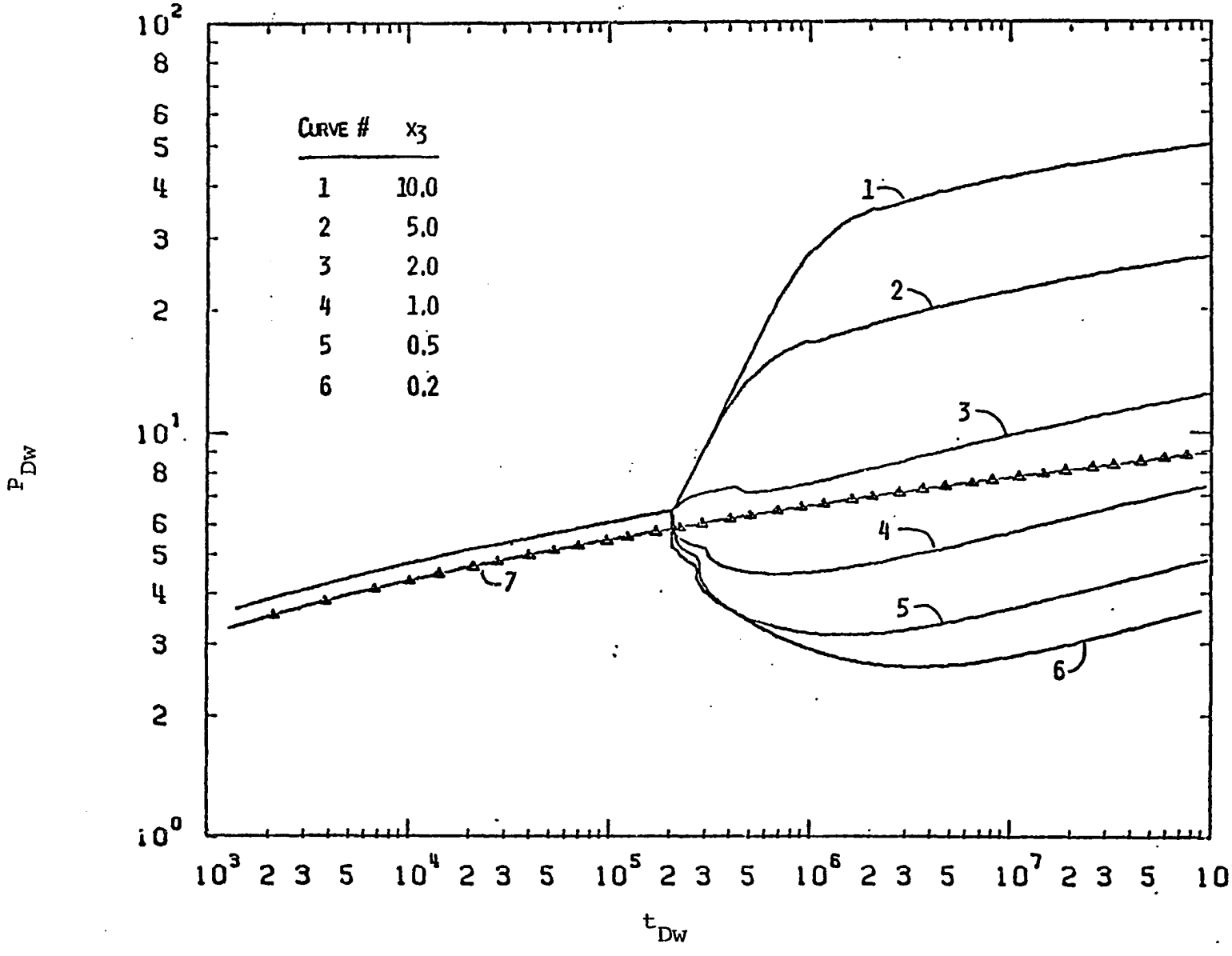

Figure D.5: Type-curve plot of P_{Dw} versus t_{Dw} for a two-layer two-region system with z=1., x_1=0.2 and x_2=2..

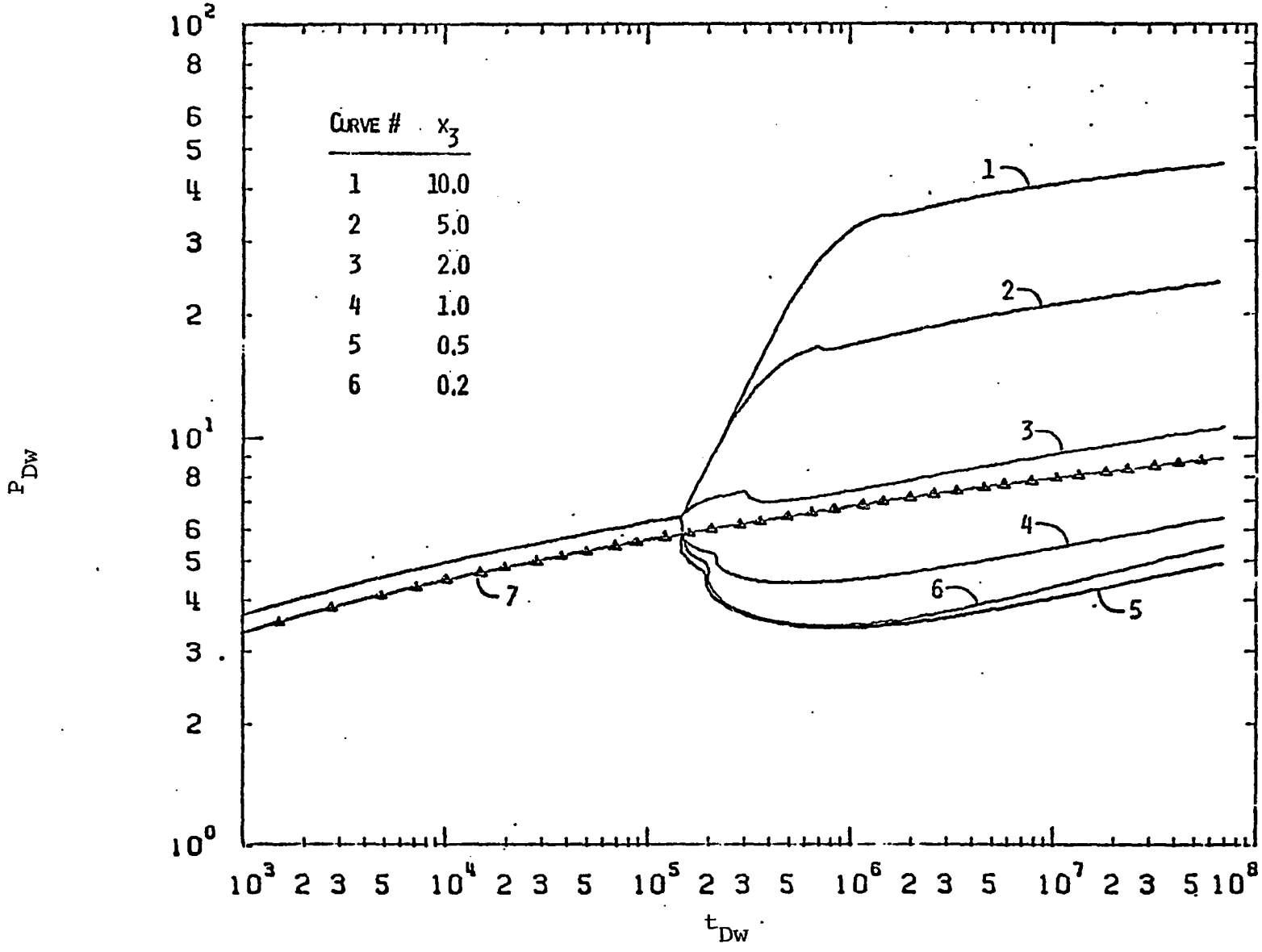

Figure D.6: Type-curve plot of P_{Dw} versus t_{Dw} for a two-layer two-region system with z=1., x_1=0.5 and x_2=2..

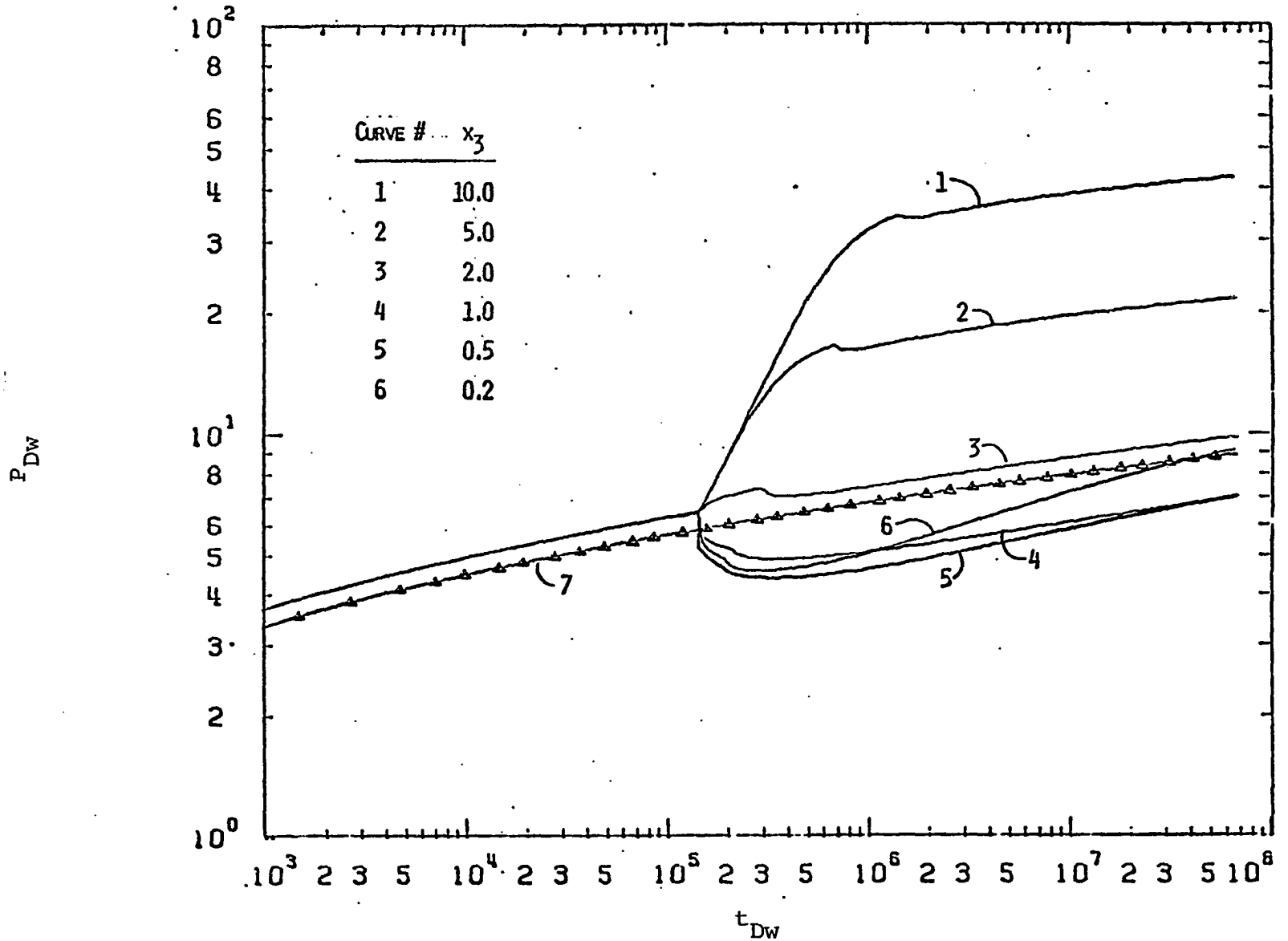

Figure D.7: Type-curve plot of P_{Dw} versus t_{Dw} for a two-layer two-region system with z=1., x_1=1. and x_2=2..

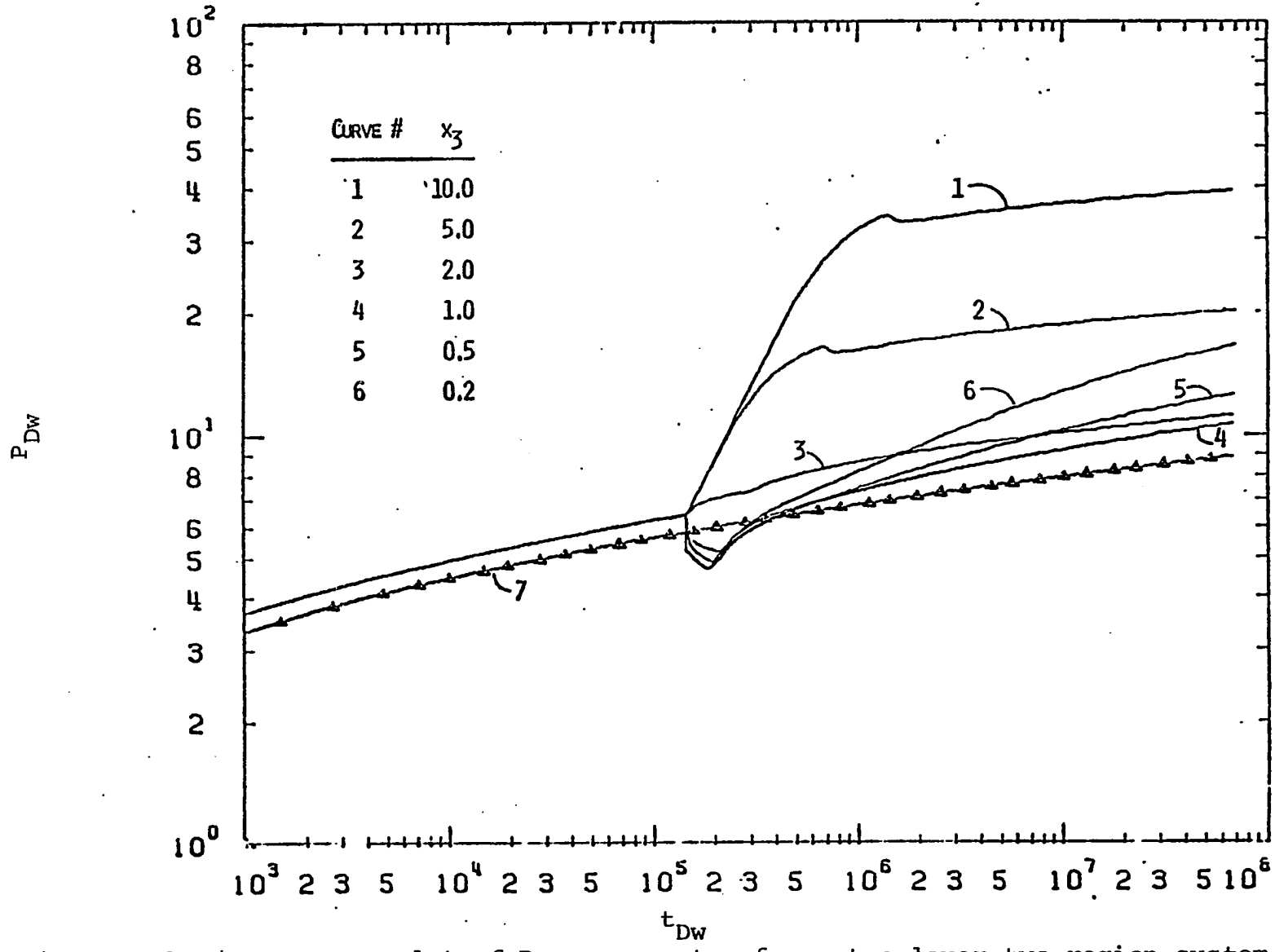

Figure D.8: Type-curve plot of P_{Dw} versus t_{Dw} for a two-layer two-region system with z=1., x_1=2. and x_2=2..

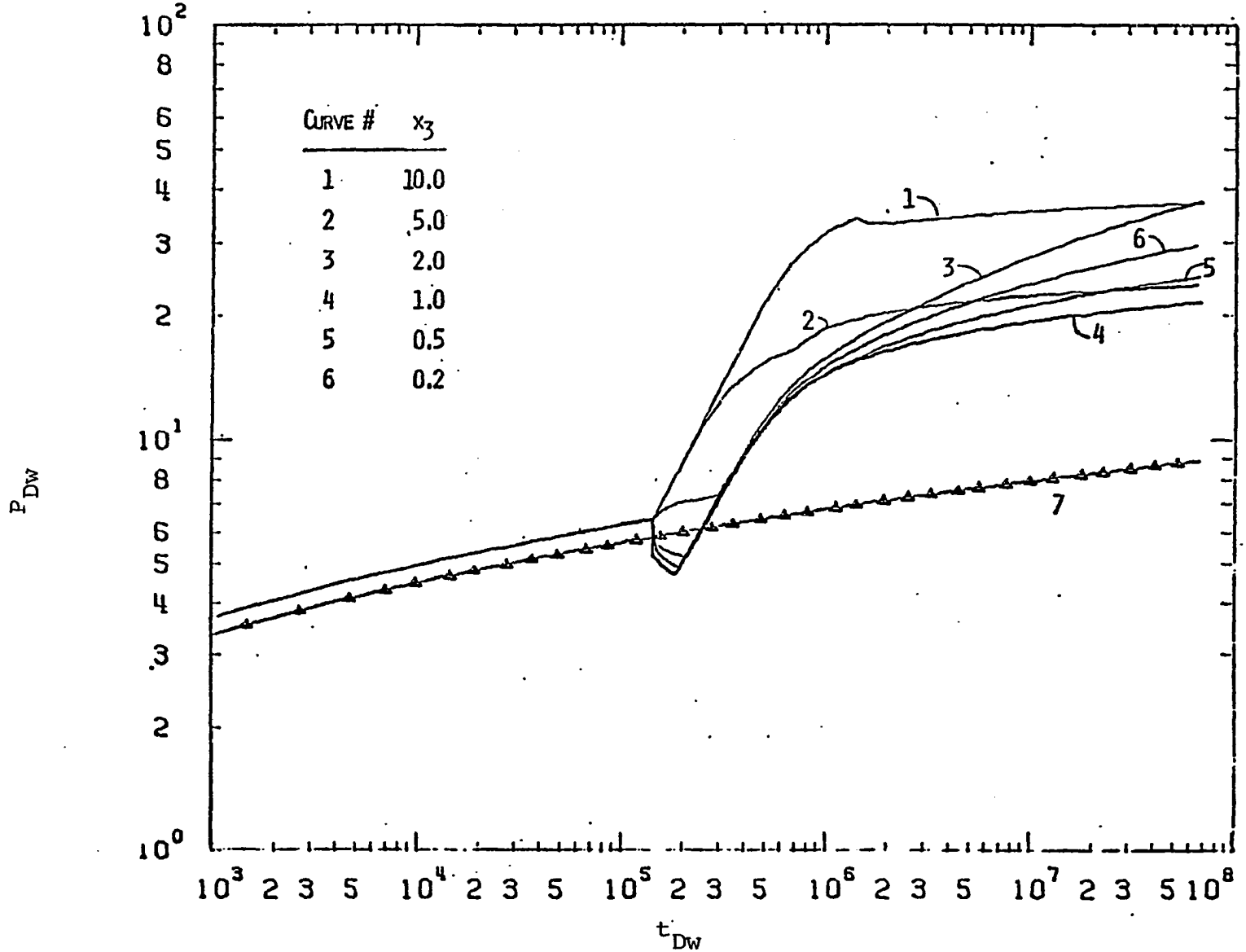

Figure D.9: Type-curve plot of P_{Dw} versus t_{Dw} for a two-layer two-region system with z=1., x_1=5.0 and x_2=2..

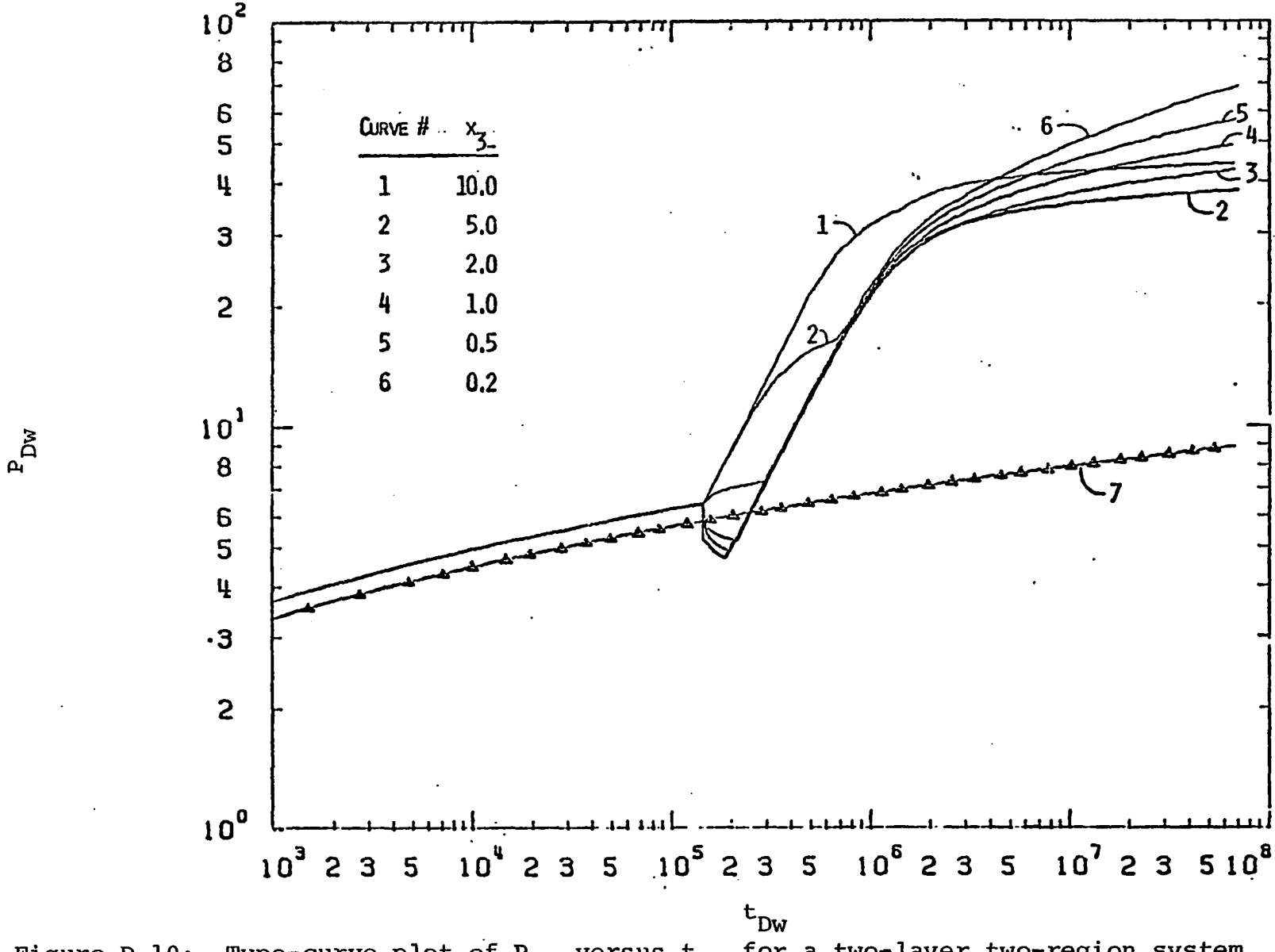

Figure D.10: Type-curve plot of P_{Dw} versus t_{Dw} for a two-layer two-region system with z=1., x_1=10. and x_2=2..

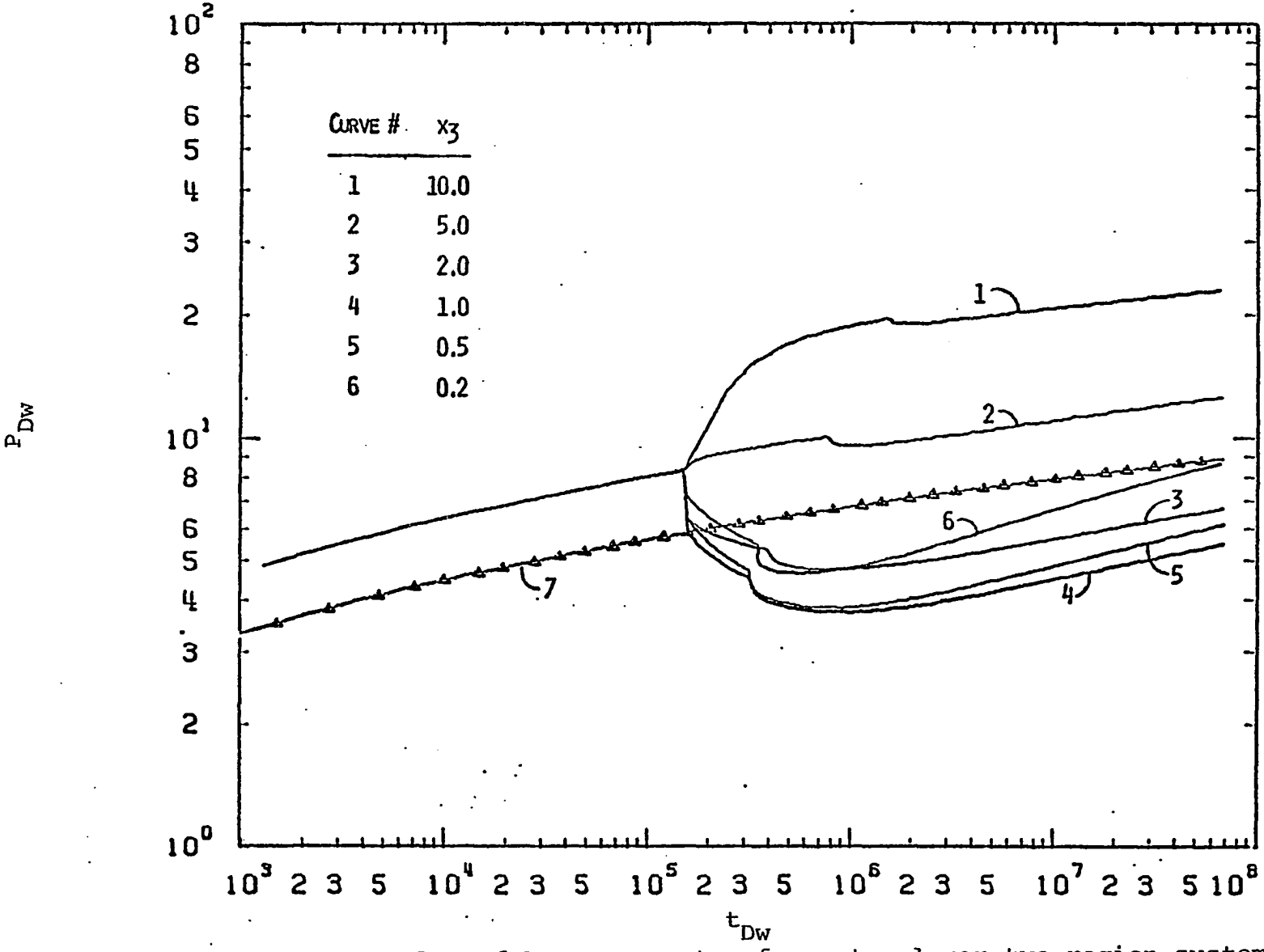

Figure D.11: Type-curve plot of P_{Dw} versus t_{Dw} for a two-layer two-region system with z=1., x_1=1. and x_2=5..

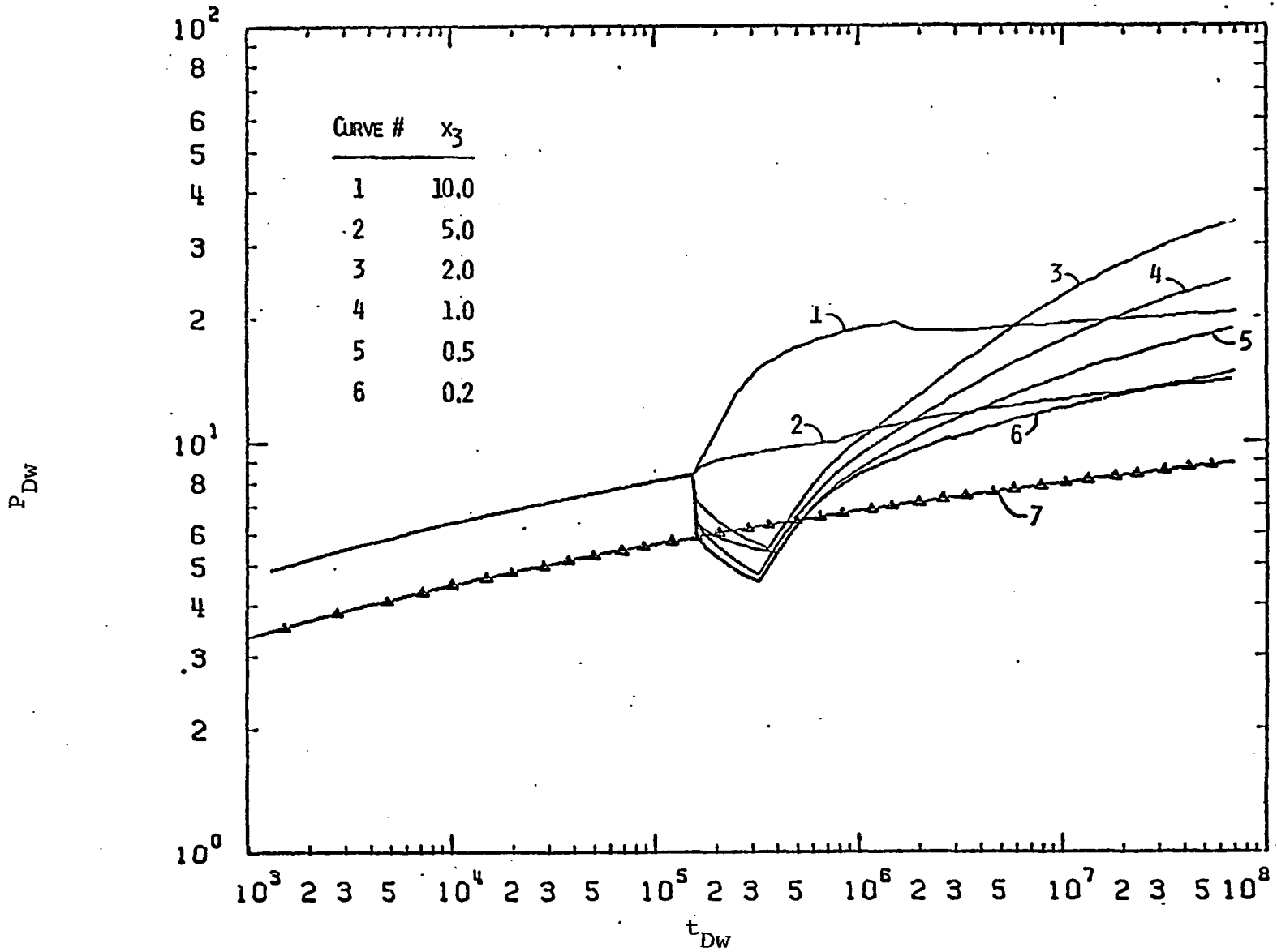

Figure D.12: Type-curve plot of P_{Dw} versus t_{Dw} for a two-layer two-region system with z=1., x_1=5. and x_2=5..

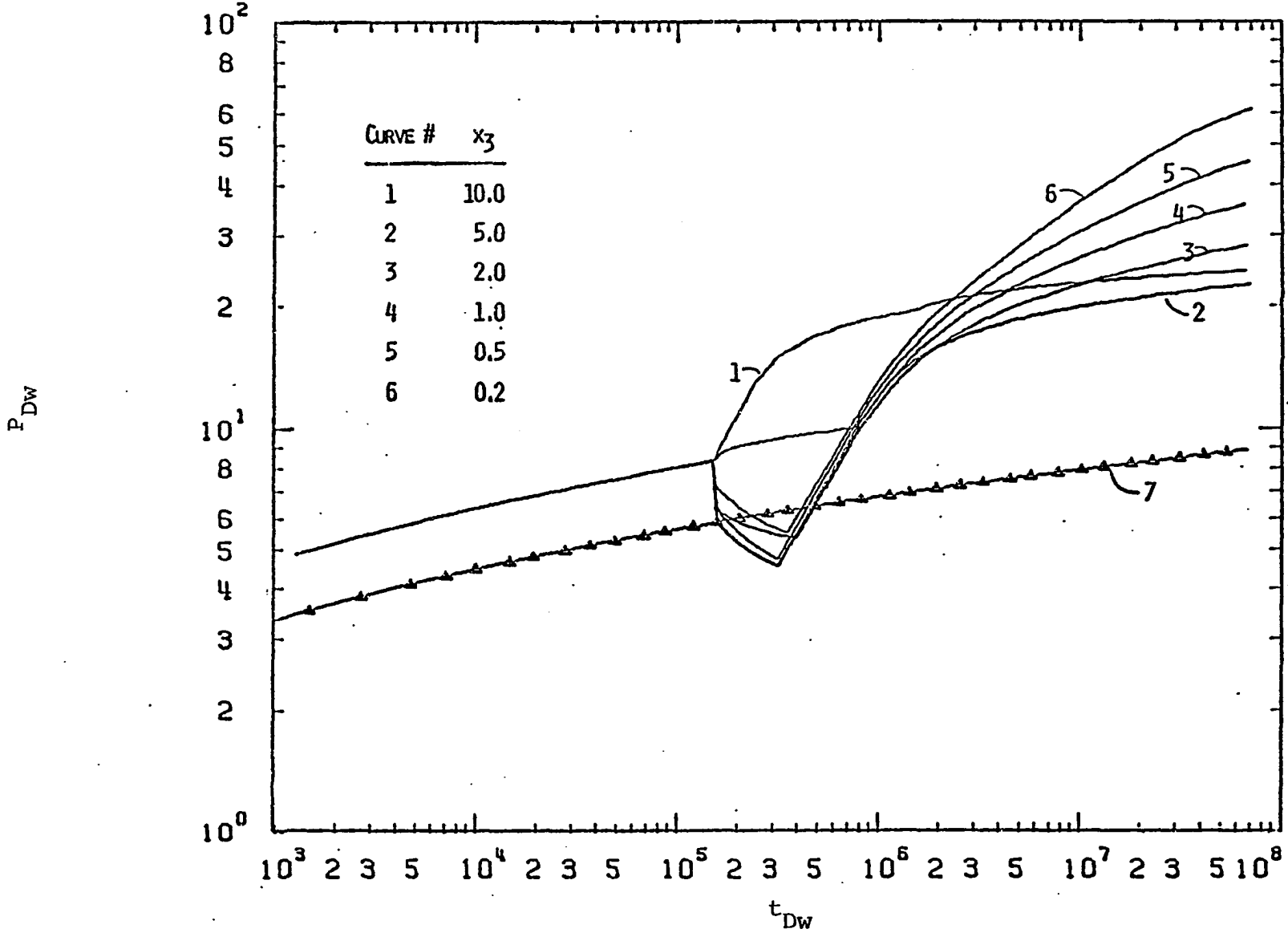

Figure D.13: Type-curve plot of P_{Dw} versus t_{Dw} for a two-layer two-region system with z=1., x_1=10. and x_2=5..

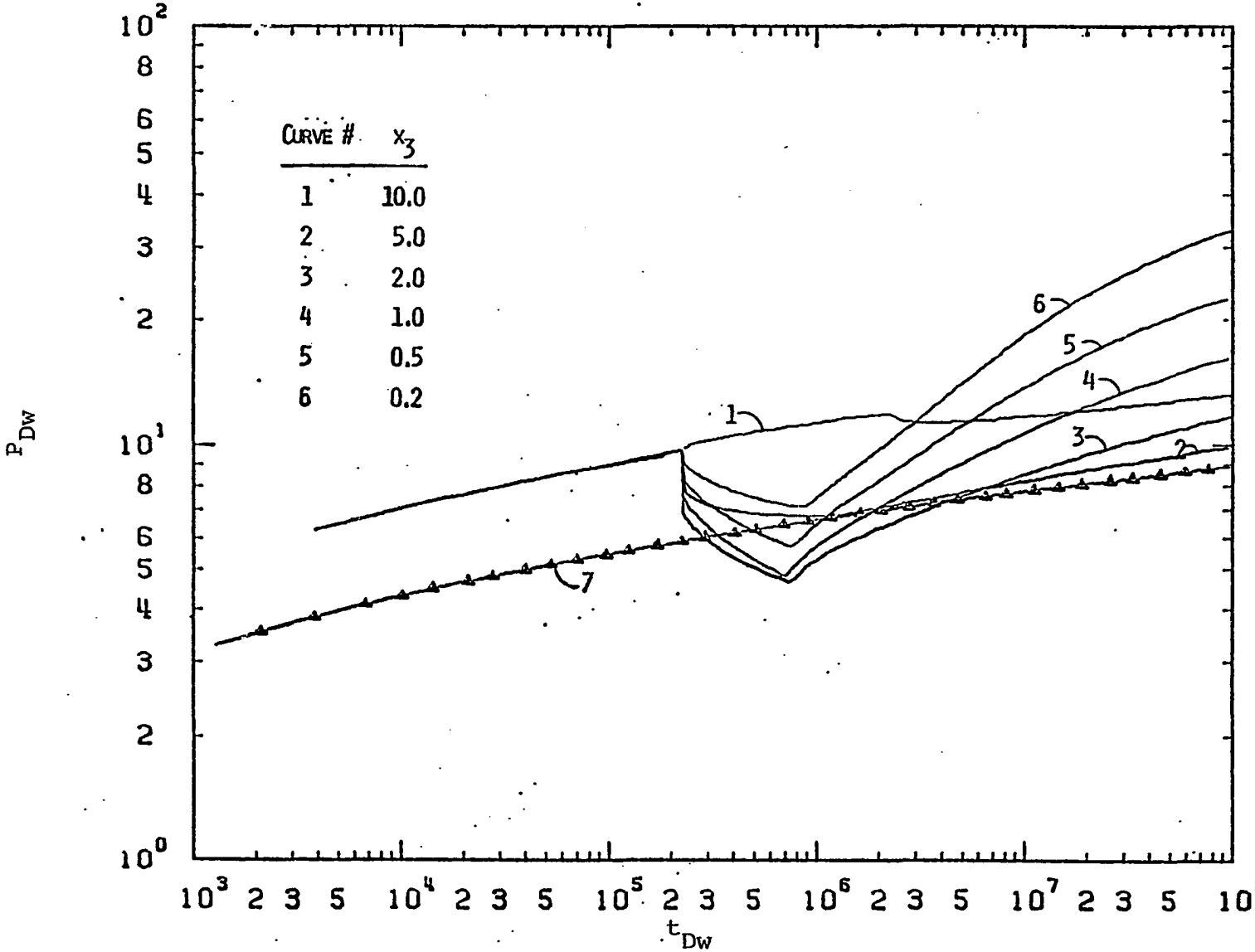

Figure D.14: Type-curve plot of P_{Dw} versus t_{Dw} for a two-layer two-region system with z=1., x_1=5. and x_2=10..

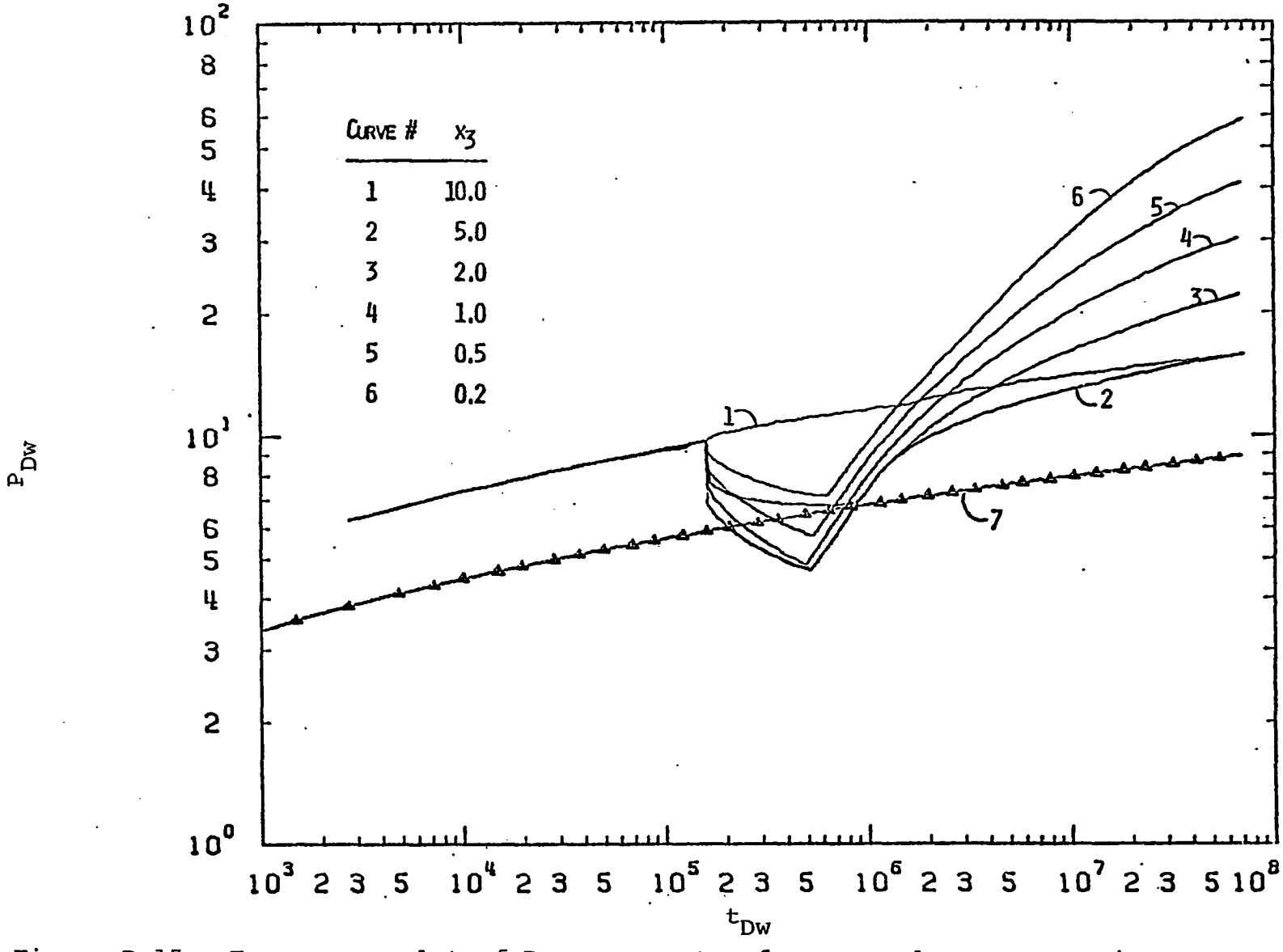

Figure D.15: Type-curve plot of P_{Dw} versus t_{Dw} for a two-layer two-region system with z=1., x_1=10. and x_2=10..

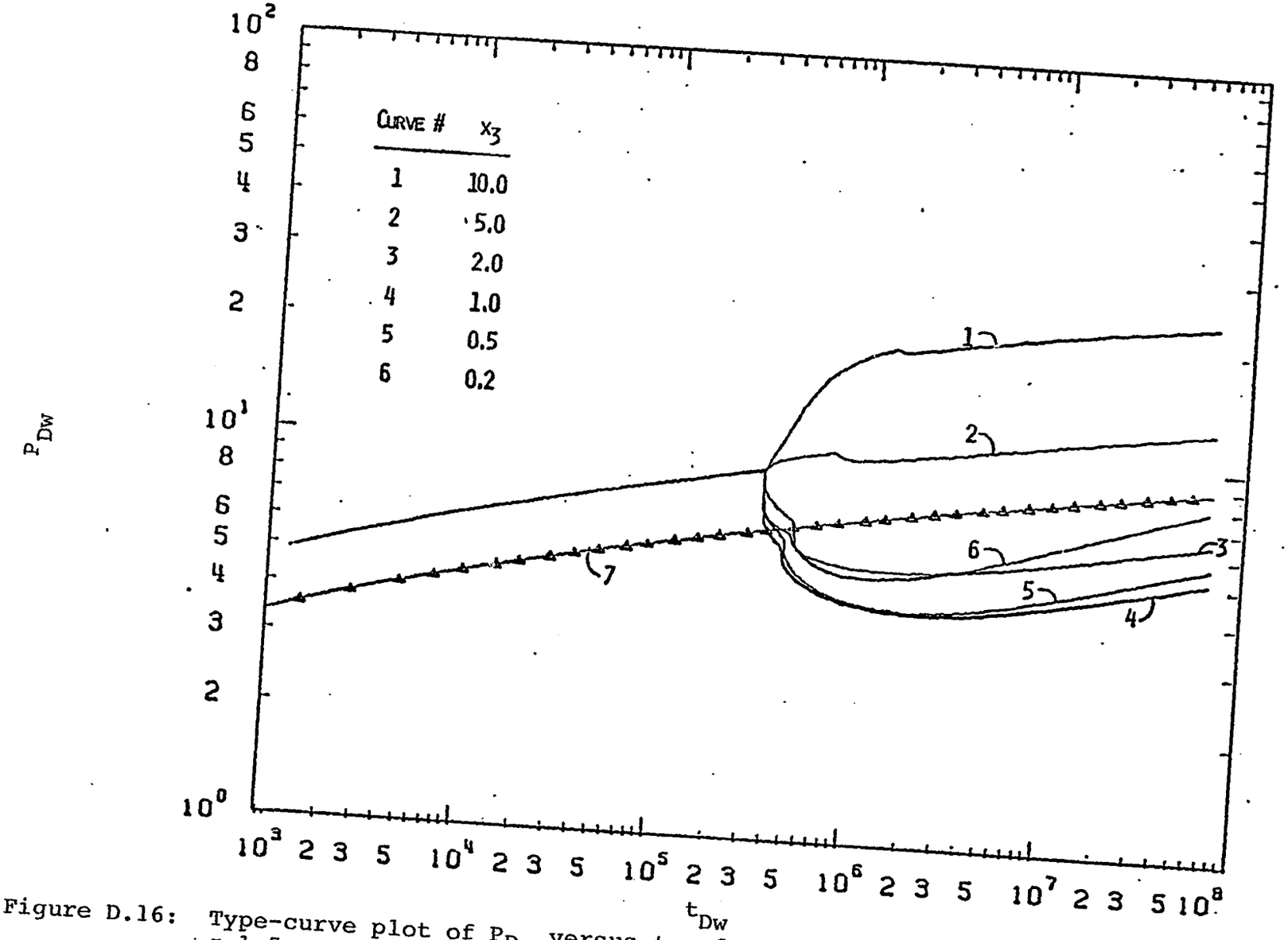

Figure D.16: Type-curve plot of P_{Dw} versus t_{Dw} for a two-layer two-region system z=1.5, x_1=1. and x_2=5..

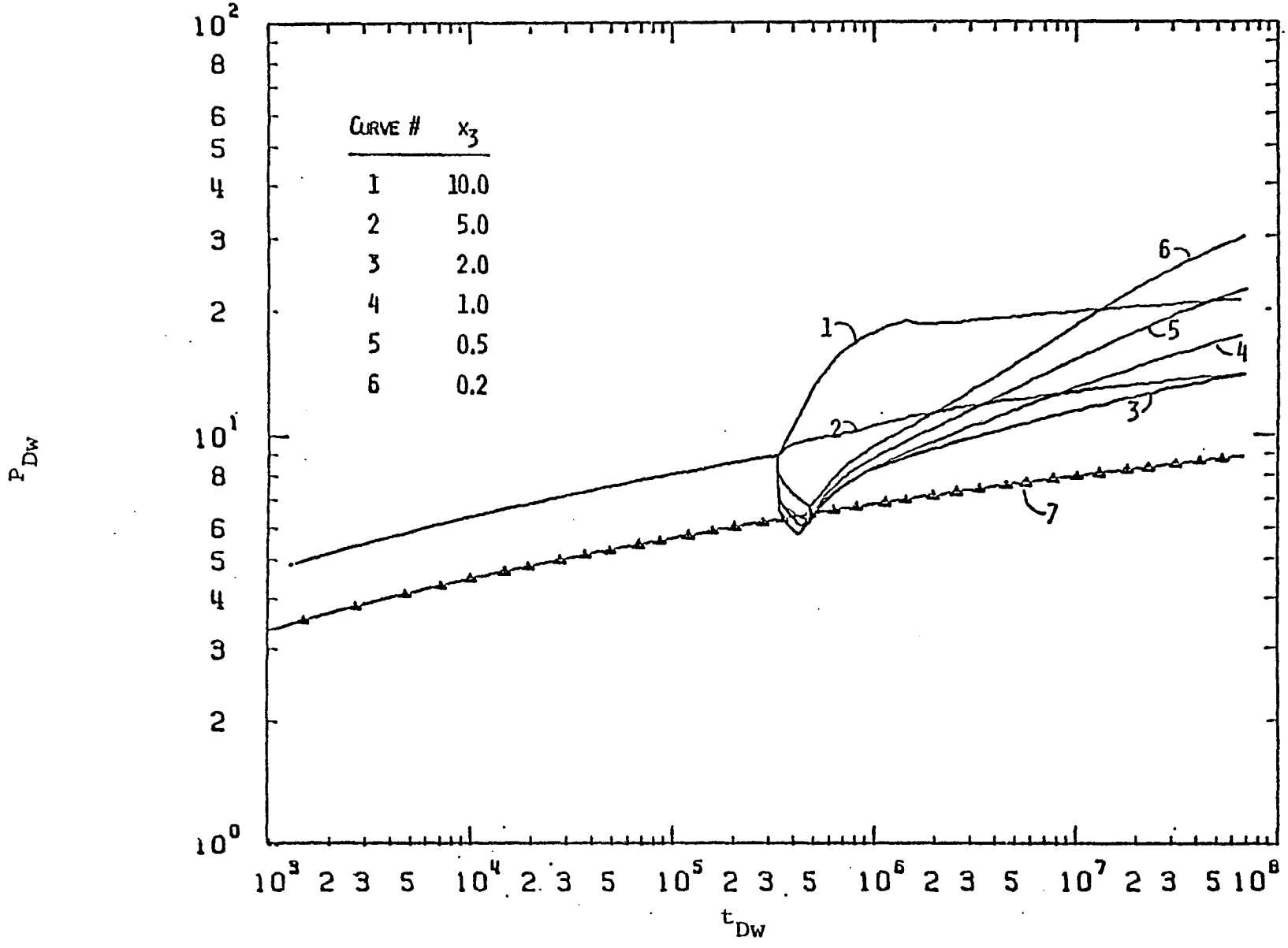

Figure D.17: Type-curve plot of P_{Dw} versus t_{Dw} for a two-layer two-region system with z=1.5, x_1=5. and x_2=5..

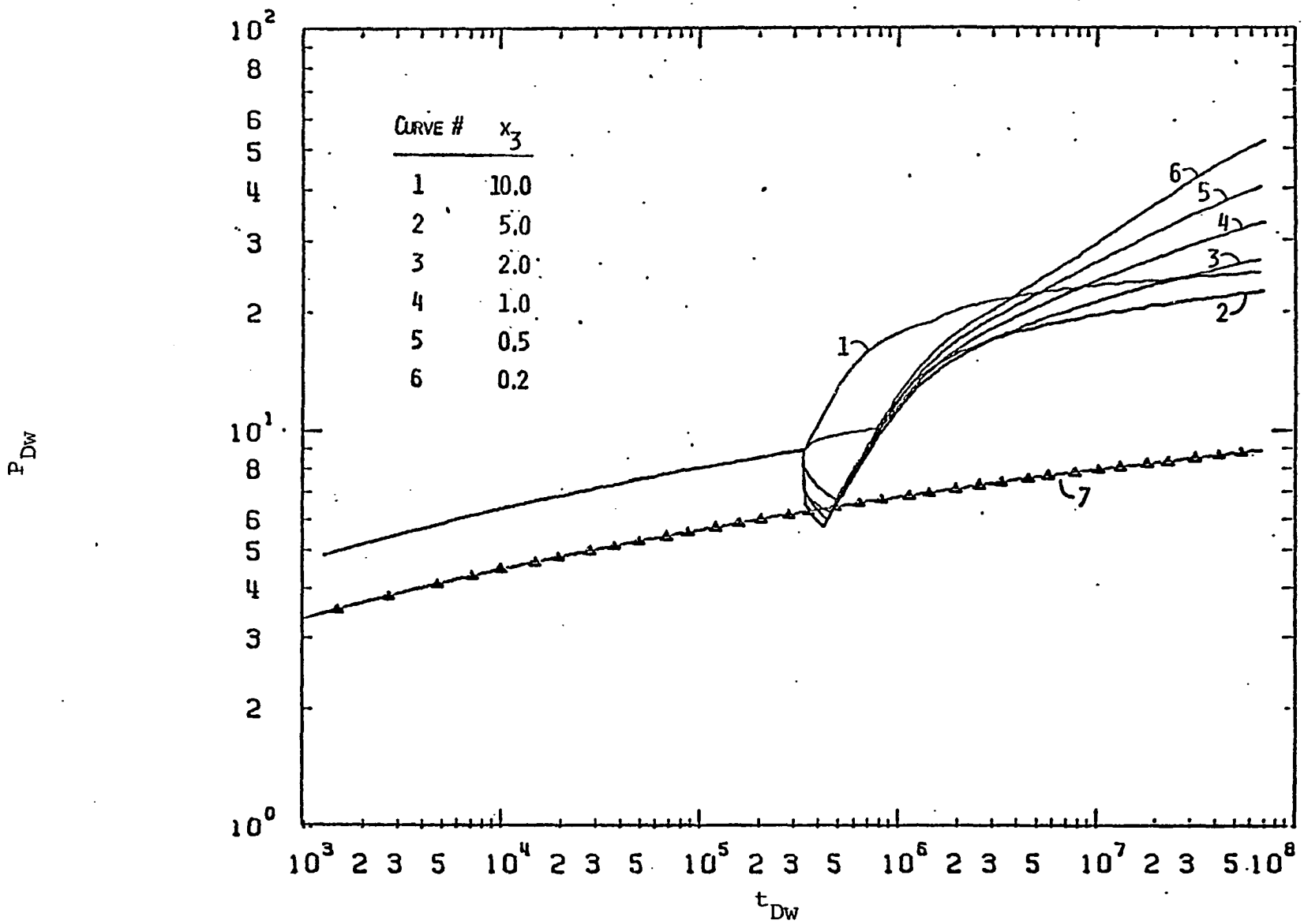

Figure D.18: Type-curve plot of P_{Dw} versus t_{Dw} for a two-layer two-region system with z=1.5, x_1=10. and x_2=5..

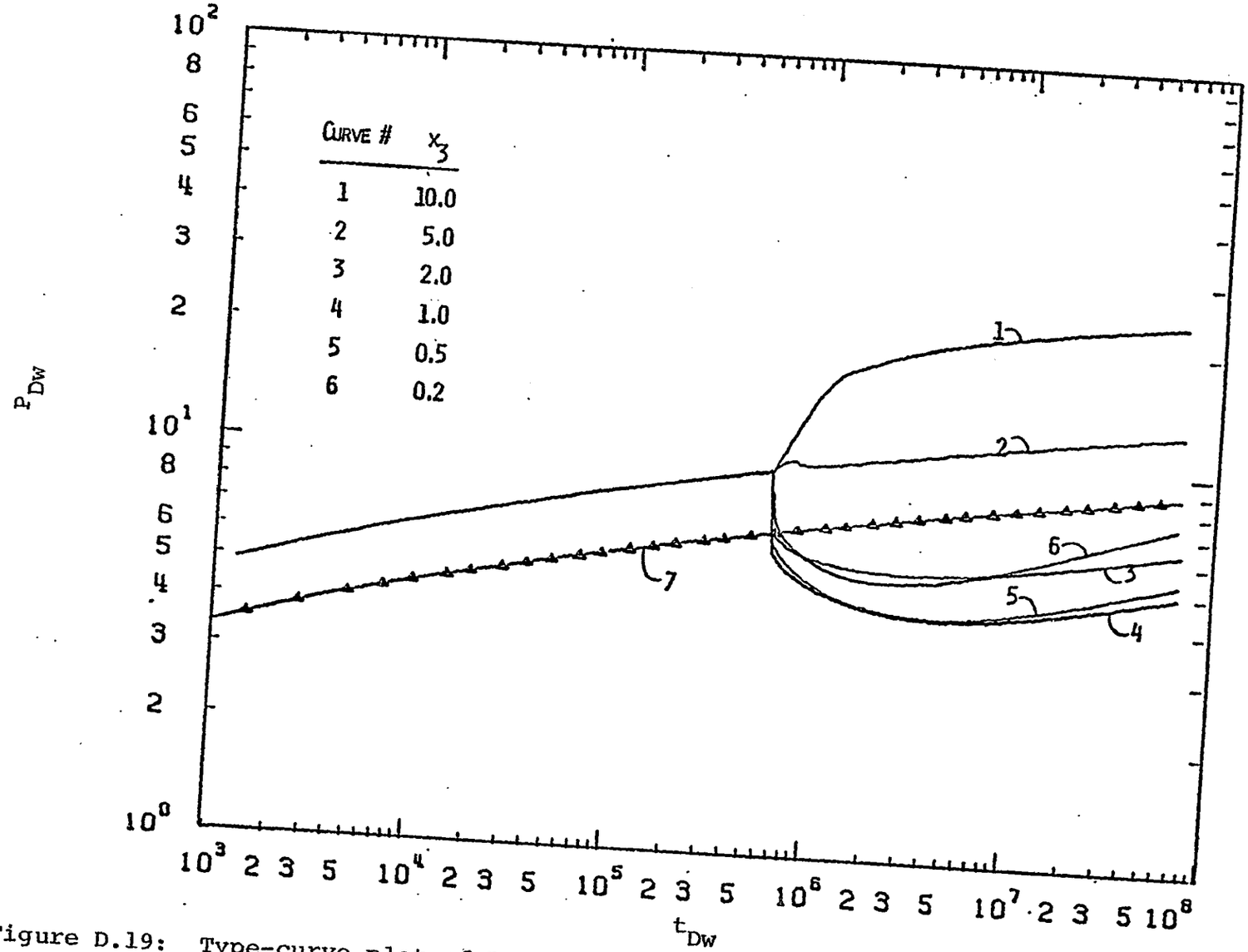

Figure D.19: Type-curve plot of p_{Dw} versus t_{Dw} for a two-layer two-region system with z=2., x_1= 1. and x_2=5..

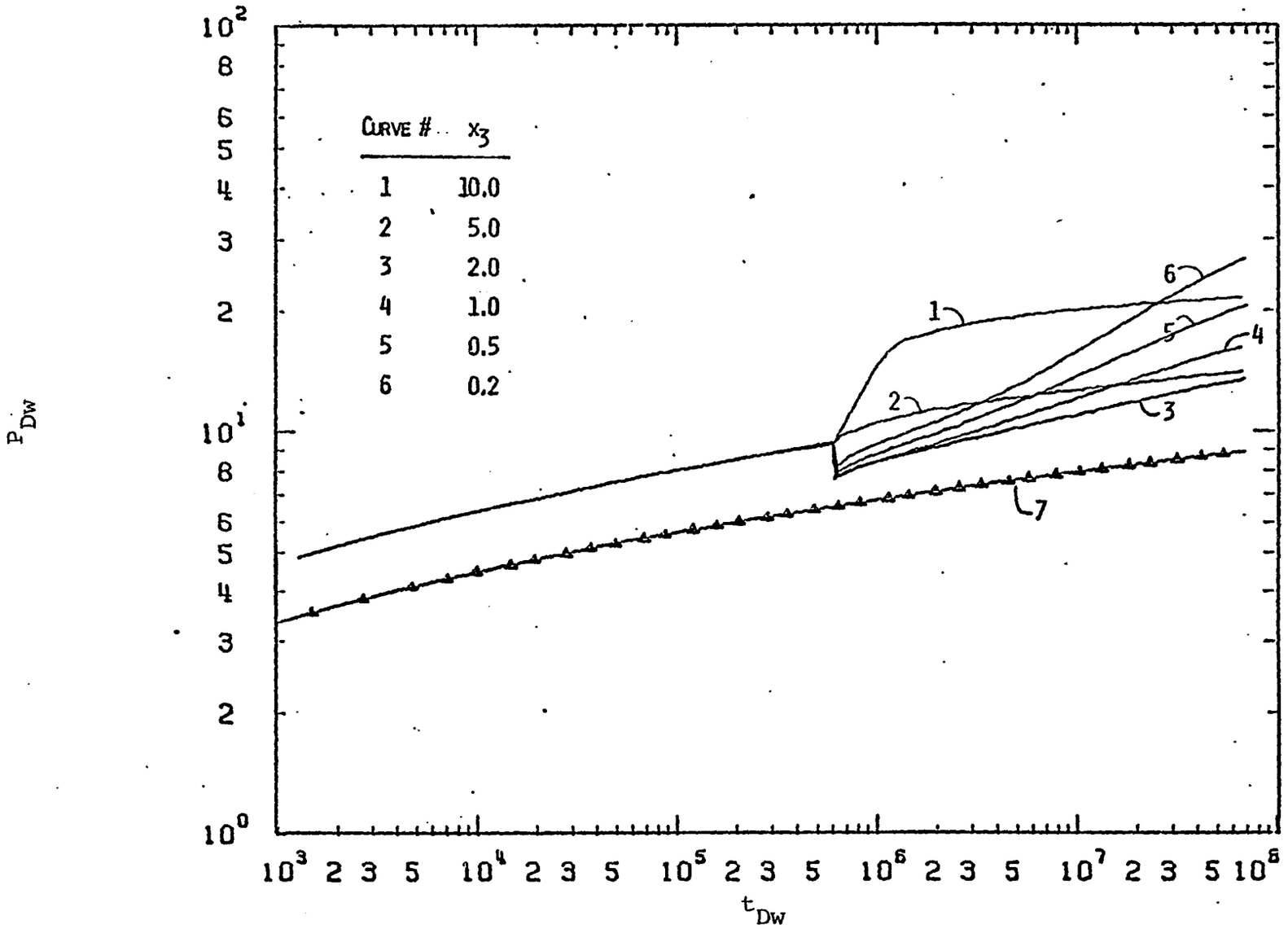

Figure D.20: Type-curve plot of P_{Dw} versus t_{Dw} for a two-layer two-region system with z=2., x_1=5. and x_2=5..

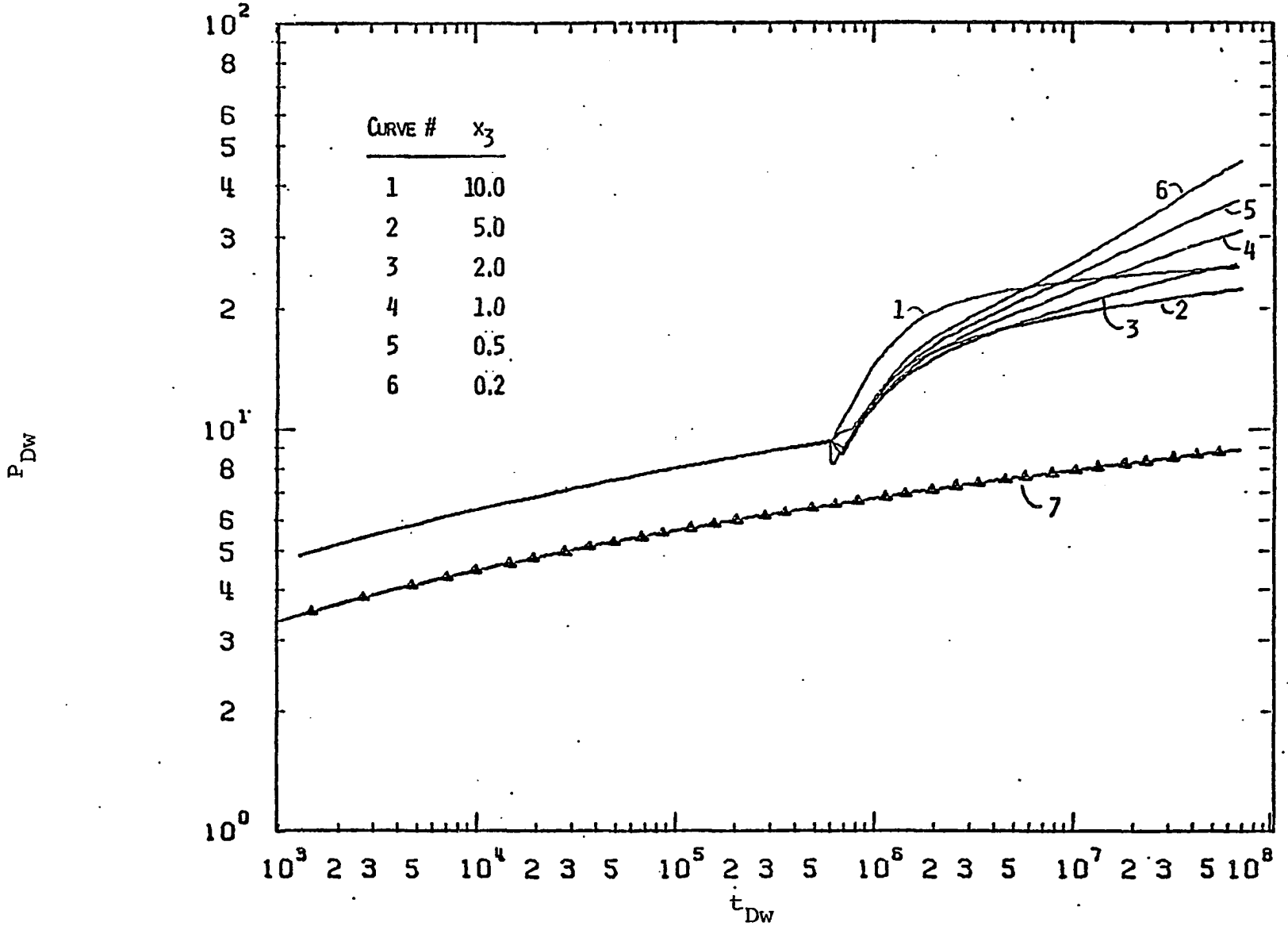

Figure D.21: Type-curve plot of P_{Dw} versus t_{Dw} for a two-layer two-region system with z=2., x_1=10. and x_2=5..

APPENDIX E

FRACTIONAL FLOW RATE BEHAVIOR PLOTS FOR DIFFERENT SYSTEMS WITH CONSTANT STORAGE ($y_1=y_2=y_3=1.$)

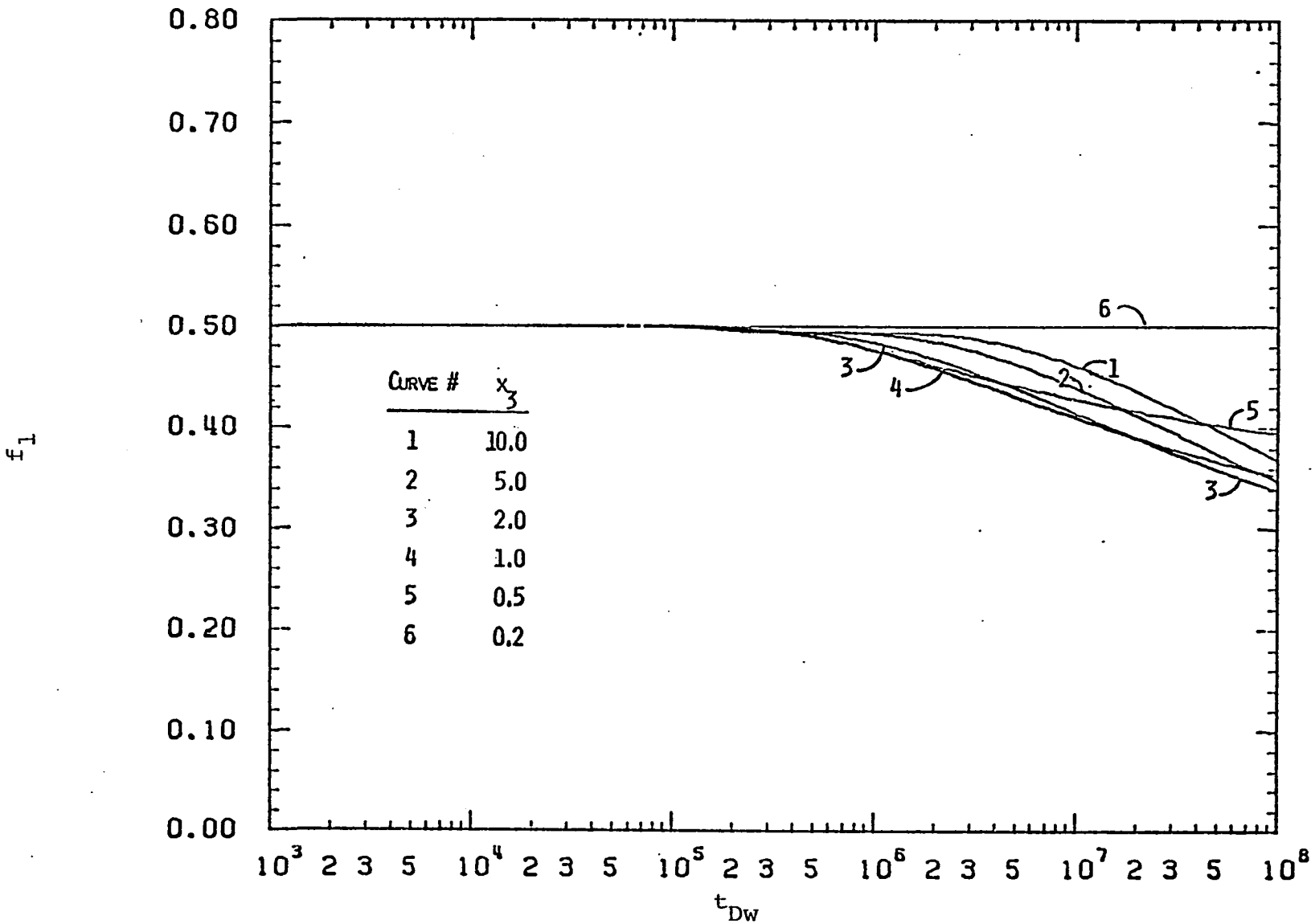

Figure E.1: Fractional flow rate from layer 1 of a two-layer two-region system with z=1., x_1=0.2 and x_2=1..

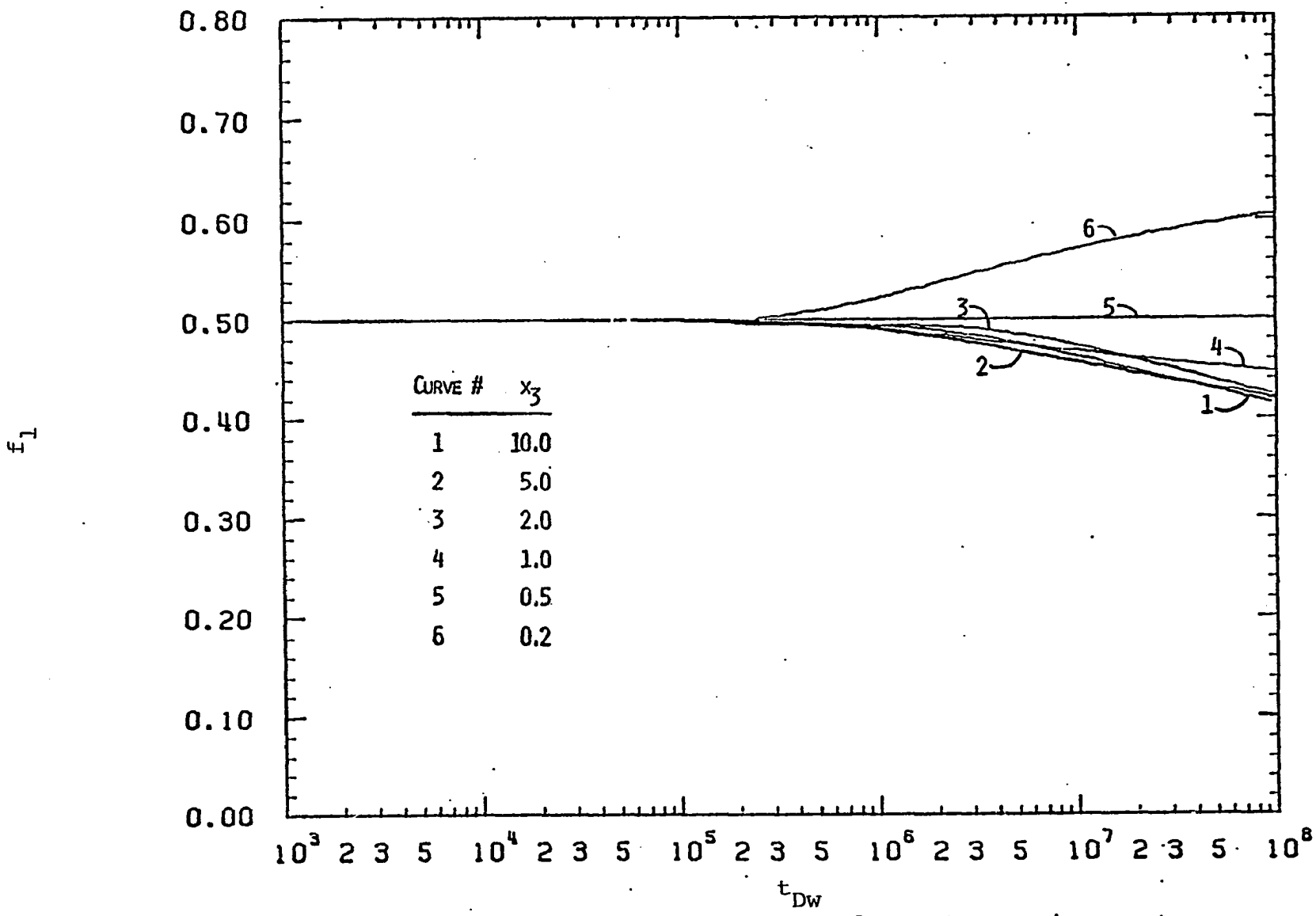

Figure E.2: Fractional flow rate from layer 1 of a two-layer two-region system with z=1., x_1=0.5 and x_2=1..

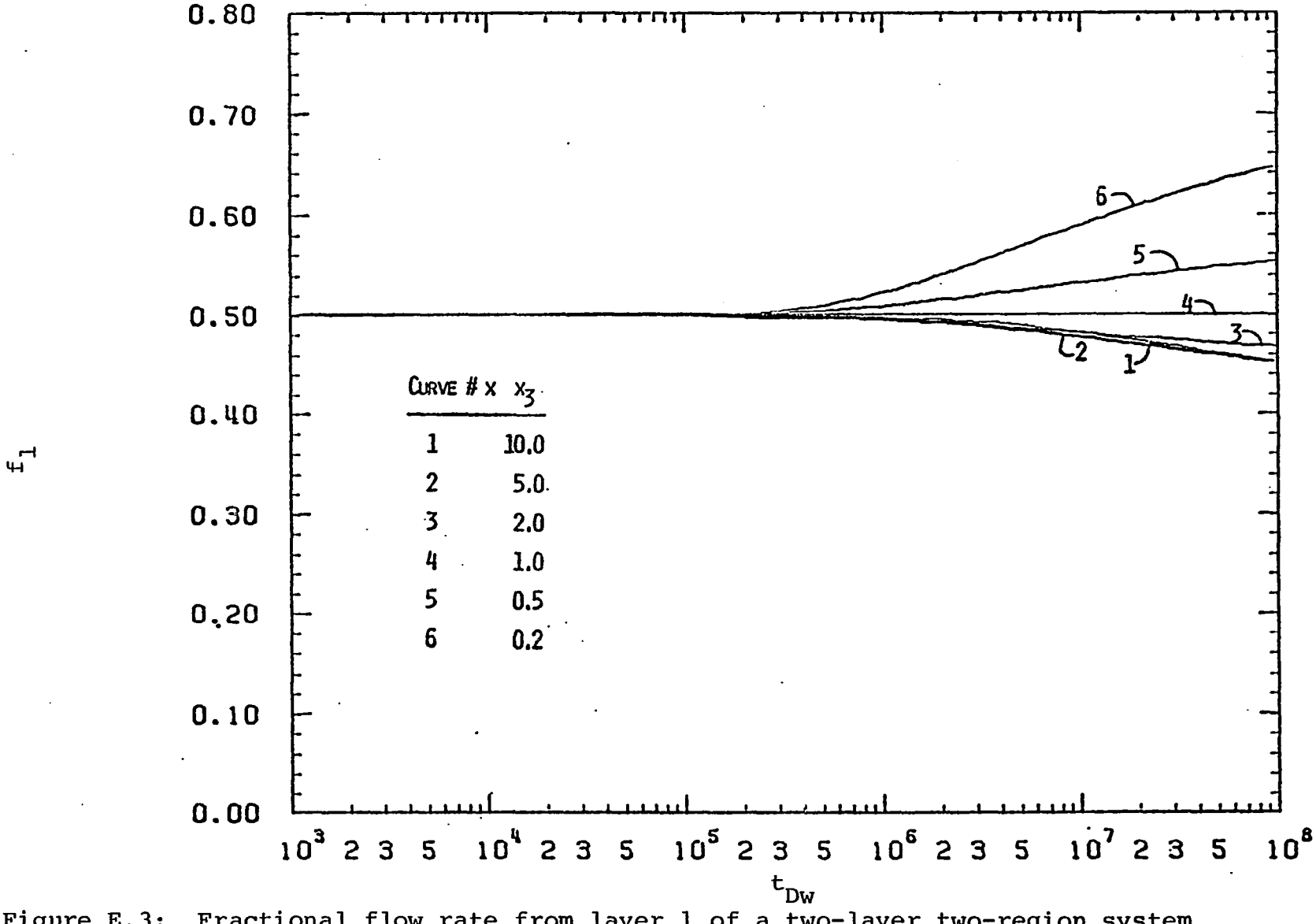

Figure E.3: Fractional flow rate from layer 1 of a two-layer two-region system with z=1., x_1=1. and x_2=1..

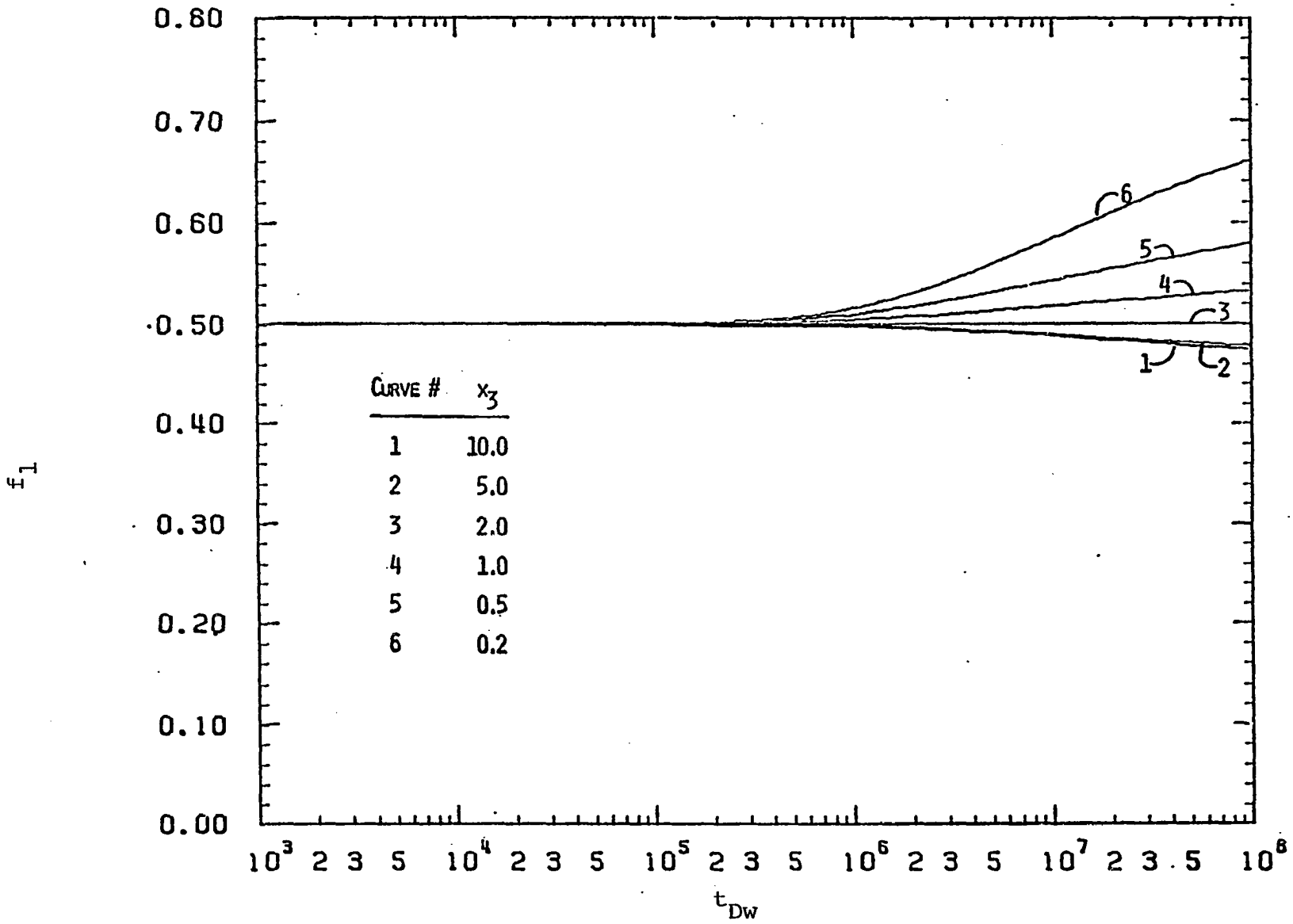

Figure E.4: Fractional flow rate from layer 1 of two-layer two-region system with z=1., x_1=2. and x_2=1..

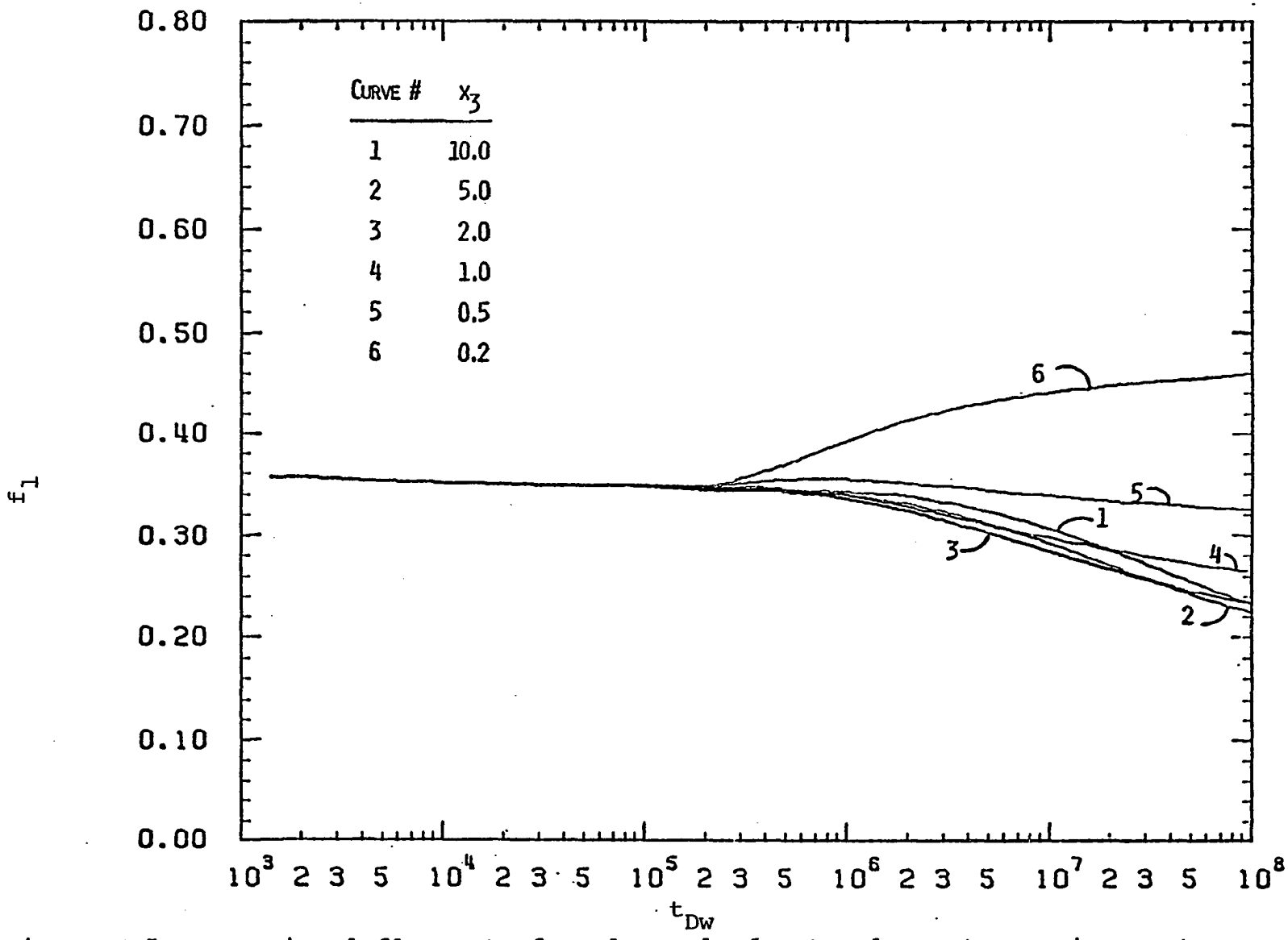

Figure E.5: Fractional flow rate from layer 1 of a two-layer two-region system with z=1., x_1=0.2 and x_2=2.0.

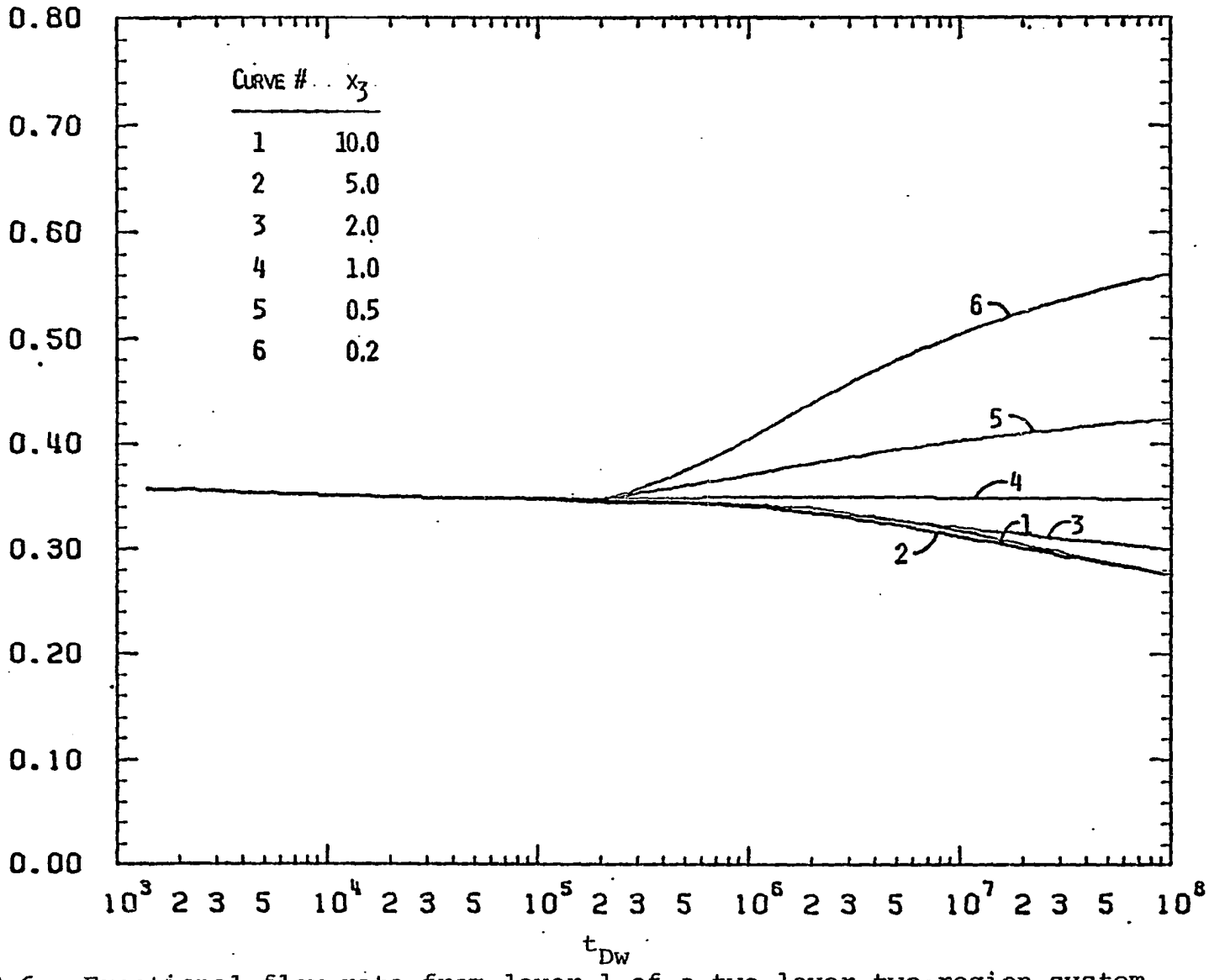

Figure E.6: Fractional flow rate from layer 1 of a two-layer two-region system with z=1., x_1=0.5 and x_2=2..

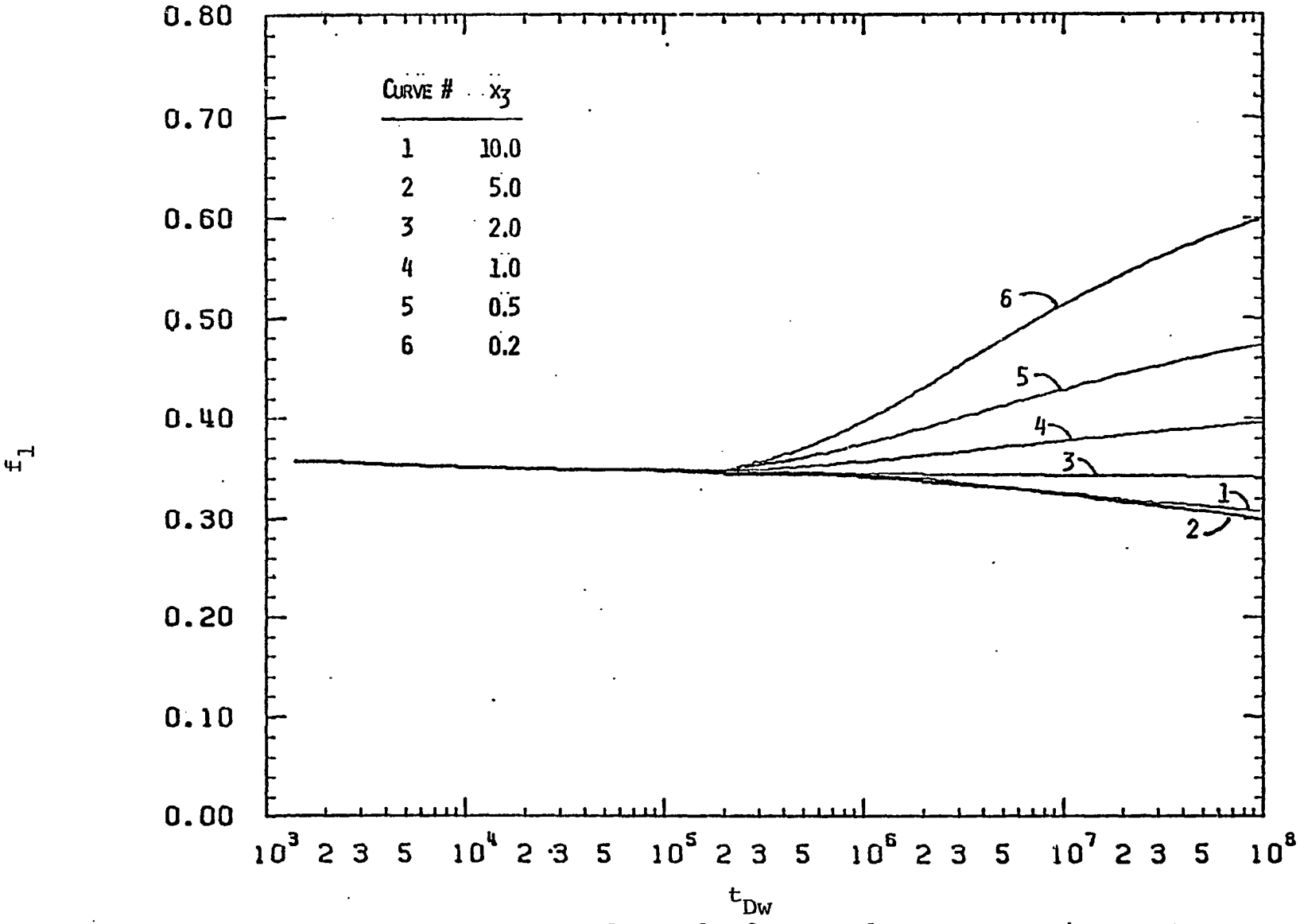

Figure E.7: Fractional flow rate from layer 1 of a two-layer two-region system with z=1., x_1=1. and x_2=2..

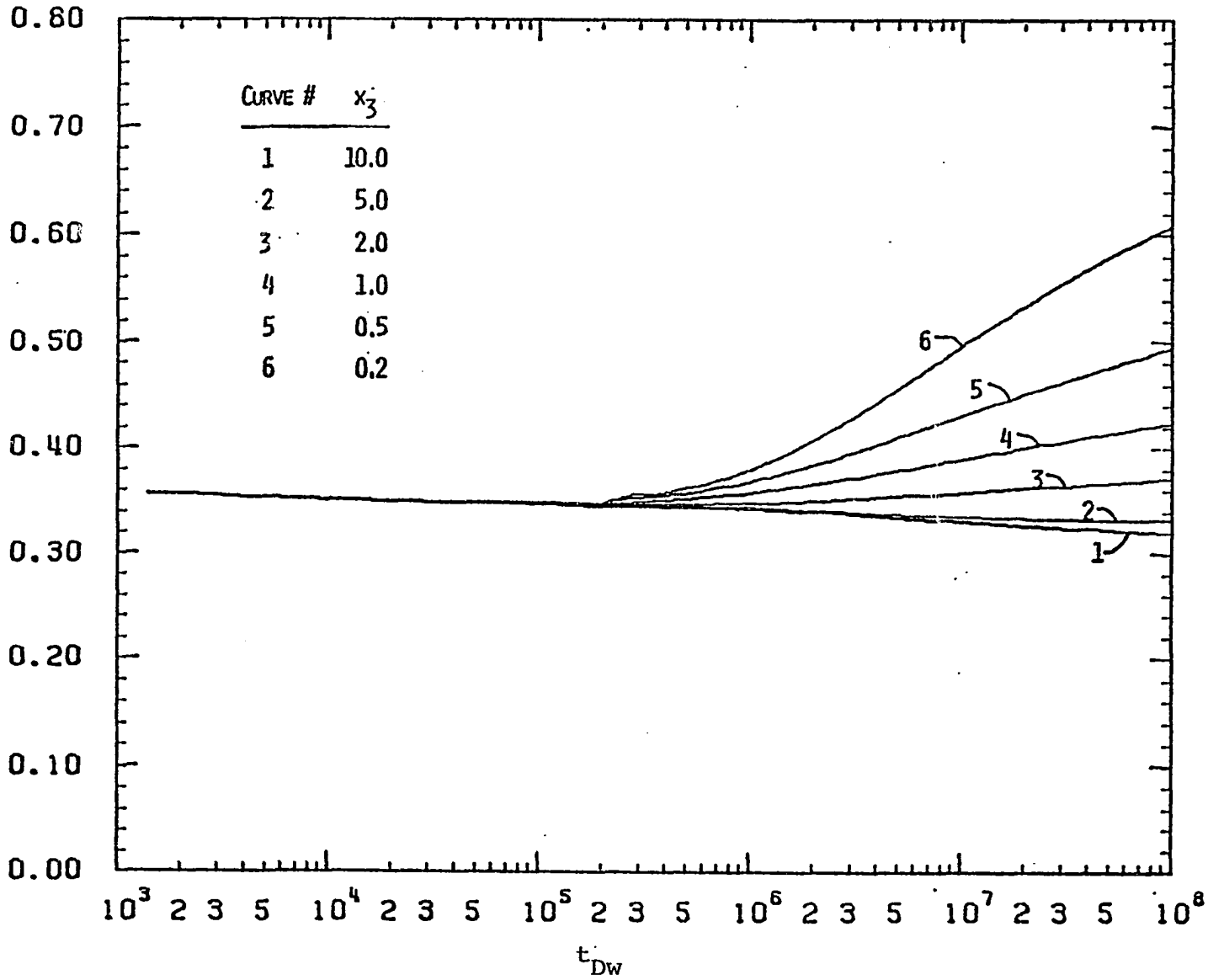

Figure E.8: Fractional flow rate from layer 1 of a two-layer two-region system with z=1., x_1=2. and x_2=2..

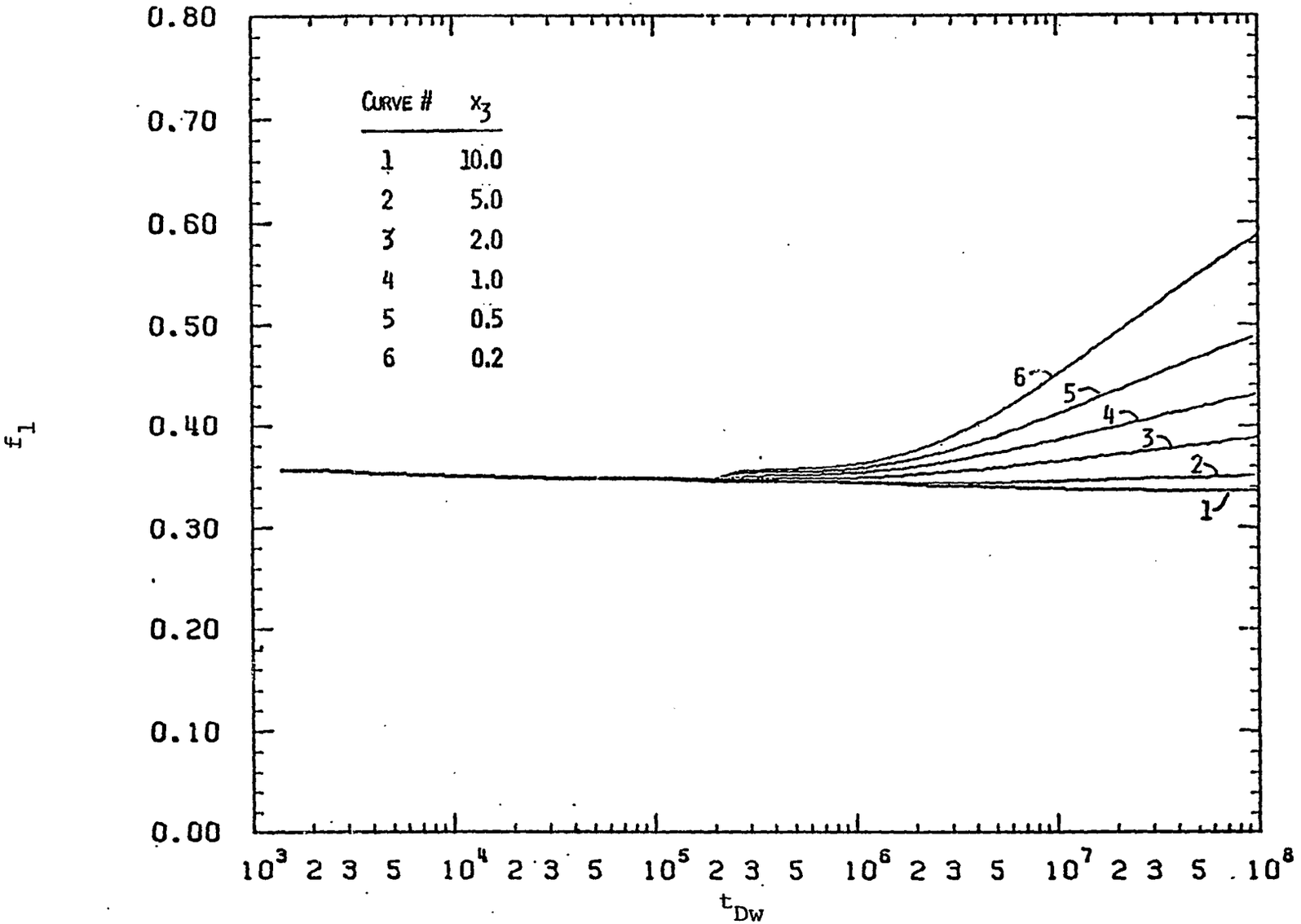

Figure E.9: Fractional flow rate from layer 1 of a two-layer two-region system with z=1., x_1=5. and x_2=2..

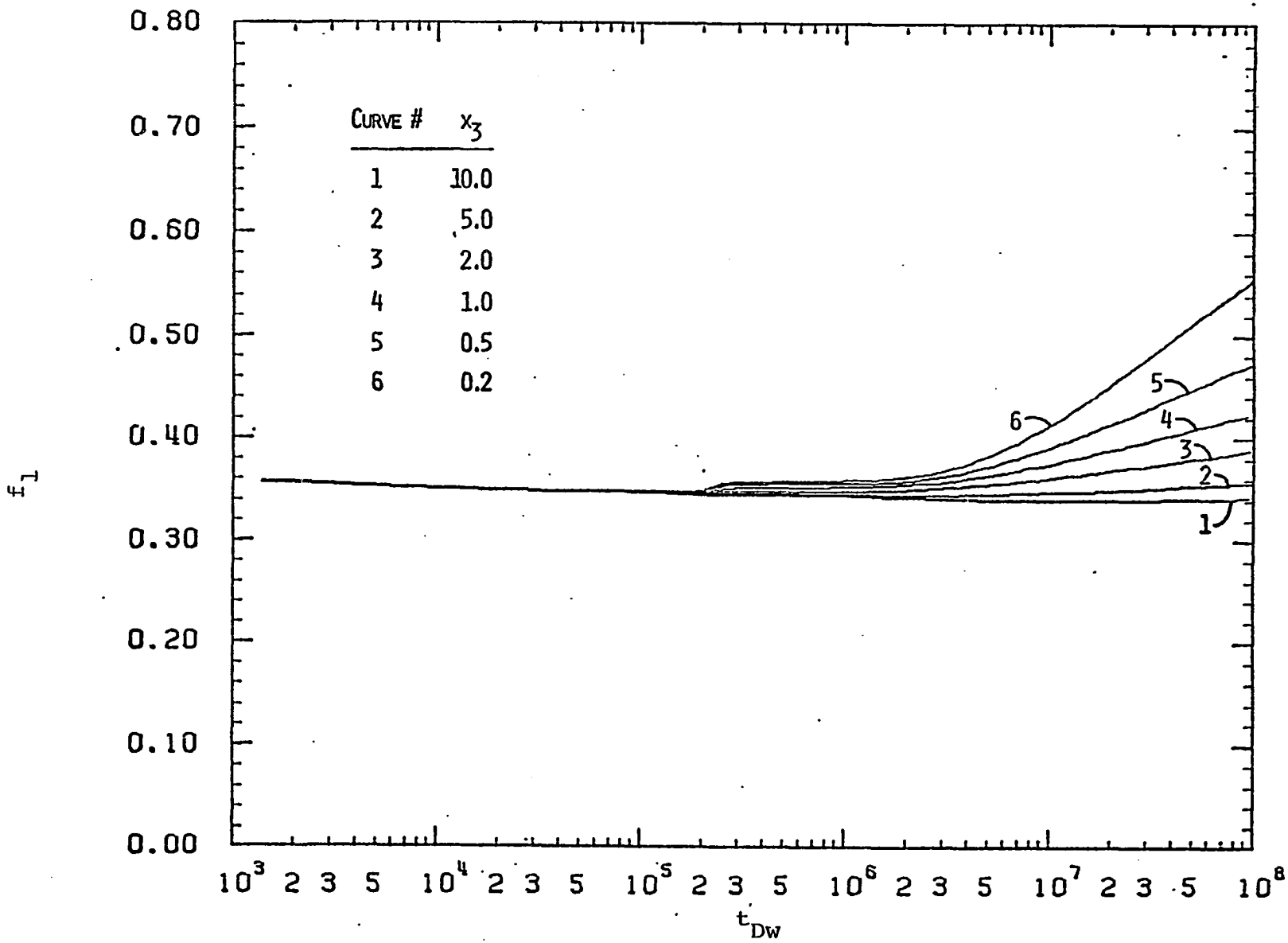

Figure E.10: Fractional flow rate from layer 1 of a two-layer two-region system with z=1., x_1=10. and x_2=2..

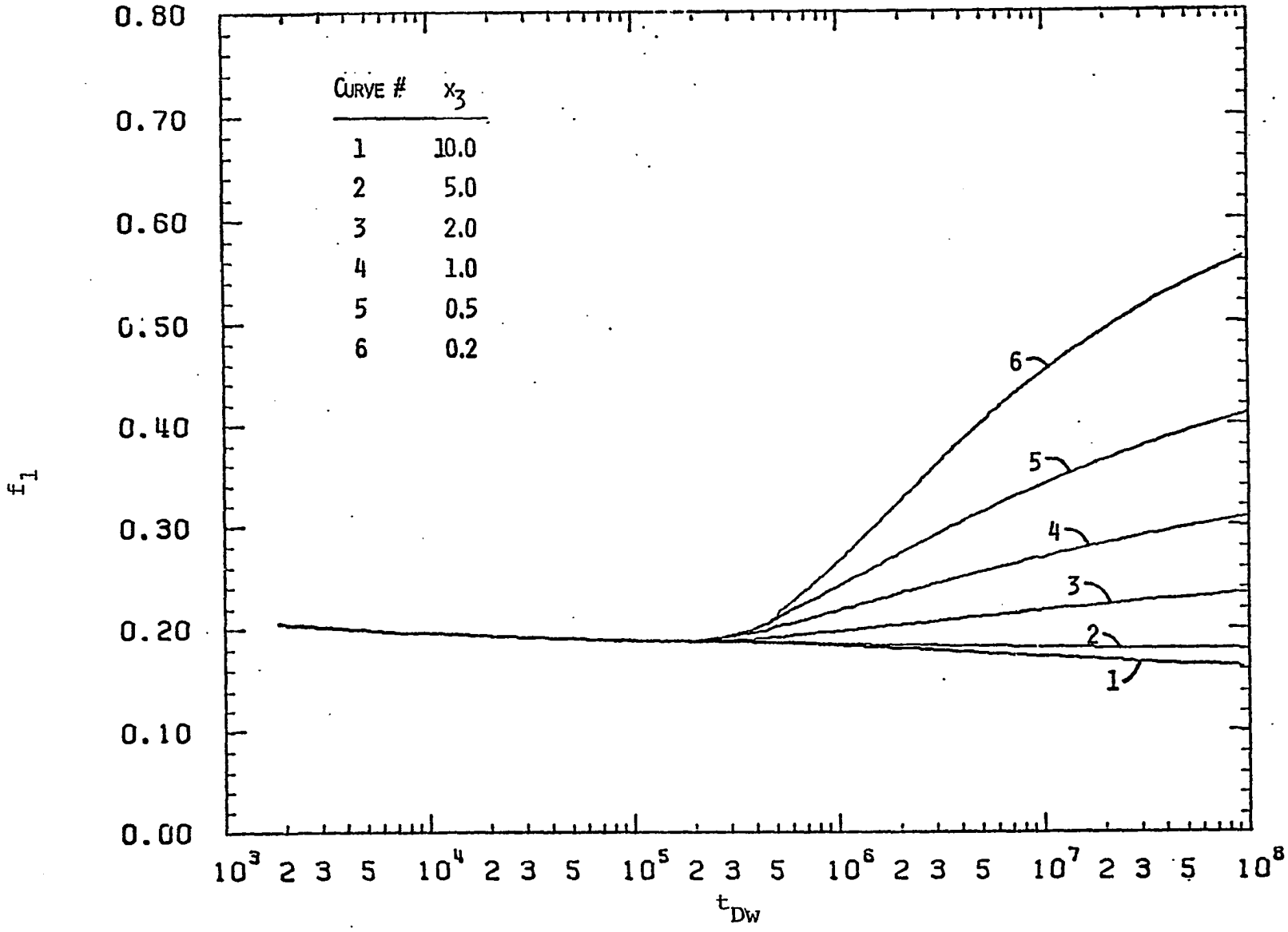

Figure E.11: Fractional flow rate from layer 1 of a two-layer two-region system with z=1., x_1=1. and x_2=5..

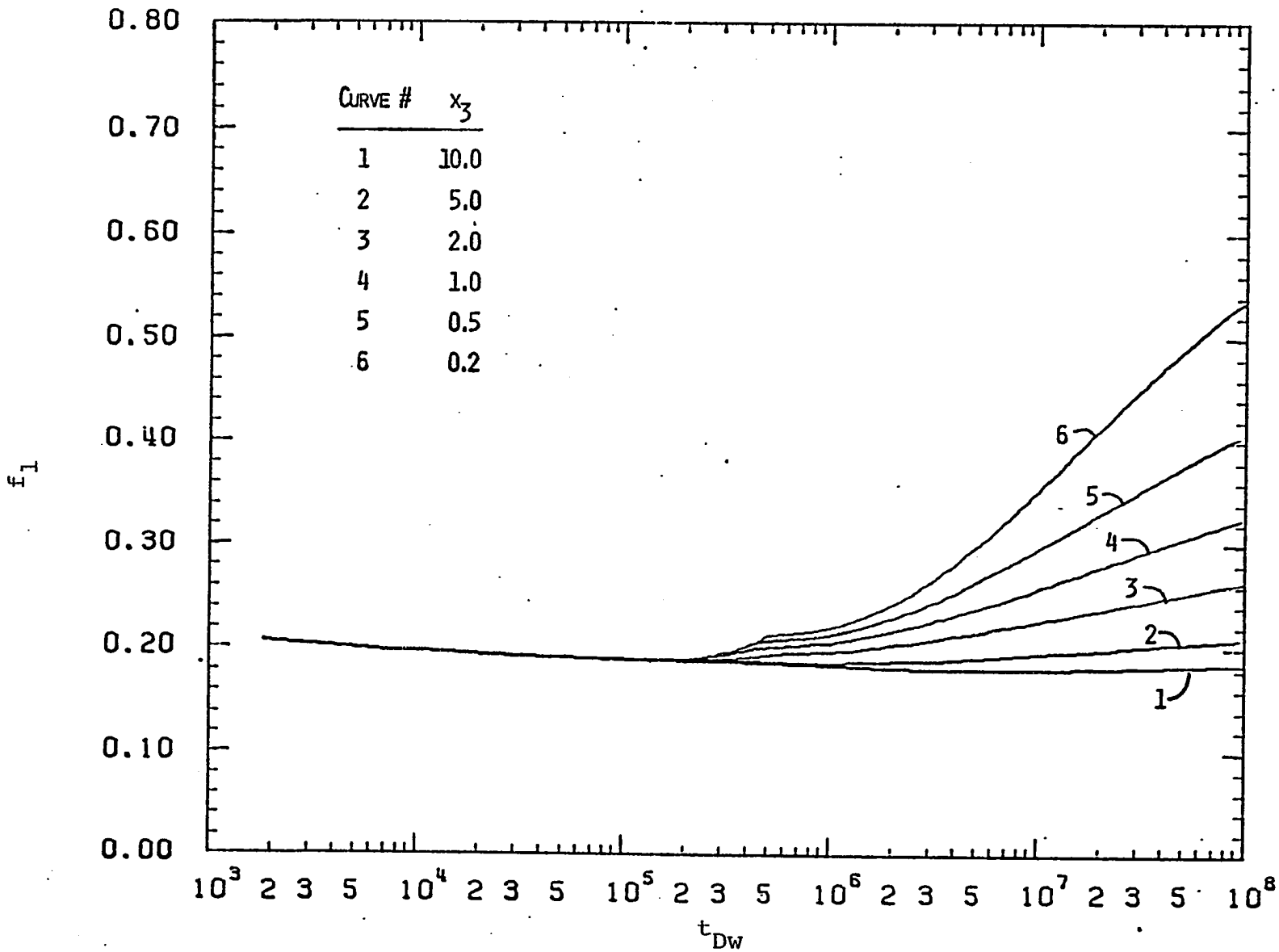

Figure E.12: Fractional flow rate from layer 1 of a two-layer two-region system with z=1., x_1=5. and x_2=5..

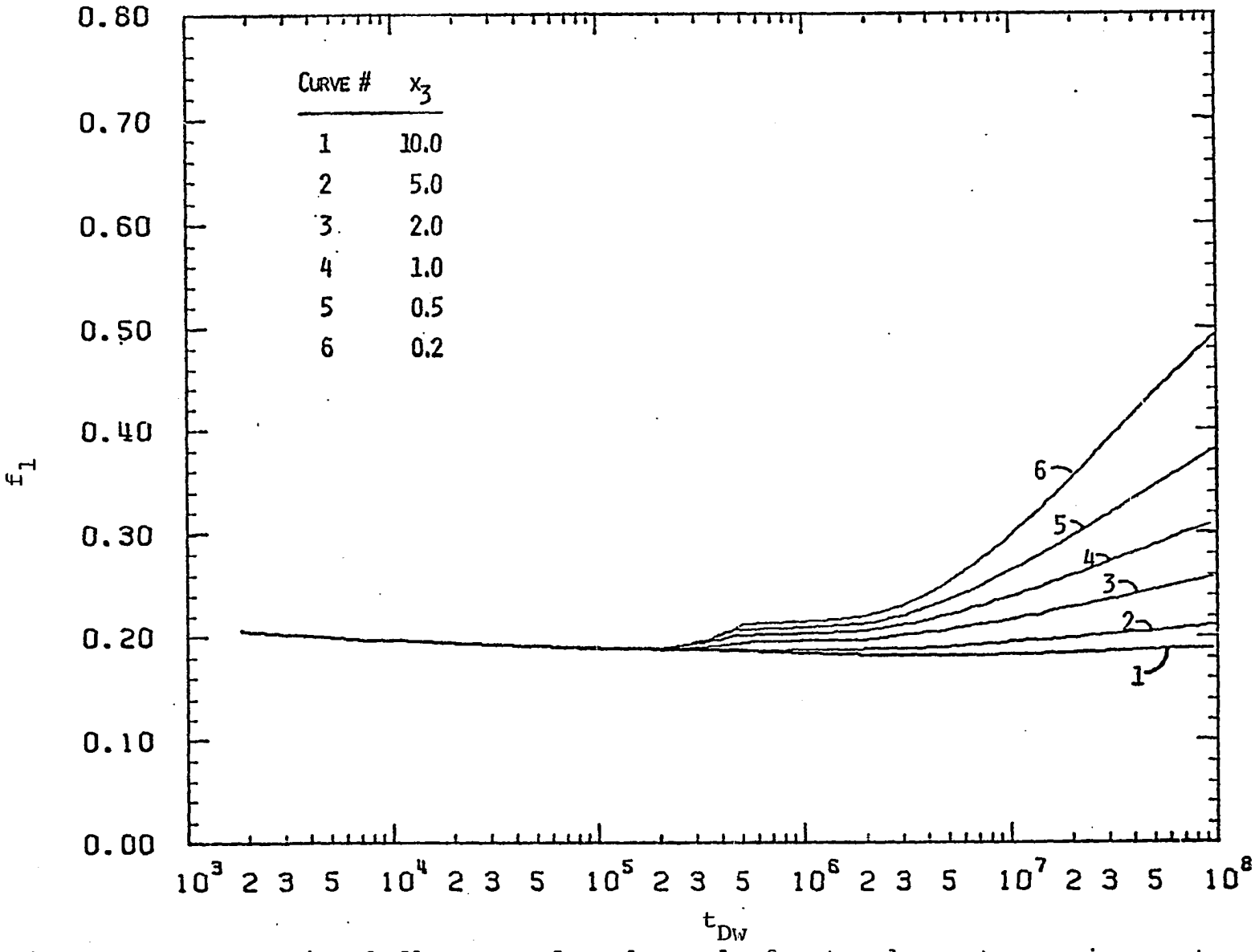

Figure E.13: Fractional flow rate from layer 1 of a two-layer two-region system with z=1., x_1=10. and x_2=5..

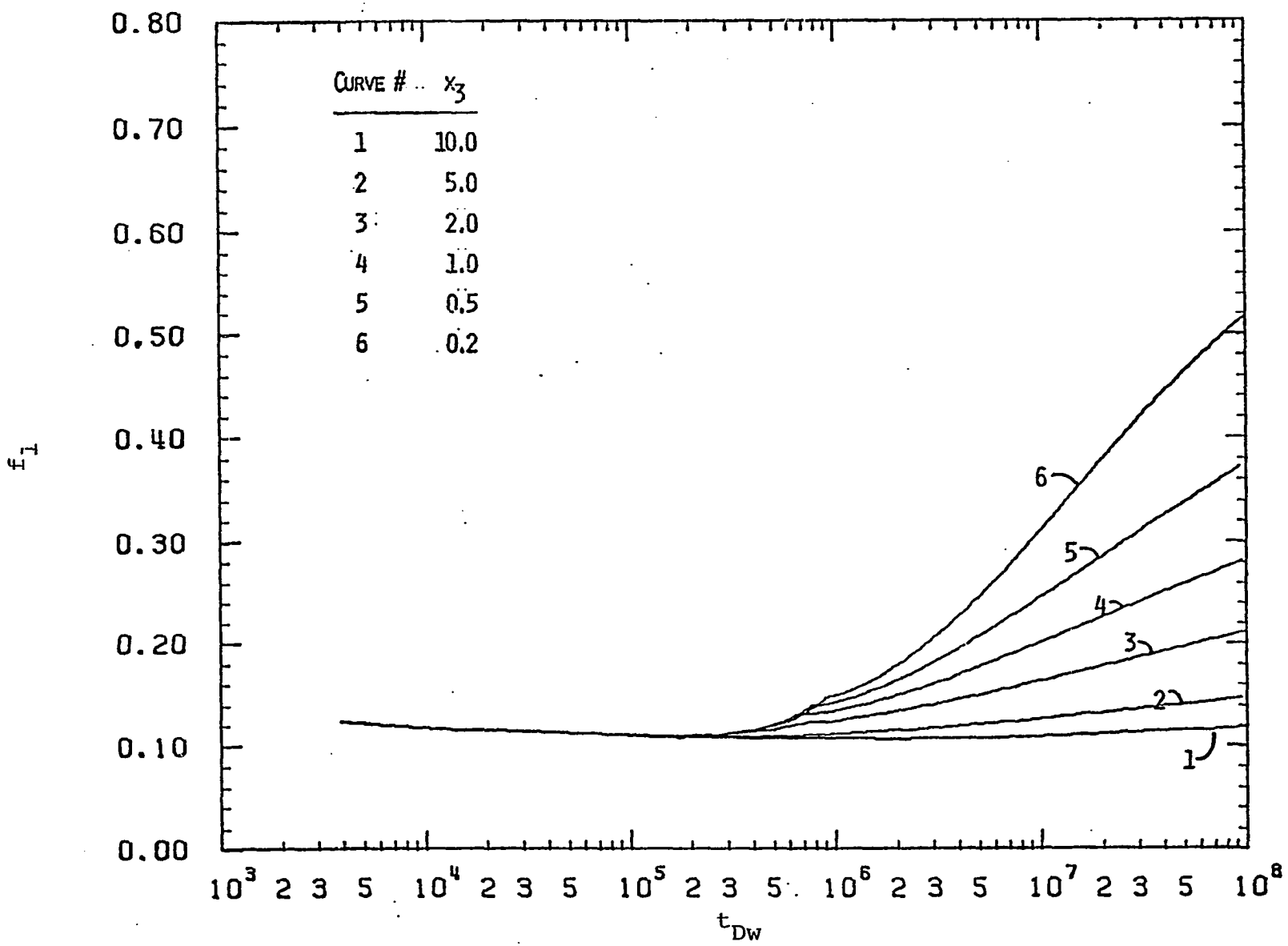

Figure E.14: Fractional flow rate from layer 1 of a two-layer two-region system with z=1., x_1=5. and x_2=10..

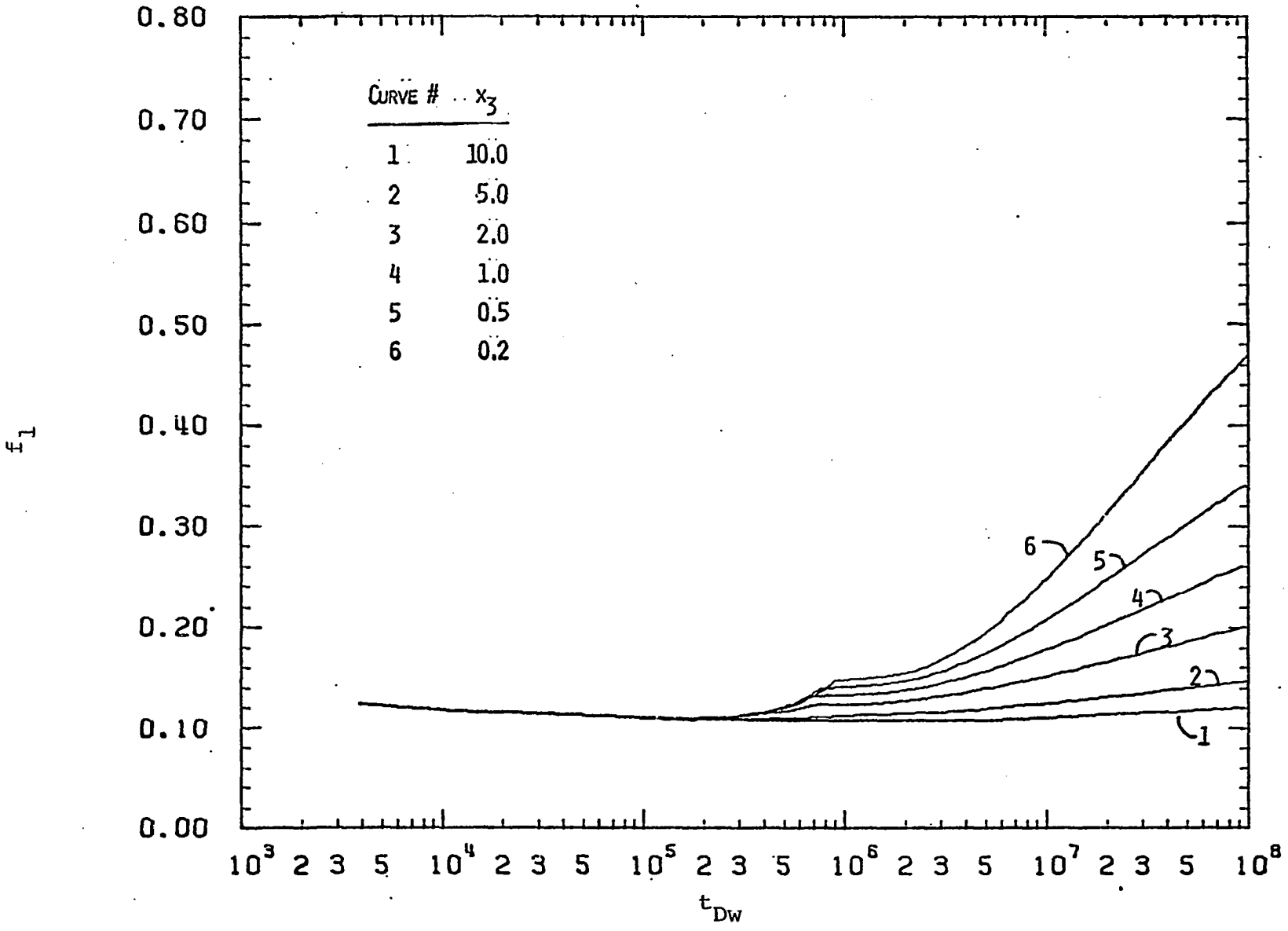

Figure E.15: Fractional flow rate from layer 1 of a two-layer two-region system with z=1., x_1=10. and x_2=10..

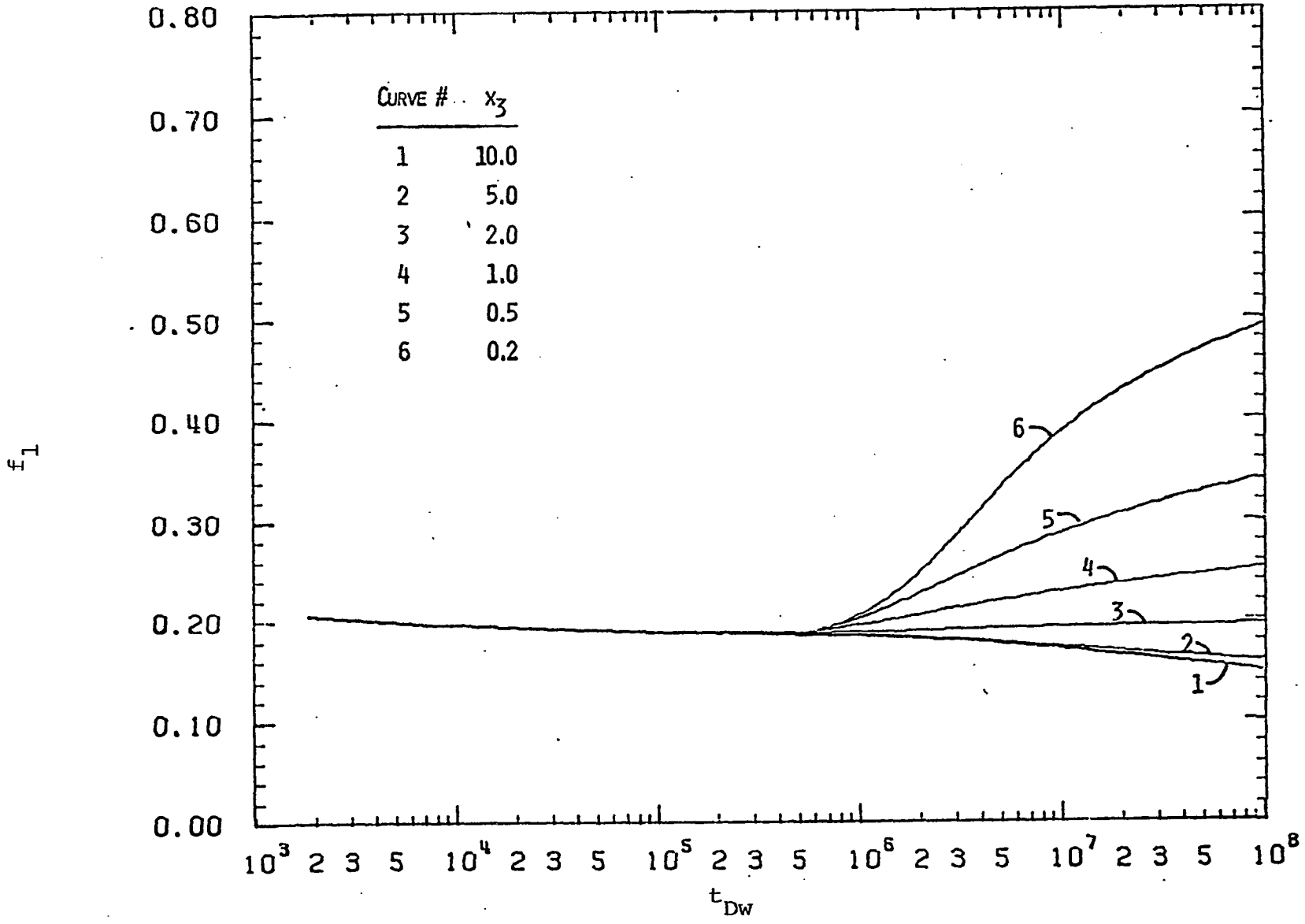

Figure E.16: Fractional flow rate from layer 1 of a two-layer two-region system with z=1.5, x_1=0.5 and x_2=5..

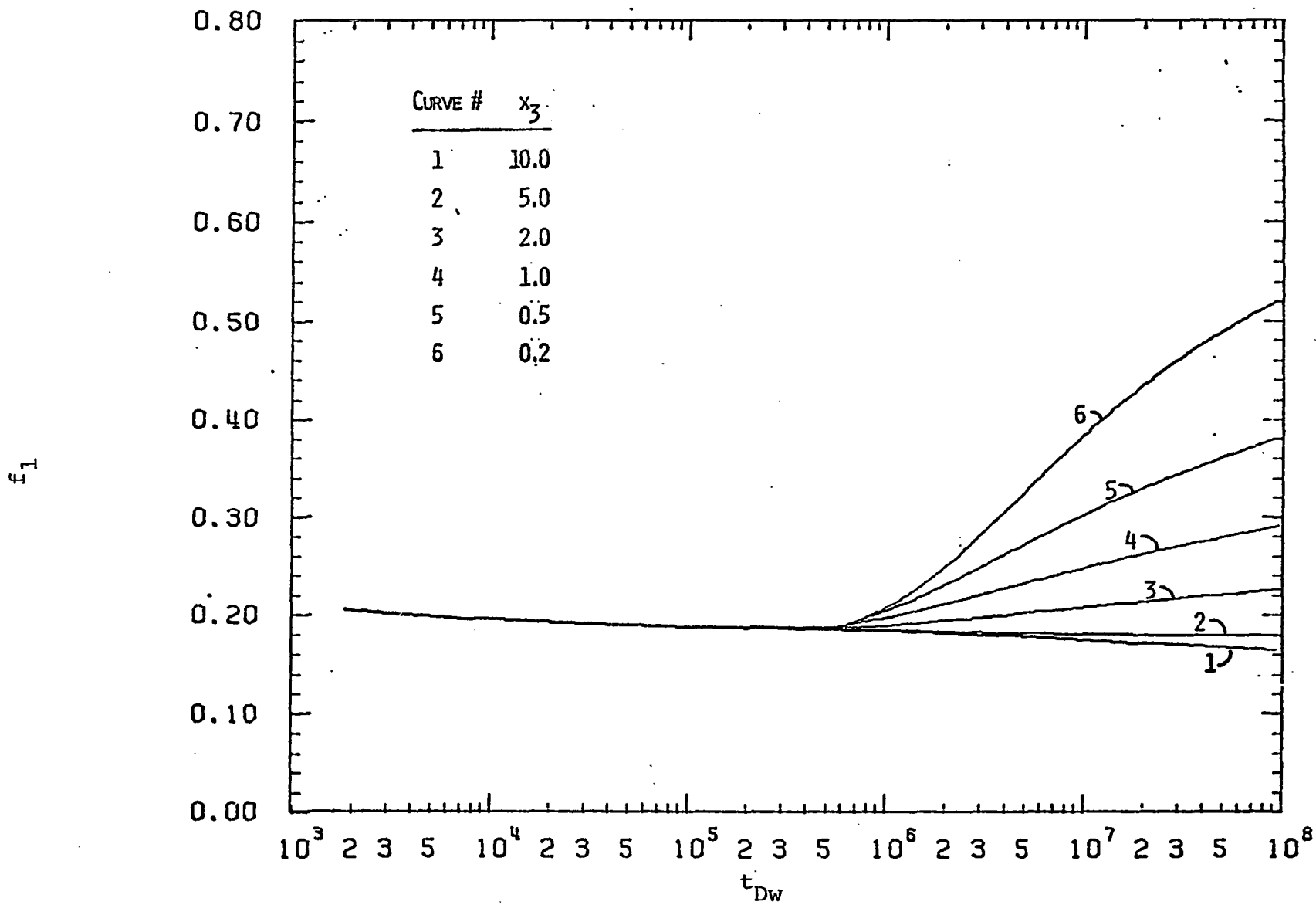

Figure E.17: Fractional flow rate from layer 1 of a two-layer two-region system with z=1.5, x_1=1. and x_2=5..

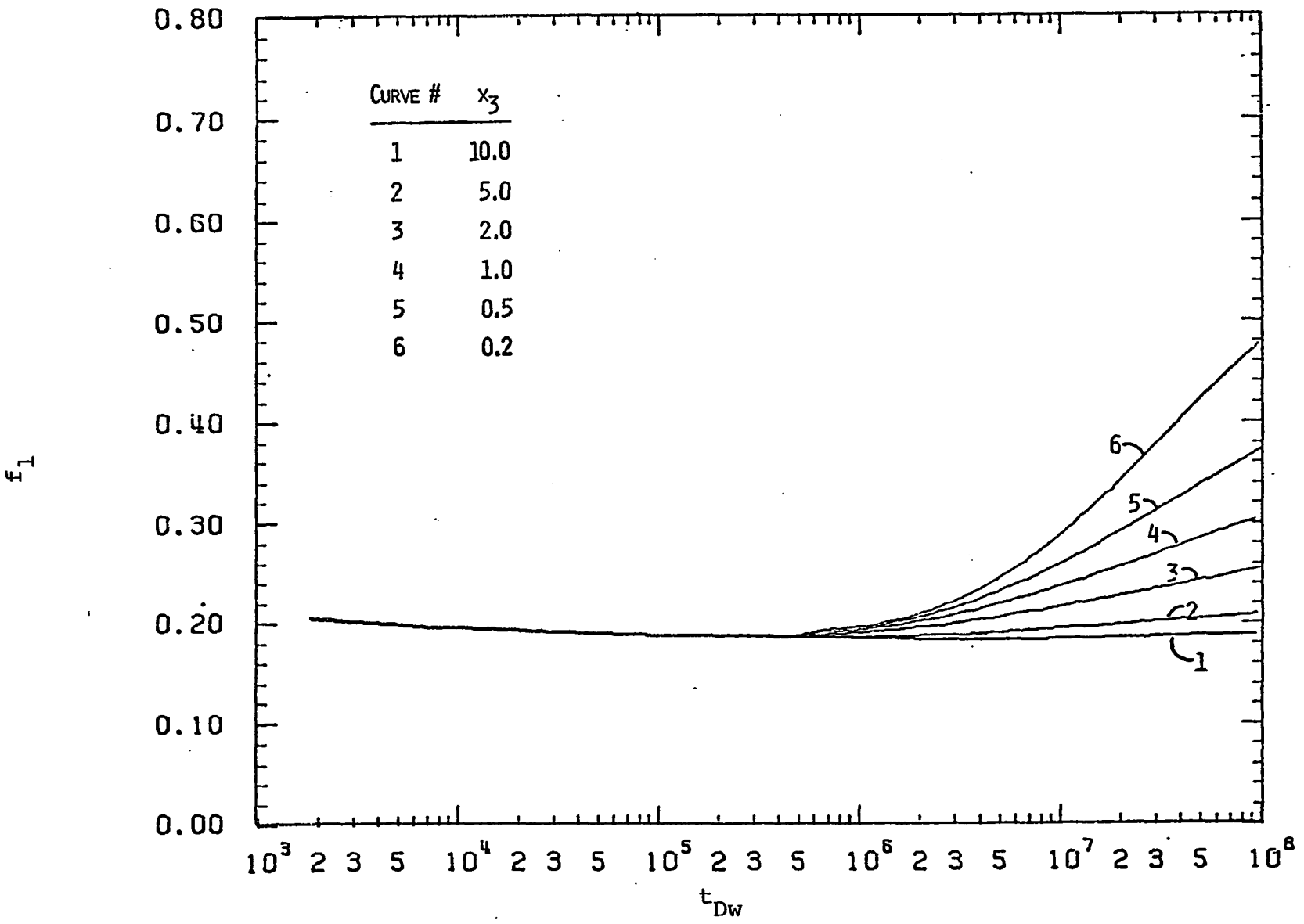

Figure E.18: Fractional flow rate from layer 1 of a two-layer two-region system with z=1.5, x_1=5. and x_2=5..

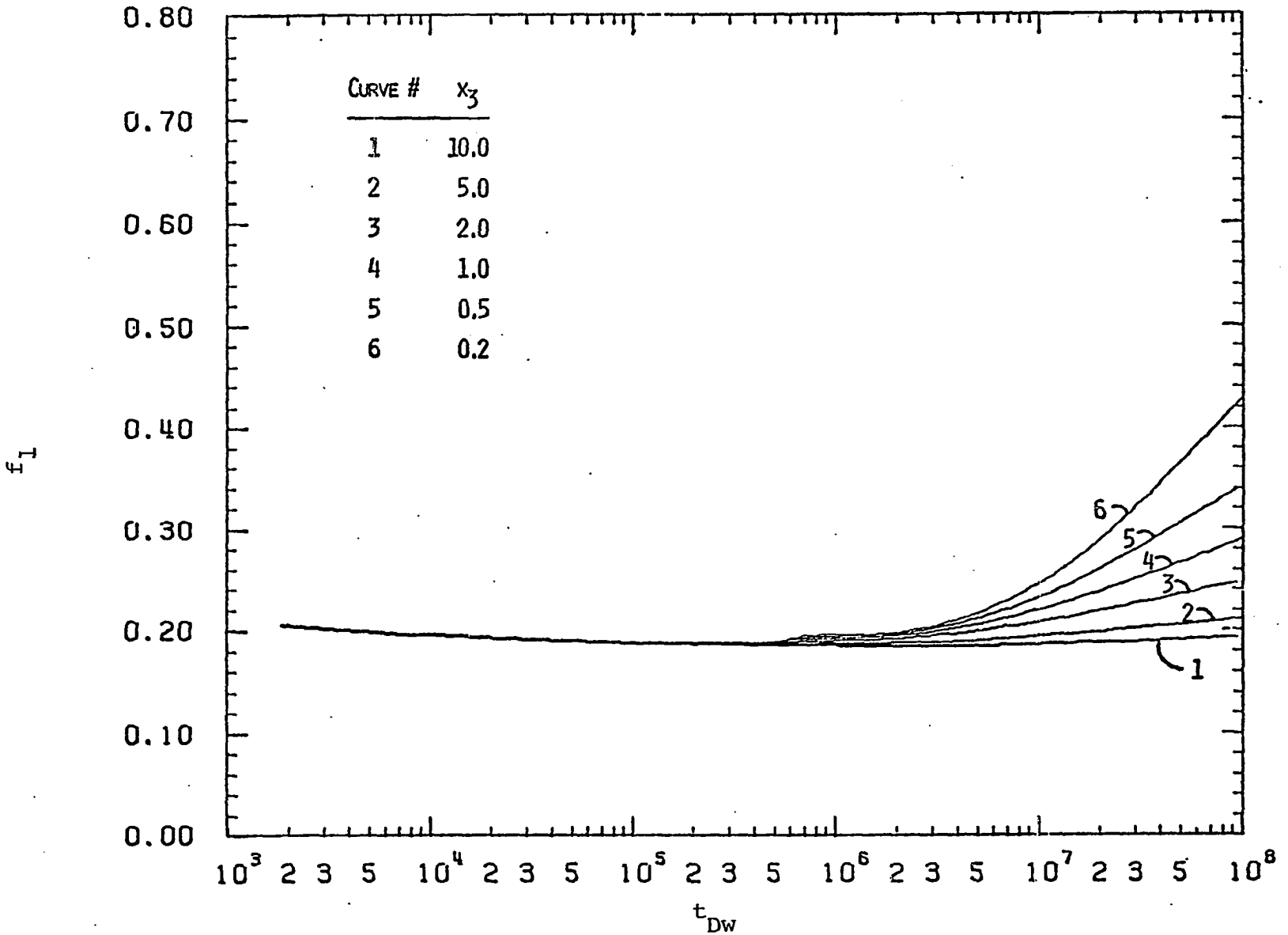

Figure E.19: Fractional flow rate from layer 1 of a two-layer two-region system with z=1.5, x_1=10. and x_2=5.0.

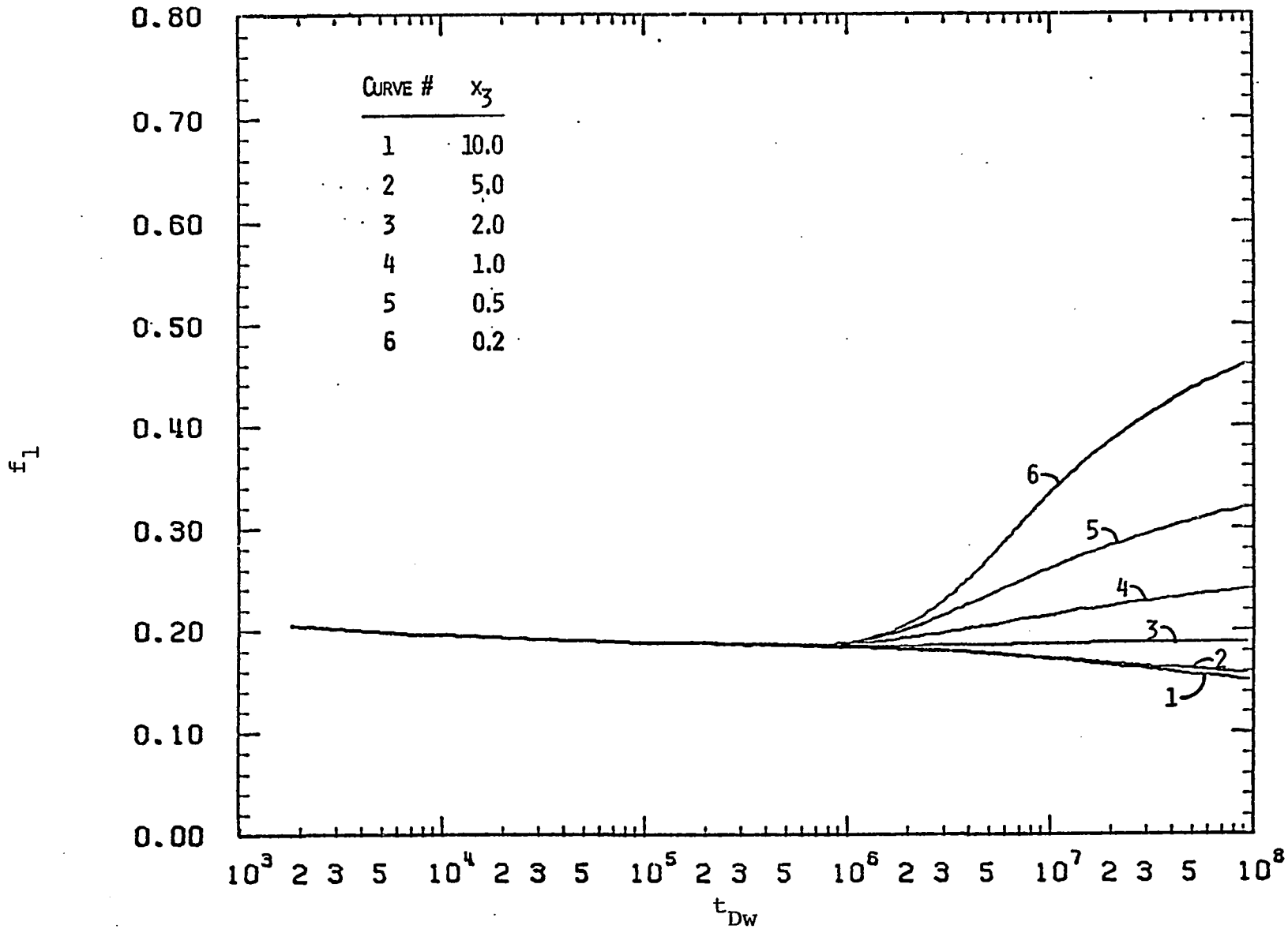

Figure E.20: Fractional flow rate from layer 1 of a two-layer two-region system with z=2., x_1=0.5 and x_2=5..

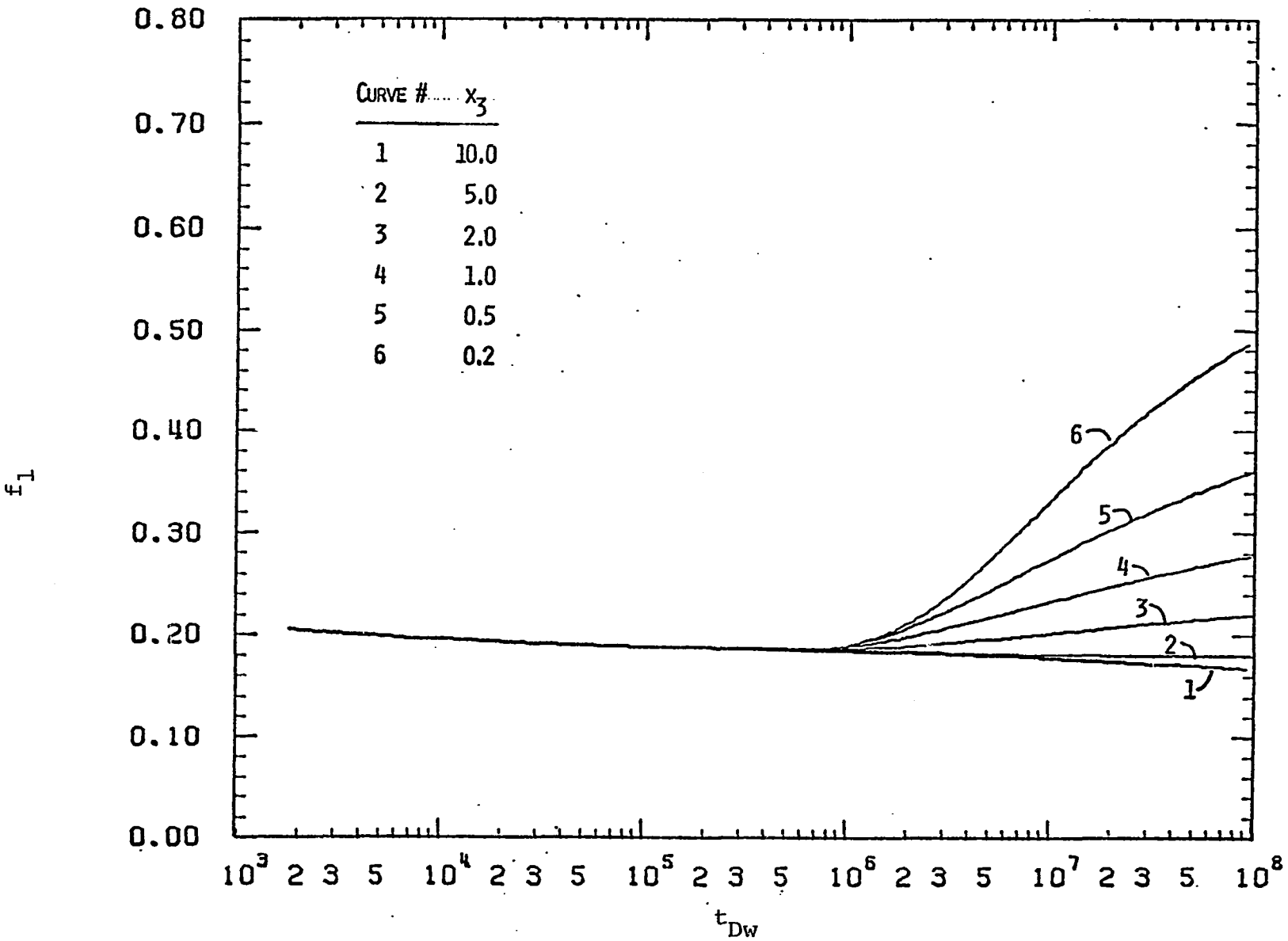

Figure E.21: Fractional flow rate from layer 1 of a two-layer two-region system with z=2., x_1=1. and x_2=5..

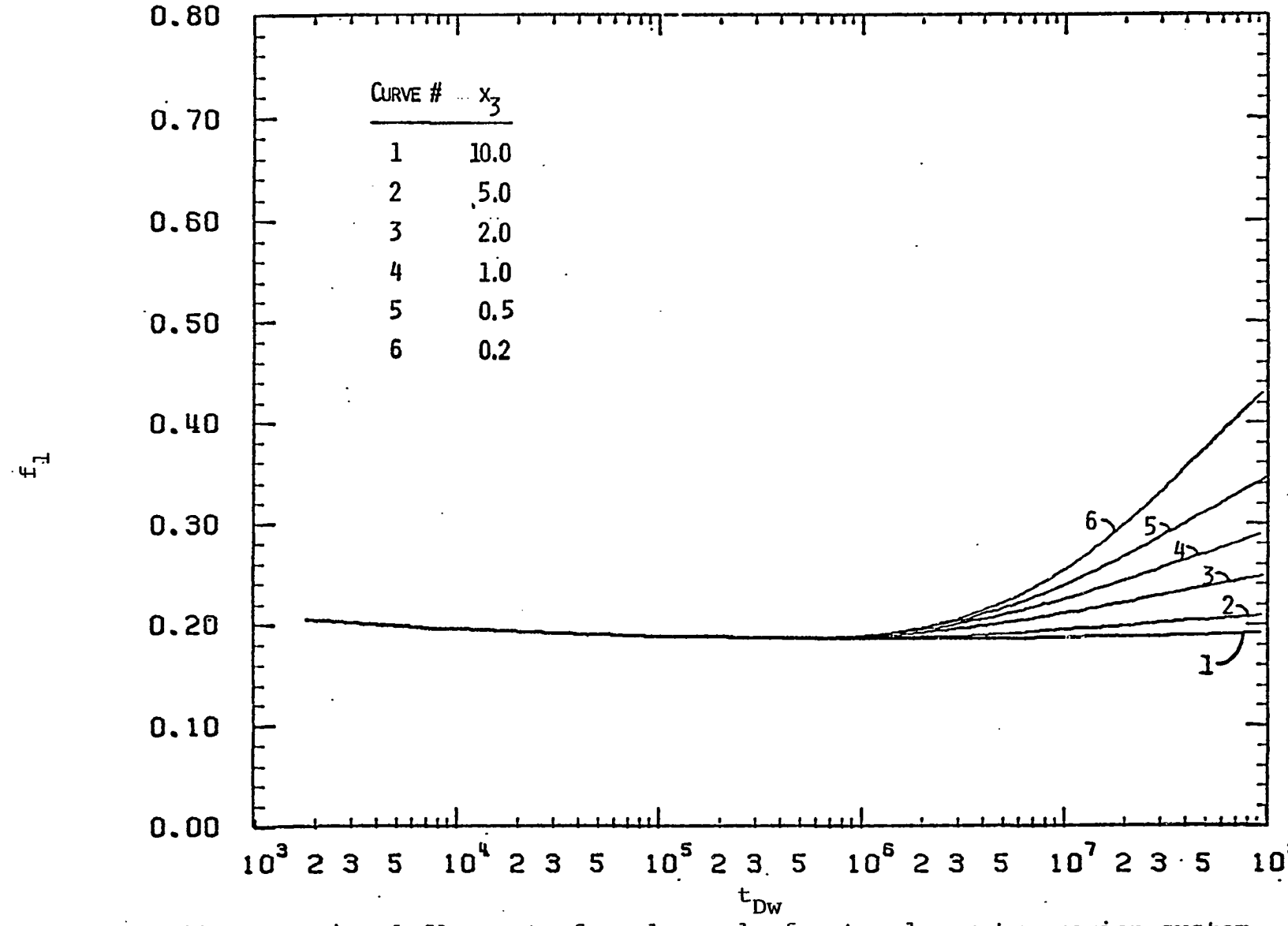

Figure E.22: Fractional flow rate from layer 1 of a two-layer two-region system with z=2., x_1=5. and x_2=5..

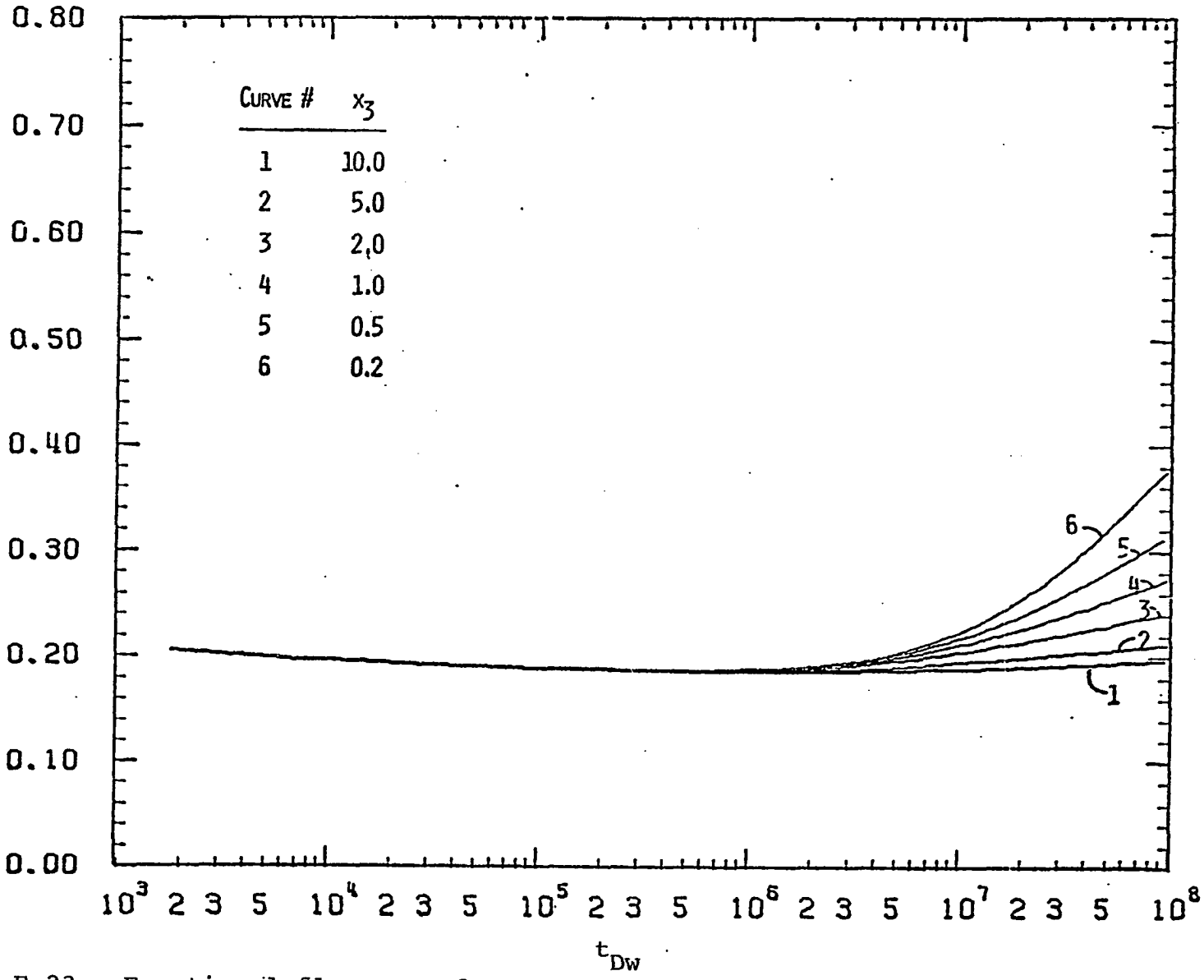

Figure E.23: Fractional flow rate from layer 1 of a two-layer two-region system with z=2., x_1=10. and x_2=5..